CFTRI-MYSORE
1810
Chemical archite.

FRONTIERS IN CHEMISTRY

Volume V

frontiers in chemistry

VOLUME V

Published under the Auspices of

WESTERN RESERVE UNIVERSITY

CHEMICAL ARCHITECTURE

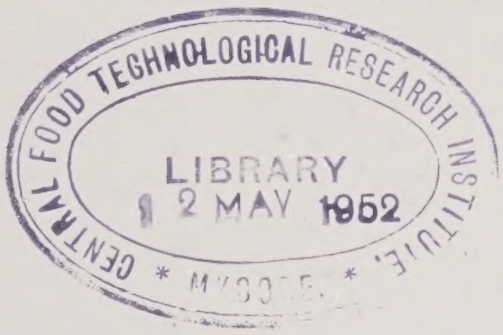

EDITORS

R. E. BURK
Plastics Department
E. I. du Pont de Nemours & Co.
Wilmington, Delaware

OLIVER GRUMMITT
Morley Chemical Laboratory
Western Reserve University
Cleveland, Ohio

1948

INTERSCIENCE PUBLISHERS, INC. • NEW YORK
INTERSCIENCE PUBLISHERS LTD. • LONDON

1810

Copyright, 1948, by
INTERSCIENCE PUBLISHERS, INC.
215 Fourth Avenue, New York 3, N. Y.

All Rights Reserved

E"2,1,N47

N48

PRINTED IN THE UNITED STATES OF AMERICA
BY THE WILLIAM BYRD PRESS, INC., RICHMOND, VA.

CFTRI-MYSORE
1810
Chemical archite.

PREFACE TO VOLUMES V AND VI

As time goes on, the task of keeping up with the flow of new chemical information becomes increasingly difficult. The contribution of the Frontiers in Chemistry lectures and publications to meeting this problem continues to be well received by audiences in this area and by the larger reading public. Since the start of the lecture programs in 1942 and the publication of Volumes I and II in 1943, several similar projects have been undertaken at various universities throughout the country. We find this to be both encouraging and flattering, and we hope that the trend will continue.

Continued success depends on the quality of the lecturers and on well-organized programs. To the contributors to these volumes a vote of thanks is extended for their excellent lectures and chapters.

September, 1947

R. E. Burk
Oliver Grummitt

PREFACE TO VOLUMES I AND II

The burdens of keeping abreast with the forward movement of science must be felt even by the brightest minds and the most energetic souls in that profession. This problem presents itself with particular force to universities who seek to train graduate students to be well-informed research workers. It is the custom for universities to have a rather small number of professors who may be specialists in certain fields such as physical, organic, inorganic, and analytical chemistry; but one or a few professors in each of these fields can no longer hope to master the entire field, nor therefore to present a well-proportioned impression of the subject to graduate students.

The problem of keeping abreast of science is also an important one to industrial research departments and to the individuals therein. There is a great tendency for the individual industrial research man to work in a rather narrow practical field. He may serve well in his capacity, yet actually be less valuable at the end of a few years' work because he may have lost touch with broader aspects of his field and become somewhat obsolete as far as attacking a new and somewhat different problem is concerned.

To meet these difficulties, Western Reserve University conceived the idea of inviting distinguished scientists in the field of chemistry and closely related fields to be professors for a day. Each of these men delivers two lectures. This gives him an opportunity to present a substantial view of his work. The lecturers who follow present somewhat different, though definitely related fields, so that at the end of a series one has what is, after all, a connected course of lectures, but one in which each lecture is given

by a real expert. Thus far two courses of twelve lectures each have been presented. They have met with outstanding success, and the plan may well appeal to others.

The participants in the lectures enjoyed the personal contact with the lecturers. The reader of the following pages is not in the same fortunate position. To compensate for this lack, we have added, in the biographical part of the book, pictures of the lecturers and short biographical sketches about each of them.

R. E. Burk
Oliver Grummitt

PREFACE TO VOLUMES III AND IV

The Western Reserve University Frontiers in Chemistry lectures have demonstrated their worth as a mechanism for presenting to graduate students the flow of chemical research, and for keeping industrial chemists abreast of their science. In spite of the shortage of gasoline and rubber, and in spite of the forty-eight hour work week, they have drawn an ample, an attentive, and an enthusiastic audience. They are highly appreciated in the Cleveland-Akron industrial area, and are recognized as a force therein.

The lectures are characterized by the distinction of the lecturers, by organization of their over-all subject matter, and by the effort which the individual lecturers evidently have put into their contributions. It is no wonder that, already, they have been imitated—this is to be encouraged.

The publication of these lectures in book form makes them available to a much wider audience, and allows those who have heard them to assimilate the material more completely. In many cases, the lectures are published in the colloquial style in which they were presented. This, as a matter of fact, was the request made of the lecturers. Others, however, have elaborated upon their lectures and, in some cases, developed them into striking and thoroughgoing contributions to the chemical literature.

David Rittenberg of the College of Physicians and Surgeons, Columbia University, who had delivered the lectures on "Isotopes, Recent Progress

and Applications in Chemistry and Medicine," because of severe illness was unable to provide us with the manuscript for Chapter I. A. S. Keston, also of the College of Physicians and Surgeons, was kind enough to write, on very short notice, an original article on the subject of Dr. Rittenberg's lectures. We wish to express our appreciation to Dr. Keston for the time and effort he has devoted to the preparation of his contribution.

R. E. Burk
Oliver Grummitt

COLLABORATORS

HUGH S. TAYLOR, Princeton University, Princeton, New Jersey

CHARLES P. SMYTH, Princeton University, Princeton, New Jersey

W. CONARD FERNELIUS, Syracuse University, Syracuse, New York

B. E. WARREN, Massachusetts Institute of Technology, Cambridge, Massachusetts

H. MARK, Institute of Polymer Research, Polytechnic Institute of Brooklyn, Brooklyn, New York

MIROSLAV W. TAMELE, Shell Development Company, Emeryville, California

Dr. Hugh S. Taylor is Professor of Chemistry, Chairman of the Department of Chemistry, and Dean of the Graduate School at Princeton University. He has served for many years as a member of the Committee on Contact Catalysis of the National Research Council. He was awarded the Nichols Medal by the New York Section of the American Chemical Society in 1928, the Mendel Medal by Villanova College in 1933, the Cross of the Order of Leopold II in 1937, and the Longstaff Medal of the London Chemical Society in 1942. Dr. Taylor is internationally known for his work in the field of physical chemistry, particularly in the fields of catalysis, thermodynamics, and activated adsorption.

Dr. Charles P. Smyth is Professor of Chemistry in Princeton University. After receiving an A.B. and A.M. at Princeton, and serving as a 1st Lieutenant in the Chemical Warfare Service in World War I, he completed his graduate studies at Harvard University and received a Ph.D. in 1921. He has been a member of the Princeton faculty since 1920 and has worked, principally, upon problems concerned with the structure of matter, in particular, refraction, dielectric constant and loss, dipole moment and molecular structure, and molecular rotation in solids. During World War II, he worked on a project for the Manhattan District Project, Corps of Engineers, U. S. Army, and also served as Expert Consultant with the U. S. Army in the European Theater of Operations.

Dr. W. Conard Fernelius is Chairman of the Department of Chemistry at Syracuse University. He received his academic training at Carnegie Institute of Technology and Stanford University and has studied at Munich and Western Reserve University. From 1928 to 1942 he was a member of the staff of the Department of Chemistry at Ohio State University, and from 1942 to 1947 Professor of Inorganic Chemistry at Purdue University. Dr. Fernelius was on leave with Monsanto Chemical Company from 1943 to 1946 to conduct work for the Manhattan District Project. He is well known for his researches in liquid ammonia and coordination compounds.

Dr. Bertram E. Warren, now Professor of Physics at Massachusetts Institute of Technology, received the Sc.D. degree from that institute in 1929 and has remained with the Physics Department since that time. He is the author of about seventy papers on x-ray diffraction studies of crystalline silicates, glasses, randomness in structures, and order-disorder changes in alloys. He is a former president of the American Society for X-Ray and Electron Diffraction.

Dr. Herman Mark is an internationally known authority in the field of high polymers. He is Professor of Organic Chemistry and Director of the Institute of Polymer Research at Polytechnic Institute of Brooklyn. Dr. Mark has served as Research Manager of the Canadian International Paper Company in Hawkesbury, Ontario, Canada, as Professor of Chemistry at the University of Vienna, and as a Research Director for I. G. Farbenindustrie. His principal researches have been on x-rays and their use in studying the structure of matter, on the diffraction of electrons, on the structure of high polymers, particularly cellulose and rubber, on the mechanical properties of long-chain molecules, on the mechanism of polymerization reactions, and on the size and shape of macromolecules in solution.

Dr. Miroslav W. Tamele is Associate Director of Research and Head of the Department of Colloid Chemistry of Shell Development Company. He received his academic training at Charles University in Praha, Czechoslovakia. Thereafter he was international research fellow and research associate at the University of California, then research chemist with the California Ink Company, and, since 1929, a member of the staff of Shell Development Company in Emeryville, California. Dr. Tamele has played a prominent part in the development of the utilization of petroleum raw materials in the chemical industry and in the introduction of catalytic processes in petroleum refining.

CONTENTS

PAGE

Preface to Volumes V and VI v

Preface to Volumes I and II vi

Preface to Volumes III and IV vii

Introducing the Collaborators ix

Applications of Molecular Geometry in the Field of Reaction Mechanism. By HUGH S. TAYLOR, Princeton, N. J. 1

I. Introduction 1
II. The Concept of Activation Energy 3
III. Geometry in Homogeneous Reactions 5
IV. Geometry in Heterogeneous Reactions 8
V. Geometry in Homogeneous Liquid Systems 19
References 21

Dipole Moment, Resonance and Molecular Structure. By CHARLES P. SMYTH, Princeton, N. J. 23

I. Introduction 23
II. The Molecule as an Electric Dipole 23
III. Experimental Determination of Dipole Moments 24
IV. Use of Dipole Moment to Determine Geometrical Structure 26
V. Movable Dipoles and Restricted Rotation 28
VI. Dipole Moment as a Measure of Resonance 31
References 49

Structure of Coordination Compounds. By W. CONARD FERNELIUS, Syracuse, N. Y. 53

I. Introduction 53
II. Fundamental Definitions 54
III. Nature of Coordination Linkages 59
IV. Methods for Deduction of Structure 65
V. Results 83
VI. Conclusion 97
References 98

X-Ray Studies of Randomness in Various Materials. By B. E. WARREN, Cambridge, Mass. 101

I. Introduction 101
II. Structures of Ideally Crystalline Materials 102
III. Randomness in Structures 108
References 120

Light Scattering in Polymer Solutions. By H. MARK, Brooklyn, N. Y. 121
I. Introduction 121
II. A Few Principles of Light Scattering 123
III. Scattering of Light from a Pure Liquid 127
IV. Scattering of Light from Solutions of Small Molecules 131
V. Scattering of Light from Solutions Containing Particles Comparable with the Wave Length of Light 139
VI. Depolarization of Scattered Light 147
VII. Experimental Methods for Measuring Turbidity and Dissymmetry 150
VIII. Experimental Data and Discussion 163
References 171

The Nature of Inorganic Gels. By MIROSLAV W. TAMELE, Emeryville, California 175
I. Introduction 175
II. Definition of Gel 176
III. Formation of Inorganic Gels 177
IV. Inorganic Sols 180
V. Sol–Gel Transformation 184
VI. Structural Changes on Drying of Gels 188
VII. Solid Framework of Dried Gels 189
VIII. Porosity of Gels 190
References 195

Subject Index 199

I. *Applications of Molecular Geometry in the Field of Reaction Mechanism*

HUGH S. TAYLOR

Frick Chemical Laboratory, Princeton University, Princeton, N. J.

I. Introduction

THE ASSOCIATION of molecular geometry with reaction mechanism is no new concept. Lucretius explained that the difference between substances which have a sweet or bitter taste consists in the bitter things being sharp and jagged and the sweet things, round and smooth. Lemery, among the later alchemists, asserted that "acids consisted of sharp, pointed particles. . . The angular or needle-shaped form of crystals was cited as further proof of the pointed shape of acid particles and the variety in the avidity with which different acids attacked different metals was alleged to be due to the degree of sharpness of the points and edges of such particles. Alkalis, on the other hand, were composed of particles so formed that the points of the acid particles readily stuck into and divided them" (1). Brown, who records these early concepts, points out that "of all this theory only one idea had a foundation in truth, that any conception which we may form as to the shapes of the ultimate atoms of bodies, and their mode of combination, must be such as to explain the facts of crystallization as well as the facts of chemical change" (1).

Mitscherlich's discovery of isomorphism and the relationship between

chemical constitution and crystalline form was the first significant demonstration of the connection between molecular geometry or architecture and the interactions of different chemical systems. Compounds of several elements having similar chemical constitutions not only possessed the same crystalline form as determined by angular measurements, but also, in many cases, combined with the same number of molecules of water of crystallization and crystallized as one crystal. The knowledge that has been gained in the past thirty years concerning atomic and ionic radii has made our knowledge of the conditions for isomorphism more precise; it has also revealed that the actual structure which a crystal assumes is determined by the ratio of the numbers, the ratio of the sizes, and the properties of polarization of the structural units (atoms or ions) of which the crystal is composed. Goldschmidt (1924–1929) incorporated these concepts in a fundamental law of crystal chemistry and applied them to simple substances of the types AX and AX_2 and to compounds of greater complexity. Thus, for substances of the general formula AX, there are six principal crystalline forms characterized by the coordination numbers 8, 6, 6, 4, 4, 3, representing the number of nearest neighbors to any particular atom in a space-lattice. It can be calculated that for eight negative ions, assumed to be spherical, to surround and touch an inner positive ion, as in the CsCl-type structure, the ratio of the ionic radii, r_+/r_-, must be greater than 0.73. For coordination numbers of 6, 4, and 3, the radius ratios must lie between 0.73 and 0.41, 0.41 and 0.22, and 0.22 and 0.15, respectively. The occurrence of the cesium chloride structure (coordination number 8) and the sodium chloride structure (coordination number 6) in the chlorides, bromides, and iodides of the alkali elements conforms to these conclusions. That the fluorides are exceptions to this conclusion is attributed to the low polarization of the fluoride ion. Similar generalizations emerge from a consideration of the more complex crystal structures.

It is beyond the scope of this article to present more detailed discussion of such crystallographic problems, since they are of little concern in the problem of reaction mechanism. This is true also of the field of stereoisomerism which played such a large part in the theories of organic chemistry since the original independent observations on this topic by Le Bel and van't Hoff in 1874. Isomeric forms are, of course, of profound significance in many problems of chemical reactivity. One need only recall the differences in reactivity between such simple structural isomers as *n*-butane and isobutane, or between position isomers (for example, ortho-, meta-, and para-substituted benzenes), or between functional group isomers such as acetone and propionaldehyde, to realize that these differences are important

consequences of molecular geometry. The detailed recording of such data would require an entire volume. Typical examples in this field will only be employed as they are pertinent to the lines of development that will be set forth in the succeeding sections.

The large body of evidence on molecular structure which the organic chemist accumulated by processes of brilliant inductive reasoning, combined with ingenious experimental research, has been confirmed, extended, and made quantitative by modern research in the areas of X-ray and electron scattering in gases, liquids, and solids, by the supplementary data obtained from Raman and infrared spectroscopy, from the investigation of dipole moments, and other measurements. Research in these fields continues to yield an increasingly important body of evidence concerning the shape, size, and spatial configurations of molecules. The tetrahedral symmetry of the carbon atom is confirmed. Triatomic molecules may be linear or nonlinear; tetratomic molecules may be planar, nonplanar, or pyramidal. The data become quantitative when the effective atomic diameters in the molecule or the bond distances are determined. It is these advances which have made possible a detailed approach to the problem of molecular geometry with reference to reaction mechanism.

II. The Concept of Activation Energy

Reaction mechanism is associated, in modern physicochemical science, with the concept of activation energy, the minimum energy which the system must acquire before it can undergo the appropriate change. With several alternative possibilities of change, the relative frequency of their occurrence will be determined mainly by the Boltzmann factor, $e^{-DE/RT}$, where DE represents the difference in activation energy between two alternative paths. The activation energy of a single process may be represented as a potential-energy barrier of definite height separating two potential-energy minima, representative of the initial and final states of the reaction. The accompanying diagram (Figure 1) represents schematically the variation of potential energy in the simplest possible reaction mechanism for a reaction between three univalent atoms, X, Y, and Z:

$$X + YZ = XY + Z$$

The activation energy for the process in the forward direction is E, the heat of reaction is ΔH, and the activation energy of the process in the reverse direction is $(E + \Delta H)$. The molecular system, $X \cdots Y \cdots Z$, at the top of

the potential-energy barrier is a particular configuration of the three atoms in question, which is determined by the atoms themselves and the energy relations between them. It is now generally termed the *activated state*. It is actually the configuration of the complex of the three atoms in question at the *lowest* potential-energy barrier intervening between the initial and final states of the system.

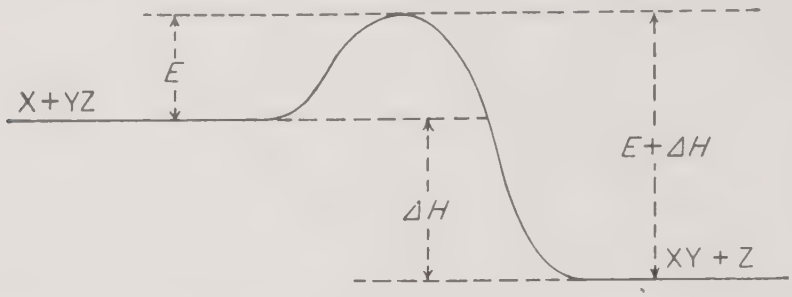

Fig. 1. Potential energy, activation, and heat of reaction for a reaction between three univalent atoms, X, Y, and Z.

It is a consequence of our valency concepts that the three univalent atoms in question must exist, in their lowest energy state, as one atom and one molecule. Classical concepts of the binding forces between atoms were not adequate for the expression of these valency rules. The quantum mechanics, however, represents the binding energy, P, of a system of two atoms as the sum or difference of two quantities, the classical coulombic interactions of the electric charges in the system, (more briefly, the coulomb energy, A) and a quantum-mechanical interchange or exchange energy, α, such that:

$$P = A \pm \alpha$$

The exchange energies are so named because they represent energy quantities which can be interpreted in terms of an electron exchange between two atoms, or *sharing* of an electron. It is these exchange energies which, according to Heitler and London (1a), yield the valence forces and account for saturation of a single valence in terms of two shared electrons. The quantity $P = A + \alpha$ represents the binding energy of two atoms which will yield a stable molecule. The term $P = A - \alpha$ represents a repulsive state between the two atoms. In a hydrogen molecule the respective contributions of coulombic and interchange energies are approximately 15 and 85 per cent of the total.

It was the extension by London of these quantum-mechanical concepts of the nature of the forces between atoms to systems of three or more atoms

which led directly to the modern work on the significance of molecular geometry in reaction mechanism. The binding energy of a system of three atoms, XYZ, in a planar, triangular configuration (shown in Figure 2), where the respective binding energies between two atoms for formation of molecules, when the third is far distant, are given by $(A + \alpha)$, $(B + \beta)$, and $(C + \gamma)$, is given by the London equation:

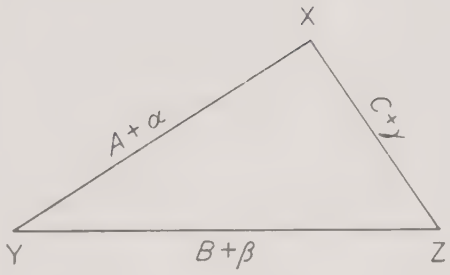

Fig. 2. Binding energies of three-atom system, XYZ.

$$P_{XYZ} = A + B + C + \sqrt{\alpha^2 + \beta^2 + \gamma^2 - \alpha\beta - \beta\gamma - \gamma\alpha}$$

The coulombic terms are additive. The exchange terms add vectorially in a manner which is capable of easy graphical computation (2).

III. Geometry in Homogeneous Reactions

The London equation permits an evaluation of the potential energy of all configurations of three atoms at any distances one from another. Application of this equation by Eyring and his colleagues (2) to a system of three hydrogen atoms revealed that the approach of a hydrogen atom to a hydrogen molecule along the line of centers of the nuclei of the molecule constituted the energetically easiest path for approach and reaction. Approach at right angles to the line of centers gave rise to high potential energies of the three-atom system such that the kinetic energy of the approaching atom was rapidly converted into the potential energy of the three-atom system; the approaching atom lost all its kinetic energy before it entered into the range of reaction. The collision was elastic and the atom reversed its pathway when it receded from the molecule along the line of approach, reacquiring its kinetic energy as the potential energy of the system of three atoms decreased. This analysis provided the first example of the molecular geometry of the *intermediate complex* in a reaction mechanism. In the case in question it is a linear array of the three hydrogen atoms represented in the following equation:

$$\underset{a}{H} + \underset{b}{H}\text{—}\underset{c}{H} \rightleftharpoons \underset{a}{H}\cdots\underset{b}{H}\cdots\underset{c}{H} \longrightarrow \underset{a}{H}\text{—}\underset{b}{H} + \underset{c}{H}$$

The quantitative treatment of the potential energies of this three-atom system indicated that, in the linear activated complex, the outer hydrogen

atoms are equidistant from the central atom and at a distance of 0.90 Å from it. Furthermore, the potential energy of the activated complex is about 14 kcal. or some 7.8 kcal. more than the zero-point energy of the molecule before the approach of the atom, namely, 6.2 kcal. This energy difference between reactants and activated complex, 7.8 kcal., is in best agreement with the experimental value for the activation energy of the reaction between hydrogen atoms and hydrogen molecules as determined by the conversion of parahydrogen to orthohydrogen under conditions of photosensitization by mercury vapor atoms by the resonance radiation of mercury $\lambda = 2536.7$ Å; the excited mercury thus produced, endowed with 112 kcal. per gram atom, is sufficient to cause dissociation of hydrogen on collision with such excited atoms. The concordance between experiment and calculation in this case has a twofold significance. It indicates the method of theoretical calculation of the activation energy, E, of a reaction mechanism which could previously be ascertained only from experimental measurement of reaction rates at two or more temperatures. It also reveals that one collision is not as good as another; that, in this case, the most fruitful molecular geometry in the reaction mechanism is the linear array of the three atoms in question. In many other atom–molecule reactions, *e.g.*, $H + Cl_2$, $H + Br_2$, $H + I_2$, $H + HCl$, $H + HBr$, $H + HI$, $Cl + H_2$, and $Br + H_2$, the linear array of the three atoms represents the most favorable geometry for the intermediate complex.

The extension of the method developed for three-atom systems to reactions involving four atoms was shown by Eyring to permit the study of reaction velocity between two diatomic molecules, reactions which may be generalized by the equation:

$$WX + YZ = WY + XZ$$

The London expression for the energy of a system of four atoms takes the form:

$$P_{WXYZ} = A_1 + A_2 + B_1 + B_2 + C_1 + C_2 + [(\alpha_1 + \alpha_2)^2 + (\beta_1 + \beta_2)^2 + (\gamma_1 + \gamma_2)^2 - (\alpha_1 + \alpha_2)(\beta_1 + \beta_2) - (\beta_1 + \beta_2)(\gamma_1 + \gamma_2) - (\gamma_1 + \gamma_2)(\alpha_1 + \alpha_2)]^{1/2}$$

In such a system of four atoms we see the possibility of six separate bonds between the atoms with binding energies, $(A_1 + \alpha_1)$, $(A_2 + \alpha_2)$, etc., when the other *two* atoms are remote. In certain systems, notably the interaction of hydrogen and halogen molecules, it was found that the molecular geom-

etry of the activated complex was a *planar* array of the four atoms. By such studies Eyring was able to show that the *molecular* collision of hydrogen molecules and iodine molecules was an easier pathway to reaction than the alternative pathway *via* the iodine and hydrogen atoms in a chain sequence of reactions to form hydrogen iodide. The most surprising result, however, in this group of hydrogen–halogen studies of reaction mechanism concerned the case of fluorine as the halogen. Contrary to all prevailing experimental conclusions, Eyring found that the reactions of H_2 with F_2 and of F with H_2 were surprisingly slow; calculation indicated that these reactions require activation energies of the order of 50 kcal. and 6–10 kcal., respectively. Experimental work by von Wartenburg, concurrently with Eyring's calculations, confirmed the essentially nonreactive nature of hydrogen and fluorine molecules at room temperature and the slowness of the reaction of atomic fluorine with hydrogen. This nonreactivity can be traced to the high potential energy of the planar configuration of the activated complex of the four-atom system due to the small distances of separation of the four atoms in the geometry of the complex. The same condition occurs in the bimolecular reaction between hydrogen molecules and deuterium molecules and leads to the result that a bimolecular interaction would require a four-atom complex with a potential energy, and therefore activation energy, some 90 kcal. above that of the zero-point energy of the separated molecules. This is in agreement with experimental result which shows that the homogeneous thermal reaction between hydrogen and deuterium at about 600°C. is not kinetically bimolecular, but close to 1.5 in order; that is, the process occurs by dissociation of the molecules to atoms followed by reactions:

$$H + D_2 = HD + D \qquad \text{and} \qquad D + H_2 = HD + H$$

The activation energy of such a 1.5-order process would be about 60 kcal., composed of half the heat of dissociation of the molecule (52 kcal.) plus the activation energy of the atom–molecule reaction (7 kcal.). These examples must suffice to indicate the utility of considerations based on the geometry of the activated complex in formulating reaction mechanisms in four-atom systems.

Reactions in more complex polyatomic systems are capable of approximate treatment by the same methods that are used in four-atom systems. Thus, the addition of halogens to an ethylenic bond can be so considered as an approximation and yields the result, which is in agreement with experiment, that such reactions in the homogeneous gas phase actually require significant activation energies. They occur normally, therefore, not in the

gas phase but as reactions catalyzed by wall surfaces. In the addition of halogen molecules, X_2, to conjugated dienes it is found that the geometry of the activated complex is such that all six atoms, C=C—C=C + 2 X, are in one plane; this may be regarded as the path by which the majority of the halogen molecules will react with a conjugated system of double bonds. Furthermore, it is also revealed that 1,4 addition may be expected to occur more readily than 1,2 addition.

IV. Geometry in Heterogeneous Reactions

The pattern of success which attended these early excursions into the significance of molecular geometry in reaction mechanism led immediately to the exploration of its significance in surface catalytic reactions. Even before the theoretical exploration, there was an intuitive empirical predisposition in this field to anticipate the significance of geometry. Speculation had dwelt on the possibility that the binding energy of the molecule to the contact mass might not be sufficient to yield total dissociation of the adsorbed material into fragments. The adsorbed molecule while not dissociated might, so to speak, be expanded or extended. Activation energy would be necessary for complete fragmentation. Concepts covering complete dissociation and deformation of adsorbate arose at intervals from 1906 by Raschig (3), Boeseken (4), Bodenstein (5), and others. Burk in 1926 (6) developed a concept of catalytic change involving *multiple adsorption* of a molecule at two or more centers in the catalyst surface, leading to reaction. The theory took on a more definite form in the *multiplet hypothesis* of Balandin (7). To the postulate that the binding between atoms of the adsorbed substance is broken when they are attracted by two different surface atoms, Balandin added a further postulate that a bond is closed between atoms bound to the same surface atom. For example, in the dehydration and dehydrogenation of alcohols which occur simultaneously on various oxides, the following scheme will interpret the processes:

The dots represent catalyst atoms and, on the basis of the two postulates, ethylene and water are formed in the first case, acetaldehyde and hydrogen in the second. Catalysis arises through the geometrically determined action of various catalytic centers.

The most specific suggestion as to correlation of surface geometry

with catalytic activity was put forward by Balandin in the case of dehydrogenation of hydroaromatic rings. Here it was shown that the six-membered ring can be symmetrically arranged on the octahedral face of a face-centered cubic metal lattice, this face having a regular triangular array of metal atoms occupying the corners of the triangle as shown in the accompanying diagram (Fig. 3). In the dehydrogenation process the metal atoms (*4*, *5*, and *6*) attract pairs of hydrogen atoms from the pair of nearest carbon atoms in the adsorbed cyclohexane and, causing them to combine, produce the observed dehydrogenation. This sextet model leads to the conclusion that only face-centered cubic metals can effect the dehydrogenation process and that, for compatability between hydroaromatic ring and octahedral face, the lattice constants of the metal must lie within certain limits. Actually, dehydrogenation and the reverse process of hydrogenation of benzene are possible with metals whose lattice constants lie between 1.397 Å (Pd) and 1.237 Å (Ni). Metals with constants lying only slightly outside these limits are inactive.

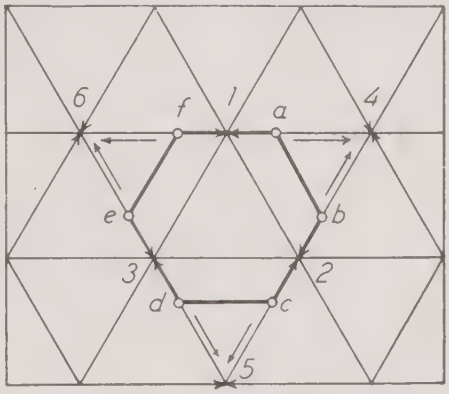

Fig. 3. Dehydrogenation of a six-membered ring (Balandin).

Balandin attempted to reinforce his argument with considerations that were not actually real or pertinent. Thus, his observation that dehydrogenation of cyclopentane and cycloheptane does not occur under conditions which are efficient for dehydrogenation of cyclohexane is not due to the absence of geometrical correlation between the cycloparaffin and the catalyst surface but is due to the unfavorable equilibrium, that found with cyclohexane being unduly favorable due to the resonance energy of benzene (8). That the problem is one of equilibrium and not geometry is evident from the fact that the hydrogenation of cyclopentenes and cycloheptenes occurs readily on the face-centered cubic metal lattices under consideration (9). Lazier and Vaughen (10) indicated that the sextet model was not a necessary condition for the dehydrogenation of cyclohexane and showed that this process occurs readily on chromium oxide gel which does not possess the geometry of the face-centered metal lattices. It also occurs on several metal chromite catalysts. This indicates, as Balandin has pointed out (11), that dehydrogenation of cyclohexane can occur by edgewise adsorption on a catalyst surface. This does not signify that

dehydrogenation on an octahedral metal lattice does not occur *via* the sextet model already discussed.

The principal experimental work that can be cited in support of the Balandin hypothesis is due to Long, Frazer, and Ott (12). They showed that, in a series of catalysts composed of alloys of iron, cobalt, and nickel, all the catalysts which were active for benzene hydrogenation below 200°C. had face-centered cubic structures. In those instances in which two structures were present (iron–nickel mixtures) the activity was in reasonable relationship to the amount of face centered structure observed. There was, however, a conspicuous anomaly in the metals studied. Copper in a face-centered structure was found to be inactive. According to Ipatieff, Corson, and Kurbatov (13) the activities of copper (in the hydrogenation of benzene) previously reported, are to be ascribed to the nickel content of the copper catalysts used.

Emmett and Skau (14) amplified the data of Long, Frazer, and Ott by coupling activity measurements on various catalysts with surface-area measurements of the catalysts used. They confirmed the inactivity of copper which contained not more than 0.0006% nickel, even though its surface area was greater than that of a pure nickel catalyst which, at much higher space velocities, produced 90% cyclohexane at 140°C. Iron having a large surface area (from precipitated oxide) and iron having a much smaller surface area (iron–synthetic ammonia catalysts) were both inactive and body-centered cubic in structure, conforming to the Balandin thesis. Emmett and Skau confirmed the Long, Frazer, and Ott data with mixed iron–cobalt catalysts. Palladium is active, silver is inactive, although both are face-centered cubic. Silver lies outside the Balandin limits. Emmett and Skau reach the general conclusion that "a necessary but not a sufficient requirement for a low-temperature metal catalyst is that it falls within the square of activity originally delineated by Balandin for metals having face-centered cubic or hexagonal lattices." The inactivity of copper, falling as it does within the Balandin limits, constitutes a continuing challenge to all those who would aspire to scientific elucidation and interpretation of catalytic processes.

That the geometry of a surface does have an influence on the rate of interaction of a gas with the surface emerges from the theoretical analysis by Sherman and Eyring (15) of the interaction between an approaching hydrogen molecule and two atoms of carbon in a carbon surface. Their study was an extension of the method of attack used by Eyring in the study of rate processes in homogeneous systems. The process may be visualized as the approach of a hydrogen molecule to two particular carbon atoms in

the surface and the formation of two C—H bonds. The solution obtained can at best be only approximate since it assumes negligible interactions between the molecule and other atoms in the surface. It does, however, emphasize the magnitude of the activation energy as a function of the distance between a pair of atoms in a surface as a function of the lattice distance separating these atoms. The form of the curve connecting activation energy with lattice distance is shown schematically in Figure 4. Quite

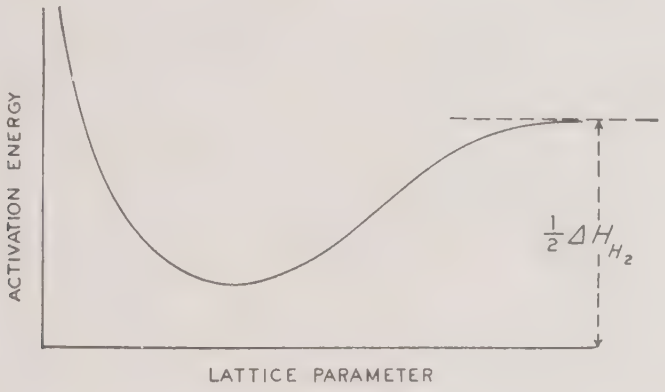

Fig. 4. Activation energy of adsorption of hydrogen molecule as function of lattice distance of surface atoms.

generally, the activation energy for the approach of a hydrogen molecule to two surface atoms will be high for small values of the lattice distance, due to the repulsive forces operative between the approaching hydrogen atoms in the molecule and the lattice atoms at such small distances. As the lattice parameter grows, these repulsive forces will decrease in importance and the activation energy will fall. At very large lattice–atom distances the activation energy required will approach asymptotically the value of one-half the dissociation energy of hydrogen, since the process consists virtually in moving the two atoms of hydrogen to an infinite distance (requiring that $E_{act} = 1/2\ \Delta H_{H_2}$) and bringing these atoms up to the surface atoms, a process which will not require activation energy. The curve for activation energy versus lattice distance will therefore show a minimum at some intermediate lattice parameter. On such a surface the *chemisorption* of hydrogen should occur with a minimum of activation energy. Sherman and Eyring calculated that with two carbon atoms in a surface the minimum would be found at about 3.6 Å. Similar calculations on the adsorption of hydrogen by nickel were carried out by Okamoto, Horiuti, and Hirota (16). The actual magnitudes of the calculated activation

energies are certainly much too high, but the factor of geometry is well established from these theoretical studies.

Direct proof of the influence of lattice spacing on the velocity of reactions at surfaces emerges from the studies of Beeck and his co-workers (17). These workers studied the influence of evaporated metal films on the velocity of hydrogenation of ethylene. The initial studies showed that evaporation of nickel from a heated nickel wire yielded a randomly oriented film of nickel. When the evaporation was effected in presence of a few millimeters pressure of an inert gas such as nitrogen, the film formed was definitely oriented. In the case of nickel it was found that the (110) plane of the nickel was parallel to the glass walls on which the film was deposited. This plane is actually the least densely packed plane of nickel, which is a face-centered cubic crystal. With iron, which is body-centered, evaporation in an inert atmosphere again gave the least densely packed plane—in this case the (111) plane—parallel to the glass backing.

Such nickel films have an extraordinarily high activity for the hydrogenation of ethylene. Experiment showed that per unit surface of nickel the oriented nickel film was some five times more active in the hydrogenation process than the randomly oriented nickel. Since the oriented film shows the (110) plane in preferred amount, it appears natural to associate the activity in the reaction with the lattice dimensions of this plane and probably with the longer dimension in the plane, with Ni–Ni distances of 3.5 Å.

Further support for this point of view arose from an extension of these studies to other face-centered cubic metals evaporated as films on glass surfaces. The activity was found to be extraordinarily sensitive to the lattice dimension in a manner suggesting that the critical dimension was close to that obtained in the lattice of rhodium. Subsequent test confirmed this conclusion as shown in the accompanying diagram (Fig. 5) in which the *logarithm* of the velocity is plotted as a function of the lattice parameter. Rhodium shows the most rapid rate of reaction by about one order of magnitude over palladium, its nearest competitor.

While it was at first believed that this influence of lattice parameter might be associated with the activation energy of adsorption of hydrogen, experiment showed that chemisorption of hydrogen on such films was rapid even at liquid-air temperatures. Measurements of heats of adsorption showed that the adsorbed hydrogen at $-183°$ and 0°C. forms a mobile film with initial heats of adsorption of 30 kcal. per mole on a bare surface, decreasing to 18 kcal. per mole when the monolayer is complete. With ethylene, the initial heat of adsorption is 60 kcal. per mole, the process

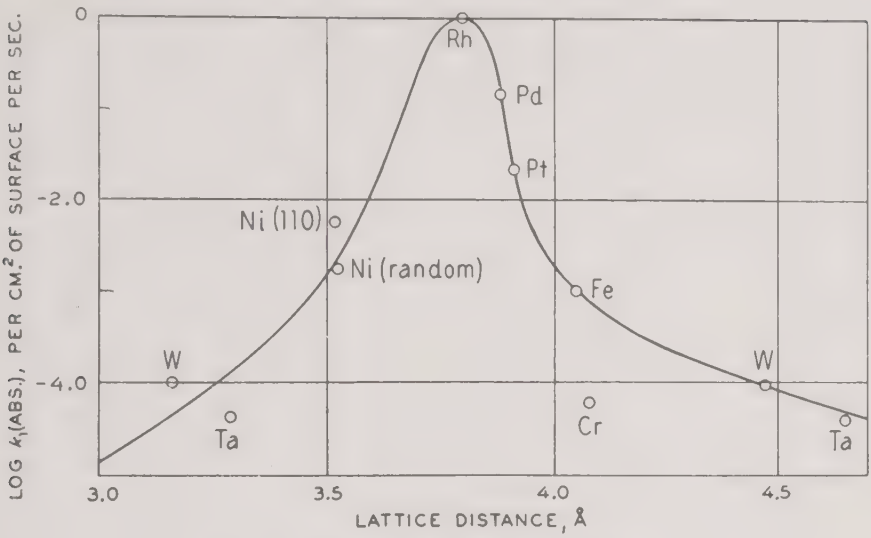

Fig. 5. Activity *vs.* lattice distance, 0°C.

being complicated by dissociation of the ethylene into acetylenic *residues* and adsorbed hydrogen atoms. This leads to selfhydrogenation with evaporation of ethane and retention on the surface as a poison of acetylenic residues.

Since the kinetics of the hydrogenation of ethylene on the surface is independent of ethylene pressure and first order with respect to hydrogen, Beeck finally concluded that the surface available for the hydrogenation step must be proportional to the hydrogen pressure and inversely proportional to the ethylene pressure; the kinetic expression becomes:

$$+ d[C_2H_6]/dt = k[C_2H_4] \times [H_2]/[C_2H_4] = k[H_2]$$

This requires that the acetylenic complexes which are capable of poisoning the reaction are removed from the surface by hydrogenation and it is the rate of this removal which determines the rate of reaction. It is in this slow, rate-determining, second hydrogenation process, and not in the fast hydrogenation which gives the reaction product, that the crystal parameter effect must be operative. In support of this point of view experimental measurement of the rate of removal of preadsorbed acetylenic complexes by hydrogen on nickel and rhodium surfaces indicated that several hours were required to clean 20% of a nickel surface whereas, with rhodium, 80% could be cleaned in a few minutes.

Beeck calls attention to the fact that the activation energy for the reaction, which must be the activation energy of the slow rate-controlling hydrogenation, is the same (10.7 kcal.), not only for oriented and non-

oriented nickel films but also for iron, platinum, palladium, and rhodium; these measurements cover about a thousandfold range in the rate constant. This leads to the conclusion that the rate differences are to be located in the so-called temperature-independent term, A, in the empirical Arrhenius equation: $k = Ae^{-E/RT}$. Modern analysis of this factor A recognizes that it corresponds in part to an entropy factor and can be called an entropy of activation. It is known that steric factors and/or *active centers* will be important terms in such entropies. The experimental evidence, however, indicates that an important item in the A term is actually the fraction of the total available surface on which, under the experimental conditions, the slow hydrogenation step occurs. Evidence seems to indicate that it may be as low as 10^{-3} to 10^{-4} in the case of nickel, and 10^{-1} to 10^{-2} in the case of rhodium.

Brunauer and Emmett (18) have sought also to interpret the chemisorptions of hydrogen on synthetic ammonia catalysts in terms of the crystal faces on which the gas is adsorbed. Differences in chemisorption of hydrogen characterized as Type A and Type B are associated with chemisorption on the outermost iron atoms in the case of Type A and on the second layer of iron atoms which are accessible in the less dense (100) and (111) crystal faces of iron. With respect to the chemisorption of carbon monoxide at −78°C. on iron they suggest that, "because of the very dense packing of iron atoms in the (110) plane, it is necessary to assume that two iron atoms are required for the chemisorption of a carbon monoxide molecule, whereas one iron atom is sufficient in the (100), (111), or (211) planes. The influence of sintering on the ratio of the two types of hydrogen chemisorption, on the ratio of the two types to carbon monoxide chemisorption and on the ratio of chemisorbed nitrogen to physically adsorbed nitrogen required to form a monolayer is, in every case, consistent with an assumption that the (110) planes preferentially increase on sintering."

In an earlier contribution the author described in detail the results of studies of hydrogen and deuterium isotopes in the reduction of carbonyl compounds (19), with especial reference to the direct reduction of acetone to propane on pure platinum catalysts. Isopropyl alcohol is reduced much more slowly than acetone on such catalysts. Platinum catalysts to which iron has been added in the course of the preparations give, on the other hand, the usually anticipated isopropyl alcohol. The direct production of propane from acetone was associated with an activated state in which the C—O bond was sufficiently stretched to permit the entry of two hydrogen atoms with formation of propane, which evaporates leaving oxygen on the

surface to be removed by reduction and formation of water. It was suggested by examination of the lattice parameters and a molecular model of the acetone molecule that, in the case of platinum, the lattice parameter is very favorable to such a concept.

Twigg and Rideal (20) utilized the results on deuterium exchange reactions with olefins, together with the ideas of Beeck, Smith, and Wheeler (17), to analyze the relation between molecular structure and catalyst geometry. They concluded that adsorption of the olefin occurred by opening of the double bond and attachment of the two carbon atoms to two nickel atoms. They calculated that this mode of attachment involved very little distortion of the adsorbed molecule. From a discussion of the effect of interatomic spacing of the catalyst atoms they concluded that this was an important factor in the hydrogenation of double bonds where two-point contact was involved. The recent work of Beeck cited previously (17) would indicate that the slow process is not hydrogenation of ethylenic linkages but rather the hydrogenation of poisonous acetylenic residues.

Qualitative calculations were also made by Twigg and Rideal of the interactions between neighboring adsorbed olefin molecules. They showed that, especially on the (110) crystal plane, there is little or no interaction between adsorbed molecules. Ethylene should therefore cover the whole catalyst surface. With the higher olefins, even in the case of propylene with only one substituent methyl group, there will be considerable interaction between the adsorbed molecules such that, even on the (110) plane, the whole surface could not be covered. Twigg and Rideal tested for extent of bare surface by following the equilibration reaction: $H_2 + D_2 \rightleftharpoons 2\,HD$, in the presence of ethylene, isobutylene, and trimethylethylene. The experimental evidence obtained indicated that ethylene covers the whole surface at temperatures up to 160°, beyond which temperature bare spots arise. With trimethylethylene at 160° the equilibration reaction proceeds very fast, indicating that the surface is considerably bare. With isobutylene at temperatures as low as 84° equilibration of hydrogen and deuterium is relatively fast, indicating again that methyl-substituted ethylenes are unable completely to cover the whole catalyst surface. In the light of Beeck's studies one is forced to ask whether these conclusions can be wholly ascribed to geometry or whether the rate of a slow rate-determining removal of a poison might not dictate the equilibration results obtained.

Herington and Rideal (21) have recently addressed themselves to the interesting question of geometry in the poisoning of metal catalysts. There are several interesting cases of selective and progressive poisoning which have been recorded in the literature and which were used by the

writer in support of his original concept of active centers on catalyst surfaces. Thus, Vavon and Husson (22) noted that successive additions of carbon disulfide to a hydrogenation catalyst rendered it inactive for the hydrogenation of acetophenone (0.4 mg. of carbon disulfide), for cinnamic acid (0.5 mg.), nitrobenzene (0.8 mg.), and benzene (1.1 mg.). Kubota and Yoshikawa (23) found that nickel could be poisoned by thiophene for the hydrogenation of benzene, the catalyst being still active for the hydrogenation of phorone. They suggested in a second paper that there are three sites on a nickel surface specific for ethylene, benzene, and nitrobenzene, respectively, which could be poisoned by ethyl sulfide, thiophene, and hydrogen sulfide. Maxted and his co-workers have made numerous studies of poisoning of platinum catalysts (24). While Maxted's poisoning studies indicate mainly a linear poisoning effect, certain cases showing breaks in a linear curve point to the possibility of two sites.

Herington and Rideal (21) set out to show that much of the data on progressive poisoning which suggests *active centers* on heterogeneous surfaces of catalysts can be reinterpreted on the basis of a set of uniform catalyst sites. With such a uniform set of sites the nature of the poisoning would be dependent on the number of contact points between reactant and poison and the catalyst surface. When reactant and poison both occupy single sites the relationship between activity and poisoning is linear; when the poisoning becomes 100 per cent the activity is zero. The curve for two-point contact deviates slightly from the linear in the direction of increased poisoning for a given percentage of the poison required for complete suppression of reaction. With seven-point contact of reactant the deviation from linearity is strongly emphasized, the amount of adsorbed reactant falling steeply with relatively small percentages of poison employed. Qualitatively these results are in agreement with many of the observations. They must, however, be only a first approximation since the study only concerns itself with one crystal face and the evidence is definite that several faces have activity. There is a classical example of poisoning reported by Pease and Stewart (25), which was cited by the writer in his first discussion of poisoning and active centers, namely, the extraordinary efficacy of carbon monoxide as a poison in the hydrogenation of ethylene on copper. In this reaction and its poisoning it is difficult to think of more than two-point contact of either ethylene or the poison. And yet, expressed in modern terms, Pease and Stewart found that 0.05 cc. of adsorbed carbon monoxide which could cover less than one per cent of the total surface, destroyed 90 per cent of the normal reactivity of the surface. Such a result would be hard to bring within the framework of the Herington-Rideal treatment.

What is definitely true in the considerations which Herington and Rideal raise is that the more highly organized the association between reactant and surface, the more vulnerable this association is to the effect of poisons. Another aspect of this same topic is that the more highly organized the reactant and surface are, the more specific will be the chemical effects which emerge from their interaction. This is clearly at the heart of the problem of biological specificity. In biological systems we are dealing with highly organized systems reacting in the presence of other highly organized systems such as enzymes, bacteria, and the like. It is here that the *lock-and-key* concept of Ehrlich may be applied which Pauling (26) has recently reemphasized, with appropriate experimental material, and with the thesis of structural complementariness to account for serological specificity. As Pauling has pointed out in a recent address, "the phenomenon of specificity so common in biology, is rare in chemistry," with the sole exception of crystallization to which we referred in the opening paragraphs. It is, however, in surface catalysis, and especially with the more highly organized organic chemicals as reactants, that we should expect to find and do find the most cogent examples of specificity in chemistry. It may well be, however, that even in the most complex cases of organization among the reactants that the minor variations in the surfaces (*e.g.*, lattice parameters, crystal faces) are so minor as virtually to eliminate most of the specificity from the event. That nickel, copper, rhodium, palladium, and platinum cause the rapid hydrogenation of ethylene, whereas copper is ineffective in the low-temperature hydrogenation of benzene is one evidence of specific behavior that can be correlated with structural organization. As against this paucity in chemical phenomena the examples of biological specificity are numerous. As Pauling has pointed out, the number of examples in which biological specificity and structural similarity have been established is increasing continuously. As an example of physiological activity he cites the antipyretic-antineuralgic activity of 4-isopropylantipyrine and that of 4-dimethylaminoantipyrine (pyramidon) to be associated with the similarity in size and shape of the isopropyl and dimethylamino groups. In enzymatic activity the activated complex is probably the substrate molecule in a strained configuration, the strain arising from the association of substrate and enzyme due to a complementariness in each. Chemotherapeutic agents may be said to "exercise their activity by acting as inhibitors to an enzyme action through competition with an essential metabolite of similar structure." Pauling cites the bacteriostatic action of sulfanilamide which results from an inhibitory competition with *p*-aminobenzoic acid . . . "The metabolite and inhibitor are closely related

in molecular shape, differing in the replacement of a carboxyl group by a sulfonamide group." A further illustration of Pauling's is the inhibition of thiamin by pyrithiamin; the competition between a five-membered ring containing sulfur and six-membered rings not containing sulfur—as shown by the formation of solid solutions by thiophene and benzene—is the suggested structural interpretation.

A further avenue of exploration of the significance of molecular geometry in the field of reaction mechanism has been developed recently in researches of Johnson and Eyring on the kinetic characteristics of luminescent processes (27). Here again we are dealing with biological systems in which a high degree of organization of the reactant and catalyst is an essential element in the problem. The approach is again through absolute rate theory of chemical reactions which formulates a rate process in terms of an equilibrium between an activated complex and the reactants. From the abnormal variation of the luminescent processes with temperature (maximum in luminescence is between 20° and 30°C.) and with pressure (luminescence is very sensitive to much smaller ranges of pressure, 1 to 700 atmospheres, than are significant in reactions between small molecules), interesting conclusions can be drawn as to the nature of the intermediate complex. Thus, from the pressure coefficient of the reaction it can be deduced that in the transition from the normal to the activated state of the reaction there is a molal volume change as large as 64 cc. The magnitude of this change suggests that a protein is involved which undergoes a denaturation resulting in a volume increase, and that high pressure represses this denaturation—to a large degree because of the large molal volume increase involved. The equilibria involved are sensitive to hydrogen ion concentration, the variations in equilibrium paralleling the variations in luminescence intensities. Poisons such as sulfanilamide, urethan, and alcohol influence the luminescent intensities. Sulfanilamide acts on luminescence in a manner very much like that of hydrogen ions at acidities between *p*H 4 and *p*H 6.5. The sulfanilamide equilibrium with the enzyme involves one inhibitor molecule to one enzyme molecule. Urethan and alcohol act in a manner that promotes the breaking of the types of bonds that are broken in both the reversible and irreversible denaturation. They, therefore, promote the irreversible denaturation and so affect luminescence as a function of time, whereas with sulfanilamide inhibition remains constant with time. These processes are, therefore, extraordinarily suggestive as to the mechanism of activation in highly organized materials such as the proteins. They merit, and are receiving, further and more extensive study.

V. Geometry in Homogeneous Liquid Systems

Reactions in homogeneous liquid systems in general involve relatively small molecules where the influence of molecular geometry on mechanism is less readily demonstrable except in those cases of isomerism that have already been specifically excluded from the range of our observations. There is, however, one area of observations in which it has been suggested that molecular geometry of the reactants in a homogeneous system may be responsible for the reactions achieved. We refer to a set of hydrocarbon reactions involving alkenes in which the processes that may occur include isomerization, polymerization, alkylation, and hydrogen isotope exchange reactions. All these apparently diverse reactions have a feature in common which is that the processes are all accelerated by the same series of catalysts. These catalysts include sulfuric and phosphoric acids, sulfonic acids, perchloric acid, hydrofluoric acid, but not strong acids like hydrochloric or trichloroacetic acid. Some of these materials, when spread on suitable supports, will reproduce in a heterogeneous system the same reactions which occur homogeneously. Phosphoric acid on various supports can be so employed. Phosphates, sulfates of copper and aluminum, moist aluminum chloride, as well as nickel and lime, are among the agents listed for securing these reactions in heterogeneous systems.

Explanation for these reactions of hydrocarbons in homogeneous systems has been sought in several directions. A prototropic mechanism due to Whitmore can be illustrated in the case of isomerization by the following mechanism:

$$CH_3CH_2CH{=}CH_2 \xrightarrow{H^+} [CH_3CH_2CHCH_3]^+ \xrightarrow{-H^+} CH_3CH{=}CHCH_3$$

A mechanism involving ester formation, sponsored by Ipatieff, can be illustrated thus:

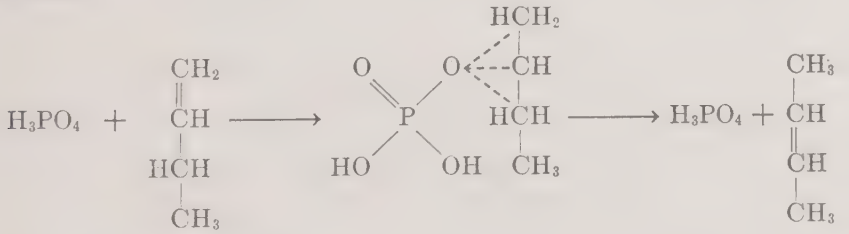

This involves an ester linkage and the transfer of a hydrogen to the α-carbon in 1-butene and withdrawal of a hydrogen from the γ-carbon in the same molecule to achieve the isomerization of 1-butene to 2-butene. With

respect to such prototropic and ester mechanisms one might ask why the strong acids such as hydrochloric and trichloracetic acids are not effective.

Turkevich and Smith (28) seek an explanation for all these reactions on a basis which may be illustrated by the case of sulfuric acid. Concentrated sulfuric acid such as is used is not to be regarded as a proton-yielding agent. Instead, it must be thought of as a tetrahedral molecule, 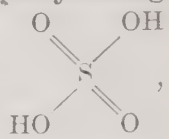 , whose parameters are such that they are geometrically suited to simultaneous acceptance of a hydrogen from an α-carbon and withdrawal of a hydrogen from a γ-carbon atom in the hydrocarbon molecule. Schematically, the postulated mechanism can be illustrated thus:

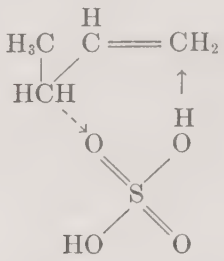

Alkylation, polymerization, and the isotope-exchange process can be similarly formulated in terms of a similar simultaneous switch of hydrogen atoms on the hydrocarbon and the sulfuric acid molecules. Turkevich and Smith emphasize that perchloric, phosphoric, and sulfonic acids share this same tetrahedral geometry with compatible lattice parameters and that hydrofluoric acid, as HFFH, can act similarly. Moist aluminum chloride also conforms in the tetrahedral structure of $HAlCl_4$. It is of interest also to note in this connection that it has been found by Twigg (29) that the isomerization of alkenes on nickel surfaces proceeds when the surface is partly covered by hydrogen and not in the absence of this adsorbed gas. One may speculate that on the various contact surfaces a similar switch of hydrogen atoms is responsible for the reaction.

A comparison of the rates of exchange and isomerization by Turkevich and Smith using tritium phosphoric acid and by Farkas (30) using deuterophosphoric acid indicates that these two reactions occur at similar rates, the activation energies differing by small amounts which might well be accounted for by zero-point energy differences. Farkas gives a detailed discussion of mechanism, along the lines of the ester mechanism of Ipatieff, with modifications suggested by his work with the deuterium exchange.

It is perhaps of significance that one of the intermediate stages, III, suggested by Farkas to account for his observations on the exchange reaction is virtually identical with the intermediate step involved in the hydrogen switch of Turkevich and Smith. The latter postulate does not involve, however, any P—O—C ester bond such as was included in the Ipatieff mechanism.

We are at the beginning of an era in which, since the actual shapes and sizes of molecules have acquired a large degree of reality in the scientific consciousness, the problems of mechanism in chemical and biological systems will be referred back more and more frequently to the actual molecular architecture and the energies of atoms and molecules in the given geometrical configurations. It is both an old and a new area of activity which invites continuously new thoughts from fresh minds.

References

1. Brown, J. C., *History of Chemistry*. Blakiston, Philadelphia, 1920.
1a. Heitler and London, *Z. Physik.*, **44,** 455 (1927). London, in P. Debye, *Probleme der modernen Physik*, Hirzel, Leipzig, 1928, p. 104; *Z. Elektrochem.*, **35,** 552 (1929).
2. For such details consult Glasstone, Laidler, and Eyring, *The Theory of Rate Processes*. McGraw-Hill, New York, 1941.
3. Raschig, *Z. angew. Chem.*, **19,** 1748 (1906).
4. Boeseken, *Rec. trav. chim.*, **45,** 458 (1926).
5. Bodenstein, *Ann.*, **440,** 177 (1924).
6. Burk, *J. Phys. Chem.*, **30,** 1134 (1926).
7. Balandin, *Z. physik. Chem.*, **B2,** 289 (1929); **B3,** 167 (1929).
8. Taylor, *J. Am. Chem. Soc.*, **60,** 627 (1938).
9. Kistiakowsky, *ibid.*, **58,** 137, 146 (1936).
10. Lazier and Vaughen, *ibid.*, **54,** 3080 (1932).
11. Balandin, *Acta Physicochim., U. R. S. S.*, **14,** 223 (1941).
12. Long, Frazer, and Ott, *J. Am. Chem. Soc.*, **56,** 1101 (1934).
13. Ipatieff, Corson, and Kurbatov, *J. Phys. Chem.*, **43,** 589 (1939). Corson and Ipatieff, *ibid.*, **45,** 431 (1941).
14. Emmett and Skau, *J. Am. Chem. Soc.*, **65,** 1029 (1943).
15. Sherman and Eyring, *ibid.*, **54,** 2661 (1932).
16. Okamoto, Horiuti, and Hirota, *Sci. Papers Inst. Phys. Chem. Research Tokyo*, **29,** 223 (1936).
17. Beeck, Smith, A. E., and Wheeler, *Proc. Roy. Soc. London*, **A177,** 62 (1940). Beeck, *Rev. Modern Phys.*, **17,** 61 (1945).
18. Brunauer and Emmett, *J. Am. Chem. Soc.*, **62,** 1732 (1940).

19. Taylor in *Frontiers in Chemistry*, Vol. III. Interscience, New York, 1945, p. 19.
20. Twigg and Rideal, *Trans. Faraday Soc.*, **36,** 533 (1940).
21. Herington and Rideal, *ibid.*, **40,** 505 (1944).
22. Vavon and Husson, *Compt. rend.*, **175,** 277 (1921).
23. Kubota and Yoshikawa, *Sci. Papers Inst. Phys. Chem. Research Tokyo*, **3,** 33, 223 (1925).
24. Maxted *et al.*, *J. Chem. Soc.*, **1921,** 225; **1934,** 26; **1935,** 393; **1938,** 2070; **1940,** 469.
25. Pease and Stewart, *J. Am. Chem. Soc.*, **47,** 1235 (1925).
26. Pauling, George Westinghouse Centennial Address, see *Chem. Eng. News*, **24,** 1375 (1946).
27. See Johnson, Eyring, Steblay, Chaplin, Huber, and Gherardi, *J. Gen. Physiol.*, **28,** 463 (1945), for a comprehensive report and bibliography.
28. Smith, R. K., *Thesis*, Princeton University, 1944.
29. Twigg, *Trans. Faraday Soc.*, **35,** 934 (1939).
30. Farkas, A., and Farkas, L., *Ind. Eng. Chem.*, **34,** 716 (1942).

II. *Dipole Moment, Resonance and Molecular Structure*

CHARLES P. SMYTH

Princeton University, Princeton, New Jersey

I. Introduction

IT IS THE PURPOSE OF THIS CHAPTER to review briefly the uses of the dipole moment in investigating the structure of matter and to describe in some detail the use of dipole moments in certain recent investigations of resonance in unsaturated aliphatic compounds. In the general review, only those examples will be discussed which may seem desirable as illustrations of the phenomena under consideration; in the more detailed description, material that is less significant or not particularly pertinent is commonly omitted. The bibliography does not attempt completeness, but should provide the reader with an amplification and continuation of the subject matter.

II. The Molecule as an Electric Dipole

The molecule as an electric dipole may be illustrated by an oversimplified view of the hydrogen chloride molecule. The chloride ion is a symmetrical distribution of negative electricity about a positive nucleus and, because the total negative charge exceeds the positive by a single electronic charge, may at a sufficient distance be regarded as a single negative charge acting at the ionic center, the nucleus. The attachment of a hydrogen ion to this structure to give a hydrogen chloride molecule forms an electric dipole, the positive end of which coincides with the hydrogen ion

and the negative end, with the chlorine nucleus. The size of the dipole is determined by the dipole moment, μ, a vector quantity, which is the product of either of the two equal but opposite charges, 4.80×10^{-10} e.s.u., and the distance between them, found from the infrared spectrum of hydrogen chloride to be 1.28×10^{-8} cm., that is, $\mu = (4.80 \times 10^{-10}) \times (1.28 \times 10^{-8}) = 6.14 \times 10^{-18}$. Since 10^{-18} is often called a debye unit, the moment calculated for this oversimplified structure is 6.14 debye units, or, for the sake of brevity, 6.14, a value nearly six times as large as the experimental value, 1.04, obtained from the measurements of the dielectric constant of the vapor over a range of temperature. This discrepancy was explained in a semiquantitative fashion (1,2) by a rough calculation of the distortion of the electronic distribution of the chloride ion by the attraction of the positive charge of the hydrogen ion, which displaces the center of gravity of the negative charges so far toward that of the positive as to shorten the axis of the dipole by an amount sufficient to reduce the moment to 1.04. A less approximate calculation (3) of the charge distribution led to a value of 1.15 for the moment.

An approach to the problem quite different from the easily visualized one of ionic distortion is that of resonance. According to this concept, the structure of the hydrogen chloride molecule is described (4) as a linear combination of the undistorted ionic structure, H^+Cl^-, for which the moment (6.14) has just been calculated, and a purely covalent structure, H—Cl, to which a zero moment is somewhat arbitrarily assigned. The hydrogen-chlorine bond is then said to possess a fractional amount of ionic character, which may be calculated as the ratio of the observed moment to the moment calculated for the purely ionic structure, or $1.04/6.14 = 0.17 = 17\%$. The remaining 83% of the bond character is, accordingly, covalent.

III. Experimental Determination of Dipole Moments (2,5)

The dielectric constant, ϵ, of a substance is measured by determining the capacity, C_0, of an empty condenser and the capacity, C, of the same condenser filled with the substance in question. Then $\epsilon = C/C_0$. The capacity is usually measured by the substitution method with high-frequency heterodyne or resonance circuits, which are capable of high precision, or in some cases with a capacity bridge. The dipole moment of a molecule may be calculated from measurements of the dielectric constant of a vapor by the Debye equation (6,7):

$$\frac{\epsilon - 1}{\epsilon + 2}\frac{M}{d} = \frac{4\pi N}{3}\alpha_0 + \frac{4\pi N}{3}\frac{\mu^2}{3kT}$$

in which ϵ is the dielectric constant, M is the molecular weight, d is the density, $N = 6.023 \times 10^{23}$ (the Avogadro number), α_0 is the molecular polarizability, μ is the dipole moment, $k = 1.38 \times 10^{-16}$, the Boltzmann constant, and T is the absolute temperature.

This may be written in the form:

$$P = a + b/T$$

in which the molar polarization $P = (\epsilon - 1)M/(\epsilon + 2)d$, where $a = 4\pi N\alpha_0/3$, which (as an approximation) may be replaced by the molar refraction for the D sodium line, $R_D = (n^2 - 1)M/(n^2 + 2)d$, where n is the refractive index and $b = 4\pi N\mu^2/9k$.

Measurements over a range of temperatures give a straight line when P is plotted against $1/T$. The dipole moment may then be calculated from the slope, b, of this line. Commonly, the measurements are simplified by the replacement of a by the molar refraction, which permits the moment to be calculated from measurements at a single temperature, although, with vapors, the measurements are extended over as wide a temperature range as may be conveniently employed.

Polar liquids or solids are measured in solution in a nonpolar liquid, such as benzene, in order to reduce the often large effects of molecular interaction. The polarization, P_{12}, of the solution is then assumed to be given by the equation:

$$P_{12} = \frac{\epsilon - 1}{\epsilon + 2}\frac{c_1M_1 + c_2M_2}{d} = c_1P_1 + c_2P_2$$

in which c represents mole fraction and the subscripts refer to the nonpolar component, 1, and the polar component, 2. The dielectric constant, ϵ, and the density, d, are measured for several solutions and the corresponding value of P_2 is calculated by means of the above equation, P_1 being assumed to be constant. The values of P_2 are plotted against c_2 and extrapolated to $c_2 = 0$ to obtain P_∞, the polarization at infinite dilution, which differs from that in the gaseous state only by a small amount because of the effect of the solvent–solute interaction, called the *solvent effect*, and may, therefore, be used to calculate the moment. The extrapolation may also be carried out by means of empirical equations (8,9). The solvent effect depends upon the shapes and polarizabilities of the molecules involved (10,11,12), but causes a change in the apparent moment value, compared with the value found for the gas, of about -12 to $+5\%$, a small decrease being the commonly observed effect. Because of this effect, measurements in the vapor state are preferable, but, for structural considerations involving

arge differences in moment or small differences between rather similar molecules, the much simpler and more generally used solution measurements are adequate.

IV. Use of Dipole Moment to Determine Geometrical Structure

The simplest example of the use of a dipole moment in the approximate solution of a structural problem is demonstrated in the determination of the structure of the water molecule. At a time when the water molecule was regarded as a symmetrical linear structure, H—O—H, and it was customary to expect valence bonds to be so arranged as to give maximum molecular symmetry, the determination of the moment of the water molecule showed it to be unsymmetrical (1). Another simple example was the discovery (13) that *cis*-dichloroethylene had a moment of 1.9, although the *trans* form had zero moment, corresponding to the symmetrical planar structure written for it by the organic chemist:

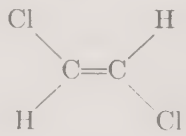

At a time when the organic chemist, though occasionally formulating a more intricate geometrical structure, was generally content with the Kekulé structure for benzene easily written on a sheet of paper, the physical chemist, misled by overoptimistic interpretations of x-ray analyses, formulated a puckered structure for the ring, with the atoms attached to the ring pointing alternately upward and downward from the ring. The measurement of the dipole moments of simple substituted benzenes indicated (13–16) the correctness of the plane Kekulé model, an indication subsequently confirmed by electron diffraction and further x-ray measurements. The method of reaching this conclusion regarding the structure of benzene illustrates the use of the dipole moment as a vector and some of the difficulties of the method. The moments observed for chlorobenzene and the three dichlorobenzenes in solution are given in Table I, together with the values calculated for the plane hexagonal models of the three dichlorobenzenes, on the assumption that each C—Cl bond has associated with it a dipole moment equal to that of monochlorobenzene and acting in the direction of the bond. The observed values given are the values measured in solution, about 10% lower than the values later obtained in the vapor state.

TABLE I

DIPOLE MOMENTS (IN DEBYE UNITS) OF CHLOROBENZENES, MEASURED IN BENZENE SOLUTION (16)

Compound	Observed	Calculated
C_6H_5Cl	1.56	—
o-$C_6H_4Cl_2$	2.25	2.70
m-$C_6H_4Cl_2$	1.48	1.56
p-$C_6H_4Cl_2$	0	0

The moment is calculated for each of the three dichlorobenzenes by means of the formula, $\mu = 2 \times 1.56 \cos \theta/2$, where θ, the angle between the two dipoles, is 60° for the ortho compound, 120° for the meta, and 180° for the para. The puckered model would also have zero moment for the para compound, but a value approximately double the observed value for the meta, and an approximately zero value for the ortho in contrast to the large observed value. The puckered ring was thus eliminated from consideration, as were certain other structures which had been suggested for the benzene ring. The moments of other substituted benzenes and naphthalenes led to the same conclusion.

The discrepancy between the observed and calculated values of *o*-dichlorobenzene is typical of what happens when two dipoles are in close proximity and may be attributed (17) to the lowering of each of the two component dipole moments by the inductive action of the other. This illustrates the point that the dipole moment associated with a bond or group may be altered by the molecular environment. The effect here is one of induction, but resonance may often play an important part. The association of a dipole moment with a particular bond is a useful concept and, in the case of a diatomic molecule like hydrogen chloride, a relatively simple one, but, in polyatomic molecules, the value assigned to a bond moment is a somewhat arbitrary and often variable quantity. The bond moment is valuable in throwing light on the relative electronegativities of the bonded atoms, in interpreting the nature of the bond in the terms of resonance which have been applied to the discussion of the hydrogen chloride molecule, and in drawing conclusions as to geometrical structure, but, except for the simplest molecules of known structure, cannot be calculated with any approach to accuracy. For the calculation of the moment that a particular molecular structure should have, the group moment (18), which is the resultant of the moments of one or more bonds

within a group of atoms and the secondary moments arising in the rest of the group, is more valuable. For the treatment of the structures of the dichlorobenzenes, the moment of monochlorobenzene was taken as the group moment of chlorine linked to phenyl. The group moment of chlorine linked to alkyl is 0.4 higher, a difference which was not understood until an explanation was offered in terms of resonance (19).

V. Movable Dipoles and Restricted Rotation

The majority of the calculations of molecular dipole moments from bond or group moments, and all of those so far discussed in this chapter, treat the bond or group moments as fixed vectors, the resultant of which is the molecular moment. In the two dichloroethylenes, the moment vectors are fixed by the rigidity of the double bond, but, in ethylene dichloride, rotation of the $—CH_2Cl$ groups around the single C—C bond between them can place the two principal C—Cl dipoles in a great variety of positions relative to one another. For molecules containing two equal dipoles of moment, m, each making an angle, θ, with an axis about which both are free to rotate without restriction, the molecular dipole moment, μ, was calculated (20) as $\mu = \sqrt{2}\, m \sin \theta$.

When the molecule contains more than two dipoles which are free to rotate, or more than one axis of rotation between two dipoles, the averaging of the moments over all possible directions in which they might point in space becomes more complicated. The problem was investigated jointly and the results of the investigation published separately (21,22). It was assumed that, when rotation occurred around an axis, all positions attainable by such rotation were equally probable. Equations derived for the resultant moments, μ, of certain types of molecules are given below as illustrations. In the equations, the moments acting in the indicated bond directions are represented by m, the carbon valence angle by θ, and the oxygen valence angle by α:

$Br(CH_2)_nBr$, m_1 = C—Br,
$$\mu = m_1[2 - 2\,(-\cos\theta)^n]^{1/2}$$

$CH_2BrCHBrCH_2Br$, m_1 = C—Br,
$$\mu = m_1(3 + 4\cos^2\theta + 2\cos^3\theta)^{1/2}$$

$HO(CH_2)_2OH$, m_2 = C—O, m_3 = H—O,
$$\mu = [2(m_2^2 + m_3^2 - m_2^2\cos^2\theta - m_3^2\cos^2\alpha\cos^2\theta + 2m_2m_3\cos\alpha\sin^2\theta)]^{1/2}$$

A general equation was derived at the same time for the resultant of such a set of movable vectors, which can best be stated in words. For free rotation

about connecting lines, the mean square sum of n vectors is equal to the sum of the squares of the lengths of the separate vectors, plus twice all the possible products of the lengths of two vectors multiplied by the product of the cosines of the angles made by the directed lines connecting the pair (21). It will be seen that the above equations are specific examples of this rule. When $n = 2$ for a polymethylene bromide, the equation for this series becomes identical with that shown for a molecule with two equal dipoles rotating around a single axis, *e.g.*, ethylene dibromide.

When freedom of rotation around the bonds between the dipoles is unrestricted, or when several bonds of somewhat restricted freedom intervene between the dipoles, the equations give satisfactory agreement between the calculated and the observed moments and can be very generally used. Thus, the moment calculated for decamethylene bromide is 2.69 and the observed value is 2.56, the moment calculated for ethylene glycol is 2.1, as compared with an observed value of 2.0, the differences in both cases being no greater than the uncertainties in the bond moment values (22). However, in ethylene dibromide, the calculated moment is 2.0, while the observed values vary from 0.8 to 1.05, increasing with rising temperature.

It was shown (23,24) that, in molecules like the ethylene dihalides, repulsion between the two dipoles was at a maximum when they were on the same side of the axis of rotation in a *cis* position, which would give maximum resultant moment, and at a minimum when they were opposite one another in a *trans* position, which would give zero moment. Consequently, the potential energy of repulsion would tend to force the dipoles into a *trans* position, but the thermal energy of the molecule would cause a rotational vibration through the *trans* position at the bottom of a potential energy trough. The *cis* position would then be at the top of a potential energy barrier over which sufficiently high thermal energy of rotational vibration could cause the dipoles to pass. Only when the thermal energy was so high as to give freedom of passage over the potential barrier could the simple equation be used with accuracy to calculate the resultant of the two dipole moments. Equations derived both from classical and from quantum mechanics (23–25) showed that repulsive potential energy would lower the resultant moment below the value calculated on the basis of complete freedom of rotation about the C—C bond and give rise to an increase of moment with rising temperature, which would increase the freedom of rotation by increasing the rotational energy. This dependence of moment upon temperature was observed for ethylene dichloride, ethylene chlorobromide, ethylene dibromide, diethyl succinate, and other molecules

(24,26,27) in which the freedom of rotation of two dipoles was hindered by repulsive forces. It was found also that the magnitude of the variation of moment with temperature was what would be expected from the heights calculated for the restrictive potential energy barriers. Development of our knowledge of interchange forces made possible a more comprehensive and less approximate calculation of the potential energy barriers and correlation with their effects upon dipole moments (28).

The dependence of certain dipole moments upon temperature gave definite evidence of the hindrance of rotation about single bonds in certain molecules and gave a clearer picture of what was occurring than could be obtained from the limited evidence available from other experimental methods of attack upon the problem. When the experimental data on dipole moments were used to calculate the heights of the potential barrier which had to be crossed in the complete rotation of a group around a bond, it was calculated that free rotation of the $—CH_2Cl$ group in ethylene dichloride was restricted by a potential barrier of 4 kcal. per mole, while the barrier in ethylene chlorobromide was 5, and that in ethylene dibromide, 6 kcal. per mole (29). Similar calculations from dipole measurements on ethylene cyanide (28) over a 180° range of temperature gave a potential barrier of 1.2 ± 0.5 kcal., over which the $—CH_2CN$ had to pass in order to rotate completely around the central bond to the other $—CH_2CN$ group, a result in better agreement with the value calculated from the intramolecular forces than was warranted by the basic assumptions. These barriers obtained from dipole moment measurements are of the same magnitude as those calculated from thermal measurements, 3 kcal. in ethane and propane, and 0.6–0.8 in propylene (30).

The restriction of rotation of groups within a molecule is not infrequently a factor in determining the molecular moment and, hence, the dielectric constant; the restriction of rotation of molecules in a solid or liquid may often have an important influence upon the properties of the material and, if the molecules are polar, upon its dielectric constant. The phase transitions which occur in the solid state when molecules acquire rotational freedom may be investigated by means of dielectric constant measurements when the molecules have dipole moments. When the molecules lose all rotational freedom, the second term of the Debye equation becomes zero and the dielectric constant drops to a low value, in the neighborhood of two. The energy changes involved are shown by specific heat measurements, but the mechanism is more evident in the dielectric constant measurements. The large body of evidence as to the effect of molecular rotation upon solid–solid transitions and melting given by dielec-

tric constant measurements cannot appropriately be treated here, but a few references are given (31–39).

VI. Dipole Moment as a Measure of Resonance

1. Ionic Character

If a bond is viewed as possessing a definite fraction of covalent character and a definite fraction of ionic character, the fractions may be calculated (4) from the bond moment, as in the case of the H—Cl bond discussed on page 24. Unless the bond is the only one in the molecule, the assignment of a value to it may be made inaccurate by the presence of other dipoles. In Table II the percentages of ionic character calculated from the

TABLE II

AMOUNTS OF IONIC CHARACTER OF BONDS CALCULATED FROM DIPOLE MOMENTS (4,40,43,44)

Bond	Bond moment, debyes	Ionic character, %	Bond	Bond moment, debyes	Ionic character, %
H—F	1.91	43	Pb—Cl	>4.1	>34
H—Cl	1.04	17	Pb—Br	>4.0	>31
H—Br	0.78	11	Pb—I	>3.4	>25
H—I	0.38	5	Na—I	4.9	35
Ge—Cl	>2.0	>19	K—Cl	6.3	47
Ge—Br	>2.2	>19	K—I	6.8	44
Sn—Cl	>3.1	>27			

dipole moments of the hydrogen halides measured (40,41) in the vapor state and of three alkali metal halides measured by the molecular beam method (42) are consistent with the differences in electronegativity of the bonded atoms. The same may be said of the less accurate fractions calculated from bond moments obtained as lower limits from the moments of organometallic molecules containing other bonds of more or less uncertain moment.

2. Aromatic Resonance

Because of the polarizabilities of the two molecules in the vicinity of the C—Cl bonds, *tert*-butyl chloride and chlorobenzene might be expected to have approximately equal dipole moments, but the vapor state value for the former is 2.13 (45) and that for the latter, 1.72 (46). In terms of the Kekulé formula, one can write two structures for chlorobenzene:

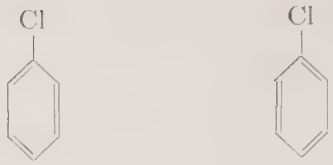

each of which should have a moment of about 2.13, residing largely in the C—Cl bond, with a positive charge on the carbon and a negative on the chlorine, but with small H—C bond moments and small secondary moments in the ring. However, in terms of the resonance theory, one can write, in addition, three less stable structures capable of making small but appreciable contributions to the structure of the molecule:

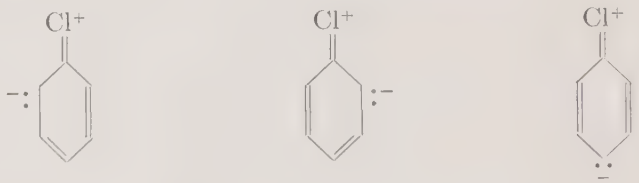

These structures arise through the shift of an unshared pair of electrons from the chlorine to the C—Cl bond, leaving a positive charge on the chlorine and causing an electron shift within the ring to put a negative charge on an ortho or para carbon. Because these three structures would have large dipole moments more or less opposite in direction to those of the two Kekulé structures, their contributions should decrease the moment of the molecule to a value below that expected for the Kekulé structures. The amount of the decrease, 0.41, may be used (43) to estimate the amount of the contribution of these three structures with the carbon-chlorine double bond to the structure of chlorobenzene in much the same way that the amount of ionic character in the H—Cl bond was calculated. Evidence of contributions from these structures is given by electron diffraction measurements, which show a shortening of the C—Cl bond, from the normal length for the single bond toward that for the shorter double bond (4). The total amount of the contribution of the three double-bonded structures is calculated from the C—Cl bond shortening to be 14%, while the moment lowering indicates the amount to be 3%. This discrepancy is larger than that usually encountered between the resonance contribution calculated from bond shortening and that calculated from dipole moment lowering, although the former method normally gives a higher result than the latter. As both methods of calculation are arbitrary and approximate in their assumptions, there is no reason why they should not differ quantitatively in their results.

In nitrobenzene, resonance elevates the moment above the values for the nitroparaffins, instead of lowering it. For this molecule, two Kekulé structures can be written with one oxygen of the nitro group negative, and two with the other negative, as in the following:

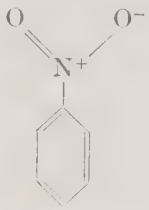

These structures should have a moment close to that of 2-nitro-2-methylpropane, 3.71; the observed value is 4.25, both values being measured in the vapor state (45–47). As in the case of chlorobenzene, structures can be written with a double bond between the ring and the attached group, but now the second electron pair comes from the ring:

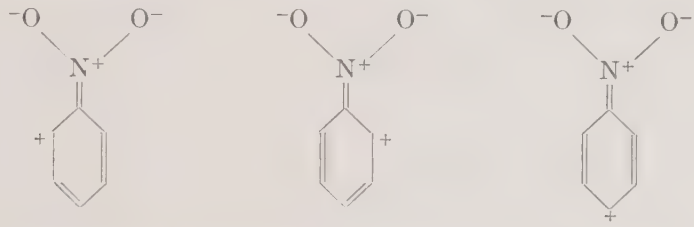

These structures would have large moments acting in the same general direction as those of the Kekulé model, so that small contributions from them are sufficient to give the large elevation of the moment, 0.54, above that of 2-nitro-2-methylpropane, which differs by no more than 0.01 or 0.02 from the values for nitroethane, 1-nitropropane, and 2-nitropropane (45).

The moments of *p*-chloronitrobenzene and *p*-fluoronitrobenzene are approximately 0.2 higher than the difference between the moment of nitrobenzene and that of the monohalogenated benzene, presumably because the presence of the nitro group increases the shift of negative charge from the halogen to the ring, thereby decreasing the ring-to-halogen moment and increasing the difference between the two opposing moments (46). A similar effect (4) is more pronounced in *p*-nitrodimethylaniline which has a moment value, measured in solution, of 6.87, whereas the solution values of dimethylaniline and nitrobenzene are 1.58 and 3.95, respectively. In the absence of additional resonance, the moment of dimethylaniline would not act in exactly the same direction as that of nitrobenzene, but, even if it did, the sum of the two moments would be

1.34 below the observed value. However, the contribution from the structure:

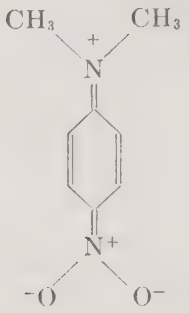

can easily account for the large increase in moment. In this structure, the unshared electron pair of the nitrogen is drawn into the double bond, as are the unshared halogen electron pairs in the molecules just discussed.

The resonating structures which raise the moment of nitrobenzene to a value 0.54 above that of 2-nitro-2-methylpropane impart so much double-bond character to the carbon-nitrogen bond that the two oxygens of the nitro group should lie in the plane of the ring. The moment value found in solution (48,49) for nitrodurene:

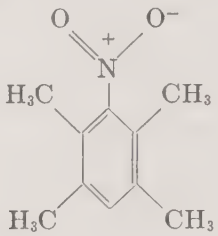

which is symmetrical as far as the two opposite pairs of methyl groups are concerned, is 3.39, in close agreement with the values found in the writer's laboratory for the nitroparaffins in benzene solution: 3.37 for 1-nitropropane, 3.41 for 2-nitropropane, and 3.45 for 2-nitro-2-methylpropane (50). The atomic dimensions are such that the adjacent methyl groups should repel the oxygen atoms when they are in the plane of the ring. It has been suggested that this repulsion forces the oxygen atoms out of the plane of the ring by twisting the nitro group around its bond to the ring, thereby destroying the double-bond character of the bond and eliminating the contributions of the polar structures, which are responsible for the elevation of the dipole moment above the values for the nitroparaffins. To put it in another way, the potential energy of repulsion increases the energies of the polar, double-bonded structures, thereby reducing their stabilities relative to the other structures and, consequently, the contributions which

they make to the structure of the molecule. The dipole moment is, therefore, practically the same as for the nitroparaffins.

The effect is even more striking in the case of *p*-aminonitrodurene.

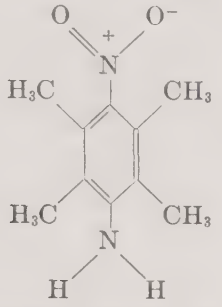

p-Aminonitrodurene

the moment of which measured (48) in solution is 4.98, as compared with 6.32 for *p*-nitroaniline. The value, 4.98, is almost identical with the sum, 4.99, of the solution values for aniline, 1.54, and 2-nitro-2-methylpropane, 3.45, and less than 0.2 more than the sum of the primary aliphatic amine moment and the nitroparaffin moment, pointing again to the elimination or reduction of the polar, double-bonded structures by steric repulsion.

These aromatic molecules have been discussed as examples of the effects of resonance because the symmetrical and fairly rigid structure of the benzene ring makes the effects stand out clearly. A fact not commonly mentioned in such discussions of resonance but implicit in them is that a bond written as, for example, the C—Cl bond in the Kekulé structures for chlorobenzene is the resultant of contributions from an ionic structure, C^+Cl^-, and a covalent structure, C—Cl, just as H—Cl was described in terms of resonance as the resultant of two forms, H^+Cl^- and H—Cl.

As a final and less obvious example of aromatic resonance, the toluene molecule will be examined. Its small moment, 0.36, has been attributed (51) to small contributions to its structure from polar structures arising through hyperconjugation (52), such as:

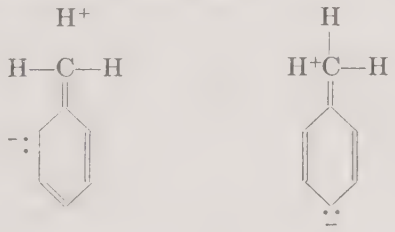

Because nine such structures can exist in addition to the two stable Kekulé structures, the moment would result from very small contributions from

them. It is well known that the orienting effect of the methyl group, and of the other groups which have been discussed, upon further substitution in the ring is consistent with the charge distributions given by these resonating structures (53).

3. Aliphatic Resonance

No dipole moment has yet been found for a saturated aliphatic hydrocarbon, although it appears reasonable to expect very small moments (perhaps too small to detect by present methods) in at least some of the branched-chain molecules. The symmetrical unsaturated molecules of ethylene and acetylene have zero moments (54), as would be expected. The reasons for the very small, or zero, moment of the paraffin molecules are tetrahedral symmetry of the C atom, zero moment of the C—C bond, and small size of the H—C bond moment, of which no absolute determination has been made. Quantum-mechanical calculations (18) and bond energies calculated from thermal measurements (4) indicate a moment value of 0.3–0.5 for the H—C bond, with the positive end of the dipole toward the hydrogen. The symmetrical methane and ethane molecules have zero moments. The methyl group has an axis of symmetry, in which its valence acts and its dipole moment lies. The tetrahedral valence angles are such that the component of each of the three H—C bond moments in the axis of symmetry is one-third of the H—C moment and the resultant moment of the methyl group is equal to that of the H—C bond. On the basis of symmetry, therefore, replacement of a hydrogen in a hydrocarbon by a methyl group should produce no moment, which is borne out by the zero moment found for propane (55) and other unsymmetrical hydrocarbons. Steric repulsion and possible differences in the effects of hyperconjugation (52) might be expected to give rise to small moments, as indicated by differences in bond energies in branched-chain molecules, but the indications are that any such moments should, at most, be of the magnitude of the present experimental uncertainty in measuring a moment close to zero.

The replacement of a hydrogen adjacent to a double or triple bond alters the charge distribution considerably as shown by the moment, 0.35, of propylene (55) and the moment, 0.72, of methylacetylene (56,57). Further lengthening of the carbon chain has only a slight or negligible effect in increasing the moment.

In addition to the normal structure for propylene, three polar structures may be written for the molecule of the type:

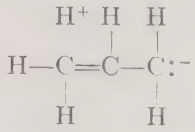

This structure is identical with the polar parts of the structures for toluene (moment = 0.36), written with an unshared electron pair on an ortho carbon. Small contributions from these polar structures are sufficient to account for the small moment of the propylene molecule. Larger contributions from analogous structures for methylacetylene:

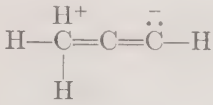

would account for the moment of its molecule. Infrared spectra and electron diffraction (4) show a considerable shortening of what is normally the single C—C bond below the normal C—C bond length, indicating that it possesses the considerable amount of double-bond character required by the dipole moment.

For butadiene, the more probable resonating forms are:

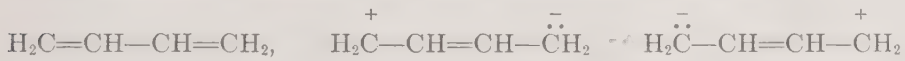

The polarity arising from the contribution of one polar structure just cancels that from the other, whether the molecular structure is *cis* or *trans* with respect to the central bond, which is shown by the shortening of the bond found by electron diffraction to possess 18% double-bond character, enough to give some stabilization of the two positions:

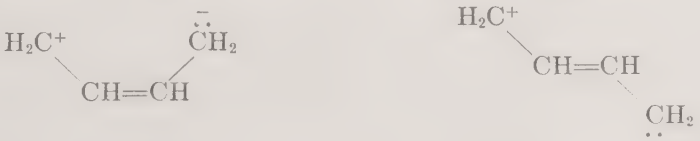

Additional structures may be written involving ionic hydrogen-carbon bonds (52), which could cause small moments in the *cis* form, but would cancel out in the *trans*. The zero moment, or a value experimentally indistinguishable from zero, observed (59) for the molecule will serve as a basis for the discussion of substituted butadienes, rather than as evidence of the structure of the simple molecule, although it is consistent with the predominance of the *trans* structure indicated by electron diffraction and spectroscopic measurements (60).

For the isoprene, or 2-methylbutadiene molecule (I), polar structures such as II may be written. The polar part of this structure is analogous to the polar structure contributing to the propylene structure, and the moment found (59) for the molecule, 0.38, is experimentally indistinguishable from that of propylene.

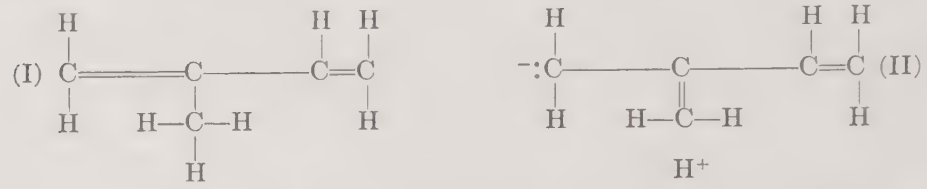

The moment, 0.68, of *trans*-piperylene, or 1-methylbutadiene (59), should be due to contributions from polar structures analogous to those of propylene and 2-methylbutadiene, except that the negative charge is displaced through the conjugated system two carbons farther away from the methyl hydrogens to give:

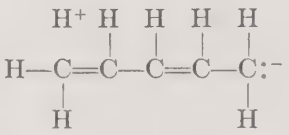

Since the contributions of three such polar structures are primarily responsible for the moment of the molecule, as in the cases of propylene and 2-methylbutadiene, the ratio of the resultant moment to that of 2-methylbutadiene should be approximately the same as the ratio of the distance between the two charges in the polar structures of the two molecules provided that the stabilities of the two sets of structures are the same. Measurement of models for these structures shows that, if 1-methylbutadiene has the probable *trans* configuration with respect to the central single bond of the butadiene structure, the ratio of the two charge separations is 1.8, which is just the ratio of the two dipole moments.

The moment, 0.52, of 2,3-dimethylbutadiene (59) and measurements (60a) on 1,2-dimethylbutadiene, 1,3-dimethylbutadiene, ethylbutadiene, and cyclopentadiene lend themselves to interpretation in terms of analogous polar structures, thus supporting the validity of this general treatment of the structures of these molecules. It is interesting to note that for styrene, as for butadiene, a moment experimentally indistinguishable from zero is found (60a). Many polar structures can be written as contributing to the structure of this molecule. The fact that their resultant moment is approximately zero points to the equal stabilities of structures having opposing moments. A simpler way of explaining this approxi-

mately zero moment is to state that the attachment of a methyl to a vinyl radical to form propylene gives practically the same moment as the attachment of a methyl to a phenyl radical to form toluene and, therefore, the attachment of a phenyl to a vinyl radical to form styrene should give zero moment.

The lowering of moment when a double bond is adjacent to a halogen is greater than that in the halogenated benzenes and the lowering when a triple bond is adjacent to a halogen is much greater still. The moment of vinyl chloride (61) is 1.44, as compared with 2.05 for ethyl chloride (62), whereas the moment of chloroacetylene is only 0.44 and that of bromoacetylene is actually zero (63). As in the halogenated benzenes, a structure may be written in which an unshared electron pair of the halogen moves into its bond with the carbon to form a double bond:

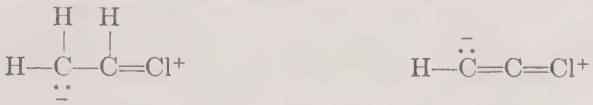

Contributions from these structures would oppose the normal dipole moments, such as those found in the alkyl halides, and reduce the molecular moment. Shortening of the carbon-halogen bond length (63,64) found by electron diffraction gives evidence of considerable amounts of double-bond character in these bonds. Electron diffraction and dipole moments, with their much greater lowering in this case, give more nearly equal values for the magnitudes of the contributions of these polar structures than were found in the case of the halogenated benzenes.

In 1-chloropropylene, contributions from polar structures like those written for propylene oppose the moments due to structures with positive chlorine. The result is evident in the higher moments (64a), 1.71 for *cis*-1-chloropropylene and 1.97 for the *trans* form. The same effects are apparent in the moment, 1.99, of isocrotyl chloride (51), in which two methyl groups are opposite the chlorine on the double bond. Contributions from structures such as:

would oppose that from the structure:

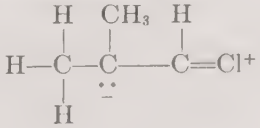

The resultant moment is close to that of isobutyl chloride, 2.04 (45). That the contribution from the structure with the double carbon-chlorine bond is reduced below that from the analogous structure in the case of vinyl chloride is indicated by the fact that electron diffraction shows the shortening of the carbon-chlorine bond by double-bond character to be about half as great in isocrotyl chloride (65) as in vinyl chloride (64). When the double bond is not adjacent to the carbon-chlorine bond, its effect is small, as shown by the fact that allyl chloride has a moment of 1.98 (64a), only 0.12 lower than that of propyl chloride (62).

The value, 2.0, calculated (51) for the carbon-oxygen double-bond moment from the moment of formaldehyde, 2.27, is slightly more than double that calculated (66) for the carbon-oxygen single bond. In terms of the resonance description of these bonds, the single bond is the resultant of contributions from the covalent structure, C—O, and the ionic structure, $C^+O:^-$, and the double bond is the resultant of contributions from C=O and $C^+—O:^-$. The moments listed in Table III give interesting evidence as to the nature of the varying charge distribution in aldehydes.

TABLE III

DIPOLE MOMENTS OF ALDEHYDES MEASURED IN THE VAPOR STATE (40,51)

Aldehyde	Formula	Moment, debyes
Formaldehyde	$H_2C=O$	2.27
Acetaldehyde	$CH_3—HC=O$	2.72
Propionaldehyde	$C_2H_5—HC=O$	2.73
Butyraldehyde	$C_3H_7—HC=O$	2.72
Acrolein	$CH_2=CH—HC=O$	3.04
Methacrolein	$CH_2=C(CH_3)—HC=O$	2.68
trans-Crotonaldehyde	$CH_3—CH=CH—HC=O$	3.67
Ketene	$CH_2=C=O$	1.45

The large increase of moment, 0.45, from the formaldehyde to the acetaldehyde molecule and a smaller increase, 0.16, from the acetaldehyde to the acetone molecule can be explained on the basis of inductive distortion of the methyl groups by the carbonyl bond moment, as can an analogous rise from the methyl to the ethyl halides (51,62,67). Indeed, calculation of the inductive effects shows a roughly quantitative agreement with the observed moment rises. A small additional rise with lengthening of the carbon chain of the aldehydes, and also of the unlisted ketones, would

be expected from the small inductive effects in the more distant parts of the chain, but it has been pointed out that curling of the chain could prevent such increases.

The description of the molecules in terms of resonance gives an entirely satisfactory explanation of the observed variations in moment, which, in turn, give an excellent indication of the magnitudes of the contributions from different polar structures. The simplest structures to be written for formaldehyde are the nonpolar formula (I), and the polar (II), but two structures involving hyperconjugation (52), as in the cases of the unsaturated hydrocarbons, may be written as in formula (III). For acetaldehyde, in addition to three structures analogous to the three written for formaldehyde, three structures such as (IV) may be written. A shortening of the C—C bond by 0.04 Å below the length of the normal single C—C bond found by means of electron diffraction (68), corresponds to about 8% double-bond character in this bond, arising from structures such as (IV) below. That the large rise in moment observed from formaldehyde to

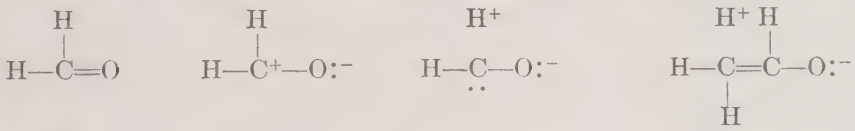

(I) (II) (III) (IV)

acetaldehyde is not even larger is probably due to the fact that the contributions from these highly polar structures should replace, in part, contributions from the structure:

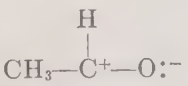

The acrolein molecule forms a conjugated system analogous to that of butadiene. Consequently, in addition to structures like those written for formaldehyde and acetaldehyde:

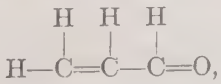

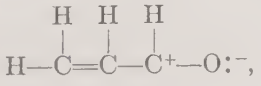

etc.

we may write such structures as:

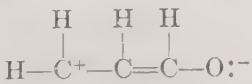

and

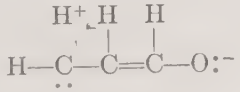

exists for such an extensive charge shift throughout the length of the chain. In methacrolein, the tendency of the methyl group to put a negative charge on the terminal carbon by giving rise to contributions from structures containing charge shifts like those in propylene, as in the following:

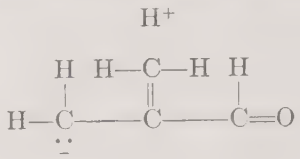

approximately compensates the charge shifts made possible by the conjugated system, the moment being reduced 0.04 below the moments of acetaldehyde and butyraldehyde.

The large rise in moment, 0.63, from acrolein to *trans*-crotonaldehyde indicates contributions from structures analogous to those which cause the moment of 1-methylbutadiene for, in addition to structures analogous to those written for the aldehydes already considered, one can write three highly polar structures, such as:

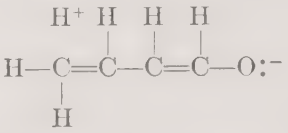

This large increase in moment made possible by transmission of charge through the conjugated system is in marked contrast to the absence of moment change when a methyl group is added to the carbon chain of acetaldehyde.

Electron diffraction (69) showed that the carbon-oxygen distance in ketene was about 0.04 Å shorter than the length of the carbon-oxygen double bond, while the carbon-carbon distance was 0.02 Å longer than the normal carbon-carbon double-bond length. This was explained by assuming that, in addition to contributions from normal structures analogous to those written for the aldehydes, $H_2C{=}C{=}O$ and $H_2C{=}\overset{+}{C}{-}\overset{\cdot\cdot}{\underset{-}{O}}:$, a 25% contribution was made to the structure by $H_2\overset{\cdot\cdot}{\underset{-}{C}}{-}C{\equiv}O$. The moment calculated for the resultant of the contributions of these structures is 1.13, with its positive end toward the oxygen. The accuracy of the bond-length determinations and the calculation from them of the contributions of the different structures, and from these, in turn, of the moment, do not warrant the attachment of much significance to the value of the moment calculated or perhaps even to its sign. The moment, 1.45, observed (69a) for ketene, as compared with the much higher values of the other ketones and the

aldehydes does, however, indicate a considerable contribution from the structure with a triple bond between the carbon and a positive oxygen in qualitative agreement with the results of electron diffraction. The structures written for the ketene molecule show analogy to those for the carbon monoxide molecule:

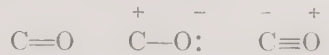

in which the contributions from the two polar structures are so nearly equal as to give a moment of 0.1, experimentally almost indistinguishable from zero.

The data available on aromatic aldehydes are limited to solution measurements, with the exception of an approximate vapor determination of the moment of benzaldehyde (51) as 3.16. The moments of the aromatic aldehydes, however, indicate small contributions from structures of the types:

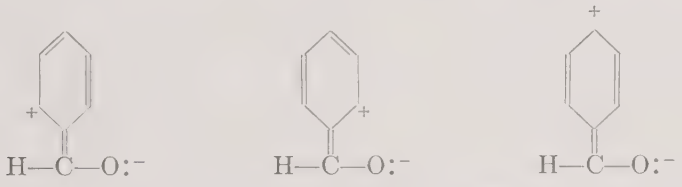

analogous to those written for nitrobenzene. The moment observed for *p*-tolualdehyde is sufficiently higher than that calculated as the resultant of the toluene and the benzaldehyde moments to indicate small contributions from three structures, such as:

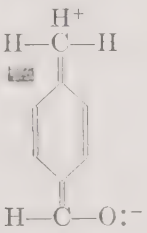

The structures of the cyanide group and the nitriles have much in common with those of the carbonyl group and the aldehydes and ketones. The difference in electronegativity between carbon and nitrogen is less than that between carbon and oxygen, the carbon-nitrogen single-bond moment, 0.45, being only about half that of the carbon-oxygen single bond (66). For hydrogen cyanide, we may write the probable contributing structures:

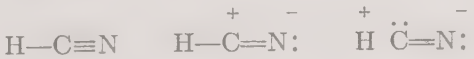

The contributions of the polar structures are responsible for the large moment of the molecule given in Table IV, together with the moment values of a number of nitriles measured in the vapor state.

TABLE IV

DIPOLE MOMENTS OF NITRILES MEASURED IN THE VAPOR STATE (51,62,69a,70)

Nitrile	Formula	Moment, debyes
Hydrogen cyanide	HCN	2.93
Acetonitrile	CH_3CN	3.94
Propionitrile	C_2H_5CN	4.04
Butyronitrile	C_3H_7CN	4.05
Valeronitrile	C_4H_9CN	4.09
Acrylonitrile	$CH_2{=}CH{-}CN$	3.88
Methacrylonitrile	$CH_2{=}C(CH_3)CN$	3.69
4-Cyano-1,3-butadiene	$CH_2{=}CH{-}CH{=}CH{-}CN$	3.90
trans-Crotononitrile	$CH_3{-}CH{=}CH{-}CN$	4.50

The rise in moment, 1.01, from hydrogen cyanide to acetonitrile is more than double that from formaldehyde to acetaldehyde. It may be attributed to a larger contribution from three polar structures of the type:

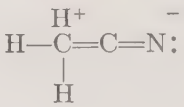

than is made by the analogous structures for the aldehydes. Indication of the contributions from such structures is given by the shortening of the carbon-carbon bond by 0.05 Å shown by electron diffraction measurements (71). Two structures analogous to the first two for hydrogen cyanide, of course, contribute as well to the resultant molecule of the nitrile. The small rise in moment from the methyl to the ethyl compound, which contrasts with the absence of rise in the aldehydes, could be due to a small inductive effect, as could the slight further upward trend to valeronitrile, which is probably within the experimental error. Indeed, the value, 4.04, obtained by Groves and Sugden (62) for propionitrile and listed for comparison with the values obtained by them for acetonitrile, butyronitrile, and valeronitrile, is 0.04 higher than the value obtained by Hurdis and Smyth (51), which will be used for comparison with that of acrylonitrile.

In view of the fact that acrolein has a moment (Table III, page 40) 0.31 higher than that of propionaldehyde, it is surprising to find the moment of acrylonitrile lower than that of propionitrile. For acrylonitrile, one may write structures analogous to those for acetonitrile:

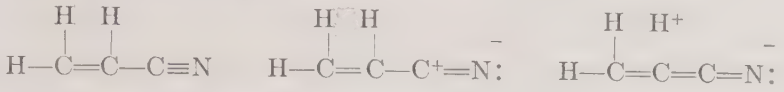

and, in addition, structures characteristic of the conjugated system as in butadiene and acrolein:

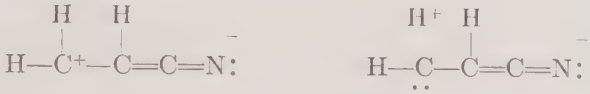

If these were the only contributing structures, their resultant would be a structure with a moment larger than that of propionitrile, instead of smaller. Another structure, which was shown for butadiene, but not for acrolein, because there was no indication of a contribution from it and because the greater electronegativity of oxygen as compared with nitrogen should make it more unstable than in the present case, may be written as:

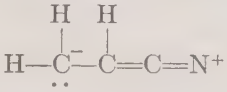

If this structure with positive nitrogen looks unstable because of the electronegativity of nitrogen, it should be remembered that—as shown by the dipole moment—the nitrogen atom of the isocyanide group also carries a positive charge, while a structure with positive oxygen has just been written for ketene and evidence for many structures with positive halogen has been cited. The lower moment of acrylonitrile as compared with propionitrile indicates the probability of a contribution from this structure with positive nitrogen sufficiently large to overcome the rise in moment due to the contributions of the other two types of structure characteristic of the conjugated system. Since 4-cyano-1,3-butadiene has a moment practically identical with that of acrylonitrile, it would appear to possess a similar compensation in the charge shifts, the contributions from a structure with positive nitrogen and negative terminal carbon overcoming the rise in moment due to the contributions of the structures with negative nitrogen and positive charge on the terminal carbon or on the hydrogens attached to it.

The case of methacrylonitrile is analogous to that of methacrolein. The methyl group tends to put a negative charge on the terminal carbon

by giving rise to structures analogous to those responsible for the propylene moment. It thus aids the structure with positive nitrogen in reducing the moment, the additional reduction being 0.19 unit, which is smaller than in the case of the aldehydes.

It is interesting to note that the large rise in moment, 0.62, from acrylonitrile to *trans*-crotononitrile is practically identical with the rise from acrolein to *trans*-crotonaldehyde, 0.63, and with the moment of *trans*-1-methylbutadiene, 0.68. Since the two rises in moment, and the entire moment in the third case, are due to contributions from analogous structures of the type:

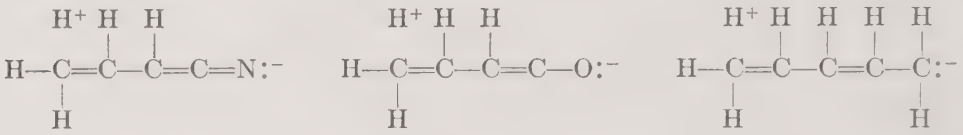

it would appear that these structures possess approximately equal stabilities as compared with the stabilities of the other structures contributing to their respective molecules.

An excellent example of the transmission of a charge through a conjugated system is given by the series of compounds (72) represented by the formula:

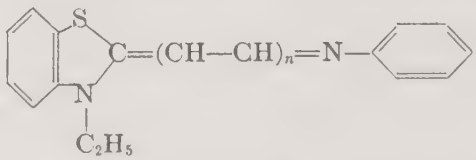

The moment calculated for this structure from group moments is 1.6 ± 0.6 when $n = 0$, and 2.0 ± 0.6 when $n = 1$ or 2. The moments measured in benzene solution are 2.37 for $n = 0$, 4.17 for $n = 1$, and 5.32 for $n = 2$. A type of polar structure capable of contributing to the structure of the molecule is:

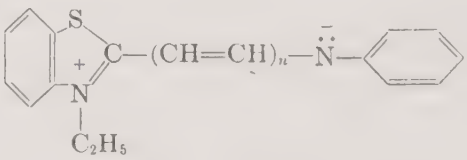

For example, when $n = 2$, the two principal types of contributing structure are:

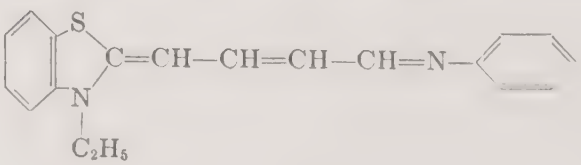

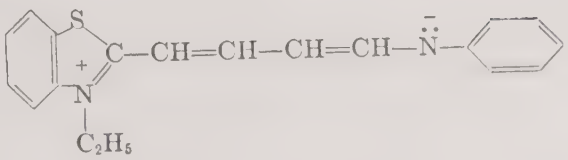

Because resonance gives some double-bond character to all the bonds of the central carbon chain, the chain tends to be linear. The rise in moment when n changes from 0 to 1 to 2 is not quantitatively proportional to the apparent increase in charge separation, as was found in the change from 2-methylbutadiene to 1-methylbutadiene. However, the observed moment increases greatly with increasing molecular length, as it should if increase in the length of the contributing polar forms does not greatly decrease their stabilities.

Resonance in such compounds is related to wave length and intensity of light absorption. Of two isomeric bases, which may be selected from a number of examples (73), 2-methyl-3-[(1-methyl-4(1)-quinolylidene)-ethylidene]-indolenine:

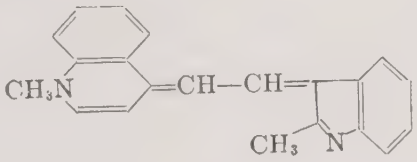

to which polar structures such as:

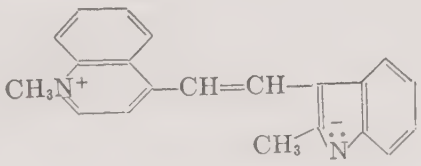

contribute, and 1,2-dimethyl-3-(β-4-quinolylvinyl)-indole:

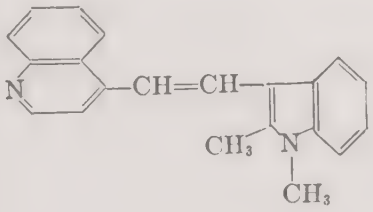

to which polar structures such as:

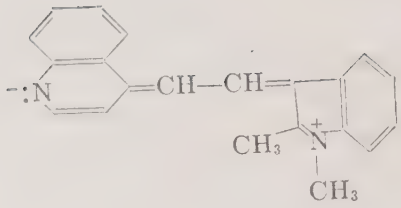

contribute, the basic behavior of the first compound points to much larger contributions from the polar structures, or greater resonance mobility, than does that of the second compound. In accordance with this behavior, as observed in other cases, the first compound is much more deeply colored. Its bluish purple pyridine solution has two absorption maxima, at 5710 and 6160 Å, while the second compound gives only a pale yellow pyridine solution, which absorbs very weakly, with its maximum at 3940 Å. The dipole moments calculated roughly for the two molecules from the group moments are the same, 2.5; the observed moments are 10.6 for the first compound and 5.43 for the second. Not only do the contributing polar structures for these molecules have large moments because of their great charge separations, but the amounts of their contributions are large. The moments indicate the contribution of the polar structures for the deeply colored first compound, the indolenine, to be about three times that in the case of the pale second compound, the indole.

The highly polar structures with widely separated charges which have been written as contributing to the structures of these rather large molecules bring to mind the relatively stable structures of dipolar or intramolecular ions. In this case, a carboxyl group in one part of the molecule loses its hydrogen to an amino group in another part of the molecule, so that the resulting $—NH_3^+$ and $—COO^-$ form a very large dipole. The high polarities of these molecules, such as those of the peptides, render them insoluble in nonpolar solvents and necessitate their study in aqueous solutions, the increment in dielectric constant produced by their solution in water giving a measure of the polarity. The many interesting properties of such solutions, which are admirably described elsewhere (74), are beyond the scope of this chapter.

Some of the differences in dipole moment which have been used as evidence of resonance and contributions from specific polar structures can be interpreted in terms of electronic shifts induced by the electric fields of the dipoles, that is, inductive distortion of the charge distribution. As has been pointed out, the existence of this effect is not only to be expected, but is generally in evidence in the observed values of the dipole moments. The description of a displacement of charge in terms of resonance may, in

some cases, amount to a description in different terms of the effect of inductive distortion. However, the development of the ideas of resonance has provided a thoroughly satisfactory explanation of many dipole moment values not previously understood and, conversely, the measurement of dipole moment provides a means of investigating, both qualitatively and, to a lesser extent, quantitatively, the phenomena of resonance.

References

1. Smyth, *Phil. Mag.*, **45,** 530 (1923).
2. Smyth, *Dielectric Constant and Molecular Structure.* Chemical Catalog Co., New York, 1931.
3. Kirkwood, *Physik. Z.*, **35,** 259 (1934).
4. Pauling, *The Nature of the Chemical Bond.* Cornell Univ. Press, Ithaca, 1940.
5. Smyth, "The Determination of Dipole Moment," in A. Weissberger, ed., *Physical Methods of Organic Chemistry.* Vol. II, Interscience, New York, 1946, Chapter XX.
6. Debye, *Physik. Z.*, **13,** 97 (1912).
7. Debye, *Polar Molecules.* Chemical Catalog Co., New York, 1929.
8. Hedestrand, *Z. physik. Chem.*, **B2,** 428 (1929).
9. Hålverstadt and Kumler, *J. Am. Chem. Soc.*, **64,** 2988 (1942).
10. Frank, *Proc. Roy. Soc. London*, **A152,** 171 (1935).
11. Higasi, *Sci. Papers Inst. Phys. Chem. Research Tokyo*, **28,** 284 (1936).
12. Conner, Clarke, and Smyth, *J. Am. Chem. Soc.*, **64,** 1379 (1942).
13. Errera, *Physik. Z.*, **27,** 764 (1926).
14. Errera, *Polarisation Diélectrique.* Presses Universitaires de France, Paris, 1928.
15. Smyth and Morgan, *J. Am. Chem. Soc.*, **49,** 1030 (1927).
16. Smyth, Morgan, and Boyce, *ibid.*, **50,** 1536 (1928).
17. Smallwood and Herzfeld, *ibid.*, **52,** 1919 (1930).
18. Smyth, *J. Phys. Chem.*, **41,** 209 (1937).
19. Sutton, *Proc. Roy. Soc. London*, **A133,** 668 (1931); *Trans. Faraday Soc.*, **30,** 789 (1934).
20. Williams, *Z. physik. Chem.*, **A138,** 75 (1928).
21. Eyring, *Phys. Rev.*, **39,** 746 (1932).
22. Smyth and Walls, *J. Am. Chem. Soc.*, **54,** 2261 (1932).
23. Meyer, *Z. physik. Chem.*, **B8,** 357 (1930).
24. Smyth, Dornte, and Wilson, *J. Am. Chem. Soc.*, **53,** 4242 (1931).
25. Lennard-Jones and Pike, *Trans. Faraday Soc.*, **30,** 830 (1934).
26. Zahn, *Phys. Rev.*, **38,** 521 (1931); *ibid.*, **40,** 291 (1932).
27. Greene and Williams, *Phys. Rev.*, **42,** 119 (1932).
28. Lewis and Smyth, *J. Chem. Phys.*, **7,** 1085 (1939).
29. Beach and Stevenson, *ibid.*, **6,** 635 (1938).
30. Kistiakowsky *et al.*, *ibid.*, **6,** 18, 407, 900 (1938).

31. Smyth and Hitchcock, *J. Am. Chem. Soc.*, **54,** 4631 (1932).
32. Smyth and Hitchcock, *ibid.*, **55,** 1296, 1830 (1933).
33. Yager and Morgan, *ibid.*, **57,** 2071 (1935).
34. White and Morgan, *ibid.*, **57,** 2078 (1935).
35. Smyth, *Chem. Revs.*, **19,** 329 (1936).
36. White and Bishop, *J. Am. Chem. Soc.*, **62,** 8 (1940).
37. White, Biggs, and Morgan, *ibid.*, **62,** 16 (1940).
38. Baker and Smyth, *Ann. N. Y. Acad. Sci.*, **40,** 447 (1940).
39. Conner and Smyth, *J. Am. Chem. Soc.*, **63,** 3424 (1941).
40. Hannay, *ibid.*, **68,** 171 (1946).
41. Zahn, *Phys. Rev.*, **27,** 455 (1926).
42. Scheffers, *Physik. Z.*, **35,** 425 (1934).
43. Smyth, *J. Am. Chem. Soc.*, **63,** 57 (1941).
44. Smyth, *J. Org. Chem.*, **6,** 421 (1941).
45. Wiswall and Smyth, *J. Chem. Phys.*, **9,** 356 (1941).
46. Hurdis and Smyth, *J. Am. Chem. Soc.*, **64,** 2212 (1942).
47. McAlpine and Smyth, *J. Chem. Phys.*, **3,** 55 (1935).
48. Birtles and Hampson, *J. Chem. Soc.*, **1937,** 10.
49. Ingham and Hampson, *ibid.*, **1939,** 981.
50. Oesper, *unpublished measurements.*
51. Hurdis and Smyth, *J. Am. Chem. Soc.*, **65,** 89 (1943).
52. Mulliken, Rieke, and Brown, *ibid.*, **63,** 41 (1941).
53. Ri and Eyring, *J. Chem. Phys.*, **8,** 433 (1940).
54. Smyth and Zahn, *J. Am. Chem. Soc.*, **47,** 2501 (1925).
55. McAlpine and Smyth, *ibid.*, **55,** 453 (1933).
56. Watson and Ramaswamy, *Proc. Roy. Soc. London*, **A156,** 130 (1936).
57. Krieger and Wenzke, *J. Am. Chem. Soc.*, **60,** 2115 (1938).
58. Schomaker and Pauling, *ibid.*, **61,** 1769 (1939).
59. Hannay and Smyth, *ibid.*, **65,** 1931 (1943).
60. Mulliken, *Rev. Modern Phys.*, **14,** 265 (1942).
60a. Hannay and Smyth, *J. Am. Chem. Soc.*, **68,** 244 (1946).
61. Hugill, Coop, and Sutton, *Trans. Faraday Soc.*, **34,** 1518 (1938).
62. Groves and Sugden, *J. Chem. Soc.*, **1937,** 158.
63. Brockway and Coop, *Trans. Faraday Soc.*, **34,** 1429 (1938).
64. Brockway, Beach, and Pauling, *J. Am. Chem. Soc.*, **57,** 2693 (1935).
64a. Hannay and Smyth, *ibid.*, **68,** 1005 (1946).
65. Beach and Stevenson, *ibid.*, **61,** 2643 (1939).
66. Smyth, *ibid.*, **60,** 183 (1938).
67. Smyth and McAlpine, *J. Chem. Phys.*, **2,** 499 (1934).
68. Stevenson, Burnham, and Schomaker, *J. Am. Chem. Soc.*, **61,** 2922 (1939).
69. Beach and Stevenson, *J. Chem. Phys.*, **6,** 75 (1938).
69a. Hannay and Smyth, *J. Am. Chem. Soc.*, **68,** 1357 (1946).
70. McAlpine and Smyth, *ibid.*, **56,** 1697 (1934).

71. Pauling, Springall, and Palmer, *J. Am. Chem. Soc.*, **61,** 927 (1939).
72. Brooker, White, Keyes, Smyth, and Oesper, *ibid.*, **63,** 3192 (1941).
73. Brooker, Sprague, Smyth, and Lewis, *ibid.*, **62,** 1116 (1940).
74. Cohn and Edsall, *Proteins, Amino Acids and Peptides.* Reinhold, New York, 1943.

CENTRAL FOOD TECHNOLOGICAL RESEARCH INSTITUTE
LIBRARY

III. *Structure of Coordination Compounds*

W. CONARD FERNELIUS

Department of Chemistry, Syracuse University, Syracuse, New York

I. Introduction

With the growth of chemistry through the years an increasing number of connotations has been attached to the term *structure*. The original planar structural formulas of the organic chemist were the embodiment of a correlation of valence rules and chemical behavior with the manner of linking between atoms in a molecule. Proof of structure consisted essentially in gathering together a sufficient mass of information about a compound to rule out all but one structural possibility. The doctrine of isomerism assumed great importance because the fundamental soundness of the concept of structural formulas was confirmed by the agreement between the number of compounds predicted for a given composition and the experimental results. For some types of compounds, more isomers were obtained than were predicted from planar models. Hence, chemists were forced to consider the space geometry of linkages between atoms within the molecule (*cis-trans* and optical isomerism).

The possibilities for the development of structural theory presented by the field of inorganic chemistry were not recognized at an early date. The demonstration of the existence of ions is, in a very limited sense, structural but there was little other development. At a later date, the theoretical attack of physicists and physical chemists on the structure of atoms and molecules proved to be very fruitful. The elaboration of the nuclear atom,

as well as the use of more powerful modern experimental methods (largely physical in character), led to the development of theories about the nature of linkages between atoms and to the direct deduction of the positions occupied by atoms in a molecule, bond angles, bond distances, and bond types.

Outstanding among the achievements of modern theory has been the breakdown of the distinction between inorganic and organic molecules with the recognition that typical compounds of each class are different manifestations of the same, or at least similar, general tendencies. The field of coordination or complex compounds is one which bridges the oft-mentioned gap between organic and inorganic compounds. In discussing the structure of coordination compounds, one may well utilize modern theory at the start. Although the larger part of our knowledge of these compounds is based on the study of classical chemical reactions, modern theory has been fitted to the field with marked success, and the application of modern experimental techniques points the way to extensive developments in the near future.

II. Fundamental Definitions

Before discussing the subject of coordination compounds we must acquire a clear concept of what a coordination compound is. Actually this task is not too simple. Although the terms, *coordination compound* and *complex compound*, are frequently used in a limited sense, they have also been extended to cover a rather wide variety of chemical combinations. Sometimes it would seem that they have even been used as catch-all terms when insufficient information was available to classify a compound definitely in one of the accepted classes of combination. European chemists have a very useful expression, *compound of higher order*, which refers to any substance formed by the union of two or more saturated molecules, *i.e.*, molecules in which all the valences of the constituents are satisfied: $AB + CD = AB \cdot CD$. In this category are included a large number of compounds, such as hydrates, ammoniates, double salts, double oxides (the familiar salts of oxyacids), and nonelectrolytic compounds which, for lack of a more suitable term, we may call molecular addition compounds (Table I). Although in some cases the strength of the union between apparently saturated molecules is so weak that the presence of the individual molecular or ionic constituents is readily demonstrated (tests for potassium, aluminum, and sulfate ions in alum), in many other cases changes so profound have taken place that the individual constituents are

TABLE I

COMPOUNDS OF HIGHER ORDER

Compounds	Empirical formula	Coordination formula
Hydrates	$BeSO_4 \cdot 4\ H_2O$	$[Be(H_2O)_4]SO_4$
	$MgCl_2 \cdot 6\ H_2O$	$[Mg(H_2O)_6]Cl_2$
Ammoniates	$Cu(NO_3)_2 \cdot 4\ NH_3$	$[Cu(NH_3)_4](NO_3)_2$
	$CrCl_3 \cdot 6\ NH_3$	$[Cr(NH_3)_6]Cl_3$
Double salts	$2\ KF \cdot BeF_2$	$K_2[BeF_4]$
	$4\ NaCN \cdot Fe(CN)_2$	$Na_4[Fe(CN)_6]$
Double oxides	$K_2O \cdot SO_3$	$K_2[SO_4]$
	$3\ H_2O \cdot TeO_3$	$H_6[TeO_6]$
Molecular addition compounds	$R_2O \cdot BF_3$	$R_2O \rightarrow BF_3$
	$R_3N \cdot SO_3$	$R_3N \rightarrow SO_3$

not recognizable. Thus, it is not possible to obtain the customary tests for the iron(II) ion in a solution of potassium ferrocyanide. In some instances it has been customary to differentiate between the two situations by calling members of the first group *double salts* and, those of the second, *complex salts*. Actually, these represent extreme tendencies, between which all gradations are encountered. The so-called *instability constant* (K_{ins}) is a quantitative measure of the tendency of a complex ion to dissociate (Table II).

TABLE II

INSTABILITY CONSTANTS OF COMPLEX IONS

$$Zn(NH_3)_4^{++} \rightleftharpoons Zn^{++} + 4\ NH_3$$

$$K_{ins} = \frac{[Zn^{++}][NH_3]^4}{[Zn(NH_3)_4]^{++}} = 2.6 \times 10^{-10}$$

$$Ag(CN)_2^- \rightleftharpoons Ag^+ + 2\ CN^-$$

$$K_{ins} = \frac{[Ag^+][CN^-]^2}{[Ag(CN)_2^-]} = 8 \times 10^{-23}$$

Werner (1), who formulated the fundamental principles in the field of coordination compounds, was impressed by the frequency with which the numbers four and six (less frequently, two and eight) were encountered among the formulas for compounds of higher order. Werner proposed an entirely new principle of molecular structure. He divided the combining power of an atom (or ion) into two spheres; an *inner*, or *coordination sphere*,

and an *outer*, or *ionization sphere*. Certain atoms have a tendency to attach to themselves a definite number of other atoms or groups, irrespective of whether these are univalent (or higher valent) atoms or groups, or whole molecules capable of independent existence. The central atom together with the atoms or groups occupying this inner sphere constitute the *coordination complex* (customarily enclosed in brackets [ ]) and the number of atoms or groups attached to the central atom is the *coordination number*.* The atoms or groups in the second (ionization) sphere are less closely attached and do not contribute to the coordination number. The manner of representing compounds containing coordination complexes is shown in the second column of formulas in Table I.

Since ions as well as neutral groups may be coordinated about a central ion or atom, the complex ions formed from a single simple ion or atom vary with the nature of the entities coordinated. The manner in which the charge on complex ions varies with the number of neutral and charged groups coordinated is shown in Table III. This simple relationship is

TABLE III

VARIATION OF CHARGE ON A COMPLEX ION WITH NUMBER OF CHARGED GROUPS COORDINATED

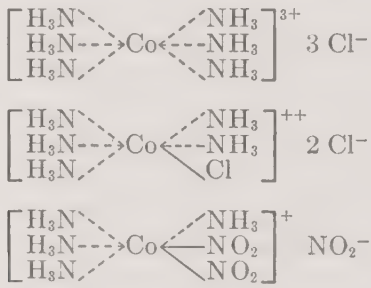

strikingly shown in Figure 1 for a group of closely related platinum(IV) compounds; the molecular conductance (roughly proportional to the number of ions present) is plotted against the number of negative ions (chloride or nitrite) coordinated to the central atom.

It is essential that the meaning of a number of terms used to describe and classify coordination compounds be clearly understood (Table IV). A

*The use of the term, coordination number, among crystallographers is similar to, but not entirely synonymous with, the usage here.

TABLE IV

TERMS USED IN CLASSIFYING COORDINATION COMPOUNDS AND COORDINATING GROUPS

Mononucleate complexes	
Nonchelate groups	
Unidentate	NH_3, F^-, CN^-
Chelate groups	
Bidentate	$NH_2CH_2CH_2NH_2$ 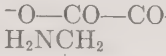
Tridentate	$HN(CH_2CH_2NH_2)_2$ 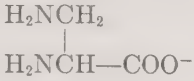
Quadridentate	$N(CH_2CH_2NH_2)_3$ 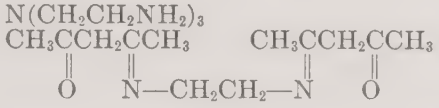
Multinucleate complexes	
	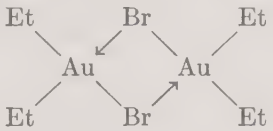
Inner complex	
First order	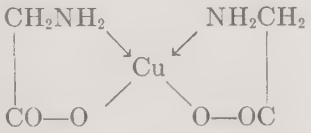
Second order	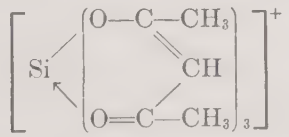

complex compound or ion may have one coordination center (*mononucleate*) or more than one (*multinucleate*). Coordinated groups may be unifunctional (*unidentate*) or multifunctional (*bi-*, *tri-*, or *quadridentate*). The latter are commonly known as *chelate* groups. Chelation is most commonly encountered among molecules which can form five- or six-membered rings.

If a neutral group and an acid group are united in the same chelate molecule, the resulting complex is known as an *inner complex salt.* Such substances constitute an especially important set of coordination compounds. If, in such a compound, the coordination number is twice the

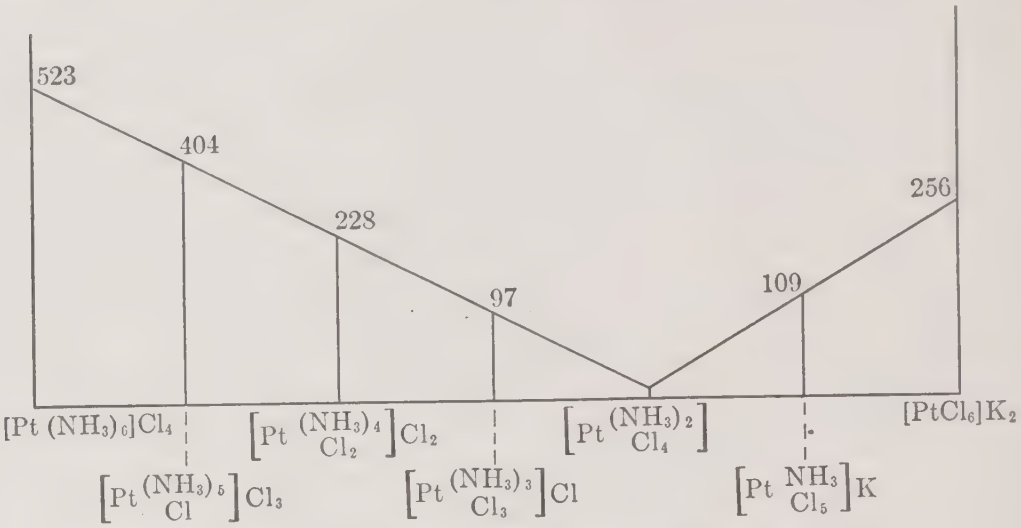

Fig. 1. Molecular conductance at 25°C. and 1000-liter dilution.

charge on the central ion the resulting coordination compound is neutral in character (*inner complex of the first order*) and has properties more like those of a neutral organic molecule than those of a salt. Beryllium acetyl-

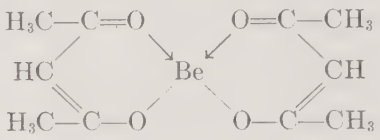

acetonate is frequently cited as a typical example. Its physical properties are given in Table V. When the coordination number of the central ion is other than twice the charge on the ion, the coordination complex as a whole

TABLE V

PHYSICAL PROPERTIES OF BERYLLIUM ACETYLACETONATE

Melting point, 108°C.	Very soluble in benzene, ether, alcohol, etc.
Boiling point, 270°C.	Slightly soluble in water.
Partial sublimation as low as 100°C.	Aqueous solutions are nonconducting.
Molecular weight has been determined by vapor density.	Aqueous solutions are nonhydrolyzed.

still bears a charge (*inner complex of the second order*). Many authors do not make this distinction but reserve the term, inner complex, for the neutral complexes.

III. Nature of Coordination Linkages

It cannot be said that chemists have as yet elaborated a single point of view sufficiently inclusive to treat completely all phases of coordination chemistry. However, some aspects of the subject are clearly recognized and are valuable as points of departure for a clearer understanding of this field. These various aspects will be considered in order.

1. Ion–Dipole Bond

It will be noted that the coordination center is most often a positive ion. One picture of the coordination linkage is that the positive charge of the central ion attracts negative ions or the negative part of polar molecules. This electrostatic attraction constitutes the linkage between the two parts of the complex. It would be expected that the strength of such an attraction would be greater (*1*) the smaller the ions and (*2*) the higher the charge. Table VI shows that, in general, the conditions leading to strong attraction are those which give the most stable complexes.

TABLE VI

IONIC POTENTIAL AND FORMATION OF COMPLEX IONS (2)

Ion	Ionic radius, Å	Ionic potential, $= \frac{\text{charge}}{\text{radius}}$	Remarks
Cs^+	1.67	0.61	↑ Ions not hydrated, no complex compounds formed ↓
Rb^+	1.48	0.67	
K^+	1.33	0.71	
Na^+	0.98	1.0	
Ba^{2+}	1.31	1.4	
Hg^{2+}	1.12	1.8	
Cd^{2+}	1.03	1.9	
Ca^{2+}	0.98	1.9	↑ Ions invariably hydrated ↓
Zn^{2+}	0.83	2.4	
Co^{2+}	0.82	2.4	↑ Ions readily ammoniated ↓
Ni^{2+}	0.78	2.5	
Fe^{3+}	0.67	4.5	↑ Ammines and inner complex salts readily formed ↓
Co^{3+}	0.66	4.5	
Cr^{3+}	0.65	4.6	
Al^{3+}	0.57	5.3	
Pt^{4+}	0.66	6.0	
Be^{2+}	0.39	5.9	

It must be recognized, however, that there are certain limitations to the point of view just presented. Although it accounts adequately for the difference in stability of the coordination compounds of cobalt(II) and cobalt(III), certain predictions are not at all in accord with the facts. Thus, the ability of iron(III) and cobalt(III) to form complex compounds is not approximately equal and aluminum is not the triply charged ion most likely to form complex compounds. There are complex ions which are held together by essentially attractive forces, but there are others in which the bonds are of a fundamentally different character. The conditions of high charge, small cation, and large anion (or highly polarizable neutral group), are the very conditions which produce the maximum distortion of coordinated groups and which cause the change from an electrovalent (or ionic) to a covalent bond (Fajans' rules) (3).

2. Coordinate Covalence

Two principal types of valence bonds are usually recognized: *electrovalence* and *covalence* (Table VII). The first type is, in one sense, not a

TABLE VII

TYPES OF VALENCE

1. Electrovalence:

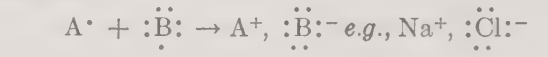

Completion of, or reversion to, a stable electronic configuration by gain or loss of one or more electrons; electrostatic attraction.

2. Covalence:

Completion of stable electronic configurations by sharing of one or more pairs of electrons; definite bond, directed in space.

Normal:

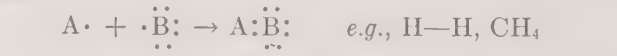

One electron for each pair contributed by both atoms.

Coordinate:

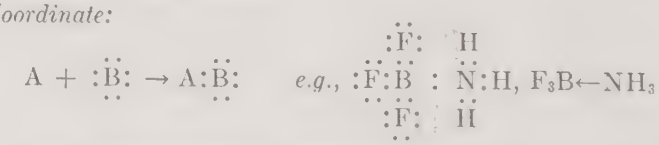

Both electrons of a pair contributed by one atom (lone pair); donor-acceptor relationship.

bond at all but an electrostatic attraction between ions and arises from the completion of, or reversion to, a stable electronic configuration by the gain or loss of one or more electrons. The second type is a definite bond, directed in space, in which the completion of stable electronic configurations takes place by the sharing of one or more pairs of electrons. Many workers find it convenient to divide covalent bonds into two classes: *normal* and *coordinate*. In the former, the electron bond arises from the contribution of one electron from each of the two linked atoms. In the latter, both electrons of a pair are contributed by one of the two atoms linked. This type of linkage has also been called a semipolar, or a dative, bond. Several things are to be noted: the donor-acceptor relationship involved in this type of bond, the necessity for the availability of a lone pair of electrons on the part of the donor, the necessity for an electronic unsaturation on the part of the acceptor, and the, at least partial, polar character of the linkage. However, it must be understood also that it is not always possible to distinguish between normal and coordinate covalence.

In the formation of covalent bonds of both types, there seems to be a definite maximum number of such bonds which can be formed by any atom (Sigdwick's *Rules of Maximum Covalence*) (4). This number varies, not with the periodic group to which an element belongs, but with the period in which it occurs (Table VIII). The search for a theoretical explanation underlying these empirical rules has shown that there are two

TABLE VIII

SIDGWICK'S RULES OF MAXIMUM COVALENCE

Period	Elements	Maximum covalence	Shared electrons	Examples			
				Binary compound	Complex ion		Nonelectrolyte complex
					Cation	Anion	
	H	2	[a]	$(HF)_x$		HF_2^-	Hydrogen bond
1*st* short	Li-F	4	8	CCl_4	$Be(NH_3)_4^{++}$	BF_4^-	$Be(C_5H_7O_2)_2$[b]
2*nd* short	Na-Cl	6	12	SF_6	$Ca(H_2O)_6^{++}$	SiF_6^{--}	$Al(C_5H_7O_2)_3$
1*st* long	K-Br	6	12	SeF_6	$Cr(NH_3)_6^{3+}$	$Mn(CN)_6^{3-}$	$Co(NH_3)_3(NO_2)_3$
2*nd* long	Rb-I	8	16			$Mo(CN)_8^{3-}$	$Sn(C_{32}H_{16}N_8)_2$[c]
3*rd* long	Cs-Tc	8	16	OsF_8	$Pb(C_{12}H_8N_2)_4^{++}$[d]	TaF_8^{3-}	$Hf(C_5H_7O_2)_4$
4*th* long	Fr-A	8	16			$U(C_2O_4)_4^{4-}$	$Th(C_9H_6NO)_4$[e]

[a] The hydrogen bond is not due to the sharing of two pair of electrons but to resonance between two different structures.

[b] $C_5H_7O_2$ is the acetylacetonate group, $CH_3CO—CH=C(CH_3)O—$.

[c] $C_{32}H_{16}N_8$ is the phthalocyanine nucleus.

[d] $C_{12}H_8N_2$ is the orthophenanthroline group.

[e] C_9H_6NO is the 8-hydroxyquinolinate group.

aspects which must be considered: (*1*) the availability of electronic orbitals and (*2*) spatial relationships.

(*A*) *Electronic Orbitals and Effective Atomic Number.* An abbreviated list of electronic configurations is given in Table IX. It is to be noted that

TABLE IX

ELECTRONIC CONFIGURATIONS

Z		1*s*	2*s*	2*p*	3*s*	3*p*	3*d*	4*s*	4*p*	4*d*	4*f*
2	He	2									
5	B	2	2	1							
10	Ne	2	2	6							
13	Al	2	2	6	2	1					
18	A	2	2	6	2	6					
20	Ca	2	2	6	2	6		2			
21	Sc	2	2	6	2	6	1	2			
22	Ti	2	2	6	2	6	2	2			
23	V	2	2	6	2	6	3	2			
24	Cr	2	2	6	2	6	5	1			
25	Mn	2	2	6	2	6	5	2			
26	Fe	2	2	6	2	6	6	2			
27	Co	2	2	6	2	6	7	2			
28	Ni	2	2	6	2	6	8	2			
29	Cu	2	2	6	2	6	10	1			
30	Zn	2	2	6	2	6	10	2			
31	Ga	2	2	6	2	6	10	2	1		
36	Kr	2	2	6	2	6	10	2	6		

the first major quantum group ($n = 1$) consists only of *s* electrons, the second ($n = 2$) consists of both *s* and *p* electrons, whereas the third and subsequent groups consist of *s*, *p*, and *d* electrons. The importance of these facts becomes evident when we inquire why boron forms the complex ion, BF_4^-, whereas the corresponding ion for aluminum is AlF_6^{3-}. The answer is that, because of the absence of available *d* orbitals in boron, its electronic system cannot be expanded beyond the limits permitted by *s* and *p* orbitals. Hence, its maximum coordination number is four, signifying the sharing of four pairs of electrons. In the case of aluminum, on the other hand, *d* orbitals are available ($n = 3$); and, hence, a coordination number of six is possible, signifying the sharing of six pairs of electrons.

The tendency toward the formation of complex compounds is very prominent among the transition elements. In a sequence of the elements in order of increasing atomic number, the transition elements are the ones

in which previously unoccupied *d* orbitals are progressively filled with electrons. That the tendency to fill the *d* orbitals extends beyond the number of electrons available in the neutral atom is evidenced by the ease with which complex compounds are formed. In general, an atom tends to add a sufficient number of electrons (by sharing) to realize the *effective atomic number* (E.A.N.) of the inert gas at the end of that period of the periodic system, *i.e.*, the *d* orbitals of one major quantum group are filled, as well as the *s* and *p* orbitals of the next higher quantum group.

Let us consider the case of the complex ion, $Co(NH_3)_6^{3+}$. The central Co^{3+} has associated with it 24 electrons (three less than the atomic number); hence, the electronic balance sheet is:

Co^{3+} (at. no. − 3) donates	24 electrons
6 NH_3 donate	12 electrons
E.A.N. of Co in $Co(NH_3)_6^{3+}$ =	36

The next higher inert gas is krypton with an atomic number of 36. A somewhat more complex case is presented by the interesting carbonyl, $Re(CO)_5Cl$, which appears to have the formula:

$$(:O\vdots\vdots C:)_5Re:\underset{\cdot\cdot}{\overset{\cdot\cdot}{X}}:$$

Electrons of Re	75
Contribution of the Cl atom to pair formation	1
5 CO contribute	10
Total:	86

The computed E.A.N. would be the same if the coordination center were considered to be Re^+, and $:\underset{\cdot\cdot}{\overset{\cdot\cdot}{Cl}}:^-$ one of the coordinated groups. Thus, the E.A.N. of Re in the carbonyl is the same as the atomic number of the inert gas, radon.

The results of such computations for a group of complexes of the platinum metals are given in Table X. An even more extensive list could be compiled for iron, cobalt, and nickel. It will be noted that the E.A.N. of the central atom in most of these compounds is that of the next higher inert gas. In a few cases, the E.A.N. is one or two units less than that of the corresponding inert gas. Infrequently, the E.A.N. may be one or two units more than that of the corresponding inert gas. In such cases, the oxidation state represented by the compound is usually unstable, *e.g.*, consider the ease with which $Co(CN)_6^{4-}$ (E.A.N. of Co = 37) is oxidized to $Co(CN)_6^{3-}$ (E.A.N. of Co = 36).

(*B*) *Radius Ratio Rules.* The existence of a chemical union between

TABLE X

EFFECTIVE ATOMIC NUMBER OF THE PLATINUM METALS IN COMPLEXES (5)

$M_4[Ru(CN)_6]$	44 − 2 + 12	54	Xe
$M_2[Ru(CN)_5NO]$	44 − 2 + 12	54	Xe
$M_2[RuCl_5NO]$	44 − 2 + 12	54	Xe
$M_3[Rh(CN)_6]$	45 − 3 + 12	54	Xe
$M_2[PdCl_6]$	46 − 4 + 12	54	Xe
$M_2[Pd(CN)_4]$	46 − 2 + 8	52	
$M_2[OsCl_6]$	76 − 4 + 12	84	
$M_3[OsCl_6]$	76 − 3 + 12	85	
$M_2[OsCl_5NO]$	76 − 2 + 12	86	Rn
$M_4[Os(CN)_6]$	76 − 2 + 12	86	Rn
$M_3[Ir(CN)_6]$	77 − 3 + 12	86	Rn
$M_2[PtCl_6]$	78 − 4 + 12	86	Rn
$M_2[PtCl_2(CN)_4]$	78 − 4 + 12	86	Rn
$M_2[Pt(CN)_4]$	78 − 2 + 8	84	

AB_2 $A/B > 0$
Two-coordination

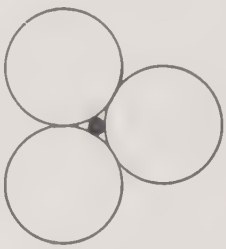

AB_3 $A/B \geqslant 0.15$
Three-coordination

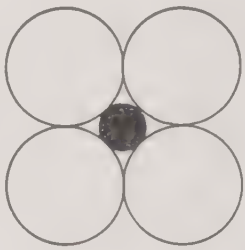

AB_4 $A/B \geqslant 0.41$
Planar four-coordination

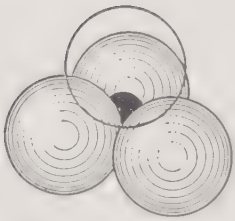

AB_4 $A/B \geqslant 0.22$
Tetrahedral four-coordination

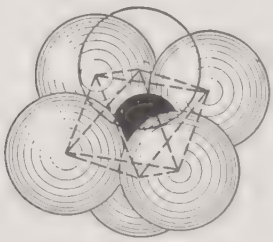

AB_6 $A/B \geqslant 0.41$
Six-coordination

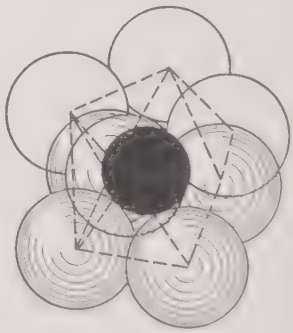

AB_8 $A/B \geqslant 0.65$
Anti-prismatic eight-coordination

Fig. 2. Coordination: ratios of radii.

two atoms implies direct contact between the atoms. The maximum coordination number of a central atom cannot be realized if that atom is too small to permit the packing of the necessary number of coordinated groups around it. Thus, for each coordination number (or geometrical configuration for a given coordination number) there is a limiting ratio (*radius ratio rules*) of central atom to coordinated atoms which must be met in order to realize experimentally that type of coordination (Fig. 2). The application of these radius ratios to the oxygen compounds of a limited number of elements is shown in Table XI. In general, the agreement with the experimental facts is very satisfactory.

TABLE XI

RADIUS RATIOS, ELEMENT:OXYGEN, AS FOUND IN CRYSTALS (6)

Be^{2+} 0.24	B^{3+} 0.19	C^{4+} 0.16	N^{5+} 0.14	RO_3^{n-} region		
Mg^{2+} 0.47	Al^{3+} 0.41	Si^{4+} 0.37	P^{5+} 0.34	S^{6+} 0.30	Cl^{7+} 0.28	RO_4^{n-} $M(H_2O)_4^{n+}$ region
Zn^{2+} 0.50	Ga^{3+} 0.46	Ge^{4+} 0.43	As^{5+} 0.40	Se^{6+} 0.37	Br^{7+} 0.35	
Cd^{2+} 0.65	In^{3+} 0.59	Sn^{4+} 0.55	Sb^{5+} 0.51	Te^{6+} 0.47	I^{7+} 0.44	
		RO_6^{n-} $M(H_2O)_6^{n+}$ region				

IV. Methods for Deduction of Structure

With these salient facts concerning the nature of coordination compounds in mind, we may proceed with a consideration of the methods which are available for the determination of structure and of the types of phenomena which are encountered in such studies. For convenience we may assume that the compounds to be considered have previously been prepared and purified and that the compositions have been determined. These qualifications are not always easy to meet. On several occasions mixtures have been mistaken for pure compounds with consequent difficulty in interpretation. Furthermore, all complex compounds are not

equally stable and many undergo changes in composition during operations designed to give information concerning their structures.

1. Identification of Ions

One simple approach to the structure of a complex compound is the identification of the ions present. Often this may be accomplished by chemical reactions. Thus, the structures $[Co(NH_3)_6]Cl_3$ and $[Co(NH_3)_5Cl]Cl_2$ are indicated for the compounds $CoCl_3 \cdot 6\,NH_3$ and $CoCl_3 \cdot 5\,NH_3$ because treatment of their aqueous solutions with silver nitrate precipitates three equivalents of silver chloride in the first case and only two in the second. The failure of a solution of $Co(NO_2)_3 \cdot 3\,NH_3$ to respond to the usual tests for the nitrite ion implies that all of the nitrite groups are coordinated to the cobalt. In many instances, specific reactions have been found for complex ions so that their presence can usually be demonstrated. Conductance data (Fig. 1), apparent molecular weights, and rates of diffusion have all been used to good advantage in determining the number and size of ions present.

2. Isomerism

The existence of isomers was of tremendous importance in establishing structural organic chemistry on a firm basis. Isomers have also played a leading role in developing the structural elements of coordination compounds. For convenience the cases of isomerism in this field may be classified into a number of types.

(*A*) *Simple Structural Isomerism.*

(1) Linkage Isomerism. If a given linkage has two possible points of attachment to a central atom, isomers may be expected, depending upon which point of attachment is involved in a given compound. In the case of the compounds having the composition $[Co(NH_3)_5NO_2](NO_3)_2$, one is red and unstable, the other yellow-brown and stable. The chemical transformations by which these compounds are formed indicates that both salts contain nitrite in complex ions. Further, the equivalent conductance indicates that both salts furnish the same number of ions. The relationships between the two series are summarized in Table XII. It would seem that the only source of the isomerism lies in the nitrite group. Since compounds like $[Co(NH_3)_5OH_2]Cl_3$, in which oxygen is undoubtedly attached to cobalt, are red, whereas those like $[Co(NH_3)_6]Cl_3$, in which only nitrogen atoms are attached to cobalt, are yellow, the nitrite group in the

TABLE XII

RELATIONSHIPS BETWEEN NITROSO AND NITRO COMPLEXES (7)

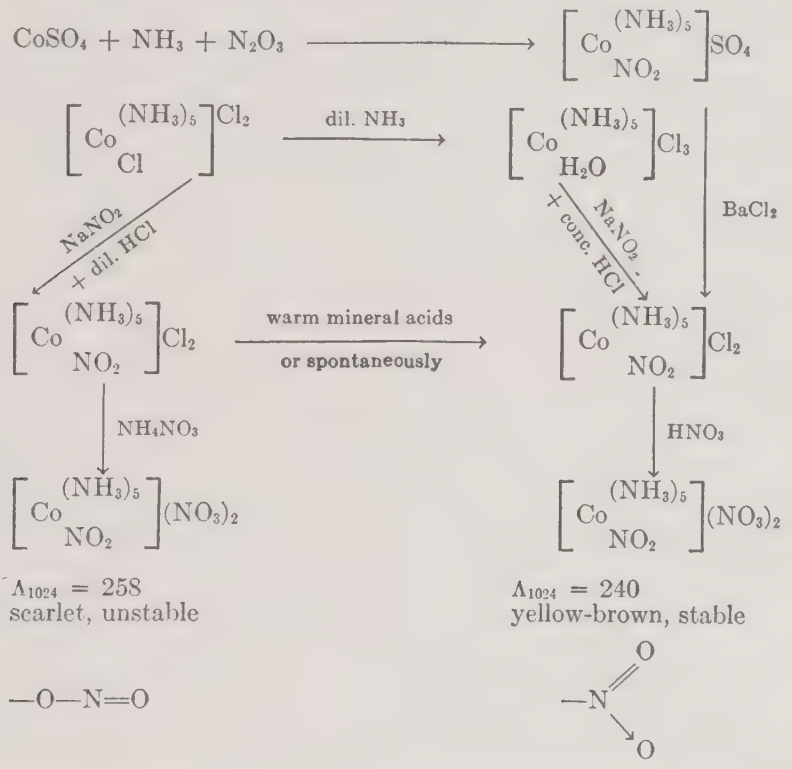

red unstable isomer is assigned the linkage —O—N=O, whereas in the yellow stable isomer, it is assigned the linkage —N(=O)→O. All that is known about these and similar nitrite complexes justifies these assignments. The claim that a similar example of linkage isomerism was shown by the thiocyanate group: —S—C≡N and —N=C=S has not been substantiated.

(2) COORDINATION ISOMERISM. Two compounds of identical composition may consist of entirely different complex ions because different groups are coordinated about the same coordination centers:

$[Co(NH_3)_6]^{3+},[Cr(CN)_6]^{3-}$ $\qquad$ $[Cr(NH_3)_6]^{3+},[Co(CN)_6]^{3-}$

(3) IONIZATION ISOMERISM. A condition of isomerism very similar to the above is shown in the two compounds:

$[Co(NH_3)_5Br]^{++},SO_4^{--}$ $\qquad$ $[Co(NH_3)_5SO_4]^{+},Br^{-}$

The two compounds give quite different reactions with common reagents. It is interesting to note that the sulfate group which is coordinated to cobalt in the second compound occupies only one coordination position although it carries two negative charges.

(4) Polymerization. The following compounds are not isomers although they have the same empirical composition:

$$[Co(NH_3)_3(NO_2)_3] \qquad [Co(NH_3)_6]^{3+}[Co(NO_2)_6]^{3-}$$

It is obvious that they would exhibit entirely different chemical behavior. Several such polymeric pairs have been encountered in the study of coordination compounds.

(*B*) *Stereoisomerism.*

(1) Cis-Trans (Geometrical) Isomerism. Of the possible spatial arrangement of six equivalent bonds about a central atom (six-coordination), all the facts support an octahedral arrangement (Fig. 3). The number of isomers obtained for various types of complexes justifies this conclusion. For convenience of representation the complex diagram of Figure 3 is usually abbreviated to that of Figure 4. It is to be remembered

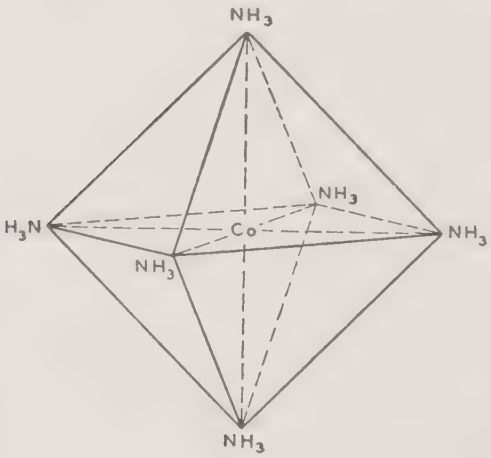

Fig. 3. Octahedral configuration of $[Co(NH_3)_6]^{3+}$.

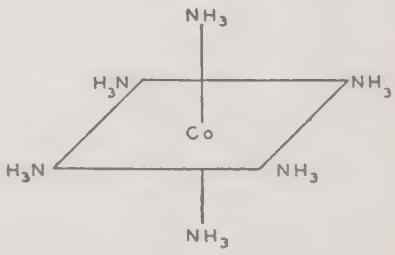

Fig. 4. Conventionalized representation of $[Co(NH_3)_6]^{3+}$.

that there is no difference between the bonds in the plane and those along the axis. Thus, the two representations of Figure 5 are equivalent.

It is evident that there can be no isomerism for a complex of the type $[Ma_5b]$. However, for those of the types $[Ma_4b_2]$ and $[Ma_4bc]$ only two

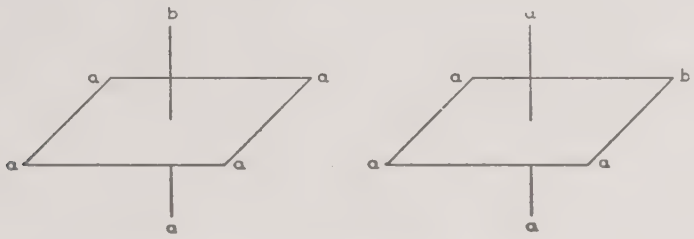

Fig. 5. Equivalent representations of [Ma_5b].

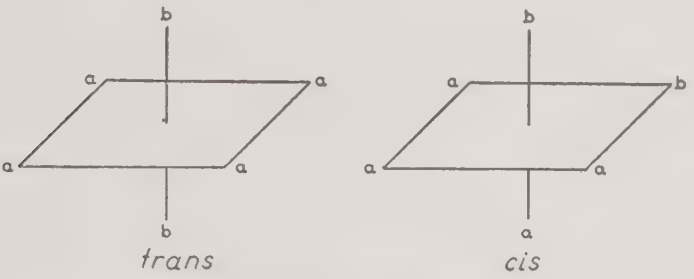

Fig. 6. Isomeric forms of [Ma_4b_2].

isomers are to be expected (Fig. 6). This conclusion is completely justified by the experimental findings. Similarly, only two isomers are to be expected for complexes of the type [Ma_3b_3] (Fig. 7).

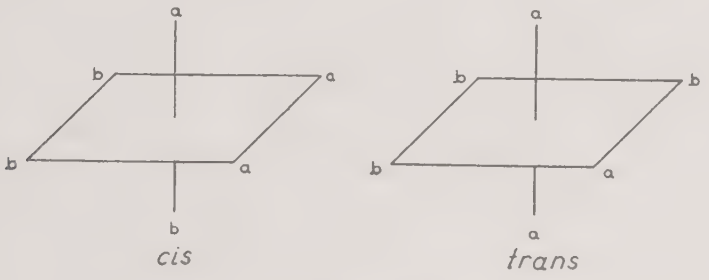

Fig. 7. Isomeric forms of [Ma_3b_3].

The common arrangement of four equivalent bonds in space (four-coordination) is tetrahedral, *e.g.*, the carbon atom. For a mononucleate complex exhibiting tetrahedral coordination, no *cis-trans* isomerism is possible. However, the four-coordinate compounds of a few elements, such as platinum, palladium, and nickel, exhibit a planar distribution of bonds. Here *cis-trans* isomerism is encountered among complexes of the type [Ma_2b_2]:

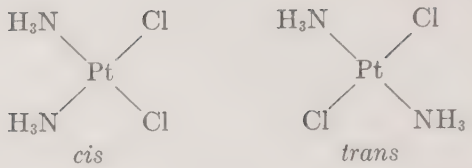

It is to be remembered at all times that the existence of isomers and their actual isolation are not synonymous. If a complex dissociates readily it may not be possible to isolate the pure isomers, but only an equilibrium mixture. Further, if one form is more stable, the less stable form may be readily converted into the more stable form. Fortunately, a sufficient number of coordination complexes are stable enough (some remarkably so) to justify the theoretical conclusions completely. In specific instances, this may not be true.

(2) Optical (Mirror Image) Isomerism. Although geometrical isomerism occurs among comparatively simple types of nonchelate coordination compounds, enantiomorphic pairs are not encountered until the types with at least three different kinds of coordinated groups are reached, such as $[Ma_2b_2c_2]$ and $[Ma_3bcd]$. However, there are few, if any, authenticated examples of such types of compounds; so any search for optical isomerism among coordination compounds must be in other directions.

In contrast to the unidentate types, some of the simplest chelate types show optical isomerism. Thus, any coordination complex of the type $[M(AA)_3]$, where AA represents a symmetrical bidentate group like ethylenediamine or oxalate ion, will exist in mirror image forms (Fig. 8). Many

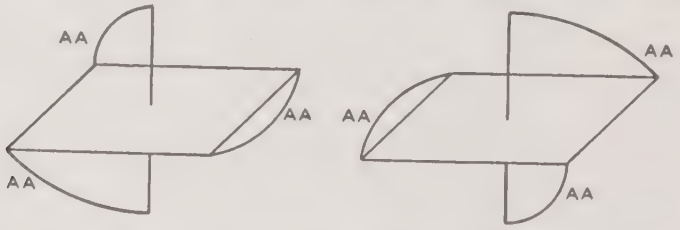

Fig. 8. Mirror-image forms of $[M(AA)_3]$.

examples of such enantiomorphic pairs have been resolved experimentally. The types $[M(AA)_2b_2]$ and $[M(AA)_2ab]$ are interesting because they exist in three forms: one enantiomorphic pair and one inactive compound (Fig. 9). There are definite and sometimes serious limitations to the experimental realization of the theoretically expected substances. Among these limitations are: ready racemization (large instability constant), steric hindrance preventing or restricting the formation of certain isomers, and

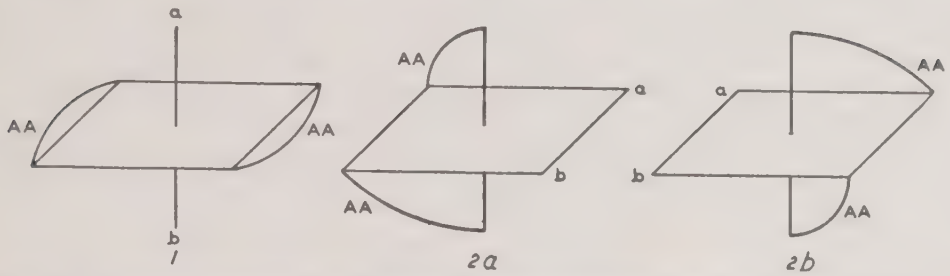

Fig. 9. Isomeric forms of $[M(AA)_2ab]$: (*1*) inactive; (*2a*) and (*2b*) enantiomorphic pair.

lack of means of resolution, such as unfavorable solubility relationships of compounds formed with resolving agent and, for nonelectrolyte complexes, lack of a reactive group for attachment of resolving agent.*

3. Substitution Reactions

The organic chemist has utilized the proof of structure by means of chemical reactions. Much the same type of reasoning may be employed in the determination of the configuration of a coordination complex. There are two assumptions which must be made: (*1*) that there is no *trans* bridging of a bifunctional group and, (*2*) that when such a chelate is replaced by, or replaces, two unidentate groups, they must also be *cis*. In one sense the first of these is hardly an assumption because it follows from molecular dimensions that many of the common chelate groups are too short to bridge *trans*. The second assumption implies that no intramolecular change of configuration takes place during a reaction. Although this is not always true, it is usually possible to recognize when it enters the picture. On the whole, many complexes seem to be more, rather than less, stable than might be expected.

The application of the principle of *cis* bridging to the proof of structure of typical cobalt and chromium complexes is shown in Tables XIII and XIV. There are two compounds of the composition $[Co(NH_3)_4Cl_2]Cl$, one of which is blue-violet and the other green (Table XIII). That the blue-violet salt is the *cis* isomer follows from its direct synthesis from $[Co(NH_3)_4CO_3]Cl$ in which the carbonate group occupies two coordination positions. This view is challenged by the fact that the green salt also can be obtained

*Partial resolution has been obtained by a method which is not subject to this restriction. From solutions of certain racemic complex compounds, optically active crystals (*e.g.*, quartz) preferentially adsorb one antipode. [Tsuchida, Kobayashi, and Nakamura, *J. Chem. Soc. Japan*, **56**, 1339 (1935).] The generality of this method has not been established.

Table XIII

Relationships among the Isomeric Dichlorotetrammine-cobalt(III) Salts (8)

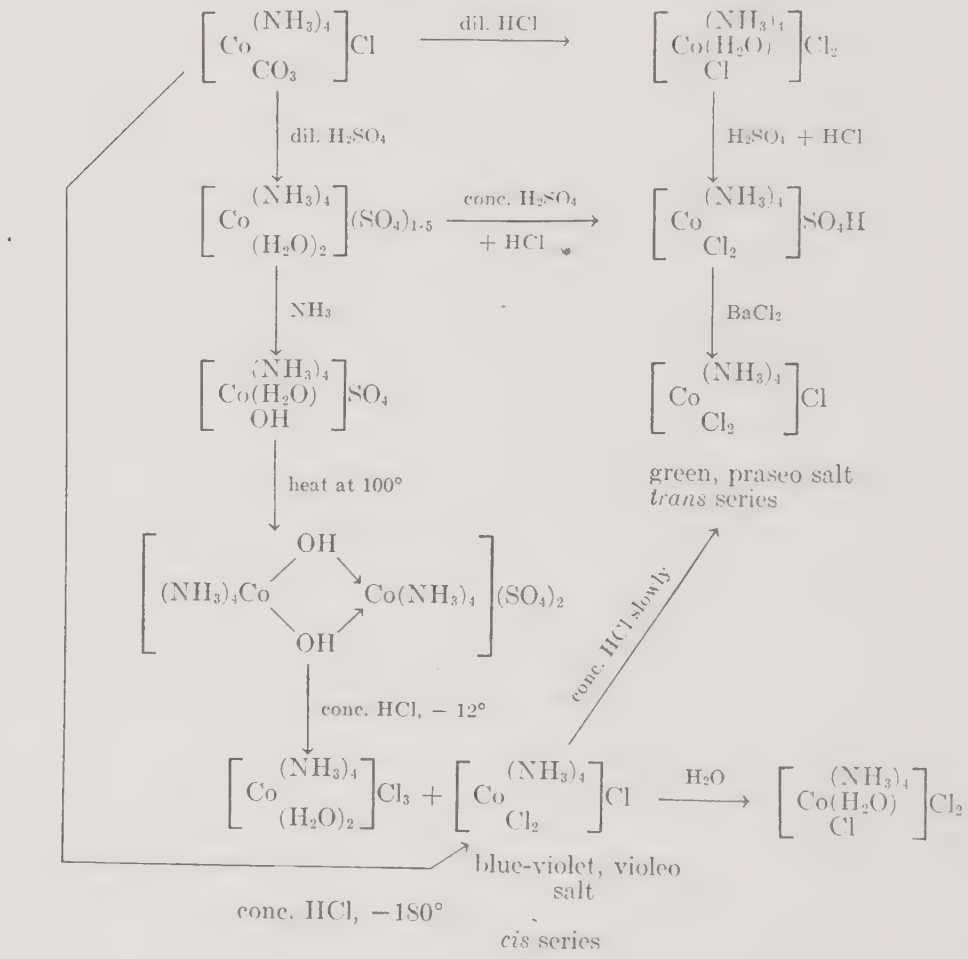

Table XIV

Relationships among the Isomers of Certain Complex Chromium Salts (9)

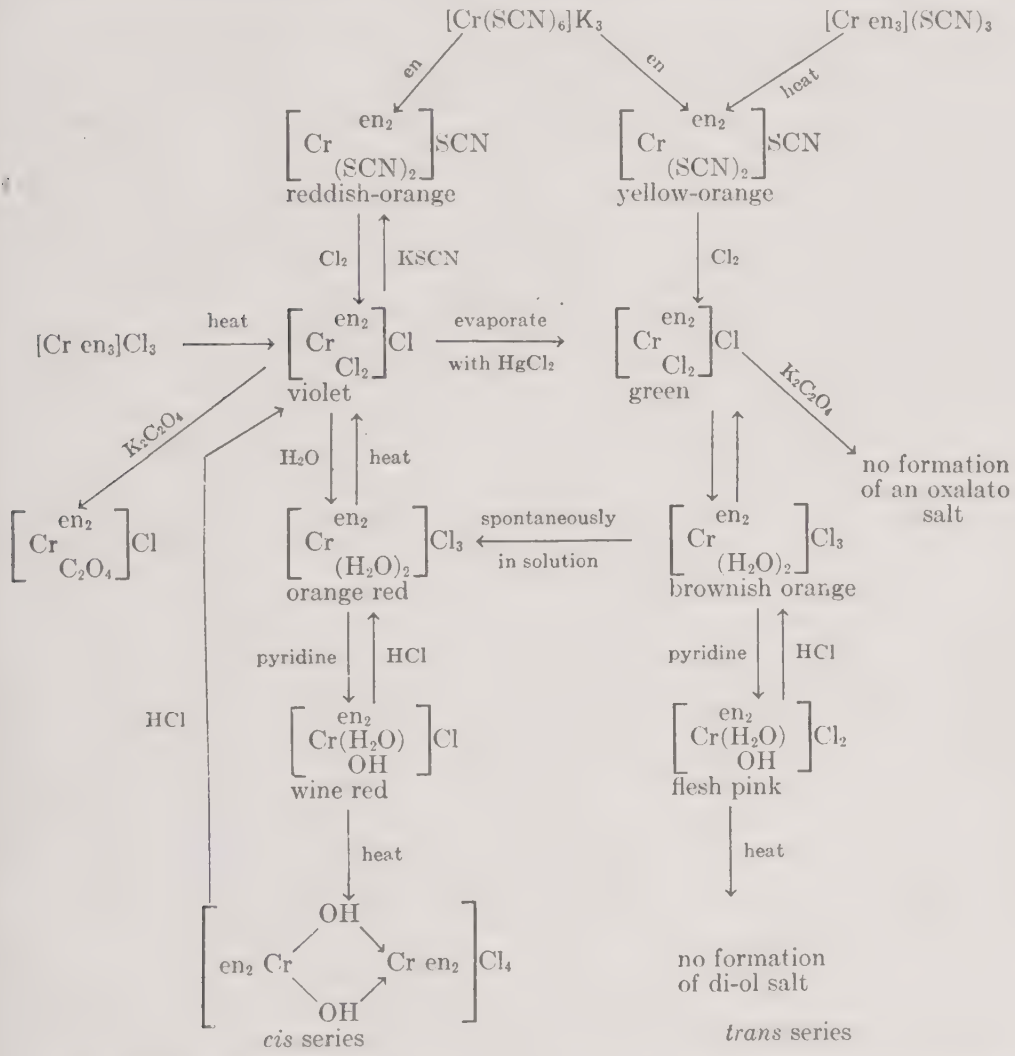

from $[Co(NH_3)_4CO_3]Cl$. However, it gains considerable support from the intermediate formation of the binuclear compound

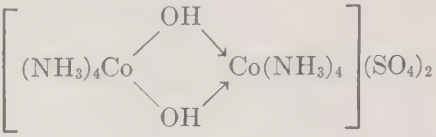

by a series of simple transformations which could hardly disturb the ammonia groups attached to the central cobalt atoms. Similarly, there are two compounds of the composition $[Cr(en)_2(SCN)_2]SCN$, where en = $H_2NCH_2CH_2NH_2$, one reddish orange, the other yellow-orange (Table XIV). The first of these can be transformed into an oxalato complex $[Cr(en)_2C_2O_4]^+$, and a diol (binucleate) complex and, hence, must be the *cis* isomer. The second thiocyanato salt forms neither an oxalato salt nor a diol, behavior which would be expected of the *trans* isomer. The transformation schemes show several cases of the transformation of a member of one series into the other series, either spontaneously or by means of some simple reagent. These transformations indicate how careful one must be in applying this particular proof of structure. Despite some outstanding cases of misinterpretation the applications of these principles have been extremely fruitful. Very frequently they constitute the only available method of approach.

4. X-Ray Studies

The application of x-rays to the study of the crystal structure of coordination compounds has been very helpful in giving information concerning the distribution of bonds about a coordination center. The advantage of the x-ray method is that it yields information about actual spatial relationships, including the sizes of the constituent parts. The disadvantage of the method is that its value is governed by the completeness of the analysis; a complete analysis is often not possible in complicated crystals. Further, the existence of an ion in a crystal does not always imply its existence as such in solution. There are two aspects to the results of a crystal structure pattern of a complex compound: the arrangement of the ions and the arrangement within the complex ion. A general survey of the results for the latter are given in Table XV.

In the purely chemical methods for the study of coordination compounds, one is concerned primarily with complex units which maintain an independent existence in solution. This situation is in sharp contrast with the highly condensed solid matter with which x-ray methods deal. It is not

TABLE XV

SHAPES OF CERTAIN IONS IN CRYSTALS (10)

Straight lines
HF_2^-, N_3^-, NCO^-, $Ag(NH_3)_2^+$, $Cd(NH_3)_2^{++}$, $Hg(NH_3)_2^{++}$, I_3^-, ICl_2^-, $Ag(CN)_2^-$
Kinked lines
NO_2^-, ClO_2^-
Triangles, central atom in plane
BO_3^{3-}, CO_3^{--}, $Cu(NH_2)_3^+$, $CO(NH_2)_2$, NO_3^-
Triangles, central atom out of plane (pyramids, or decapitated tetrahedra)
SO_3^{--}, ClO_3^-, BrO_3^-
Tetrahedra
SiO_4^{3-}, CrO_4^{--}, WO_4^{--}, MoO_4^{--}, MnO_4^-, PO_4^{3-}, SO_4^{--}, SeO_4^{--}, ClO_4^-, IO_4^-, ReO_4^-, VS_4^{3-}, AsS_4^{3-}, SnS_4^{3-}, BeF_4^{--}, BF_4^-, $Be(H_2O)_4^{++}$, $CoCl_4^{--}$, $Cu(CN)_4^{3-}$, $Zn(CN)_4^{--}$, $Cd(CN)_4^{--}$, $Hg(CN)_4^{--}$, $N(CH_3)_4^+$, $N(CH_3)_2H_2^+$, $PH_2O_2^-$, OsO_3N^-, $Zn(NH_3)_2Cl_2$
Squares, central atom in plane
$PtCl_4^{--}$, $PdCl_4^{--}$, $Pd(NH_3)_4^{++}$, $CuCl_2(H_2O)_2$, $AuBr_4^-$
Octahedra
AlF_6^{3-}, SiF_6^{--}, GeF_6^{--}, FeF_6^{3-}, $MoO_3F_3^{3-}$, $TiCl_6^{--}$, $ZrCl_6^{--}$, $PtCl_6^{--}$, $PdCl_6^{--}$, $SnCl_6^{--}$, $PbCl_6^{--}$, $SeCl_6^{--}$, $TeCl_6^{--}$, $OsO_2Cl_4^{--}$, $SeBr_6^{--}$, $Sn(OH)_6^{--}$, $Te(OH)_6$, $Co(NH_3)_6^{++}$, $Co(NH_3)_6^{3+}$, $Co(NH_3)_5H_2O^{3+}$, $NH_4(H_2O)_6^+$, $Cs(H_2O)_6^+$, $Mg(H_2O)_6^{++}$, $Al(H_2O)_6^{3+}$, $Cr(H_2O)_6^{3+}$, $Zn(H_2O)_6^{++}$, $Ni(H_2O)_6^{++}$, $Tl(H_2O)_6^+$, $Cr(NH_3)_5Cl^{++}$, $Co(NH_3)_5Cl^{++}$, $Rh(NH_3)_5Cl^{++}$, $Co(NO_2)_6^{3-}$, $Pt(SCN)_6^{--}$

surprising that the results of the two methods differ occasionally. The term coordination number is defined by the crystallographer as the number of nearest neighbors surrounding an atom or ion in a crystal. When one of the units in a crystal is a complex one, identical with that found in a solution of the compound concerned, x-ray and strictly chemical methods yield the same results. However, it is also possible, by means of x-ray analysis, to show the existence of complexes which, because of their instability, are not readily detectable in solution.

In the case of simple binary compounds having ionic lattices, the

crystallographer's use of the term *coordination number* is not the same as that of the student of complex compounds. Consider lithium fluoride with the sodium chloride type of structure where each ion has six close neighbors. Thus, the crystallographic coordination number of lithium is six, although the chemical coordination number never exceeds four. (Fluorine is not known to act as a coordination center in complex compounds). Similarly, the crystallographic coordination numbers of chlorine in cesium chloride and of calcium in calcium fluoride are at variance with the chemical findings. It would seem that the two usages of the term *coordination number* are not compatible when applied to binary compounds with strictly ionic lattices. On the other hand, the two usages are strictly compatible when applied to binary compounds which are dominantly covalent in character. Particularly interesting are the cases of *giant molecules* in which there are covalently linked chains or sheets extending throughout the crystal or the entire crystal is one large three-dimensional "compound," each of whose atoms is linked to its neighbors by covalent bonds (Fig. 10). The study of such compounds has given a good deal of information on the coordinating behavior of various elements. At times it has corroborated evidence from other lines of approach and, at others, has provided evidence when such was entirely lacking from other methods.

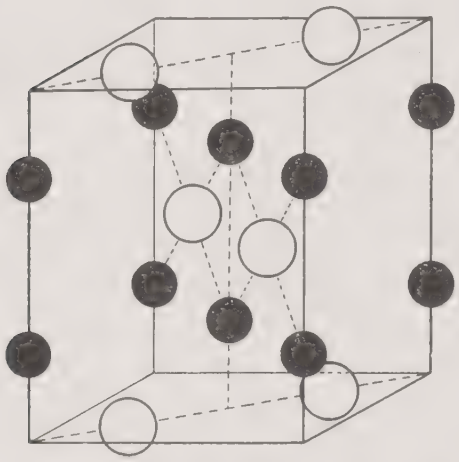

Fig. 10. Crystal structure of PtS: • = S; ○ = Pt.

5. *Electron Diffraction*

Although the electron-diffraction method has yielded very important information on many structural problems, the application of this technique to complex compounds is rather limited. Electron-diffraction studies are restricted to gaseous (or volatile liquid and solid) compounds and to comparatively simple compounds. They have been especially useful in providing information concerning the distribution of bonds in compounds representing coordination numbers which are not often encountered among complex ions (such as MX_5, representing coordination number five) and some molecular-addition compounds. Valuable information concerning bond types has been obtained from electron-diffraction studies.

6. Dipole Moments

All molecules of the type A—A are electrically symmetrical and, hence, are not dipoles. All molecules of the type A—B should have at least some electrical dissymmetry and, hence, should have a permanent electric moment. In a polyatomic molecule, AB_n, a dipole moment is associated with each A—B linkage and the permanent dipole moment of the molecule is the vector sum of all the individual bond moments. Thus, for a molecule with a center of symmetry, the vector sum of the individual dipole moments is zero.

It is apparent that the existence of a permanent dipole in one of two isomeric coordination compounds would clearly demonstrate which compound possesses a center of symmetry. The determination of the dipole moment of a substance requires that it be soluble in a nonpolar solvent. In general, salts do not meet this qualification; so that of the large field of coordination compounds, only the soluble neutral complexes can be studied.

For compounds exhibiting planar coordination, the *trans* isomer has a center of symmetry, while the *cis* isomer does not. The results of dipole measurements of a group of *cis* and *trans* isomers of a number of platinum(II) compounds are given in Table XVI. In harmony with the prediction,

TABLE XVI

DIPOLE MOMENTS OF PLATINUM(II) COMPOUNDS OF TYPE PtA_2X_2 (11)

Compound[a]	Dipole moment, Debyes	Compound[a]	Dipole moment, Debyes
trans-$[PtBr_2(Et_3P)_2]$	0	*cis*-$[PtBr_2(Et_3P)_2]$	11.2
trans-$[PtI_2(Et_3P)_2]$	0	*cis*-$[PtI_2(Et_3P)_2]$	8.2
trans-$[PtCl_2(Pr_3P)_2]$	0	*cis*-$[PtCl_2(Pr_3P)_2]$	11.5
trans-$[PtCl_2(Et_3As)_2]$	0	*cis*-$[PtCl_2(Et_3As)_2]$	10.5
trans-$[PtI_2(Et_3Sb)_2]$	0	*cis*-$[PtCl_2(Et_3Sb)_2]$	9.2
trans-$[PtCl_2(Bu_3P)_2]$	0	*cis*-$[PtCl_2(Bu_3P)_2]$	11.5
trans-$[PtCl_2(Pr_2S)_2]$	2.35	*cis*-$[PtCl_2(Pr_2S)_2]$	9.5
trans-$[PtCl_2(Bu_2S)_2]$	2.35	*cis*-$[PtCl_2(Bu_2S)_2]$	9.2
trans-$[Pt(NO_2)_2(Pr_2S)_2]$	2.48	*cis*-$[Pt(NO_2)_2(Pr_2S)_2]$	13.1
trans-$[PtBr_2(Et_2S)_2]$	2.26	*cis*-$[PtBr_2(Et_2S)_2]$	8.9

[a]Et = ethyl; Pr = propyl; Bu = butyl.

the *trans* phosphine compounds have no dipole moment, whereas the *cis* compounds have a definite moment. Although the *cis* sulfide complexes

possess a considerably larger moment than the *trans* compounds, the latter nevertheless exhibit a definite moment which does not vary greatly among the different compounds. This situation is accounted for by the lack of symmetry due to the unshared pair of electrons of the sulfur atom (Fig. 11).

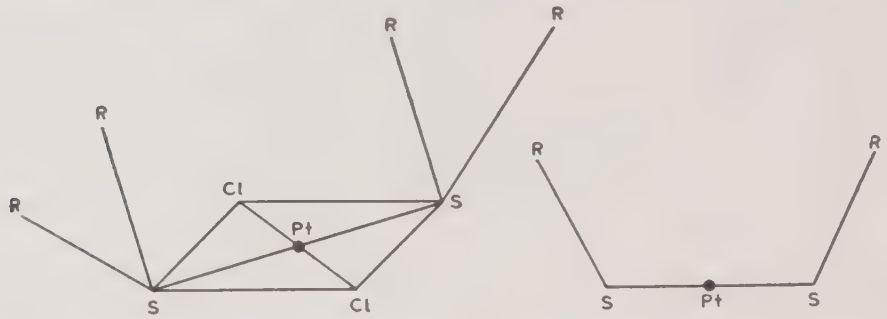

Fig. 11. *Trans*-planar structure for $[PtCl_2(R_2S)_2]$ showing that the S—C moments are not directed along the direction of the Pt—S bonds.

7. *Theory of Orbitals*

On the basis of quantum-mechanical considerations, Pauling has developed a theory of the electronic orbitals involved in bonding and their direction in space (12). As Table XVII shows, when two p orbitals are involved,

TABLE XVII

ATOMIC ORBITALS AND BOND CONFIGURATIONS

Orbitals	Configuration
p^2	Right angle
sp^3	Tetrahedral
dsp^2	Planar
d^3s	Tetrahedral
d^2sp^3	Octahedral

the bonds are at right angles to each other. Likewise, the hybridization of one s orbital with three p orbitals leads to a tetrahedral distribution of bonds. Similarly, the hybridization dsp^2 leads to a planar distribution, d^3s to a tetrahedral, and d^2sp^3 to an octahedral distribution. The application of these principles to specific complexes is illustrated in Table XVIII.

It is to be remembered that this treatment applies only to covalent bonds (not ionic) and then only to those which are free to arrange (nonforced configuration).

Table XVIII

Atomic Orbitals and Bond Configurations

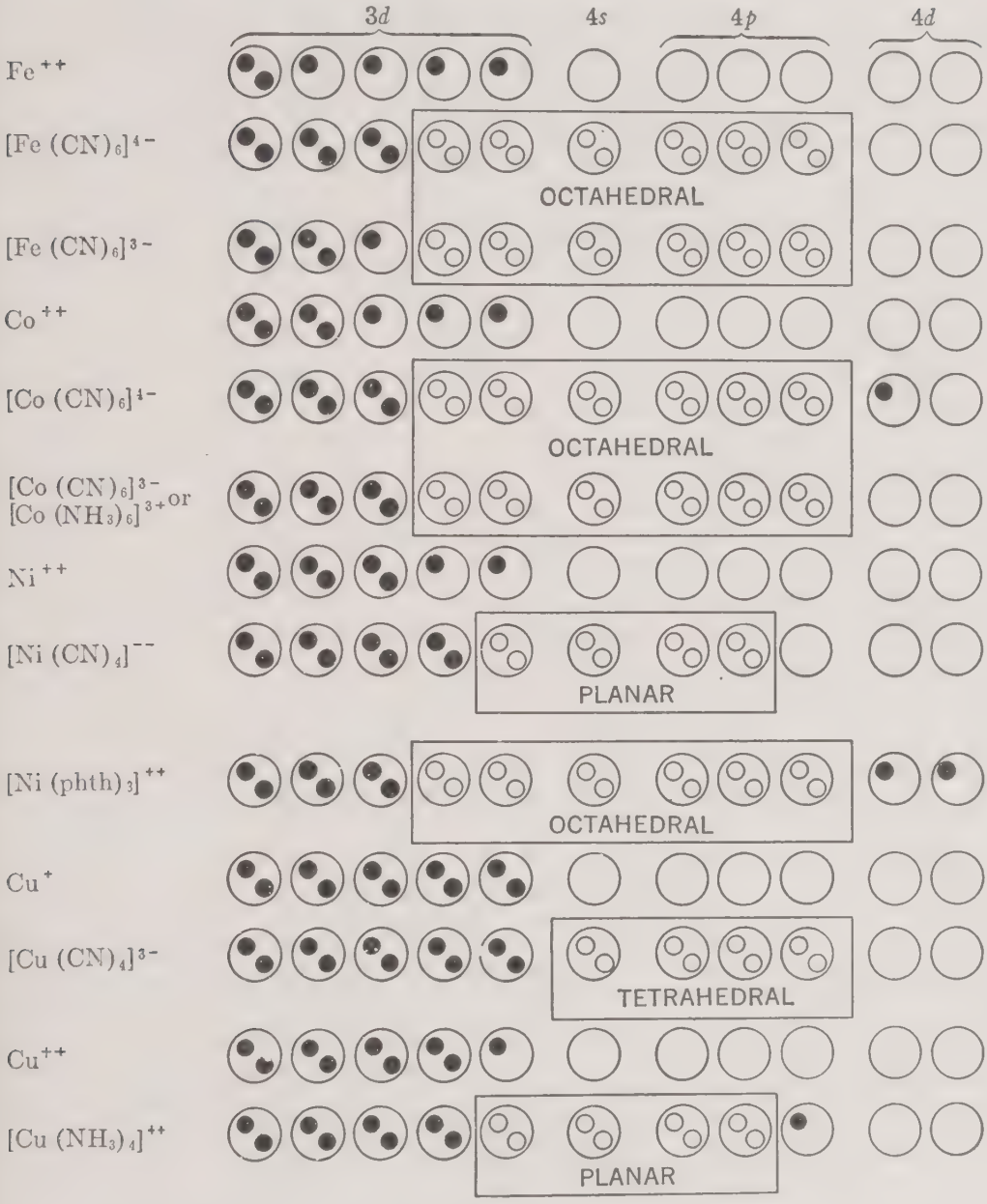

8. Magnetic Considerations

Paramagnetism is due to unpaired electrons in a given system and its magnitude is related to the number of unpaired electrons. In this connection the approximate relationship: $\mu = \sqrt{n(n+2)}$, when μ is the effective magnetic moment in Bohr magnetons and n is the number of unpaired electrons, is very useful. Completely closed configurations (filled quantum groups) are diamagnetic. Thus, $[Fe(CN)_6]^{4-}$ (Table XVIII) has a completely closed configuration and is diamagnetic, whereas $[Fe(CN)_6]^{3-}$ has one unpaired electron and is paramagnetic. In a similar manner it is evident why $[Co(CN)_6]^{4-}$ is paramagnetic, whereas $[Co(CN)_6]^{3-}$ and $[Co(NH_3)_6]^{3+}$ are diamagnetic, why planar tetracoordinated nickel compounds are diamagnetic, whereas hexacoordinated ones are paramagnetic, and why the magnetic behavior of tetracoordinated copper compounds depends upon the oxidation state.

In this same connection Sidgwick and Bose formulated a rule earlier that the number of unpaired electrons in a complex is equal to the difference between the E.A.N. of the metal atom and the atomic number of the nearest rare gas. The paramagnetism can be calculated from the number of unpaired electrons. Table XIX shows how this rule may be successfully ap-

TABLE XIX

CALCULATION OF MAGNETIC SUSCEPTIBILITY BY THE SIDGWICK-BOSE RULE (14)

$[Cu(NH_3)_4]^{++}$		$[Ni(dipyridyl)_3]^{++}$	
Cu^{++}	27 electrons	Ni^{++}	26 electrons
$4\ NH_3$	8	3 dipyridyl	12
Total E.A.N.	35	Total E.A.N.	38
36 − E.A.N. =	1 unpaired electron	E.A.N. − 36 =	2 unpaired electrons
μ (calculated)	1.73 Bohr magnetons	μ (calculated)	2.83 Bohr magnetons
μ (found)	1.82	μ (found)	2.8

plied to complexes. While this rule gives the correct results for many complex salts, it cannot be successfully applied to planar four-coordinated compounds.

Magnetic data are of particular importance in the study of coordination compounds because they often serve as a criterion for distinguishing between covalent and ionic complexes. In contrast to $[Fe(CN)_6]^{3-}$ which has an effective magnetic moment of 1.73 Bohr magnetons, $[FeF_6]^{3-}$ has an effec-

tive moment of 5.9 magnetons. Since the Fe^{3+} ion with five unpaired d electrons has a theoretical effective moment of $\sqrt{5(5+2)} = 5.92$, it is evident that $[FeF_6]^{3-}$ must have a structure which is primarily ionic. Other fluoride complexes, many hydrates, and some ammines have magnetic moments corresponding to essentially ionic structures. Failure of attempts to resolve certain complex ions into their optical antipodes has been related to their ionic character (15). Thus, the magnetic susceptibilities of the unresolvable complexes $[Mn(C_2O_4)_3]^{3-}$ and $[Fe(C_2O_4)_3]^{3-}$ indicate that they are essentially ionic, whereas $[Co(C_2O_4)_3]^{3-}$ which can be resolved is essentially covalent (Table XX). By inference, $[Al(C_2O_4)_3]^{3-}$ is ionic and

TABLE XX

MAGNETIC SUSCEPTIBILITIES OF SOME OXALATE COMPLEXES

Complex	μ
$K_3Mn(C_2O_4)_3 \cdot 3\ H_2O$	4.88
$K_3Fe(C_2O_4)_3 \cdot 3\ H_2O$	5.75
$K_3Co(C_2O_4)_3 \cdot 3.5\ H_2O$	0.00

$[Cr(C_2O_4)_3]^{3-}$ covalent because the former cannot be resolved, whereas the latter can be. Such considerations as these raise several important questions. Can the difference in the molecular volume of ammonia in the so-called *normal* (normal molecular volume) and *penetration* (small molecular volume) complexes (16) be related to bond type? Is there any relationship between instability constant and bond type (or resolvability)? Are ionic bonds directed in space as are covalent bonds? It is to be hoped that further work will produce answers to these questions.

In common with other methods for studying coordination compounds, the application of magnetic data has certain limitations. The nontransition elements, as well as their complexes, are uniformly diamagnetic. In the case of chromium(III) complexes, the extreme types of electrovalence and covalence have the same number of unpaired electrons. Hence, little can be learned from magnetic measurements.

9. Radioactive Isotopes

Only a few applications of radioactive isotopes to the study of complex compounds have been made, but the meager work which has been done indicates that a good deal of information may be expected from such studies in the future.

The lack of exchange between the two sulfur atoms in $S_2O_3^{--}$ shows that they are not equivalent (17). Further light is thrown on the nature of the linkage in thiosulfates by the slow exchange between S^{--} and $S_2O_3^{--}$ and the lack of exchange in the following systems: S^{--} and SO_4^{--} in alkaline solution, SO_3^{--} and SO_4^{--} in acid or alkaline solution (36 hours at 100°), and SO_3^{--} and $S_2O_3^{--}$ at 20° (complete exchange of one sulfur does take place within an hour at 100°) (18,19). Similarly, there is no exchange between the iron atoms in a mixture of $[Fe(CN)_6]^{4-}$ and $[Fe(CN)_6]^{3-}$ either in slightly acid or slightly alkaline solution, between Fe^{3+} and $[Fe(CN)_6]^{3-}$, or between the iron atoms in precipitates of Prussian or Turnbull's blue (20). Radioactive chlorine has been used to show that the interconversion in aqueous solution of green *trans*-dichlorobis(ethylenediamine)cobalt(III) chloride to the violet *cis* isomer does not proceed by an intramolecular mechanism (21).

A very interesting application of radioactive isotopes has been made in the study of complex oxalato ions, $[M(C_2O_4)_3]^{3-}$, with oxalate ion made with radioactive carbon (22). The compounds of Fe(III) and Al(III) show rapid exchange, while those of Co(III) and Cr(III) exhibit no interchange. As mentioned in the previous section, the iron and aluminum complexes involve predominately ionic bonds and have not been resolved, whereas the complexes of cobalt and chromium are predominantly covalent and have been resolved into their optical antipodes.

10. Optical Properties

No one who has worked with coordination compounds can fail to be impressed by the array of colors which they exhibit. There can be no question but that attachment of coordination groups modifies the electronic structure of the central atom. The color of the ions of the transition elements arises from the incompleted *d* orbitals. Since it is precisely these orbitals which are involved in complex formation, their rearrangement must introduce changes in the absorption spectrum and, the more pronounced the rearrangement, the more profound the change in the spectrum. Contrast the red color of the stable $[Ni(phenanthroline)_3]^{++}$ ion with the light green of the dissociable $[Ni(H_2O)_6]^{++}$ ion or the purple of the $[Ni(NH_3)_6]^{++}$ ion.

The study of Raman spectra has contributed to our knowledge of coordination compounds. Although the color of many complex compounds has prevented the application of the Raman method, several cyanide and a few ammine complexes have been studied. For these Raman displacements have been found which must be due to the vibrational frequencies

of the coordinate link. The force constants are rather smaller than those for ordinary single bonds but are of the same order of magnitude. Some effort has been made to deduce the configuration of a complex ion from the number of lines in its Raman spectrum and the state of polarization of each line. However, it cannot be said that the method has yet reached a satisfactory stage of development.

The data of crystal optics have some usefulness in indicating the structure of complex compounds. The striking double refraction of crystals of the isomorphous series, calcium carbonate, sodium nitrate, and scandium borate, which is due to the presence of parallel planar XO_3 ions, suggested that similar optical properties would be found among crystals of compounds with planar four-coordinated units. Double refraction is high for all platinum(II) complexes so far examined; whereas only a small value would be expected for a tetrahedral configuration of the complex ions. Since double refraction depends not only on the presence of anisotropic units but also on their arrangement, one must recognize a limit to the application of the data of crystal optics. While high double refraction indicates the presence of highly anisotropic units in a structure, low double refraction does not necessarily mean that such units are absent. One must also keep in mind that double refraction is subject to dispersion and take care that measurements are not made with a wave length at which the magnitude of the effect is low or at a minimum.

V. Results

Now that we have a picture of the various methods available for the determination of the structure of coordination compounds, it is of interest to review briefly the general results of such studies, particularly to see what bond distribution has been found for individual elements, and to comment on significant findings. A convenient procedure is to consider the various coordination numbers. An excellent summary organized somewhat differently and containing a complete bibliography has been published by Sidgwick and Powell (23).

1. Coordination Number Two

The two bonds of a central atom are directed linearly or angularly (examples are given in Table XV, page 75). Whenever the valence group contains less than eight electrons: *e.g.*, Br—Hg—Br, $R_3P\rightarrow Au—I$, and $[CH_3—Tl—CH_3]^+$, the bonds are directed in a straight line. For a complete octet as found in compounds of oxygen and other elements of the sulfur

group, the valence angle is between 90° and 110°. All such compounds possess a permanent dipole moment. The *imperfect octet*, found in ClO_2, B_2H_6, $SnCl_2$, and $PbCl_2$, leads to structures which are similar to those formed with complete octets. However, when the valence group contains five pairs of electrons, three of which are inert, the structure is linear, *e.g.*, $[ICl_2]^-$.

2. Coordination Number Three

The two structures for compounds built around a central atom with coordination number of three are planar (valence angle = 120°) and pyramidal. The former is found in compounds with a valence group of six electrons, BX_3 and $(CH_3)_3B$, while the latter is invariable for a completed valence octet (compounds of nitrogen, phosphorus, arsenic, antimony, bismuth, oxygen, sulfur, selenium, tellurium, bromine, iodine). The structure of compounds containing ten electrons in the valence group ($C_6H_5ICl_2$) has not been investigated.

3. Coordination Number Four

As has already been mentioned, the possibilities in this case are the tetrahedral and planar configurations. The theoretically possible types

TABLE XXI

TYPES AND CLASSES OF COMPOUNDS OF AN ELEMENT EXHIBITING A COORDINATION NUMBER OF FOUR (24)

Class	Number of chelate groups		
	None	One	Two
	Type 1	Type 2	Type 3
i	a a a a	AA b b	AA AA
ii	a a a b	AB c c	AA BB
iii	a a b b	AA b c	AA BC
iv	a a b c	AB c d	AB AB
v	a b c d		AB CD

and classes of compounds of an element exhibiting a coordination number of four are given in Table XXI. For the element carbon all of these types are known but this is very probably not true for any other element.

(*A*) *Tetrahedral Configuration.* In Table XXII are listed the various classes of compounds of an element exhibiting tetrahedral symmetry and

TABLE XXII

ISOMERIC CLASSES AND FORMS FOR A TETRAHEDRAL CONFIGURATION (24)

Type	Class symbol	Optically active	Optically inactive	Total
1	4a	—	1	1
	3a b	—	1	1
	2a 2b	—	1	1
	2a b c	—	1	1
	a b c d	2	—	2
2	AA 2b	—	1	1
	AB 2c	—	1	1
	AA b c	—	1	1
	AB c d	2	—	2
3	2AA	—	1	1
	AA BB	—	1	1
	AA BC	—	1	1
	2AB	2	—	2
	AB CD	2	—	2

the number of forms to be expected in each class. It is to be noted that isomerism is involved in only four cases, and in these the isomerism is that of optically active pairs. Compounds of the class [Mabcd] have been prepared for a number of elements (nitrogen, phosphorus, arsenic, sulfur, silicon, etc.) and successfully resolved. Thus, there is no question of the tetrahedral symmetry of such elements.

Compounds of the class $[M(AB)_2]$, as illustrated by beryllium benzoylpyruvate:

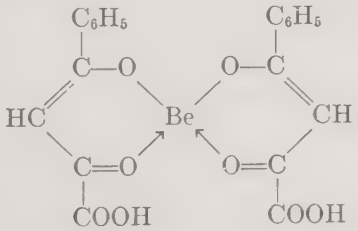

have been successfully resolved when, as in this instance, the molecule possesses a functional group capable of compound formation with a resolving agent. If beryllium benzoylpyruvate were planar, it would be expected to show *cis-trans* isomerism but not optical isomerism. Similar compounds of silver and boron have been resolved.

The question arises in all cases of whether the spatial distribution of

bonds exhibited by an atom is rigid or whether it may be bent out of the normal distribution by the application of suitable stress. This question has been settled for elements which normally exhibit square coordination in a very interesting way (25). Tris(2-aminoethyl)amine:

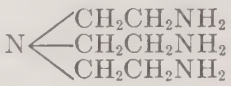

is a quadridentate group with each of the four nitrogen atoms capable of coordinating to metal atoms. If scale models of this molecule are constructed, it is found that the free rotation about each single bond permits a number of different spatial arrangements. However, in none of these arrangements are all four nitrogen atoms in the same plane and sufficiently close together to permit coordination to a central atom. On the other hand, the molecule can take a position such that the four nitrogen atoms occupy the four apexes of a tetrahedron. Hence, it follows that in the complex ion $[PtN(CH_2CH_2NH_2)_3]^{2+}$ the bonds of platinum(II) which are normally directed toward the corners of a square are distorted into a tetrahedral arrangement (Fig. 12). Such a distortion from a normal

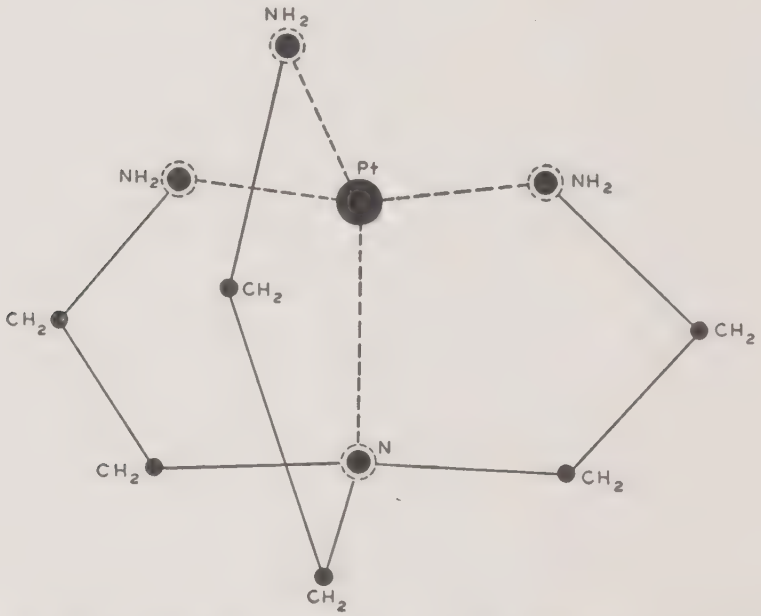

Fig. 12. Tetrahedral configuration of $[PtN(CH_2CH_2NH_2)_3]^{2+}$.

configuration is known as a *forced configuration.* Other examples will be discussed in the next section.

The elements for which tetrahedral coordination has been demonstrated by one or more means are listed in Table XXIII.

Table XXIII

Elements Exhibiting Tetrahedral Four-Coordination

	Be	B	C	N	O						
	Mg[a]	Al	Si	P	S	Cl					
			Ti	V	Cr	Mn	Fe	Co	Ni[b]		
Cu	Zn	Ga[a]	Ge	As	Se						
				Cb	Mo				Pd[b]		
Ag	Cd	In[a]	Sn	Sb[a]	Te	I					
				Ta	W	Re	Os		Pt[b]		
	Hg	Tl	Pb								

[a]Elements for which a tetrahedral configuration has been demonstrated only for compounds of the type MgTe, AlP, GaAs, InN, and GaSb by x-ray methods.
[b]With the exceptions of $Ni(CO)_4$ and $Pt(CH_3)_3Cl$, these elements are tetrahedral only in forced configurations.

Table XXIV

Isomeric Classes and Forms for a Planar Configuration (24)

Type	Class symbol	Number of isomeric forms				
		Optically active	Optically inactive			*Total*
			Cis	*Trans*	Others	
1	4a	—	—	—	1	1
	3a b	—	—	—	1	1
	2a 2b	—	1	1	—	2
	2a b c	—	1	1	—	2
	a b c d	—	—	—	3	3
2	AA 2b	—	—	—	1	1
	AB 2c	—	—	—	1	1
	AA b c	—	—	—	1	1
	AB c d	—	—	—	2	2
3	2AA	—	—	—	1	1
	AA BB	—	—	—	1	1
	AA BC	—	—	—	1	1
	2AB	—	—	2	—	2
	AB CD	—	—	—	2	2
Total		None	2	4	15	21

(B) Planar Configuration. The various classes of compounds of an element with a coordination number of four exhibiting a planar configuration and the number of forms to be expected in each class are shown in Table XXIV. It is evident that any optical activity encountered among four-coordination compounds cannot arise from the central atoms but must be attributed to the coordinating groups.

The *cis-trans* isomerism of compounds of the class $[Ma_2b_2]$ has already been discussed. That of compounds of classes $[Ma_2bc]$ and [M(AB)cd] is of the same character. The three forms expected for class [Mabcd] (Fig.

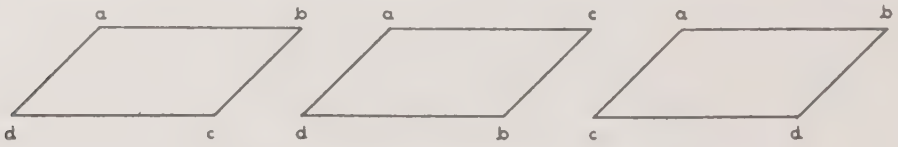

Fig. 13. Isomeric forms of [Mabcd].

13) have actually been realized for the composition $[PtNH_3(NH_2OH)C_6H_5N(NO_2)]NO_2$ (26).

The planar (rather than pyramidal) character of compounds of the class $[M(AA)_2]$ is clearly shown by the crystal structure of bis(dithiooxalato) complexes:

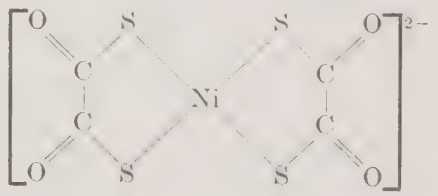

Bis(dithiooxalato)nickel(II) Ion

as deduced from x-ray studies. The planar configuration of this same class is strongly indicated by the calculations summarized in Fig. 14, in which the angles in a diamine ring attached to a platinum atom are given, on the assumptions that: (*a*) the platinum has a planar (square) configuration and (*b*) the platinum has a tetrahedral configuration (the ring is assumed

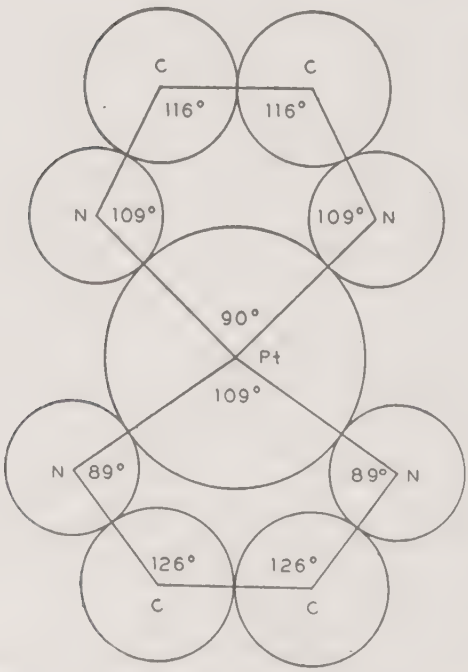

Fig. 14. Angles in a diamine ring attached to a platinum atom.

to be in a plane in both cases). Since the normal valence angles of carbon and nitrogen are tetrahedral (109.5°), there is much more strain for a tetrahedral arrangement of the platinum bonds than for a planar arrangement.

The planar character of a compound of the type [M(AA)(BC)] has been demonstrated in a rather ingenious manner. The ion shown in Fig. 15

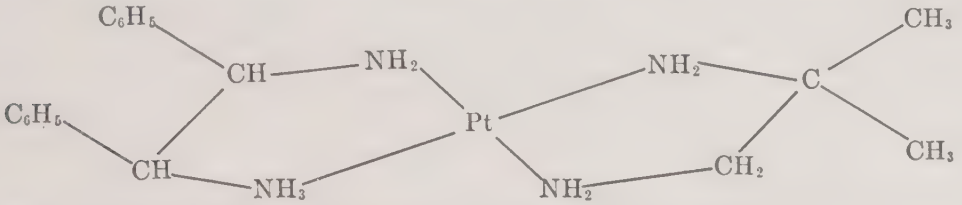

Fig. 15. Compound of the type [M(AA)(BC)] showing absence of a plane of symmetry in the planar configuration.

possesses no plane of symmetry and hence, should be optically active, which is confirmed experimentally. If one ring were horizontal and the other vertical, as would be required by a tetrahedral central atom, there would be a plane of symmetry and, hence, no optical activity.

Phthalocyanine is a remarkably stable compound whose metal derivatives have recently been studied rather extensively:

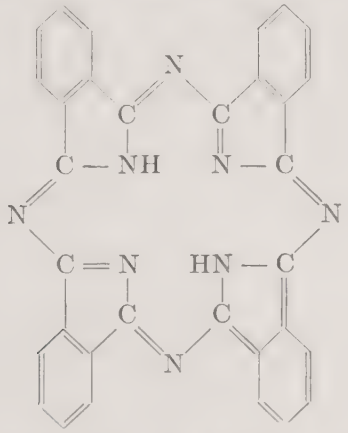

The compound is quadridentate and strictly planar. Many elements which are normally tetrahedral form stable compounds with the phthalocyanine nucleus. These cases present fine examples of forced configurations.

The elements for which planar coordination has been demonstrated are given in Table XXV. It is interesting that the ion $[ICl_4]^-$ which contains twelve electrons in the valence group (two inert pairs) is planar.

TABLE XXV

ELEMENTS EXHIBITING PLANAR COORDINATION NUMBER FOUR[a]

	Be							
	Mg	Al						
	Ca			Cr	Mn	Fe	Co	Ni
Cu	Zn							Pd
Ag	Cd		Sn	Sb		I		
	Ba							Pt
Au	Hg		Pb					

[a]Those elements which are planar only in the phthalocyanine derivatives are enclosed.

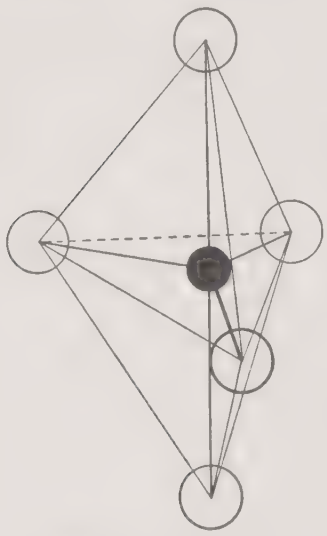

Fig. 16. Trigonal bipyramid.

4. Coordination Number Five

Typical coordination complexes exhibiting a coordination number of five are very rare; in fact, there is some question as to whether their existence has been definitely established. However, several neutral molecules with five atoms surrounding a central atom are known. Insofar as these have been studied (PX_5, CbX_5, TaX_5, $MoCl_5$, $(CH_3)_3SbX_2$, $Fe(CO)_5$), the bonds have been found to be directed toward the apexes of a trigonal bipyramid (Fig. 16).

5. Coordination Number Six

Although compounds with elements exhibiting a coordination number of six have been extensively studied, both by x-ray and various chemical methods, there is no evidence for any type of configuration other than octahedral. The only exceptions are a few giant molecules, like MoS_2, which contains trigonal prismatic Ma_6 groups. Despite much synthetic work in this field, many of the theoretically possible classes of compounds shown in Table XXVI have not been realized experimentally. The complexity of the field is clearly indicated by the number of isomers to be expected for each class (see Table XXVII). Furthermore, while several general types of reaction are evident for this group of compounds, they have not been developed to the point where the synthetic chemist has at his command a series of

Table XXVI

Types and Classes for Six-Coordination Compounds (24)

Class	Number of bidentate groups			
	None	One	Two	Three
	Type 1	Type 2	Type 3	Type 4
i	6a	AA 4b	2AA 2b	3AA
ii	5a b	AB 4c	AA BB 2c	2AA BB
iii	4a 2b	AA 3b c	2AA b c	AA BB CC
iv	4a b c	AB 3c d	AA BB c d	2AA BC
v	3a 3b	AA 2b 2c	AA BC 2d	AA BB CD
vi	3a 2b c	AB 2c 2d	2AB 2c	3AB
vii	3a b c d	AA 2b c d	AB CD 2e	AA 2BC
viii	2a 2b 2c	AB 2c d e	2AB c d	AA BC DE
ix	2a 2b c d	AA b c d e	AA BC d e	2AB CD
x	2a b c d e	AB c d e f	AB CD e f	AB CD EF
xi	a b c d e f			

Table XXVII

Isomeric Classes and Forms for Octahedral Configurations (24)

Class symbol	Number of isomeric forms								*Total*
	Optically active				Optically inactive				
	Cis	*Trans*	Others	*Total*	*Cis*	*Trans*	Others	*Total*	
Type 1	—								
6a	—	—	—	—	—	—	1	1	1
5a b	—	—	—	—	—	—	1	1	1
4a 2b	—	—	—	—	1	1	—	2	2
4a b c	—	—	—	—	1	1	—	2	2
3a 3b	—	—	—	—	1	1	—	2	2
3a 2b c	—	—	—	—	1	2	—	3	3
3a b c d	2	—	—	2	—	3	—	3	5
2a 2b 2c	2	—	—	2	—	4	—	4	6
2a 2b c d	4	—	—	4	—	4	—	4	8
2a b c d e	12	—	—	12	—	3	—	3	15
a b c d e f	—	—	30	30	—	—	—	—	30
Total	20	None	30	50	4	19	2	25	75

TABLE XXVII (*Continued*)

ISOMERIC CLASSES AND FORMS FOR OCTAHEDRAL CONFIGURATIONS (24)

Class symbol	Number of isomeric forms								Total
	Optically active				Optically inactive				
	Cis	*Trans*	Others	*Total*	*Cis*	*Trans*	Others	*Total*	
Type 2									
AA 4b	—	—	—	—	—	—	1	1	1
AB 4c	—	—	—	—	—	—	1	1	1
AA 3b c	—	—	—	—	1	1	—	2	2
AB 3c d	2	—	—	2	—	2	—	2	4
AA 2b 2c	2	—	—	2	—	2	—	2	4
AB 2c 2d	4	—	—	4	—	2	—	2	6
AA 2b c d	4	—	—	4	—	2	—	2	6
AB 2c d e	10	—	—	10	—	2	—	2	12
AA b c d e	—	—	12	12	—	—	—	—	12
AB c d e f	—	—	24	24	—	—	—	—	24
Total	22	None	36	58	1	11	2	14	72
Type 3									
2AA 2b	2	—	—	2	—	1	—	1	3
AA BB 2c	2	—	—	2	—	1	—	1	3
2AA b c	2	—	—	2	—	1	—	1	3
AA BB c d	4	—	—	4	—	1	—	1	5
AA BC 2d	4	—	—	4	—	1	—	1	5
2AB 2c	2	4	—	6	—	2	—	2	8
AB CD 2e	8	—	—	8	—	2	—	2	10
2AB c d	4	6	—	10	—	1	—	1	11
AA BC d e	8	4	—	12	—	—	—	—	12
AB CD e f	16	4	—	20	—	—	—	—	20
Total	52	18	None	70	None	10	None	10	80
Type 4									
3AA	—	—	2	2					2
2AA BB	—	—	2	2					2
AA BB CC	—	—	2	2					2
2AA BC	—	—	2	2					2
AA BB CD	—	—	4	4					4
3AB	2	2	—	4					4
AA 2BC	2	4	—	6					6
AA BC DE	—	—	8	8					8
2AB CD	4	4	—	8					8
AB CD EF	—	—	16	16					16
Total	8	10	36	54	None	None	None		54

clear-cut substitution reactions, such as is available to the organic chemist.

The examples discussed earlier included the classes $[Ma_6]$,$[Ma_5b]$,$[Ma_4b_2]$, $[Ma_4bc]$,$[Ma_3b_3]$,$[M(AA)_2b_2]$,$[M(AA)_2bc]$, and $[M(AA)_3]$. A few additional comments are in order. The existence of multinucleate complexes considerably increases the possibilities for isomerism. This is illustrated for binucleate complexes of the classes 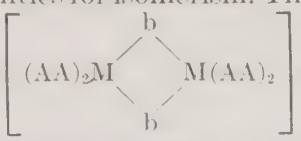 and 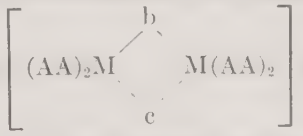 in Figure 17, in which (*a*) and (*b*) are mirror images and (*c*) is inactive by inter-

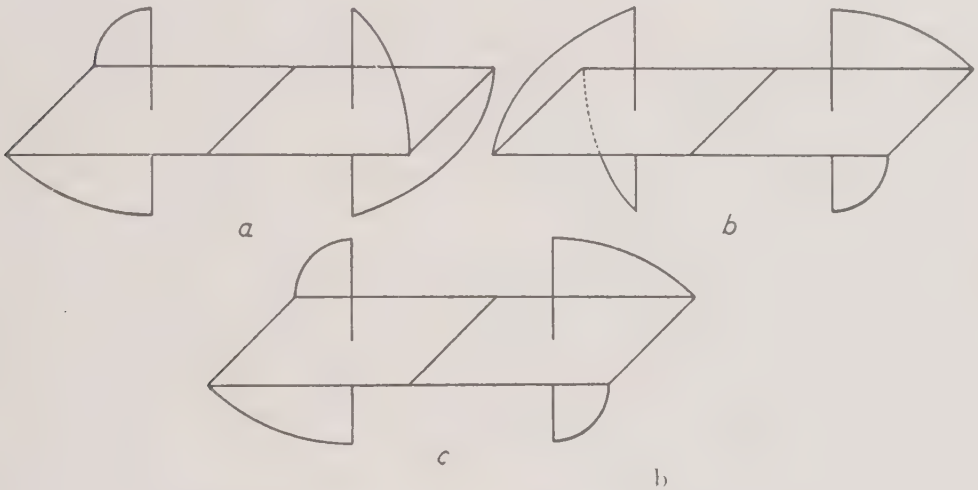

Fig. 17. Isomeric forms for 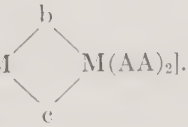 .

nal compensation. The situation closely parallels the classical case of the tartaric acids in organic chemistry. The experimental realization of the isomeric forms of 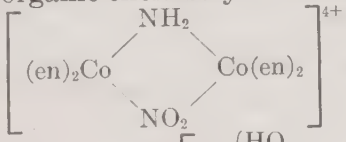 is illustrated in Table XXVIII.

The quadrinucleate complex 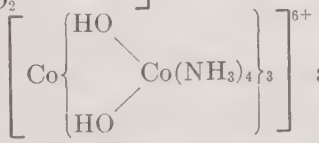 actually belongs to the class $[M(AA)_3]$ and, hence, optical antipodes are to be expected. The substance was successfully resolved by Werner in 1914 (29). As the first completely inorganic (noncarbon) compound to be resolved, it served to dispel the then prevalent misconception that the activity of the oxalato and

TABLE XXVIII

RESOLUTION OF A BINUCLEAR COMPLEX (28)

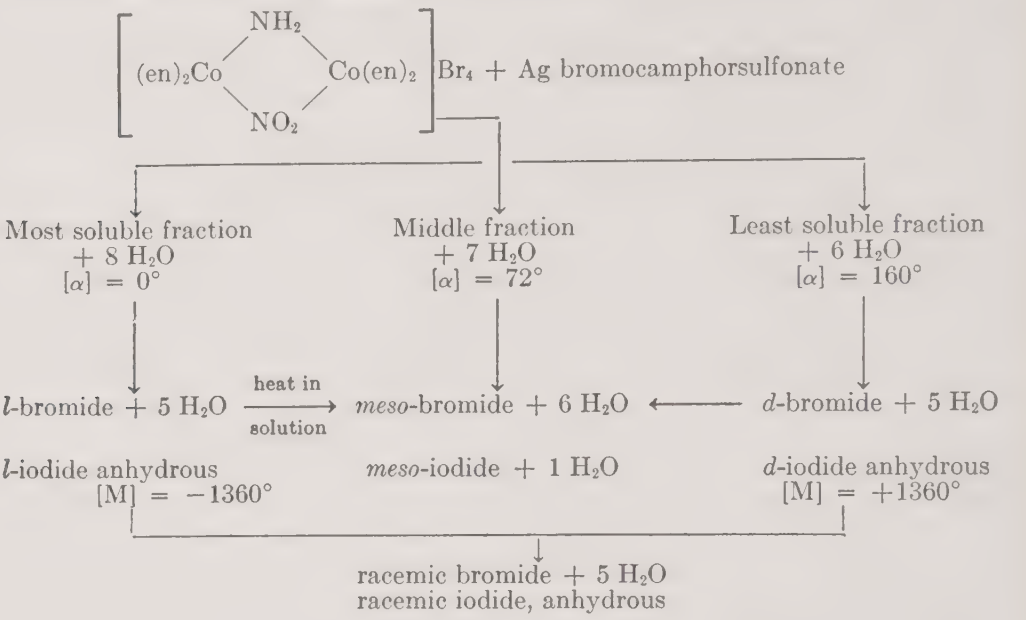

ethylenediamine complexes was in some mysterious way due to the carbon atoms present. Another strictly inorganic complex which has been successfully resolved is the sulfamide complex of rhodium: $\left[(H_2O)_2Rh\left(\begin{matrix}HN\\ \diagup\ \diagdown\\ SO_2\\ \diagdown\ \diagup\\ HN\end{matrix}\right)_2\right]^-$

The molecular rotation of many of these compounds is unusually high:

$$\left[Co\left(\begin{matrix}HO\\ \diagup\ \diagdown\\ Co(NH_3)_4\\ \diagdown\ \diagup\\ HO\end{matrix}\right)_3\right]Br_6,\ [M]_D = 47{,}600°$$

$$\left[(en)_2Co\begin{matrix}O_2\\ \diagup\ \diagdown\\ Co(en)_2\\ \diagdown\ \diagup\\ NH_2\end{matrix}\right](NO_3)_4,\ [M]_D = 68{,}550°$$

This is in part due to the special type of molecular dissymmetry involved. However, the extreme values recorded especially for cobalt complexes are to be associated largely with the fact that the measurement was made in close proximity to an optical absorption band. In this region the rotary dispersion is very great and the rotation changes its sign at the site of the absorption band. Some rotary dispersion curves are very complex.

It is interesting to note that the work of Bailar (30) has definitely established an example of the Walden inversion for a six-coordinate compound:

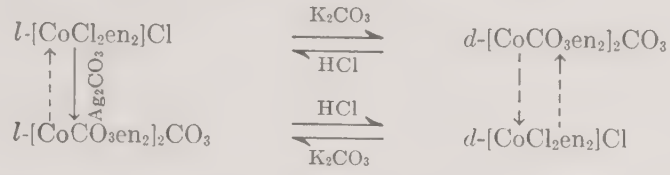

Those elements whose octahedral coordination has been definitely established are shown in Table XXIX.

TABLE XXIX

ELEMENTS EXHIBITING OCTAHEDRAL COORDINATION NUMBER SIX

	Mg	Al	Si	[P]	S				
		[Sc]	Ti	V	Cr	Mn	Fe	Co	Ni
Cu	Zn	Ga	Ge	As	Se				
		[Y]	Zr		Mo		Ru	Rh	Pd
	Cd	In	Sn	Sb	Te	I			
		[*]	[Hf]		W		Os	Ir	Pt
		Tl	Pb	Bi					

* Rare earths: Pr, Nd, Sm, Eu, Gd.

[ ] Probably octahedral.

6. *Coordination Number Seven*

Only a few compounds of elements exhibiting a coordination number of seven are known. For the limited number of compounds studied, two

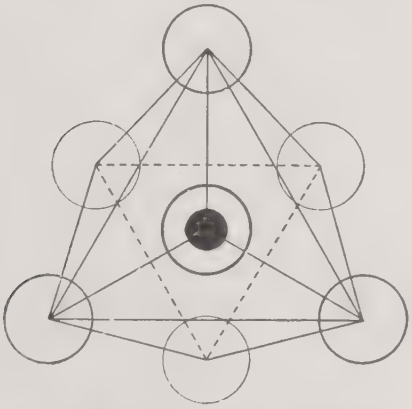

Fig. 18. Face-centered octahedron.

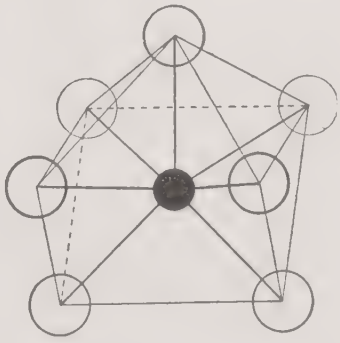

Fig. 19. Face-centered trigonal prism.

types of structure have been established: face-centered octahedron (Fig. 18) for $[ZrF_7]^{3-}$ in the potassium and ammonium salts (31) and face-centered trigonal prism (Fig. 19) for $[CbF_7]^{--}$ and $[TaF_7]^{--}$ in their potassium salts (32). The compound of the composition $(NH_4)_3SiF_7$ does not contain an element with a coordination number of seven. The crystal lattice is made up of NH_4^+, F^-, and SiF_6^{--} units (33).

7. *Coordination Number Eight*

Although the number of compounds with elements exhibiting a coordination number of eight is not large, several different types of combinations are included in the known examples: fluorides (OsF_8^{3-} and TaF_8^{3-}), acetylacetonates (zirconium, hafnium, thorium, cerium, uranium, and polonium (?)), 8-hydroxyquinolate (thorium), orthophenanthroline [lead(II)], phthalocyanine [tin(IV)], and cyanides (molybdenum, tungsten). Although it was assumed in the earlier speculations that a coordination number of eight would exhibit a cubical configuration, other configurations appear more probable (Table XXX).

TABLE XXX

POSSIBLE CONFIGURATIONS FOR EIGHT-COORDINATE COMPOUNDS (34)

Configuration	Arrangement	Remarks
d^3fsp^3	Cube	Cubic arrangement requires use of f orbitals; since there is no authentic case in which f orbitals are known, this arrangement should not ordinarily be found
d^3f^4s	Cube	
d^5p^3 d^4sp^3	Antiprism	Found for TaF_8^{3-}
d^4sp^3	Dodecahedron	Found for $Mo(CN)_8^{4-}$
d^5sp^2	Rectangular face-centered trigonal prism	Structure was predicted for such ions as TaF_8^{3-} and the molecule OsF_8
	Triangular face-centered trigonal prism	Very unlikely because of unfavorable radius ratio

By means of x-ray examination $[Mo(CN)_8]^{4-}$ has been shown to be dodecahedral (35). (Fig. 20) and $[TaF_8]^{3-}$ to be square, Archimedean, antiprismatic (36) (Fig. 21). The number of isomers of $[U(C_2O_4)_4]^{4-}$ which have been isolated definitely rules out the forms of symmetry represented by the cube and the triangular face-centered trigonal prism but do not serve to distinguish between those of the other possible forms (37). Tin(IV)

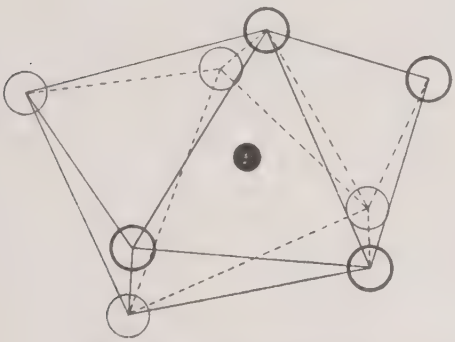

Fig. 20. Dodecahedron.

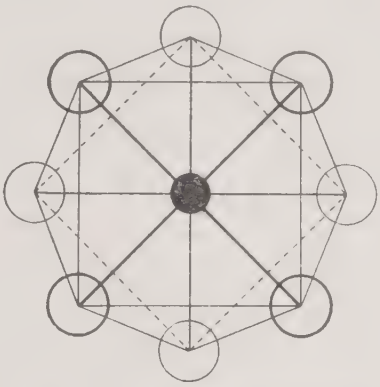

Fig. 21. Square Archimidean antiprism.

phthalocyanine would be an interesting case for study because the flatness of the phthalocyanine groups would limit the possible configurations to the cube and antiprism. Tables giving the number of classes and the theoretically possible forms within each class may be found elsewhere (38). They are not given here because of the paucity of experimental evidence. The complexity of the field is so great that chemical methods of attack (and many physical) are almost useless except in isolated cases.

VI. Conclusion

The field of coordination compounds has developed rapidly and has received valuable contributions from almost every branch of chemistry. The theory of coordination is not regarded as applying only to a special and limited area, but is recognized as an essential cornerstone of chemical thought. Further, the applications of coordination compounds in the arts and in scientific work have become so numerous that this field has become of general interest. Despite the rapid advance of the subject, numerous problems await solution. Since these are very challenging and the means for the solution of many of them are at hand, it seems reasonable that the field of coordination compounds will continue to attract the attention of

capable scientists. Thus, one may confidently expect further important advances in the not distant future.

Acknowledgment

A number of reviews and monographs have been freely consulted in the preparation of this paper, and are listed below as General References for the benefit of those who desire to pursue the subject further.

Throughout the preparation of the manuscript, the author had the benefit of frequent discussions with his colleagues: Dr. L. E. Marchi, Dr. C. L. Rollinson, and Dr. E. M. Larsen. Drs. Marchi and Rollinson have read the complete manuscript and offered many valuable suggestions. For these, the author wishes to make public acknowledgment.

References

1. Werner, *Z. anorg. Chem.*, **3,** 269 (1893).
2. Emeléus and Anderson, *Modern Aspects of Inorganic Chemistry.* Van Nostrand, New York, 1938, p. 166.
3. Fajans and Joos, *Z. Physik*, **23,** 1–46 (1924). Fajans, *Naturwissenschaften*, **11,** 165–172 (1923); *Z. Kryst.*, **61,** 18–48 (1925).
4. Sidgwick, *Trans. Faraday Soc.*, **19,** 469 (1923); *Chemistry & Industry*, **42,** 901–903 (1923).
5. Blanchard, *Science*, **94,** 311–317 (1941).
6. Rice, *Electronic Structure and Chemical Binding.* McGraw-Hill, New York, 1940, p. 317.
7. Emeléus and Anderson, *loc. cit.*, p. 85.
8. Emeléus and Anderson, *loc. cit.*, p. 89.
9. Emeléus and Anderson, *loc. cit.*, p. 90.
10. Rice, *loc. cit.*, p. 308.
11. Jensen, *Z. anorg. allgem. Chem.*, **225,** 97–114 (1935); **229,** 225–251 (1936).
12. Pauling, *J. Am. Chem. Soc.*, **53,** 1367–1400, 3225–37 (1931); *cf.* ref. 34.
13. Emeléus and Anderson, *loc. cit.*, p. 176.
14. Emeléus and Anderson, *loc. cit.*, p. 173.
15. Johnson, *Trans. Faraday Soc.*, **28,** 845–856 (1932).
16. Biltz, *Z. anorg. Chem.*, **164,** 345 (1927).
17. Anderson, *Z. physik. Chem.*, **B32,** 237–242 (1936).
18. Voge and Libby, *J. Am. Chem. Soc.*, **59,** 2474 (1937).
19. Voge, *J. Am. Chem. Soc.*, **61,** 1032–1035 (1939).
20. Kennedy, Ruben, and Seaborg, quoted by Seaborg, *Chem. Revs.*, **27,** 256 (1940).
21. Ettle and Johnson, *J. Chem. Soc.*, **1939,** 1490.
22. Long, *J. Am. Chem. Soc.*, **63,** 1353–1357 (1941).
23. Sidgwick and Powell, *Proc. Roy. Soc. London*, **A176,** 153–180 (1940).

24. Smith, *Chemistry and Atomic Structure.* Benn, London, 1924.
25. Mann and Pope, *J. Chem. Soc.*, **1926,** 482–489, 2675.
26. Chernyaev, *Ann. inst. platine U.S.S.R.*, **4,** 243–275 (1926).
27. Barrett, Dent, and Linstead, *J. Chem. Soc.*, **1936,** 1719–1736. Linstead, *Ber.*, **72A,** 93–103 (1939). Robertson and Woodward, *J. Chem. Soc.*, **1937,** 219–230. Klemm and Klemm, *J. prakt. Chem.*, **143,** 82–89 (1935). Senff and Klemm, *ibid.*, **154,** 73–81 (1939).
28. Emeléus and Anderson, *loc. cit.*, p. 100.
29. Werner, *Ber.*, **47,** 3087 (1914).
30. Bailar and Auten, *J. Am. Chem. Soc.*, **56,** 774–776 (1934). Bailar, Jonelis, and Huffman, *ibid.*, **58,** 2224–2226 (1936); Bailar and Peppard, *ibid.*, **62,** 820–823 (1940).
31. Hampson and Pauling, *ibid.*, **60,** 2702–2707 (1938).
32. Hoard, *ibid.*, **61,** 1252–1259 (1939).
33. Hoard and Williams, *ibid.*, **64,** 633–637 (1942).
34. Kimball, *J. Chem. Phys.*, **8,** 188–198 (1940).
35. Hoard and Nordsieck, *J. Am. Chem. Soc.*, **61,** 2853–2863 (1939).
36. Hoard, Sixth Annual Symposium, Division of Physical and Inorganic Chemistry, American Chemical Society, Columbus, Ohio, Dec. 1941.
37. Marchi and McReynolds, *J. Am. Chem. Soc.*, **65,** 333–335 (1943). Marchi, *ibid.*, 2257–2258.
38. Marchi, Fernelius, and McReynolds, *ibid.*, **65,** 329–333 (1943).

General References

Bailar, "The Stereochemistry of Complex Inorganic Compounds," *Chem. Revs.* **19,** 67–87 (1936).

Bailar, "The Coordinating Tendency of the Metallic Ions," *Chem. Revs.*, **23,** 65–75 (1938).

Bjerrum, *Metal Ammine Formation in Aqueous Solution.* Haase, Copenhagen, 1941.

Blanchard, "Valence Relations Among the Metal Carbonyls," *Chem. Revs.*, **26,** 409–422 (1940); "The Metal Carbonyls," *Science*, **94,** 311–317 (1941).

Blanchard, "Coordination and Valence," *J. Chem. Education*, **20,** 454–460 (1943).

Copley, Foster, and Bailar, "The Stabilization of Valences by Coordination," *Chem. Revs.*, **30,** 227–238 (1942).

Diehl, "The Chelate Rings," *Chem. Revs.*, **21,** 39–111 (1937).

Emeléus and Anderson, "Coordination Compounds and Inorganic Stereochemistry," in *Modern Aspects of Inorganic Chemistry.* Van Nostrand, New York, 1938, Chap. IV, pp. 79–178.

Hall, "The Acid-Base Properties of Complex Ions," *Chem. Revs.*, **19,** 89–99 (1936).

Jaeger, "Spatial Arrangements of Atomic Systems and Optical Activity," in *Optical Activity and High Temperature Measurements.* McGraw-Hill, New York, 1930, Part I, pp. 23–234.

Keller, "Coordination Compounds of Olefins with Metallic Salts," *Chem. Revs.*, **30,** 227–238 (1942).

Mellor, "The Stereochemistry of Square Complexes," *Chem. Revs.*, **33,** 137–183 (1943).

Morgan and Burstall, *Inorganic Chemistry: A Survey of Modern Developments.* Chemical Pub. Co., Brooklyn, 1937.

Palmer, *Valency: Classical and Modern.* Cambridge Univ. Press, London, 1945, pp. 168–178.

Pauling, *The Nature of the Chemical Bond.* Cornell Univ. Press, Ithaca, 1939.

Pfeiffer, *Organische Molekülverbindungen.* Enke, Stuttgart, 1927.

Pfeiffer, "Komplex Verbindungen" in Freudenberg, *Stereochemie,* Deuticke, Leipzig, 1933, pp. 1200–1377.

Rice, "Complex Compounds and Complex Crystals," in *Electronic Structure and Chemical Binding.* McGraw-Hill, New York, 1940, Chap. XVI, pp. 286–353.

Schwarz, *The Chemistry of the Inorganic Complex Compounds.* Translated by L. W. Bass. Wiley, New York, 1923.

Selwood, "Complex Compounds," in *Magnetochemistry.* Interscience, New York, 1932, Chap. VI., pp. 142–184.

Sidgwick, *The Electronic Theory of Valency.* Oxford Univ. Press, London, 1929.

Sidgwick, *Some Physical Properties of the Covalent Link in Chemistry.* Cornell Univ. Press, Ithaca, 1933.

Sidgwick and Powell, "Stereochemical Types and Valency Groups," *Proc. Roy. Soc. London,* **A176**, 153–180 (1940).

Smith, *Chemistry and Atomic Structure.* Benn, London, 1924.

Stilwell, "The Structures of the Werner Compounds," in *Crystal Chemistry.* McGraw-Hill, New York, 1938, Chap. IX, pp. 307–322.

Sutherland, "The Metal-ammines," in Friend, *A Textbook of Inorganic Chemistry.* Vol. X, Griffin, London, 1928.

Thorne and Ward, "Werner's Coordination Theory and the Ammines," in Ephraim, *Inorganic Chemistry,* 3rd English ed., Interscience, New York, 1939, Chap. XI, pp. 277–319; see also pp. 325–351.

Weinland, *Einführung in die Chemie der Komplex-Verbindungen.* Enke, Stuttgart, 1924.

Wells, *Structural Inorganic Chemistry.* Oxford Univ. Press, London, 1945.

Werner, *New Ideas in Inorganic Chemistry.* Longmans, Green, London, 1911.

Wittig, *Stereochemie.* Akadem. Verlagsgesellschaft, Leipzig, 1930.

IV. *X-Ray Studies of Randomness in Various Materials*

B. E. WARREN

Massachusetts Institute of Technology, Cambridge, Mass.

I. Introduction

FOR THE FIRST TWENTY YEARS after the beginning of x-ray diffraction studies in 1913, the principal interest was in structure determination. Various experimental methods were devised for obtaining x-ray diffraction patterns and considerable skill was developed in the interpretation of the patterns. More and more complicated crystalline structures were worked out and structural information, such as interatomic distances, bond angles, and coordination schemes was accumulated. A new science of structural crystal chemistry was built up. During the last ten years it has become evident that many substances do not have the perfect repeating type of structure that is associated with the idea of crystallinity. Various kinds of randomness in crystalline or semicrystalline materials have been discovered; the study of these various kinds of randomness has become an interesting new field of research. The first part of this paper will be devoted to a brief résumé of x-ray structure determination, and of the developments in this field in the last ten years. The second part will be devoted to two examples of randomness: (*1*) the parallel-layer randomness in the structure of carbon black and (*2*) the order-disorder type of randomness in the alloy Cu_3Au.

II. Structures of Ideally Crystalline Materials

1. X-Ray Diffraction Patterns

Most structure determinations are made from one or another of the various types of x-ray rotation patterns. A fine pencil of essentially monochromatic radiation, of wave length about 1 Å, falls upon a small single crystal. During the exposure the crystal is either rotated or oscillated about one of its crystal axes. The diffracted beams register upon a cylindrical film.

Figure 1 is the rotation pattern of a quartz crystal. The crystal is mounted with the c axis perpendicular to the x-ray beam and is rotated continuously about this axis during the exposure. The diffraction spots are arranged on sets of horizontal layer lines. From the distances between layer lines and the positions of the spots on the layer lines, the lengths of the crystal axes and the size and shape of the unit cell of the crystal are readily computed. For quartz the unit cell is hexagonal and the axes turn out to be: $a = 4.903\ kX$, $c = 5.393\ kX$.

Crystal dimensions are determined in terms of the Siegbahn x-ray wave lengths which are expressed in X units ($kX = 1000\ X$). The kX unit has been used loosely as though it were equal to the Å unit (1 Å $= 10^{-8}$ cm.) but actually the two differ by about 0.2%. The crystal dimensions which have been reported during the last twenty-five years in Å units are actually in kX units. The conversion factor between kX units and the absolute 10^{-8} cm. unit is now fairly definite. A crystal dimension in Å units can be obtained from the value in kX units by using the relation:

$$d_{\text{Å}}^{\circ} = 1.00202\, d_{kX}$$

The number of units of silicon dioxide per unit cell can then be computed from the volume of the cell, the density of quartz, the molecular weight of silicon dioxide, and the Avogadro number*:

$$n = \frac{V\rho N}{M} \quad \frac{4.903^2 \times 5.393 \times 0.866 \times 10^{-24} \times 2.65 \times 0.606 \times 10^{24}}{60.1} = 3.00$$

There are, accordingly, three silicon and six oxygen atoms per unit cell. The arrangement of these atoms in the unit cell must then be fixed from considerations of the symmetry of the crystal and from the intensities of the spots on the diffraction pattern. Crystal structure determination may thus be divided into two distinct steps: (*a*) the determination of the size

*If the axial lengths are expressed in Å units, the new value of the Avogadro number, 6.023×10^{23}, should be used; if the axial lengths are left in kX units, it is common practice to correct the mistake by using the old value of the Avogadro number.

and shape of the unit cell from the geometry of the diffraction pattern (this step is perfectly straightforward) and (*b*) the determination of the arrangement of the atoms within the unit cell from the intensities of the diffraction spots (this step is not at all straightforward and for many substances is so difficult that it has not yet been accomplished).

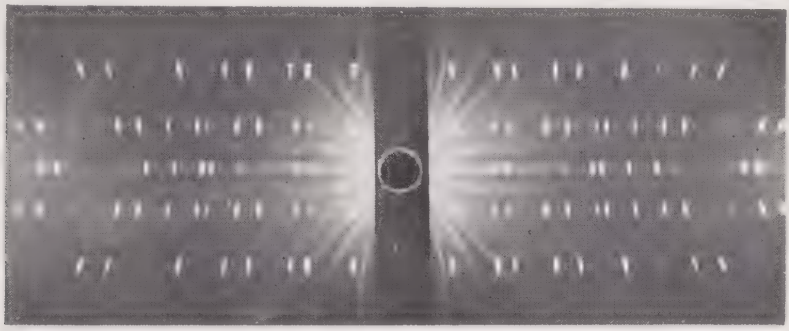

Fig. 1. Rotation pattern of a quartz crystal, rotated about the *c* axis. Radiation Cu Kα, $\lambda = 1.539$ *kX*.

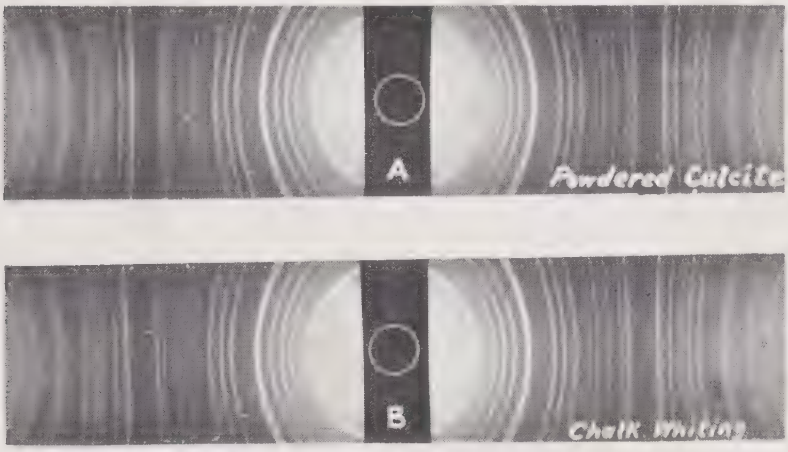

Fig. 2. X-ray powder patterns of (A) ground calcite crystal and (B) chalk whiting. Radiation Cu Kα, $\lambda = 1.539$ *kX*.

Many crystalline materials cannot be obtained in the form of single crystals of sufficient size for a rotation pattern, and for these the powder pattern must be used. A monochromatic x-ray beam falls upon a small sample of powdered material comprising an enormous number of tiny crystals which have a completely random orientation. For each set of planes (*hkl*) with spacing, *d*, there will be some crystals properly oriented with respect to the main beam to satisfy the Bragg law: $n\lambda = 2\,d \sin \theta$. For each such set of planes there will be a cone of diffracted beams and the

intersection of these cones with a cylindrical film gives the lines of the powder pattern. The calcite pattern of Figure 2 is a typical powder pattern. Structure determinations are made from a powder pattern only when rotation patterns cannot be obtained and, in general, the determination is successful only on very simple structures. However, powder patterns are used a great deal for other purposes, such as identification. The two patterns of Figure 2 are an interesting example. One of the samples was obtained by grinding up a clear calcite crystal, the other was a very fine chalk whiting powder. It is evident that the two patterns are identical and, hence, chalk whiting is simply a fine particle form of calcite.

2. Crystalline Structures

The rock-salt structure is the well-known example of a simple ionic structure. Each Na^+ ion is surrounded by six Cl^- ions, and each Cl^- ion by six Na^+ ions, the sodium-chlorine distance being 2.814 kX. There is no sodium chloride molecule in the structure; instead, it is a simple assemblage of positive and negative ions, held together by electrostatic forces. Many of the inorganic salts have ionic structures.

In general, organic crystals have structures which consist of molecules. The simplest organic structure is probably that of hexamethylenetetramine, $C_6H_{12}N_4$. The material crystallizes in the cubic system, and the diffraction pattern is readily solved. The position of each carbon and nitrogen atom in the unit cell can be uniquely determined from the intensities of the diffraction spots, and the positions of the hydrogen atoms may be approximated. Figure 3 represents (to scale) the structure which

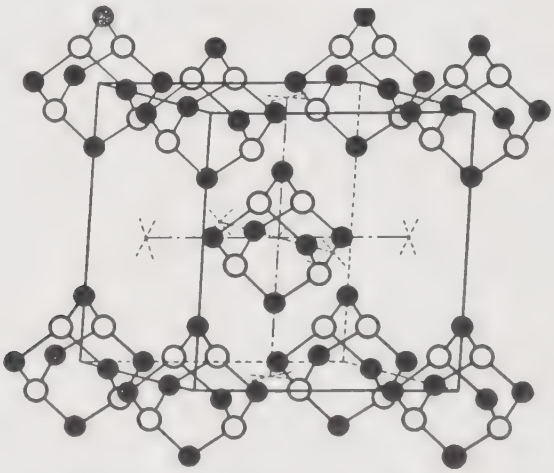

Fig. 3. Structure of hexamethylenetetramine, $C_6H_{12}N_4$. Black spheres are carbon atoms and open spheres, nitrogen atoms.

has been deduced, black spheres representing the carbon atoms and open spheres, the nitrogen atoms. The existence of the molecule, $C_6H_{12}N_4$, is clearly indicated. Molecules show up in a structure as compact assemblages of atoms, which are clearly separated from neighboring atoms. The closest atoms within an organic molecule are at distances of the order of 1.5 Å from each other, whereas the shortest distances between atoms of neighboring molecules are about 3.5 Å. After having fixed the position of each atom in a structure, such as that of Figure 3, interesting structural information, such as interatomic distances (length of the C—N bond), bond angles, and coordination numbers, is immediately available. Information of this sort derived from crystalline structures has played an important role in building up theories of chemical bonding and in testing these theories.

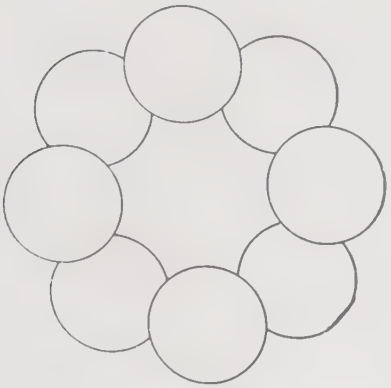

Fig. 4. Puckered-ring structure of the S_8 molecule in rhombic sulfur.

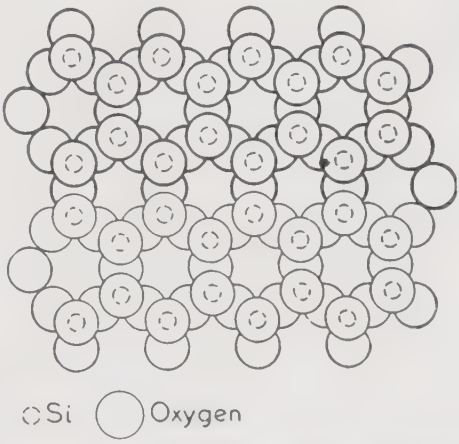

Fig. 5. Structure of tremolite showing long $(Si_4O_{11})_n$ double chains which form the basis of the amphibole structures. Each silicon is tetrahedrally surrounded by four oxygens.

There are some examples of inorganic materials with molecular structures. The x-ray analysis of rhombic sulfur leads to a complicated structure with 128 atoms per unit cell. The atoms are grouped together to form S_8 molecules, each molecule being a puckered eight-atom ring, as illustrated in Figure 4. From a complete structure determination, all dimensions of the molecule are determined and interatomic distances and bond angles are readily computed. The S—S distance turns out to be about 2.12 Å and the bond angle, about 105°. These values are just what would be expected for covalent bonding by paired *p*-electrons.

From about 1925 to 1935 the field of complex silicate structures was opened up and the rules governing such structures were established (1). The method was essentially a "brute force" determination of the simpler silicate structures, the knowledge so obtained then being used to work out more complicated structures. In spite of the apparent complexity of structures and compositions, the rules governing silicate structures turn out to be very simple. The silicon atom is always bonded tetrahedrally to four oxygen atoms, the Si—O distance being about 1.6 Å. If the ratio of oxygen to silicon atoms is four, independent SiO_4 groups exist in the structure. If the oxygen-to-silicon ratio is less than four, some of the oxygens are shared by two silicon atoms. In the limiting case when the oxygen-to-silicon ratio is two, each oxygen is bonded to two silicons. In the complex silicate, tremolite, $(OH)_2Ca_2Mg_5(Si_4O_{11})_2$, the oxygen–silicon ratio of 11:4 is satisfied by building long double chains, as illustrated in Figure 5. These chains are arranged parallel to one another and are held together laterally by the Ca^{++} and Mg^{++} ions placed in the holes between them. Since the $(Si_4O_{11})_n$ chain is the strongest unit in the structure, it is not surprising that the material should have fibrous properties. One branch of the asbestos family has structures built up of $(Si_4O_{11})_n$ chains. In the micas the effective oxygen–silicon ratio is 5:2; this ratio is satisfied by building indefinite sheets of composition, $(Si_2O_5)_n$. The flaky character of mica results from a structure built up out of such $(Si_2O_5)_n$ sheets.

3. Recent Developments in Complex Structure Determination

Up to ten years ago, most complex structures were determined by brute force and cut-and-try methods. There is no straightforward method for solving the x-ray diffraction pattern of a complex structure. The arrangement of the atoms in a structure determines the intensities of the spots in the diffraction pattern, but the connection between structure and diffraction pattern is a one-way relationship. If the structure is known, the intensities of the spots in the diffraction pattern can be readily computed; however, from a complete knowledge of the intensities of the diffraction pattern, there is no straightforward method for deriving the structure. In working out complex structures, all available evidence and experience was used to make intelligent guesses about the structure; the x-ray pattern was then used to check the accuracy of the guess and to fix precisely the coordinates of the atoms.

It is obvious that a more straightforward method of attack is highly desirable. Several recent advances have involved the use of a Fourier series. The density of scattering matter (electron density, ρ), if plotted

in space, may be used to represent the structure, since the electron density is high near the center of an atom. Hence, atoms show up as peaks in the electron-density function. For the sake of simplicity let us consider a one-dimensional electron-density function, $\rho(x)$, which, if symmetrical, can be represented by a Fourier series involving only cosine terms:

$$\rho(x) = A_0 + A_1 \cos 2\pi \frac{x}{a} + A_2 \cos 2\pi \frac{2x}{a} + \cdots \qquad (1)$$

a is the distance of repetition and the coefficients, A_j, are related to the intensities of the diffracted beams, the intensity of each diffracted beam being proportional to the square of the corresponding coefficient in the electron-density Fourier series:

$$I_j \propto A_j^2 \qquad (2)$$

Here we meet the fundamental stumbling block to crystal analysis by x-ray diffraction. From the experimental intensities we can determine the squares of the coefficients in the Fourier series; all we know is the magnitude of each coefficient, but not the sign. This has limited the direct use of the Fourier series to a few special cases when it is possible to use other information and to guess the signs of the coefficients.

A recent technique which has been used successfully has involved the actual determination of the signs of the coefficients in special cases in which isomorphous replacements were possible. An outstanding example is Robertson's analysis (2) of the phthalocyanine molecule, $C_{32}H_{18}N_8$. There is an isomorphous series of crystals of free phthalocyanine and various metal derivatives of phthalocyanine. For the nickel derivative there is one nickel atom per molecule, and crystal symmetry requires this atom to be at a symmetry center which can be taken as the origin of coordinates. Taken in this way, the sign of the scattering from the nickel is always positive, and the sign of the scattering from the phthalocyanine group can be determined by seeing whether reflections from the nickel derivative are stronger or weaker than the corresponding reflections from the free phthalocyanine. In this way Robertson was able to determine both the magnitude and the sign of all the coefficients in his Fourier series and to make a two-dimensional plot of the electron density. Figure 6 shows the electron-density plot obtained directly from the experimentally determined intensities and, for comparison, the phthalocyanine molecule which is deduced from this plot.

Since it is only the squares of the coefficients in the electron-density function which can be determined experimentally, the question arises as

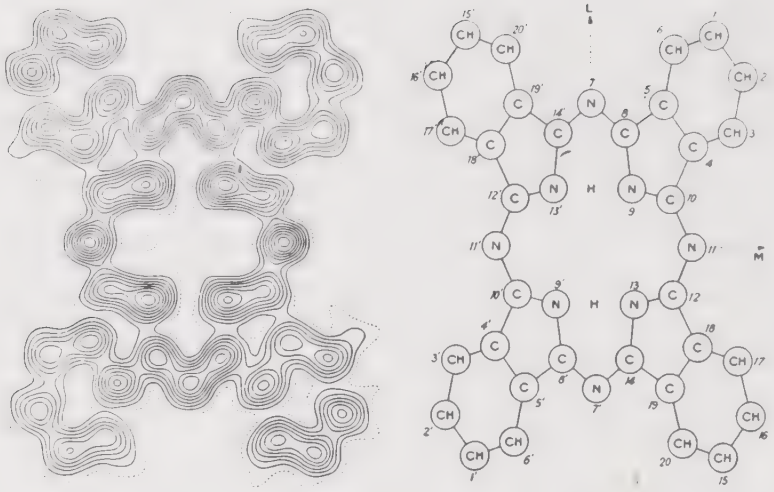

A B

Fig. 6. Two-dimensional Fourier plot of (A) electron densities in a phthalocyanine molecule, compared with (B) the idealized molecular structure (2).

to whether anything can be done with the squared coefficients. Patterson has shown that a Fourier series with the squares of the A values as coefficients has a real physical significance (3). In a Patterson plot, a peak does not indicate the position of an atom. Instead, the vector from the origin to the peak is the vector displacement of some atom from some other atom in the structure. Peaks in the Patterson plot simply indicate the terminal points of vectors from the origin, these vectors representing the various displacements of each atom from every other atom. Hence, a Patterson plot is not a picture of the structure, but rather an advanced point from which to jump off into the guessing stage. In recent years a good many extremely complex structures have been worked out by the use of Patterson plots, which probably could not have been solved by any other method.

III. Randomness in Structures

1. Random-Layer Structure of Carbon Black

A. Structure of Graphite. Graphite is one of the crystalline forms of carbon. The structure is built up of planar layers of carbon atoms, as shown in Figure 7. Within each layer the atoms are arranged in a hexagonal pattern, with a C—C distance of 1.42 Å. The layers are stacked parallel to one another, with a distance of 3.35 Å between layers. Each layer has

a definite position with respect to its neighboring layers and alternate layers are placed directly over one another. Interatomic distances are an indication of the strength of bonding, the shorter the distance the stronger the bond. The short C—C distance of 1.42 Å indicates very strong bonding within the layer. The large distance of 3.35 Å between layers indicates that the layers are held together very loosely. Hence, the layers can readily slide over one another, which is one of the reasons why graphite has good lubricating properties. The powder pattern of graphite is shown in Figure 8C. It is the usual sharp line pattern of a crystalline material.

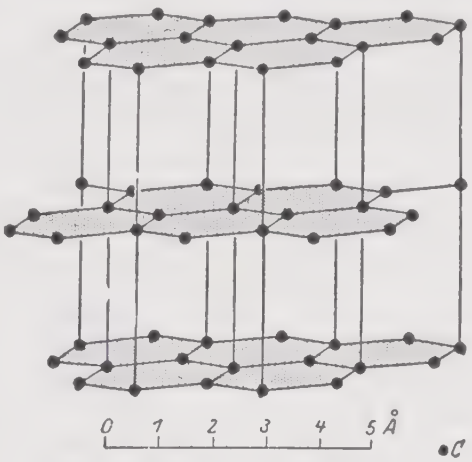

Fig. 7. Structure of graphite.

B. X-Ray Pattern of Carbon Black. The x-ray pattern of a typical fine-particle carbon black is shown in Figure 8A. The pattern consists of

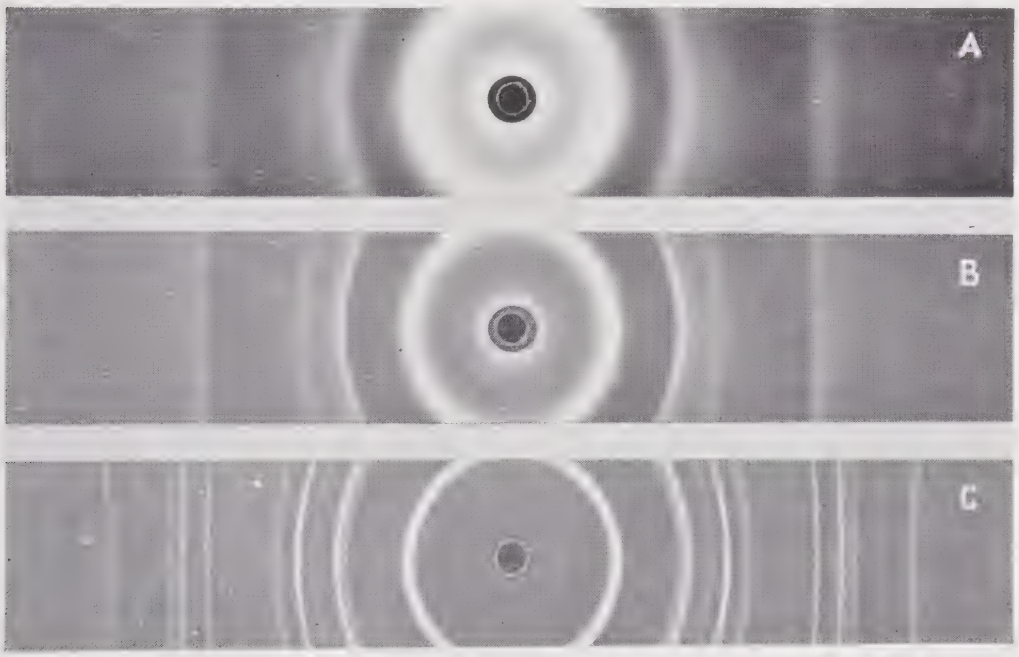

Fig. 8. X-ray diffraction patterns of carbon black and graphite. (A) Spheron Grade 6 black, unheated; (B) same material, heated for 2 hours at 2000 °C.; (C) graphite. Radiation Cu Kα.

three very diffuse rings and is similar in appearance to the diffuse ring patterns of amorphous materials or extremely fine crystalline materials. There is an obvious relation between the patterns of carbon black and graphite, the diffuse rings of the carbon black pattern occurring approximately at the positions of the strong lines of the graphite pattern. Because of this connection between the patterns, it has been a lively question for years as to whether carbon black consists merely of very fine graphite crystals, or whether it is an actual modification of carbon.

By heat-treating carbon black, the diffraction pattern sharpens up considerably, and more definite conclusions can be drawn. Figure 8B shows the pattern of a carbon black heated for two hours at 2000°C. If we attempt to index the pattern in terms of the graphite structure, we find that there are sharp crystalline reflections of the type 00*l*, diffuse reflections at approximately the positions of the reflections (*hk*0), and no reflections of the general type (*hkl*). This is the type of diffraction pattern to be expected from a structure in which the individual graphite layers are stacked together, roughly parallel and equidistant, but with each layer having a completely random orientation about the normal to the layer (4).

C. Structure of Carbon Black. Carbon black is a form of matter which is neither amorphous nor perfectly crystalline. Each graphite layer

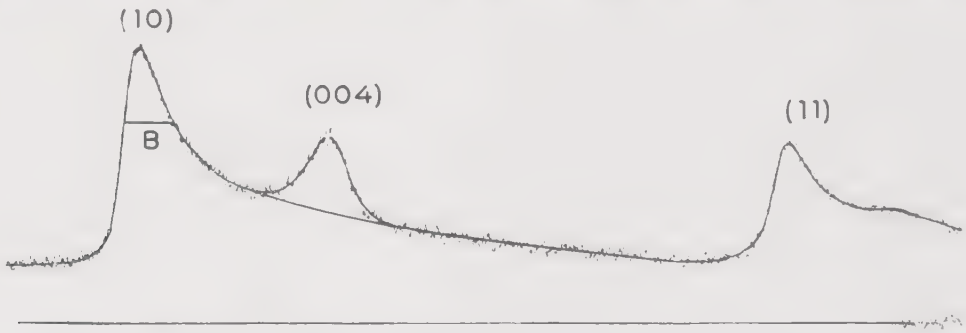

Fig. 9. Microphotometer record of the pattern of Spheron Grade 6 black, heated for two hours at 2800°C. The peaks labeled (10) and (11) are two-dimensional lattice reflections, (004) is a crystalline reflection.

is a perfect two-dimensional crystal, but the stacking of these layers in the third dimension is imperfect. The term *turbostratic* (unordered layers) has been suggested as a name for this particular class of mesomorphic solids.

The peculiar features of the diffraction pattern of carbon black are shown in the microphotometer record of Figure 9. Reflections of the type (00*l*) are not affected by the randomness in orientation of the layers. Hence, reflections of this type, such as (004), are true crystalline reflections

which fall off sharply on either side of the peak. The remaining reflections are very seriously affected by the randomness in orientation. Each layer diffracts independently, so that these reflections are those of two-dimensional crystals. The shape of these reflections can be predicted from the theory of two-dimensional crystal powder patterns. On the small angle side the reflection rises sharply to a peak and then drops off slowly on the large angle side. The peaks labeled (10) and (11) in Figure 9 are two-dimensional crystal reflections of this type.

Interatomic distances in carbon black are computed from the positions of the reflections. From the (*hk*) reflections we compute a C—C distance within the layer of 1.41 Å, which is essentially the same as the C—C distance in graphite, 1.42 Å. It would, of course, be expected that the C—C distance in carbon black or graphite would be a little larger than the C—C distance in the benzene ring. The C—C distance in graphite (1.42 Å) corresponds to 1.33 bonds, while the C—C distance in benzene (1.39 Å) corresponds to 1.5 bonds. From the (00*l*) reflections, the distance between layers in carbon black is found to be about 3.45 Å. This value is larger than the corresponding distance, 3.35 Å, in graphite. This increase in distance should be expected, since in graphite each layer sits precisely upon the preceding layer and, thus, allows a minimum separation to be achieved. In carbon black the random orientation of the layers prevents any precise setting, and a larger average spacing results.

From the widths of the reflections it is possible to compute the average size of the parallel-layer groups in carbon black. From the (00*l*) reflections, the dimension, L_c, perpendicular to the layers is obtained and from the (*hk*) reflections, the dimension, L_a, which is essentially the diameter of a layer. For a typical fine carbon black (Spheron Grade 6), without heat-treatment, the L_c dimension is about 13 Å, which corresponds to about four parallel layers. For the same material the L_a dimension is about 20 Å, which is about eight times the width of each hexagonal ring.

Heat-treatment causes an increase in the dimensions of the parallel-layer groups, as shown in Figure 10. The groups appear to grow at about the same rate in both directions, that is, the individual graphite layers grow in size and more layers stack themselves parallel. The curves indicate a fairly definite temperature (about 1000°C.) at which the rapid growth sets in. This temperature can, perhaps, be correlated with the sharp rise in the curve (Fig. 10B) which shows the percentage of hydrogen in the gas evolved at different temperatures. If the hydrogen content of the sample is chemically bonded around the edges of the graphite layers, it could presumably act as an effective barrier toward growth of the layers. Only

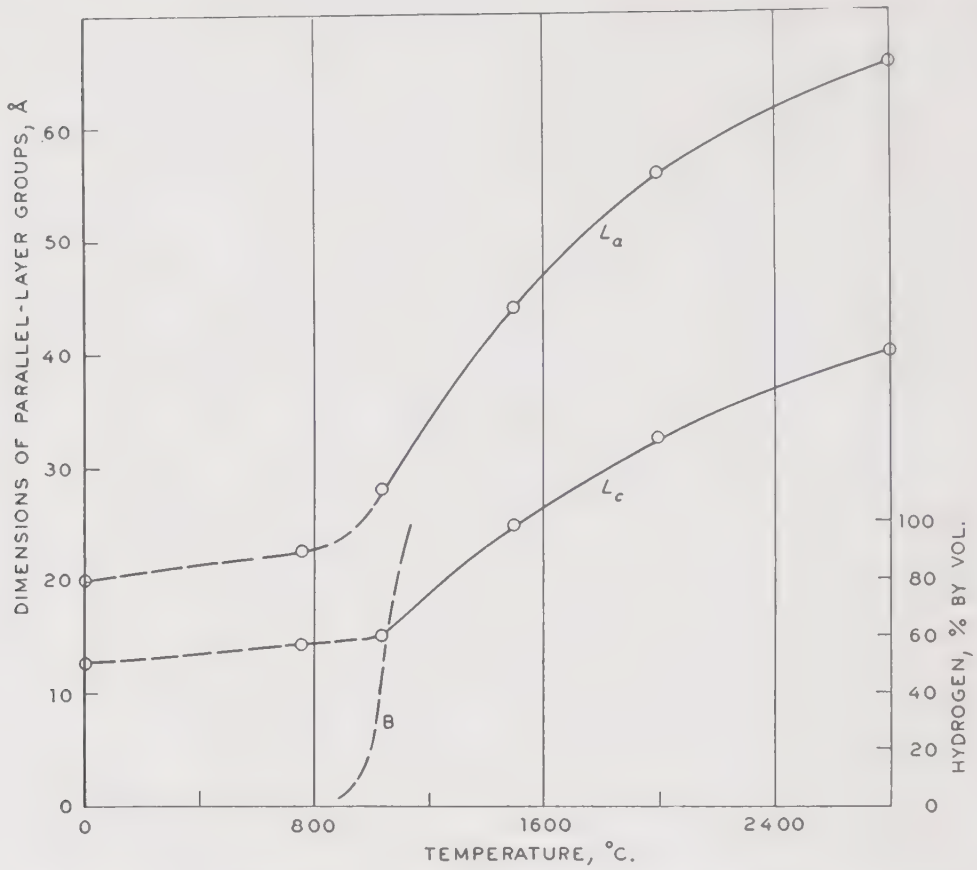

Fig. 10. (A) Dimensions L_a and L_c of the parallel-layer groups in Spheron Grade 6 black, heated for two hours at various temperatures; (B) per cent by volume of hydrogen in gas evolved at various temperatures.

at temperatures high enough to drive off this hydrogen can growth of the graphite layers take place.

D. Graphitization of Carbon Black. A pattern of carbon black heated for two hours at 2800°C. showed the two-dimensional reflections characteristic of the random-layer structure. A sample heated for two hours at 3300°C. gave the complete graphite pattern. For the Grade 6 material and our rate of heating, graphitization took place somewhere between 2800° and 3300°C. Graphitization should be a discontinuous process, since it involves the rotation of the various graphite layers into correct orientations. As the material is brought to higher temperatures, the individual layers acquire greater thermal movement and it should become easier for each layer to rotate, with respect to neighboring layers, into the graphite configuration. However, the size of each layer, L_a, increases with temper-

ature and with larger layers, it becomes increasingly difficult for the layers to rotate into the graphite structure. If the temperature could be raised so rapidly that there was no time for appreciable increase in L_a, graphitization might set in at a lower temperature.

2. *Order-Disorder in the Alloy, Cu_3Au*

A. Long-Range Order. An entirely different type of randomness is the *order-disorder* randomness in alloys such as Cu_3Au. The stable form at low temperatures is the *ordered* structure. As shown in Figure 11, the gold atoms (solid spheres) are at cube corners and the copper atoms (open spheres) at each face center. This arrangement allows each gold atom to be surrounded exclusively by copper atoms, which presumably produces the structure of lowest energy and is, hence, most stable at low temperatures. If the temperature is raised, a critical temperature is reached, at $T_c = 388°C.$, above which a *disordered* structure appears. The atomic positions remain the same, but each position may be occupied by either a copper or gold atom. In a completely disordered structure the positions are occupied indiscriminately by copper and gold atoms, the probability being 25% for a gold, and 75% for a copper atom. The reason for the change to the disordered structure is easily understood. The stable structure at any temperature is the one which has the minimum free energy: $F = U - TS$. The ordered structure has the smallest energy, U, but the disordered structure has an increased entropy due to the random distribution of the atoms. At low temperatures the term TS is small, and the ordered structure is determined by the low U. At high temperatures the large TS term for the disordered structure makes this form more stable.

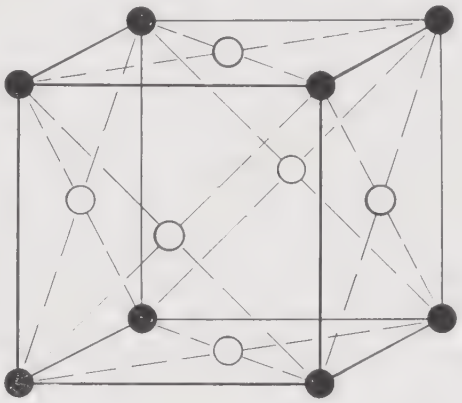

Fig. 11. Ordered structure of Cu_3Au. The solid spheres are gold atoms and the open spheres, copper atoms.

Let r_{Cu} represent the fraction of the copper atoms which are in the right position (face-centered). An order parameter, S, may then be defined as: $S = 4\,r_{Cu} - 3$. For the perfectly ordered structure, $r_{Cu} = 1.0$ and $S = 1.0$; for a completely disordered structure, the probability of finding a copper atom at a face center is 0.75 and, hence, $S = 0$. All degrees of order from

complete disorder to perfect order are represented by the order parameter, S, which varies from 0 to 1.0.

The amplitude of diffracted radiation per unit cell is called the structure factor, F. For the Cu_3Au structure there are two different expressions for F, depending upon whether the indices, hkl, are unmixed (all odd or all even) or mixed; for the partially ordered structure:

$$\begin{aligned} &(hkl) \text{ unmixed} \qquad F = f_{Au} + 3 f_{Cu} \\ &(hkl) \text{ mixed} \qquad F = (f_{Au} - f_{Cu}) S \end{aligned} \tag{3}$$

Diffraction lines for which the indices (hkl) are unmixed are called fundamental lines, since the intensities are independent of the degree of long-range order. Lines for which the indices are mixed are called superstructure lines, since their intensities depend upon the degree of order; they are strongest for perfect order and drop to zero intensity for complete disorder.

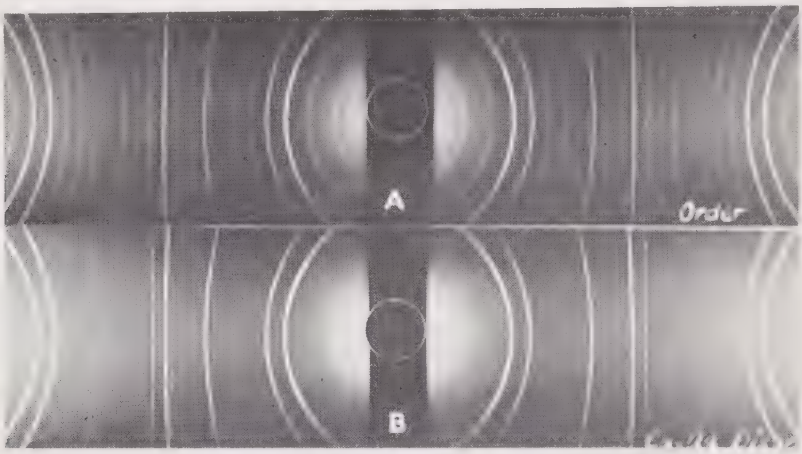

Fig. 12. X-ray patterns of Cu_3Au: (A) long-range order; (B) disordered.

It is evident from equation (3) that the degree of long-range order in the sample can be determined by measuring the intensities of the superstructure lines.

The difference between the x-ray patterns of ordered and disordered Cu_3Au is shown in Figure 12. The lines which are present in the ordered pattern, and absent in the disordered pattern, are the superstructure lines. To investigate the degree of long-range order, S, as a function of temperature, diffraction patterns were made at three temperatures: 250°, 370°, and 380°C. The sample was powdered Cu_3Au which was held at the desired temperature by being placed in a small furnace. The radiation was Cu Ka

monochromated by reflection from a rock-salt crystal. The order parameter was determined from the intensity of the superstructure line (210). The two fundamental lines, (200) and (220), were used to calibrate the (210) line. The values of the long-range order parameter, S, obtained in this way at three different temperatures, are shown by curve A of Figure 13. Curves B and C give the theoretical predictions of Bragg and Williams, and of Peierls, respectively. The experimental results indicate that the long-range order parameter is a little less than unity at low temperatures, drops slightly with increasing temperature, and drops to zero at the critical temperature, T_c = 388°C. To determine the critical temperature accurately and to investigate the variation of S in the neighborhood of the critical temperature, a series of exposures was made at temperatures in this region. At 386.0°C. the superstructure lines are prominent, at 387.5°C. they are faint, and at 389.0°C. they have disappeared completely. From these observations the probable value of T_c is estimated to be 388°C.

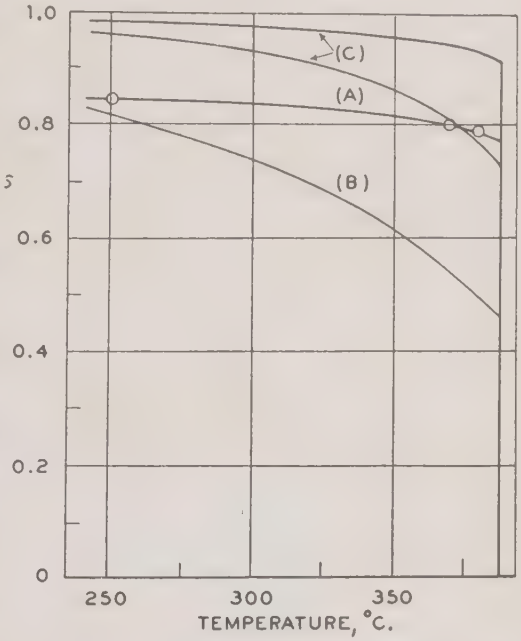

Fig. 13. Long-range order parameter, S, for Cu_3Au as a function of temperature: (A) experimental; (B) according to Bragg and Williams; (C) according to Peierls.

B. Short-Range Order. Above the critical temperature long-range order disappears, but a short-range type of order persists. A gold atom still *prefers* to be surrounded by copper atoms and a copper atom, by gold. For any particular atomic position there is no criterion on the basis of which to say whether it is a right or a wrong position for gold. However, if a certain position is occupied by gold, then there is a probability, which is higher than that of complete disorder, for finding the neighboring positions occupied by copper. The short-range order parameter, σ, gives the amount by which the kind of nearest neighbors, second nearest neighbors, etc., departs from that corresponding to complete disorder. The short-range order parameter would be expected to approach zero very rapidly with increasing neighbor distance.

Let the distance between nearest neighbors be designated as r_1, between second neighbors, r_2, etc. A gold atom will have, on the average, n_i neighbors of copper at a distance r_i, the total number of i^{th} neighbors being designated by c_i. For interatomic distances, $r_i > r_m$, when m is sufficiently large, it will be assumed that complete randomness exists. Let N_0 be the total number of diffracting atoms and $k = 4\pi(\sin\theta/\lambda)$. For a sample of Cu_3Au in which there is partial short-range order but no long-range order, the intensity of diffracted radiation is given in electron units by the equation:

$$I = \frac{3N_0}{16}(f_{Au} - f_{Cu})^2 + \frac{N_0}{16}(f_{Au} - f_{Cu})^2 \sum_{i=1}^{i=m} c_i\left(3 - \frac{4n_i}{c_i}\right)\frac{\sin kr_i}{kr_i} + \left(\frac{3}{4}f_{Cu} + \frac{1}{4}f_{Au}\right)^2 \sum_{l}\sum_{l'}\frac{\sin kr_{ll'}}{kr_{ll'}} \tag{4}$$

The first term is a continuous diffuse scattering due to the randomness and the last term is simply the crystalline reflections, which in this case would be the fundamental lines. The second term represents a fluctuating diffuse background. We will call it the short-range order term, I_{SRO}, since it involves the term $(3 - 4n_i/c_i)$ which is related to the short-range order.

The degree of short-range order may be defined by a set of parameters, σ_i, such that $\sigma_i = 0$ for total disorder and $\sigma_i = 1$ for perfect order. For i^{th} neighbors when n_i/c_i should be greater than 0.75, we define σ_i as:

$$\sigma_i = \frac{4n_i}{c_i} - 3 \tag{5}$$

For i^{th} neighbors when n_i/c_i is less than 0.75:

$$\sigma_i = 1 - \frac{4n_i}{3c_i} \tag{6}$$

$$\sigma_1 = \frac{4n_1}{c_1} - 3, \qquad \sigma_2 = 1 - \frac{4n_2}{3c_2}, \qquad \sigma_3 = \frac{4n_3}{c_3} - 3, \qquad \text{etc.}$$

Let $(c_i/16)(3 - 4n_i/c_i) = 4\pi r^2\rho(r)$. The expression for I_{SRO} involving a summation over sets of neighbors can then be expressed as an integral[4]

$$\frac{I_{SRO}}{N_0} = (f_{Au} - f_{Cu})^2 \int 4\pi r^2\rho(r)\frac{\sin kr}{kr}\,dr \tag{7}$$

By the Fourier integral theorem, this equation can be inverted so that $4\pi r^2\rho(r)$ can be obtained directly from the experimentally determined I_{SRO}. By plotting $4\pi r^2\rho(r)$ against r, the short-range order parameters, σ_i, can then be obtained from the areas under the peaks:

$$\sigma_1 = -\frac{16}{c_1}\int 4\pi r^2\rho(r)\,dr \qquad \sigma_2 = \frac{16}{3\,c_2}\int 4\pi r^2\rho(r)\,dr \qquad (8)$$

The experimental studies were made on two samples of Cu_3Au powder, brought to equilibrium at temperatures of 540°C. and 750°C., and then quenched. Figure 14 shows the Microphotometer records: (A) quenched

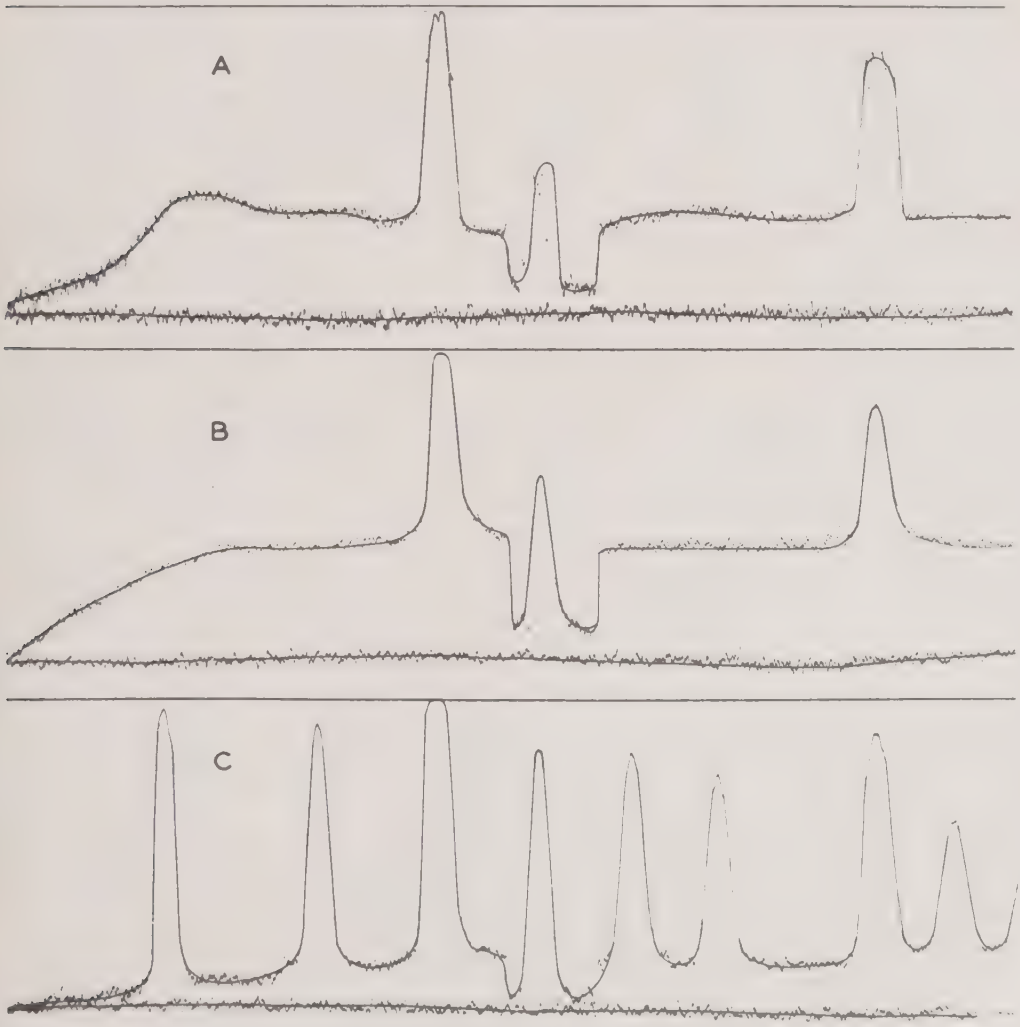

Fig. 14. Microphotometer records of patterns of Cu_3Au: (A) quenched from 540°C.; (B) quenched from 750°C.; (C) ordered sample.

from 540°C., (B) quenched from 750°C., and (C) ordered sample. On all three patterns, the (200) line was attenuated by a factor 0.251 by use of an aluminum shield, so as to facilitate the intensity measurements. The fluctuation in background which is due to the short-range order is clearly seen on curve A in the part directly under A. There is considerably less fluctuation on pattern B for the sample quenched from 750°C., corresponding to considerably less short-range order.

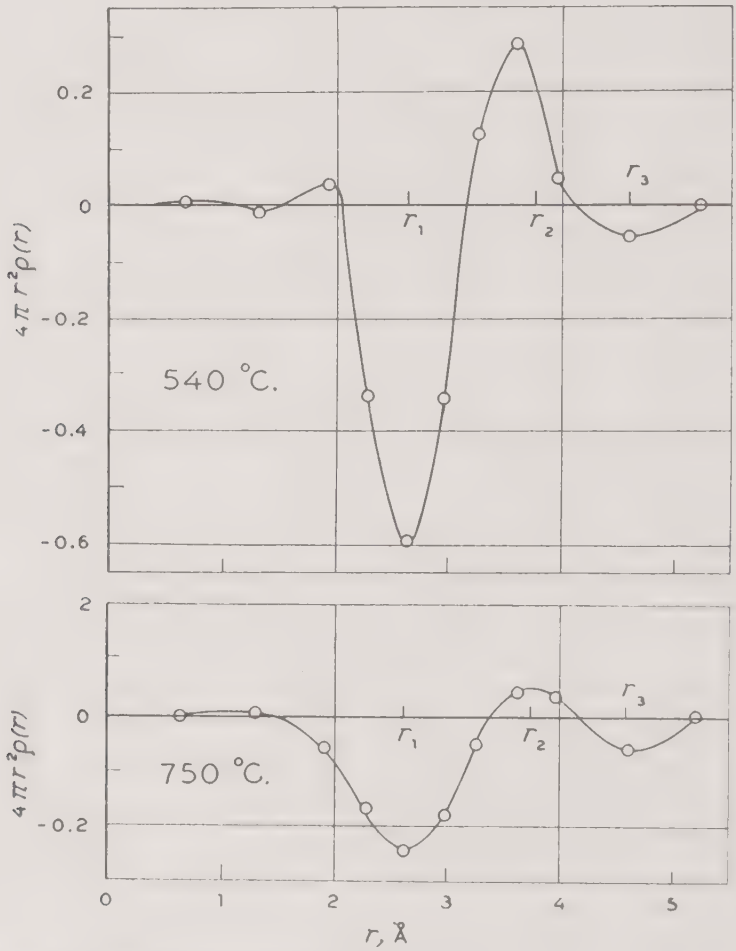

Fig. 15. Distribution curves for short-range order in samples of Cu_3Au quenched from: (A) 540°C. and (B) 750°C.

By putting these curves upon an absolute intensity basis (by means of the known integrated intensities of the fundamental lines) and correcting the background intensity for Compton modified scattering and temperature diffuse scattering, the short-range order intensity term, I_{SRO} is

finally obtained. Performing the Fourier integral inversion of equation (7), the distribution curves for short-range order of Figure 15 are obtained. If there were no short-range order, these curves would be horizontal lines coinciding with the axis of abcissas. A negative peak indicates a concentration of unlike neighbors and a positive peak, a concentration of like neighbors. The positions of the nearest neighbors, second nearest neighbors, etc., are shown by the positions marked r_1, r_2, and r_3. For the sample quenched from 540°C., there is a strong negative peak at the position r_1 indicating a preponderance of unlike atoms as nearest neighbors, a smaller positive peak at r_2 indicating a small excess of like atoms as second nearest neighbors, and a very small negative peak at r_3 corresponding to a slight excess of unlike atoms as third neighbors. At the higher temperature, 750°C., the concentrations are of the same kind but much less marked. The rapidity with which short-range order falls off with distance is clearly indicated by the two curves. From the areas under the peaks, the short-range order parameters, σ_i, are computed by means of equations (8). They are given in Table I.

TABLE I

SHORT-RANGE ORDER IN Cu_3Au

Temperature, °C.	σ_1	σ_2	σ_3
750	0.25	0.05	0.03
540	0.50	0.13	0.03

The discussion of order-disorder changes in Cu_3Au, which has been given here, is an abstract of work done by Dr. Z. Wilchinsky. I am indebted to him for making his paper (5) available to me prior to its publication.

3. Discussion of Randomness

Two examples of randomness in structures have been discussed: the random-layer structure of carbon black and the order-disorder randomness in the alloy Cu_3Au. Many different kinds of randomness have been studied: the random layer structures in platelike minerals, such as micas and clays, the random-ribbon structure in chrysotile, the randomness in structure due to thermal vibration, the rotation of groups and molecules in a crystal, various types of order-disorder changes, the randomness involved in segregation changes, the randomness involved in deformation by cold work, and many others. The x-ray study of ideal crystals gives information about

structures. The study of materials in which randomness can exist gives additional information, for here it is possible to follow changes in the material, changes which are impossible for a perfect crystal. From studies of randomness, new kinds of information can be obtained, information concerning the kinetics of changes, rates of migration and diffusion of atoms in solids, the nature of thermal vibrations in solids, and many others. This is a relatively new field of research with a very promising future.

References

1. Bragg, *Atomic Structure of Minerals.* Cornell Univ. Press, Ithaca, 1937.
2. Robertson, *J. Chem. Soc.*, **1936,** 1195.
3. Patterson, *Z. Krist.*, **90,** 517 (1935); *Phys. Rev.*, **46,** 372 (1934).
4. Biscoe and Warren, *J. Applied Phys.*, **13,** 364 (1942).
5. Wilchinsky, *ibid.*, **15,** 806 (1944).

V. *Light Scattering in Polymer Solutions**

H. MARK

Institute of Polymer Research, Polytechnic Institute of Brooklyn, Brooklyn, N. Y.

I. Introduction

DETERMINATION of the *weight, size,* and *configurational shape* of polymer molecules in solution is one of the key problems in polymer science. The results are not only interesting as such, but are also of importance for the evaluation of kinetic measurements concerning the mechanism of the formation of macromolecules, for the study of rate and equilibrium of order-disorder phenomena, and for the mechanical properties of polymers in the gel and bulk phases, such as the elastic behavior of rubbers, the brittleness of molded test pieces, and the creep and tenacity of fibers and films. Until recently the following methods were available for the determination of the weight and shape of polymer molecules.

(*a*) *Chemical Determination of End Groups.* This method is based on the assumption that certain reactive groups are located at one or both ends of a linear macromolecule; the analytical determination of these groups permits counting the molecules in a given amount of material and, from their number, computing the number average *weight* of the *individual molecule.* This method is only applicable to systems having reactive end groups and

*The author is greatly indebted to Professor P. Debye, Cornell University, and to Dr. Paul M. Doty, University of Notre Dame, for reading the manuscript of this article and for making a number of valuable suggestions for its improvement.

is, in general, restricted to molecular weights below 10,000 because of the limited accuracy of most available analytical methods. It has been of considerable value in the case of cellulose and its derivatives, polyesters, and polyamides, but there is little hope that it can be used successfully in the large field of synthetic polymers and copolymers or in cases in which branching or cross linking must be expected.

(*b*) *Osmotic Method.* This method has been described frequently in recent articles; if properly applied, it leads to the *number-average molecular weight* of the solute and to the quantity μ, which is a thermodynamical measure for the interaction between solvent and solute. This method is, in general, limited to the molecular-weight range between 20,000 and 500,000 and does not yield any direct data concerning the average shape of the dissolved macromolecules.

(*c*) *Ultracentrifugal Analysis of Polymer Solutions.* In principle, this method permits the determination of the *weight-average* and the *z-average molecular weight* of the solute and the computation of a *shape factor* which, to a first approximation, describes the deviation of the particle shape from that of a sphere by assuming that the particle can be treated as a rigid ellipsoid. It also leads (if certain assumptions are fulfilled) to the *distribution function* of molecular weights. This method has been particularly successful with globular proteins, but its application to flexible linear macromolecules has proved to be rather complicated and time consuming.

(*d*) *Observation of Degree of Flow Birefringence and of Angle under Which Maximum Double Refraction Occurs.* This method promises to give information about the shape of dissolved macromolecules and its dependence upon the rate of shear. It does not permit any conclusions about the molecular weight.

This brief summary shows that, in spite of the existence of several independent methods, a fast and reliable determination of large molecular weights and a thorough study of the average shape of macromolecules in solution is still a difficult task, for which any new experimental methods would be extremely welcome.

It was therefore of great importance for the development of the whole field when P. Debye in 1943 and 1944 drew attention to the fact that light scattering of polymer solutions could be used as an *absolute* method to determine the weight-average molecular weight of dissolved macromolecules (8). During the last few years, the theory of light scattering in polymer solutions has been expanded (31,40,41,44,45) and a number of systems

have been studied experimentally by several authors (11–18,22,24,33,39). As a result of this work it seems that the *light-scattering method* is capable of contributing very interesting data about the *weight-average molecular weight*, the *average shape*, and (under certain conditions) even about the *molecular-weight distribution curve* of dissolved macromolecules. This article intends to present a brief review of the theoretical background of this method, its experimental execution, and the results obtained to date.

II. A Few Principles of Light Scattering

Whenever a parallel beam of light passes through a transparent system, such as a gas, a liquid, a solution, or a crystal, a small part of the light is scattered in directions off the primary beam. This scattering can be formally interpreted as a certain *turbidity*, τ, of the medium which is defined by:

$$I = I_0 e^{-\tau l} \tag{1}$$

where I_0 denotes the intensity of the light beam as it enters the scattering system (such as a tube or cuvette filled with a solution), whereas I represents the intensity of the beam after it has passed through the scattering medium of the length, l. Equation (1) shows that the turbidity has the dimension of a reciprocal length (cm.$^{-1}$).

If it is desired to compute τ, it is necessary either to measure the transmitted intensity, I, or to determine the amount of light scattered in a certain direction, *e.g.*, at an angle θ with the incident beam, and then to add up the contributions in all directions. For the computation of the intensity scattered in a given direction, two factors are of importance: (*a*) the scattering from the individual molecules (scattering centers) of which the system is built up, and (*b*) the manner in which these individual scattering centers are geometrically arranged in the medium and hence cooperate in building up the field of the scattered light.

Let us review these two factors briefly.

1. Light Scattering from an Isolated Small Molecule

For the purpose of scattering it is best to consider a parallel beam of light as consisting of a number of plane electric waves, propagating in the direction of the beam, and representing an electric field which oscillates very rapidly in space and time. If we have, for example, a plane-polarized wave of the length λ, propagating in the x-direction with the velocity c, its electric field can be represented by:

$$E = E_0 \cos \frac{2\pi}{\lambda} (x - ct) \tag{2}$$

where E_0 is the amplitude of the electric vibrations.

If we now place a small molecule at a certain place, x_0, in the path of this wave, it will be subject to the periodic electric force represented by (2) and its electrons will respond by oscillating parallel to E with a frequency $\nu = c/\lambda$. Under the influence of the primary wave the molecule will thereby be transformed into an *oscillating dipole*, which (like a little antenna) acts as a *secondary light source* and radiates energy in the form of spherical waves in *all directions*. These *secondary waves* are responsible for the *laterally scattered* light. The electric moment, p, induced in the molecule by equation (2) will be proportional to E:

$$p = \alpha E \tag{3}$$

where α is the *polarizability* of the molecule and represents the degree to which its electrons respond to a field of unit magnitude. By inserting equation (2) into (3) the oscillating dipole is obtained, which is the source of the laterally scattered light:

$$p = \alpha E_0 \cos \frac{2\pi}{\lambda} (x_0 - ct) \tag{4}$$

To compute the spherical wave such an oscillating dipole produces, it must be remembered (cf. 38) that the amplitude of this wave (6,7) at a distance r is: (*a*) inversely proportional to r, (*b*) proportional to the *second derivative* of p, and (*c*) proportional to the cosine of the angle between the directions of the vibration of the electric vector of the incident and scattered rays:

$$E_{sec.\ pol} = \alpha E_0 \frac{4\pi^2}{\lambda^2 r} \cos \frac{2\pi}{\lambda} (x_0 - ct) \cos \phi \tag{5}$$

The intensity of the scattered light at the distance r is given (38) by the square of equation (5):

$$I_{sec.\ pol} = \frac{16\pi^4}{r^2} I_0 \frac{\alpha^2}{\lambda^4} \cos^2 \phi \tag{6}$$

Light-scattering experiments are usually carried out with unpolarized light, which can be considered as the superposition of two polarized beams oscillating at right angles to each other and incoherent in phase. Each one of these beams produces independent oscillating dipoles in the molecule

according to equation (4); these emit secondary waves independently of one another according to equation (5). The resulting intensity at a distance r is given by:

$$I_{sec.\ unpol} = \frac{8\pi^4}{\lambda^4 r^2} \alpha^2 I_0 (1 + \cos^2 \theta) \qquad (7)$$

where θ is now the angle between the incident beam and the direction in which scattering is observed. Figure 1 gives a geometrical representation of equation (7); it can be seen that along the circle in the YZ-plane normal to

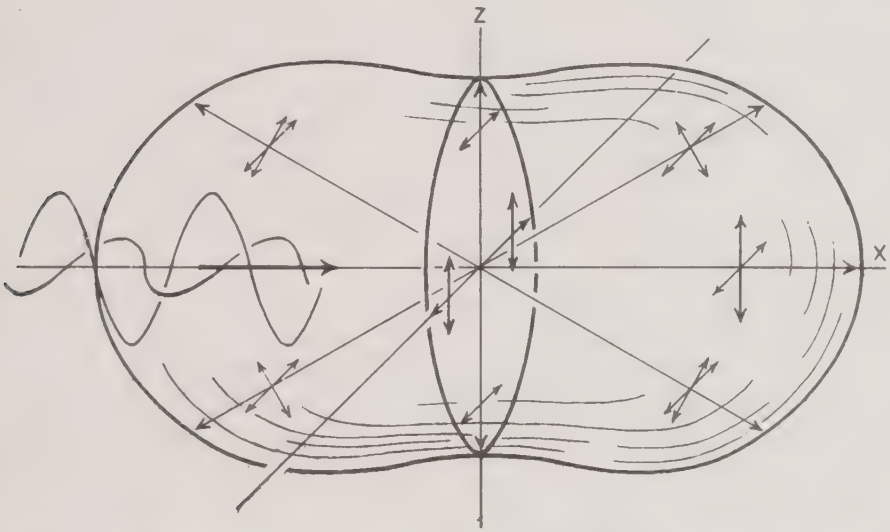

Fig. 1. The envelope indicates the magnitude of the intensity, I, of the scattered light according to equation (7). The incident beam is assumed to be unpolarized. The arrows indicate the state of polarization of the scattered light in the different directions. The scattering molecule is located at the center of the coordinate system and is assumed to be small as compared with the wave length of the scattered radiation.

the incident beam the scattered light is equally bright and completely polarized. In the forward and backward direction it is twice as bright and completely unpolarized; for intermediate values of θ, intensity and state of polarization of the scattered light are intermediate.

2. Scattering of Light from an Ideal Gas

In reality the scattering from an isolated small molecule can never be observed, but only the effect produced by a large number of them. This is the point at which the geometrical arrangement of the scattering centers

and their phase relations enter into the picture. The simplest conditions will prevail if the scattering molecules are completely independent of each other, because in this case no phase relations will exist and the intensity scattered by a multitude of independent particles, as they exist in an ideal gas, will be obtained simply by multiplying equation (7) by the number of scattering centers. If we want not only the intensity scattered by all molecules in a given direction, θ, and observed at a given distance, r, but also the turbidity of the gas as defined in equation (1) as the fractional decrease of the primary intensity per unit length, we must consider that τ is the fraction of the incident light scattered per *unit volume* of the medium in *all directions*. If there are n independent molecules per cc. of the gas, each of which scatters according to equation (7), we must multiply $I_{sec.,\ unpol}$ by n and integrate over all directions and distances. The result, which has already been obtained by Lord Rayleigh (38), [compare also (4,7,9)] is:

$$\tau = \frac{8\pi}{3}\left(\frac{2\pi}{\lambda}\right)^4 n\alpha^2 \tag{8}$$

The primary intensity I_0 has disappeared because τ is defined as its *fractional* decrease per unit length; r and θ have been eliminated by integrations; the polarizability, α, describes the optical properties of the individual scattering center and the simple multiplication by n expresses the absence of phase relations between the secondary waves. The factor $(2\pi/\lambda)^4$ originates from the second derivative, $\partial^2 p/\partial t^2$, in equation (5) and provides for the proper dimension of τ:

$$\tau(\text{cm.}^{-1}) = \frac{n(\text{cm.}^{-3}) \times \alpha^2(\text{cm.}^6)}{\lambda^4(\text{cm.}^4)} \tag{9}$$

Equation (8) permits a simple estimate of the order of magnitude of τ. By putting $n \simeq 3 \times 10^{19}$, $\lambda \simeq 5 \times 10^{-5}$, and $\alpha \simeq 1.0 \times 10^{-24}$, a value of about 10^{-7} is obtained for τ, which indicates that a tube containing an ideal gas under normal pressure has to be 10^7 cm. (or 100 km.) long in order to reduce the intensity of a light beam by scattering to $1/e$ of its original value.

The polarizability, α, is connected with the refractive index of the medium by the formula:

$$\mu - 1 = 2\pi n\alpha \tag{10}$$

which can serve to replace the molecular parameter α in equation (8) by the experimentally measurable quantity μ. By eliminating α from equations (8) and (10), the following relation is obtained:

$$\tau = \frac{32\pi^3}{3} \cdot \frac{1}{\lambda^4} \cdot \frac{1}{n}(\mu - 1)^2 \qquad (11)$$

This relation expresses the well-known fact that scattering of a gaseous system decreases sharply if a given amount of the dispersed phase is divided into a larger number of individual particles, as exemplified in the transition from a fog to a vapor; it has been used to determine Avogadro's number, N_0, by the scattering of light from vapors. A few recent figures resulting from such experiments are contained in Table I; they show rather satis-

TABLE I

AVOGADRO'S NUMBER, N_0, FROM LIGHT-SCATTERING MEASUREMENTS

Method employed	$N_0 \times 10^{-23}$
Light scattering from a mixture of 91% argon, 8.7% nitrogen, and 0.3% oxygen	6.90
Light scattering from ethyl chloride vapor	6.50
Light scattering from water vapor	6.40
Presently accepted value	6.06

factory agreement with the value of N_0 obtained by other, more accurate methods and may be considered as experimental confirmation of equation (11).

III. Scattering of Light from a Pure Liquid

An attempt to expand the simple treatment outlined above to a condensed system, such as a liquid, faces several difficulties.

(*a*) First, we must keep in mind that in a liquid the individual molecules, which act as scattering centers, are far from being independent from one another; in fact, as Debye, Lennard-Jones, and Prins have shown (compare, *e.g.*, reference 8) that there exists in a liquid a considerable degree of short-range order because of the definite volume requirement of the individual particles. If a plane wave passes through a liquid, all molecules in a given part of the incident wave front will vibrate with the same phase, but the secondary waves will now possess certain phase relations because of the quasiregular arrangement of the scattering centers. These phase relations will not affect the intensity scattered *parallel* to the primary beam, but sharply reduce the aggregated intensity under larger angles θ. Hence, it is now not possible simply to *multiply* the intensity

originating from one individual scattering center by the number of these centers per cc., as was done in the derivation of equation (8) from (7). In adopting this procedure, values of about 10^{22} would have to be used for n in liquids and it would be concluded that the turbidity of ordinary liquids should be several hundred times larger than that of ideal gases. In reality pure liquids scatter only ten to fifty times more light than their vapors at atmospheric pressure. A column of water has to be about 1000 m. long ($\tau \simeq 1.0 \times 10^{-5}$ cm.$^{-1}$) in order to reduce the incident intensity by a factor of $1/e$, whereas application of equation (11) would lead to a value of only about 200 m. ($\tau \simeq 5 \times 10^{-5}$ cm.$^{-1}$). This shows that the regular arrangement of the molecules in a liquid decreases the intensity of the laterally scattered light very substantially and must be considered if it is desired to arrive at the correct superposition of the secondary waves emanating from them.

(*b*) Another complication arises from the fact that the relation between the polarizability of the individual molecules and the refractive index of the medium is no longer as simple as that expressed in equation (10) because of the fact that neighboring molecules affect and polarize each other in a condensed system.

(*c*) Finally, it must be considered that in a dense system such as a liquid any individual molecule vibrates not only under the influence of the primary wave but also under the influence of the field produced by the displaced charges in the rest of the medium.

Zimm (43) has recently carried out a straightforward calculation of the interference part of the problem by adding up the secondary waves originating in the various molecules, considering their varying phases, and then averaging over all relative positions of the scattering centers as they exist in a liquid. This procedure is, however, rather difficult and involved and we shall therefore only refer to the original article (40,41) without giving a detailed description of it.

A simpler method of arriving at an equivalent result was originated as early as 1908 by Einstein (19,20), who pointed out that the scattering of a condensed system can be considered to be due to the existence of *thermal density fluctuations*, in the absence of which there would be no lateral light scattering at all. In fact, an ideal crystal, in which all molecules are arranged in complete order at small distances from one another, represents a completely homogeneous optical medium and scatters no light. This can be easily understood with the aid of Figure 2, in which A and B represent two volume elements of the medium which are small as compared with the

wave length of light and regularly distributed throughout the systems. Because of the regular, lattice-like arrangement of the molecules, each of these volume elements contains exactly the same number of scattering centers and the secondary waves emanating from each of them have exactly the same amplitude. At any point of observation, P, the strength of the electric fields originating from A and B will therefore be the same. The distance between A and B, however, remains arbitrary and may be chosen in such a way that the electric vibrations coming from A and B are half a wave length out of phase at the observation point and, therefore, *cancel each other*. For each volume element inside of the scattering system we can find another one which just cancels its effect on P and the total scattered intensity will, therefore, be zero. Only volume elements situated at the extreme surface of the system will remain uncancelled, but they only contribute a negligible effect.

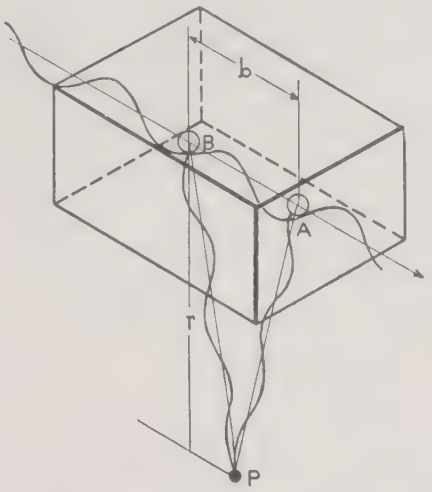

Fig. 2. Lateral scattering of light from a homogeneous medium.

It is thus apparent that a perfectly homogeneous and transparent medium scatters no light at all. A transparent liquid, however, is not perfectly homogeneous because of the thermal motion of its molecules. If we examine the two volume elements, A and B, in Figure 2, we find that molecules are continually moving in and out of them as a result of their random Brownian motion. Hence, at a given instant, the actual number of scattering centers in A will not be exactly the same as in B; the two waves in P will not have the same amplitude and, therefore, will not cancel each other completely in spite of the fact that they are half a wave length out of phase. The *local random density fluctuations* and the corresponding fluctuations of refractivity make a pure transparent liquid optically inhomogeneous and are, therefore, the reason for its turbidity. To calculate this kind of turbidity we have to know: (*1*) the magnitude of the thermal fluctuations and (*2*) the optical efficiency of each of them. These two factors must then be multiplied.

In order to compute the average magnitude of the density fluctuations in a liquid, thermal energy, kT, must be compared with the work which must be supplied to accomplish a certain density change by outside pressure.

The compressibility $\chi = -1/V \cdot \partial V/\partial p$ indicates the relative volume decrease, $-\partial V/V$, if the pressure is increased by ∂p. The larger χ is, the easier it is to produce a density change by outside pressure; the reciprocal compressibility, $K = 1/\chi$, therefore, expresses the *resistivity* of the liquid against compression and its tendency to eliminate thermal fluctuations after they have been produced by kT. The ratio kT/K will then give the average magnitude of the density fluctuations because the numerator is responsible for their creation, the denominator for their disappearance; this ratio corresponds to the number of independently scattering molecules, n, in equation (8).

The optical efficiency of these thermal density fluctuations is given by the refractive index of the medium, μ, multiplied by the change in the refractive index with pressure, $\partial\mu/\partial p$, and is, therefore, $\mu \cdot \partial\mu/\partial p$. This quantity corresponds to the polarizability, α, in equation (8) and must, therefore, appear as the second power because of the transition from the amplitudes of the electric waves in equation (5) to their intensities in equations (6) and (7). By combining the above expressions, multiplying them by a numerical factor resulting from various integrations, and considering the wave length dependence, we find that the turbidity of a pure transparent liquid can be put in the form:

$$\tau = \frac{32\pi^3}{3} \cdot \frac{1}{\lambda^4} \cdot \frac{kT}{K} \left(\mu \frac{\partial \mu}{\partial p} \right)^2 \qquad (12)$$

By comparing equation (12) with relation (11) it can be seen that kT/K replaces $1/n$, whereas $(\mu \cdot \partial\mu/\partial p)$ now stands for $(\mu - 1)$. If the expressions which are valid for an ideal gas are introduced to equation (12) for K and $\partial\mu/\partial p$, equation (12) becomes identical with (11). If the proper values for λ, K, μ, and $\partial\mu/\partial p$ are introduced into equation (12), the correct order of magnitude for the turbidity of liquids ($\tau \simeq 10^{-5}$ cm.$^{-1}$) is obtained, which indicates that a liquid column about 1000 m. in length would scatter enough light laterally to reduce the light beam to $1/e$ of its original intensity.

Raman and his school of optical physicists (4,26,35) have used equation (12) to determine the compressibility of liquids from the measurements of the turbidity, τ, the refractive index, μ, and the change in refractive index with pressure, $\partial\mu/\partial p$. The values of K obtained in this way agree reasonably well with those measured directly, which can be taken as an experimental confirmation of equation (12). We shall see later that this computation of K from three optical quantities (τ, μ, and $\partial\mu/\partial p$) corresponds exactly to the computation of the osmotic pressure, π, of a solution

from the three corresponding optical properties (τ, μ, and $\partial\mu/\partial c$). Table II contains a few numerical data referring to the turbidity of pure liquids.

TABLE II

COMPRESSIBILITIES OF LIQUIDS AT 30°C. AS OBSERVED BY LIGHT SCATTERING

Liquid	$K \times 10^6$ per atmosphere	
	From light scattering	From compression
Isopentane	238	
n-Pentane	225	
Ethyl ether	212	207
Ethyl chloride		255

IV. Scattering of Light from Solutions of Small Molecules

Next we consider the turbidity of a solution and assume first that the molecules of the solute are, in any direction, small as compared with the wave length of the scattered light. This wave length is usually in the neighborhood of 5000 Å (green light) and "small" means that the molecules of the solute should in no direction have an extension larger than about 1/15 of λ, which is about 350 Å. A solid sphere of this diameter made out of a polymeric substance like polystyrene, rubber, or cellulose acetate would have a molecular weight between twenty and thirty million. A rod-shaped particle having this molecular weight and even a randomly kinked coil would, of course, have a much larger dimension along its axis and, therefore, could certainly not be considered to be small as compared with the wave length of the scattered light. In fact, chainlike molecules with molecular weights as low as 150,000 can be compared with a wave length of 5000 Å in certain directions, *e.g.*, parallel to their longest extension, and can, therefore, not be treated as centers of simply spherical secondary waves. The intensity scattered from such molecules can no longer be represented by equation (7) and the turbidity of a gas consisting of such particles would not be given by a relation of the form of equation (8). We shall discuss the influence of the molecular size and shape on the scattering of light in the next paragraph and presently assume that the solute molecules are smaller in all directions than 1/15 or 1/20 of the wave length of the scattered light.

In a dilute solution of this kind, there will be not only local *density* fluctuations of the solvent, as discussed in the previous paragraph, but also

local fluctuations of the *concentration* of the solute. If we focus our attention on a small volume element of the solution, we will find that solute molecules in the course of their Brownian motion move randomly into this volume element and out of it again, so that the solute concentration within the element fluctuates about a certain average value. If the refractive index of the solute differs from that of the solvent, the solution will always contain volume elements of different refractivity and the medium will be rendered turbid by the presence of minute local refracting heterogeneities. In order to compute the turbidity caused by these fluctuations in solute concentration, we must calculate their *average magnitude* and multiply it by their *optical efficiency*. Einstein (20), Gans (21), and Raman (37) have already considered such fluctuations in mixtures and solutions, and Debye (9,10) has recently given a detailed theory.

Apparently we must now compare the average thermal energy, kT, available in the system with the work which is necessary to establish a certain change in concentration. This work is closely connected with the osmotic pressure, π, of the solution and Debye has shown (9) that it can be expressed by $c \cdot \partial\pi/\partial c$. Hence the magnitude of the fluctuations in solute concentration is given by the ratio $kT/(c \cdot \partial\pi/\partial c)$. The optical efficiency of these fluctuations is expressed by $\mu^2(\mu_s - \mu)^2$ where μ is the refractive index of the solvent and μ_s the refractive index of the solution. For dilute solutions $(\mu_s - \mu)$ is very nearly proportional to the concentration of the solute and can be put equal to γc. Hence the turbidity of a solution, as far as fluctuations of solute concentration are concerned, can be written as:

$$\tau = \frac{32\pi^3}{3} \cdot \frac{1}{\lambda^4} \cdot \frac{kT}{c \cdot \partial\pi/\partial c} (\gamma\mu c)^2 \qquad (13)$$

It can be seen that this equation, like equations (11) and (12), consists of four factors: (*1*) a numerical factor $32\pi^3/3$ ($\simeq 350$), (*2*) a factor $1/\lambda^4$ which expresses the wave length dependence of dipole radiation, (*3*) a factor $kT/(c \cdot \partial\pi/\partial c)$ which considers the *average magnitude* of the concentration fluctuations, and (*4*) a factor $(\gamma\mu c)^2$ which accounts for their capacity to *render the system turbid.*

For solutions of small solute molecules, the osmotic pressure can be expressed by van't Hoff's law, $\pi = nkT$, in a concentration range up to a few per cent (n is the number of kinetically independent solute molecules per cc.). By introducing this into equation (13), the following relation is obtained:

$$\tau = \frac{32\pi^3}{3} \cdot \frac{(\gamma\mu c)^2}{\lambda^4} \cdot \frac{1}{n} \qquad (14)$$

In comparing this with equation (11), it can be seen that a solution in the range of van't Hoff's law produces the same turbidity as an ideal gas, if one replaces $(\mu - 1)^2$ for the gas by $(\gamma\mu c)^2$ for the solution. Both systems—gas and solution—become less and less turbid as a given amount of matter is dispersed in a larger and larger number of independently moving particles.

If we want to introduce the molecular weight, M_2, of the solute, we have to write van't Hoff's law in the following form:

$$\pi = (N_0 kT/M_2)c \tag{15}$$

where N_0 is Avogadro's number and c the solute concentration. If equation (15) is introduced into (13), the following is obtained:

$$\tau = \frac{32\pi^3}{3} \cdot \frac{\gamma^2\mu^2}{\lambda^4} \cdot \frac{M_2 c}{N_0} \tag{16}$$

which shows again that, at a given solute concentration, the turbidity increases with M_2. The coarser the distribution of the solute, the more turbid is the system. One gram of cellobiose in 100 cc. of water is twice as turbid as one gram of glucose.

Equation (16) can be used to compute the molecular weight, M_2, of the solute, if the wave length, λ, of the scattered light and the refractive index, μ, of the pure solvent are known and if *two* quantities are measured: (*a*) the increase, γ, in the refractive index with solute concentration, and (*b*) the turbidity, τ, at a given concentration, c. For a given light source (λ) and a given solvent–solute system (λ and μ), the factor

$$32\pi^3\gamma^2\mu^2)/(3\ N_0\lambda^4)$$

assumes a certain constant value of the order of magnitude of 10^{-6} to 10^{-7}, which has been denoted by H (14). Equation (16) can then be written as:

$$\tau = HM_2c \tag{17}$$

In passing to the discussion of solutions containing (comparatively small) polymer molecules, it must be remembered that van't Hoff's law (15) does not even hold at very low concentrations. As has been found in recent investigations, even solutions containing 0.2 grams of solute per 100 cc. and less exhibit noticeable deviations from equation (15). It has been found that for such solutions, equation (15) must be replaced by an equation of the form:

$$\pi = (N_0 kT/M_2)c + Bc^2 \tag{18}$$

where B is an empirical constant which expresses the interaction between the solvent and the individual segments of the dissolved polymer molecules and which, in first approximation, is independent of the molecular weight of the solute. If equation (18) is introduced into (13), the following relation for the turbidity is obtained:

$$\tau = H \cdot \frac{M_2 c}{1 + \frac{2B}{RT} M_2 c} \tag{19}$$

This relation reduces to equation (17) whenever $M_2 c$ is so small that the second term in the denominator can be neglected as compared with unity. This will be the case for very small concentrations if M_2 is large or for larger concentrations if M_2 is not too large, just as would be expected from our knowledge about the validity of van't Hoff's law in the domain of polymer solutions.

For the actual determination of M_2 from osmotic measurements, it is common practice to rearrange equation (18) into the following form:

$$\pi/c = RT/M_2 + Bc \tag{20}$$

By plotting the *reduced* osmotic pressure, π/c, *vs.* c, a straight line is obtained, the intercept of which is RT/M_2, whereas the slope permits the determination of B. Compare, for example, reference (3).

Correspondingly, it is advantageous to rearrange equation (19) into the following form:

$$Hc/\tau = \frac{1}{M_2} + \frac{2B}{RT} c \tag{21}$$

If the *reduced transparency*, Hc/τ, is plotted *vs.* c, a straight line is also obtained, the intercept of which is $1/M_2$, whereas the slope can serve for the determination of B.

Comparison of equations (20) and (21) shows that osmotic pressure and turbidity measurements can be used to determine experimentally two important properties of a polymer solution: (*a*) the molecular weight, M_2, of the solute, and (*b*) the thermodynamic interaction as expressed by the constant B, which in turn (compare ref. 3) is given by $RT/V_1 d_2^2(1/2 - \mu_{12})$, where V_1 is the molar volume of the solvent, d_2 the density of the dry solute, and μ_{12} a magnitude which describes thermodynamically the solvent–solute interaction in a given system at a given temperature, T.

In order to determine these quantities from direct measurements of π it is necessary to carry out at least 3 (4 or 5 are better) individual osmotic

measurements and to draw the best straight line through the experimental points. In using the light-scattering method, it is necessary: (*a*) to measure the refractive index of the solution at several (4 or 5) concentrations below 1% and to determine γ; (*b*) to measure the turbidity of the solution at several (4 or 5) concentrations below 1%, to plot Hc/τ *vs.* c, and to draw the best straight line through the experimental points.

An example is shown in Figure 3 in which plots of Hc/τ *vs.* c for turbid-

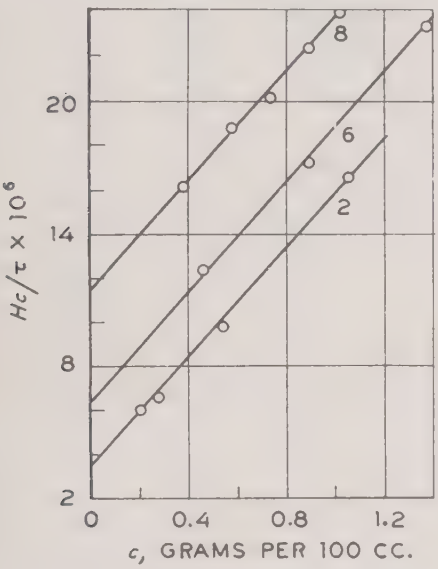

Fig. 3. Values of Hc/τ of three polystyrene fractions in toluene *vs.* solute concentration.

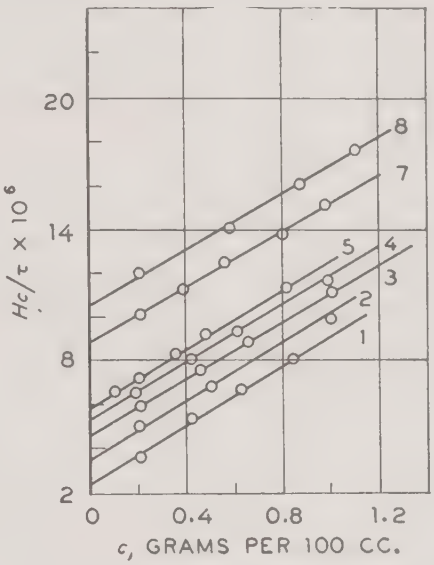

Fig. 4. Values of Hc/τ of seven polystyrene fractions in methyl ethyl ketone *vs.* solute concentration.

ity measurements of three polystyrene fractions in toluene at room temperature are given; it can be seen that the experimental points are, with reasonable accuracy, arranged along straight lines, the intercepts of which are distinctly different, as should be expected from the fact that the three fractions are supposed to have different molecular weights. Table III shows the *turbidity molecular weights* as computed from the intercepts in Figure 3 according to equation (21) and compares them with the *osmotic molecular weights* obtained by direct osmotic measurements using equation (20). It can be seen that there is agreement (to a first approximation) between the osmotic and turbidity molecular weights. Figure 3 also shows that the slopes of the three straight lines are very nearly the same, indicating that the thermodynamic interaction between the segments or submolecules of each of these fractions with toluene is about the same. This is

TABLE III

OSMOTIC AND LIGHT-SCATTERING MEASUREMENTS OF POLYSTYRENE FRACTIONS IN TOLUENE AT 25°C.

Fraction No.	M_2		μ_{12}	
	Osmotic	Turbidity	Osmotic	Turbidity
2	≃200,000	285,000	0.44	0.43
6	127,000	137,000	0.43	0.44
8	100,000	88,500	0.45	0.43

in line with expectation, because all three fractions were obtained from the same polystyrene sample by fractional precipitation; Table III contains the μ_{12}-value as computed from this slope.

Figure 4 represents Hc/τ *vs.* c plots of seven polystyrene fractions in methyl ethyl ketone at room temperature. Again it becomes apparent that the points for each individual fraction are distributed fairly well along straight lines, the intercepts of which on the ordinate determine, according to equation (21), the molecular weights of the various fractions. Table IV

TABLE IV

OSMOTIC AND LIGHT-SCATTERING MEASUREMENTS OF POLYSTYRENE FRACTIONS IN METHYL ETHYL KETONE AT 25°C.

Fraction No.	M_2		μ_{12}	
	Osmotic	Turbidity	Osmotic	Turbidity
1	≃400,000	445,000		
2	≃200,000	250,000		
3	198,000	182,000		
4	≃200,000	190,000	0.47–0.49	0.47–0.48
5	172,000	178,000		
7	91,000	107,000		
8	≃100,000	95,000		

contains the values for M_2 as obtained by turbidity and osmotic measurements and shows again that there is, in general, reasonable agreement between the values obtained by the two methods. It may also be worth while to point out that the molecular weights of fractions 2 and 8, which were measured in toluene and methyl ethyl ketone, agree reasonably well (285,000

and 85,000 in toluene, 250,000 and 95,000 in methyl ethyl ketone), whereas the μ_{12}-values in various solvents show distinct differences.

These two examples may suffice at this point to exemplify in principle the application of equation (21) and its comparison with equation (20); more details about the experimental procedure and more results on various high polymers will be given later (compare pages 163 *et seq.*).

The scale on the ordinates in Figures 3 and 4 indicates that Hc/τ is of the order of magnitude of 5×10^{-6}. Since c is about 10^{-2}, the turbidity of 1% polymer solutions amounts to about 2×10^{-3}, which indicates that a column about 5 m. in length of such solutions will scatter enough light to reduce the initial intensity of the primary beam to $1/e$ of its value. Table V

TABLE V

ORDER OF MAGNITUDE OF LIGHT SCATTERING IN A FEW TYPICAL SYSTEMS

System	Order of magnitude of turbidity, cm.$^{-1}$	Order of magnitude of D, various units
Ideal crystal	Virtually zero	Infinite
Ideal gas or vapor	10^{-7}	100 km.
Pure liquids	10^{-5}	1 km.
Solutions of ordinary small molecules in 1% concentration	10^{-4}	100 m.
Polymer solutions in 1% concentration	10^{-3}	10 m.
Rubber latex in 1% concentration	10^{-1}	10 cm.
Milk	10	1 mm.

summarizes the turbidities of a few characteristic systems according to Debye (8) and indicates the distances which are necessary to reduce the initial intensity of a light beam to $1/e$ of its original value.

This table shows that the turbidity of polymer solutions in the range of concentration in which the measurements are usually made (between 0.1 and 1.0%) is about a hundred times larger than the turbidity of pure liquids and indicates that the concentration fluctuations in polymer solutions are a hundred times more efficient in creating refracting inhomogeneities than the density fluctuations of the solvent. This is a very fortunate phenomenon because it permits neglecting the contribution of the solvent in most cases, as given by equation (12), at the side of the contribution of the solute as expressed in equation (13). The *total* scattering of a solution is represented by the sum of these two contributions:

$$\tau = \frac{32\pi^3}{3} \cdot \frac{\mu^2 kT}{\lambda^4} \left\{ K\left(\frac{\partial \mu}{\partial p}\right)^2 + \frac{1}{c} \cdot \frac{\partial c}{\partial \pi} (\gamma c)^2 \right\} \qquad (22)$$

where, for polymer solutions, the first term in the brace is usually small as compared with the second and has to be subtracted from the total effect.

In considering the two working equations, (20) and (21), which serve to determine M_2 and μ_{12}, it becomes apparent that there are a few significant differences between them.

(*a*) It is worth while to note that at very low concentrations the osmotic pressure, π, is inversely proportional to M_2, whereas the turbidity, τ, is directly proportional to it. The quantities π and τ are those which must be measured experimentally and should not be too small if the measurement is to remain accurate. This indicates that the osmotic method is particularly designed for measuring small molecular weights (between 20,000 and 200,000), whereas the turbidity method is more appropriate for larger molecular weights (between 100,000 and 1,000,000). Hence the two methods complement each other in a very satisfactory manner. The use of the osmotic method in the domain of still smaller molecular weights (less than 20,000) is, however, restricted by diffusion of the solute through the available membranes (compare the article on osmotic pressure in Volume VI of this series) and the use of the turbidity method for large molecules is complicated by the dissymmetry of the scattering. This effect renders the application of the light-scattering method less simple than it would seem to be at the beginning, but, on the other hand, contributes valuable information about the average shape of the dissolved macromolecules.

(*b*) The different relation of M_2 with π and τ, respectively, also has a very important consequence as soon as one does not investigate sharp fractions, which have a comparatively uniform molecular weight, but unfractionated samples with a broad distribution curve of molecular weights. Let us assume that we measure the osmotic pressure of a solution containing a given *amount* (say, 1 gram) of solute. If we subdivide the dissolved material into smaller and smaller units, the osmotic pressure increases because it is proportional to the *number* of independent solute particles in the system. In a mixture of molecules with different molecular weights, one measures, therefore, the *number-average* molecular weight. On the other hand, if we measure the turbidity of a solution containing a given *amount* of solute, as has already been mentioned and is immediately apparent from equation (14), τ increases as the weight of the independent solute particles increases. If the turbidity method is applied to a mixture, there-

fore, the *weight-average* molecular weight of the various species of dissolved molecules is determined.

These two averages are only identical if one operates with very sharp fractions; whenever the distribution curve extends over a wider range of molecular weights, its weight average becomes larger than its number average; the ratio M_w/M_n can even be taken as a first approximate measure of the heterogeneity of a given sample. In case of a *statistical distribution function*, as it occurs in synthetic polymerization and polycondensation products and also in degraded natural polymers, the ratio M_w/M_n is equal to two and assumes even larger values if the spread of molecular weights becomes larger than indicated by random building-up or random degradation of long-chain molecules. The combination of the osmotic and the light-scattering methods can, therefore, be used to obtain a first idea about the molecular homogeneity of a given polymer sample.

After this brief description of the fundamental features of the light scattering from solutions of molecules, that are small as compared with the wave length of light, we shall now consider the turbidity of systems containing molecules which are comparable with the wave length of the scattered light ($\lambda \simeq 5000$ to 6000 Å) and, at the same time, point out a number of refinements which must be made in order to make the theory better able to represent the actual experimental observations.

V. Scattering of Light from Solutions Containing Particles Comparable with the Wave Length of Light

Equation (22) was derived under the assumption that the solute molecules are small as compared with the wave length of the incident light, which means that the largest distances occurring in these particles do not exceed 1/10 to 1/20 of λ. In this case each molecule can be considered to be a *point source* of secondary radiation, which has then the character of a simple *spherical wave*; the dependency of the intensity of the scattered light on the angle of observation, θ, is entirely a function of the projection of the induced dipole moment on a normal to the direction of observation, and would, for unpolarized incident light, vary as $(1 + \cos^2 \theta)$. Figure 1 (page 125) shows a polar plot of this angular distribution. The scattering is symmetrically distributed about the 90° axis.

If, however, any linear dimension of the molecule approaches the magnitude of the wave length, the radiations from all of its component dipoles vary in phase, and the molecule cannot any longer be considered in its entirety as a simple point source. Since the radiation from the com-

ponent parts of any one molecule is coherent, the resulting scattered intensity will be proportional to the square of the *vector sum* of the amplitude of the scattered rays. This will result in an interference pattern which is characteristic of the size and shape of the particle.

This phenomenon may be readily illustrated with the aid of a simple example. The sphere in Figure 5 represents a scattering particle with dimensions which are of the order of magnitude of the wave length. Let us consider two scattering volume elements at A and B, and two incident rays, R_1 and R_2, which are in phase at plane P. In reaching a forward observation point, O_1, ray R_1, which travels the *shorter* distance to reach element A, travels the *longer* distance, AO_1, from A to O_1; whereas ray R_2, which travels the *longer* distance to element A, travels the *shorter* distance

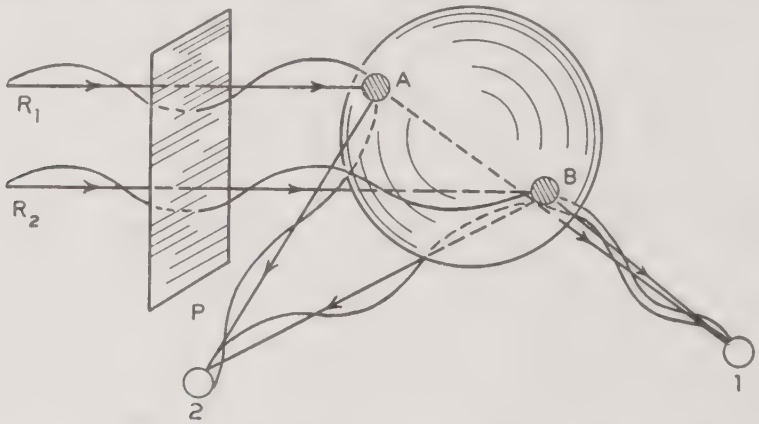

Fig. 5. Lateral scattering of light by a particle the dimensions of which are comparable with the wave length of light.

to the observation point. Thus, the differences in path lengths are partially compensated for, and the rays do not become very much out of phase in the forward direction, O_1.

For a backward observation point, O_2, however, the situation is reversed; the ray (R_2) which travels the *longer* distance from the plane to the element also travels the *longer* distance to the observation point. If, as in this illustration, the molecular dimensions are something less than one wave length, the path difference will be such as to produce a phase lag that will result in destructive interference of the two rays in the backward direction, O_2. Therefore, it may be seen that, as a result of this interference effect, there will be an all-around decrease in the scattered intensity. Since destructive interference is more probable between rays scattered in the backward direction, the radiation envelope will no longer be symmetrical.

For still larger particles, path differences greater than one-half wave length will be produced and *higher-order* interference will occur. More than one intensity maximum will then be experienced; compare (6,28,30). A typical first-order interference pattern of this type is shown in Figure 6.

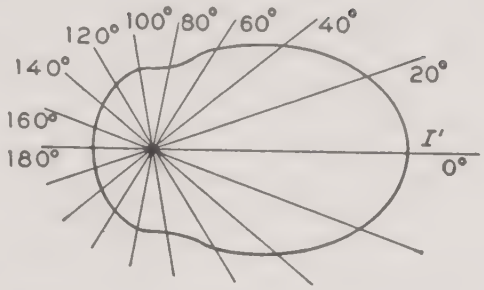

Fig. 6. The radii of the curve are proportional to the intensity of the scattered light in the direction of the radius. The envelope shows a considerable dissymmetry in favor of forward scattering as explained in Figure 5.

The evaluation of this interference effect for particles of simple geometric shape has been studied by Mie (30) and more recently by LaMer and his collaborators (28). Its exact evaluation is difficult, however, when the refractive index of the particle is much different from that of the medium in which it resides. The problem which then arises involves the determination of the effect of the polarization charges on the surfaces of the particles on the electric field acting upon a particular dipole as a function of the position of that dipole in the particle. A solution of Maxwell's equations under these conditions, even for particles of simple geometric shape, usually leads to complicated expansions, the application of which is difficult. Blumer (5) has obtained integrated solutions of this type for spheres; compare also (6).

In the more special case of polymer solutions, however, one can arrive at a simpler treatment of this problem by taking advantage of the fact that the refractive index of the solute is usually not very different from that of the solvent and that this difference can be reduced to any desired degree by choosing a proper solvent or solvent mixture. P. P. Debye and P. Debye (8,9) have shown that, for small differences in refractivity between solvent and solute, the refraction of the primary wave *inside* of the particle can be neglected and the contributions from the various elements of the scattering molecule can be added up in a reasonably simple manner. They have obtained in this way the intensity distribution of the light scattered by spheres, rods, and random coils. The last two shapes are particularly interesting from the point of view of polymer solutions and shall, therefore, be discussed here in some detail.

If polymer molecules consist of comparatively stiff chains or are strongly solvated, their shape can be approached by that of a *free-draining chain* (37,41), where the chain only exhibits slight kinks and moderate modulations. For such conditions the *rigid-rod* model appears to be a

reasonable approximation of the actual average shape of the dissolved macromolecules. P. Debye and his son (11) and Doty, Stein, and Zimm (41) arrived at the following expression for the angular intensity distribution of the light scattered from a rigid rod of length L and of very small diameter:

$$I(\theta, L/\lambda) = \frac{I^0}{x} \int_0^{2x} \frac{\sin x}{x}\, dx - \left(\frac{\sin x}{x}\right)^2 \qquad (23)$$

The factor $(1 + \cos^2 \theta)$ has been omitted from the right side because it is symmetrical about 90^0, the quantity x is defined by:

$$x = 2\pi \frac{L}{\lambda} \sin \theta/2 \qquad (24)$$

and I^0 represents the intensity scattered by particles which are small as compared with λ.

Expression (23) represents a function which decreases as the angle θ increases; the rate of this decrease depends upon the parameter L/λ, as indicated in equation (24). Hence, by measuring $I(\theta, L/\lambda)$ at several values of θ, one can first verify that the dissolved particles approach the shape of rigid rods and then determine the average length, L, of the particles in terms of λ.

If polymer molecules consist of very flexible chains and are not noticeably solvated, their shape can be approached by *randomly kinked coils* (23,27) of roughly spheroidal shape. For such particles, the intensity distribution is:

$$I(\theta, D/\lambda) = \frac{2\, I^0}{v} [e^{-v} - (1 - v)] \qquad (25)$$

$$v = \frac{2}{3} (D/\lambda)^2 (2\pi \sin \theta/2)^2 \qquad (26)$$

Equation (25) also represents a function which decreases with increasing observation angle, θ; the rate of decrease depends upon the parameter D/λ, where D is the *root mean square separation* of the ends of the chain and represents the *largest distance* which occurs in the most probable configuration of such molecules. By measuring $I(\theta, D/\lambda)$ at various angles, one can again confirm the existence of randomly coiled particles in solution and determine their largest average extension.*

*Those familiar with the theory of x-ray diffraction will notice the similarity of these functions with the atomic form factor.

Figure 7 shows how in the two cases of free-draining chains and matted particles the scattered intensity depends upon the angle of observations. For those familiar with the theory of x-ray scattering it will be apparent that these curves correspond entirely to *atomic form factor* curves as used to evaluate x-ray intensities quantitatively.

It may be emphasized here that a great deal of work on the dissymmetry of light scattering was carried out by P. Debye and his collaborators at Cornell University under a contract of the Office of Rubber Reserve, Reconstruction Finance Corporation. Some of the work has been published (12,24); most of it is not yet published but is embodied in reports to the sponsoring agency.

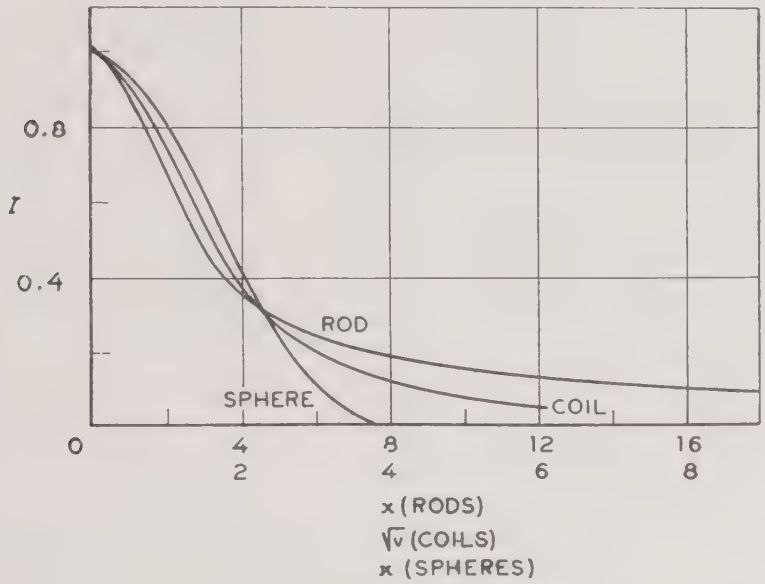

Fig. 7. Intensity of light scattered by spheres, rods, and coils having dimensions comparable with the wave length of light as dependent upon the characteristic quantities x and $\sqrt{v}$ as defined by equations (24) and (26).

In most of the work reported up to date (14,17,39) two angles (50° and 130°) of observation symmetrical about 90° have been chosen and the scattered intensities have been measured at these angles. The ratio, z, of $I(50°)$ to $I(130°)$ was termed the *dissymmetry* coefficient of the polymer under consideration in the particular solvent employed. Experiments of Zimm (42) have shown that z still depends upon the concentration of the solution and, in general, increases as zero concentration is approached. This

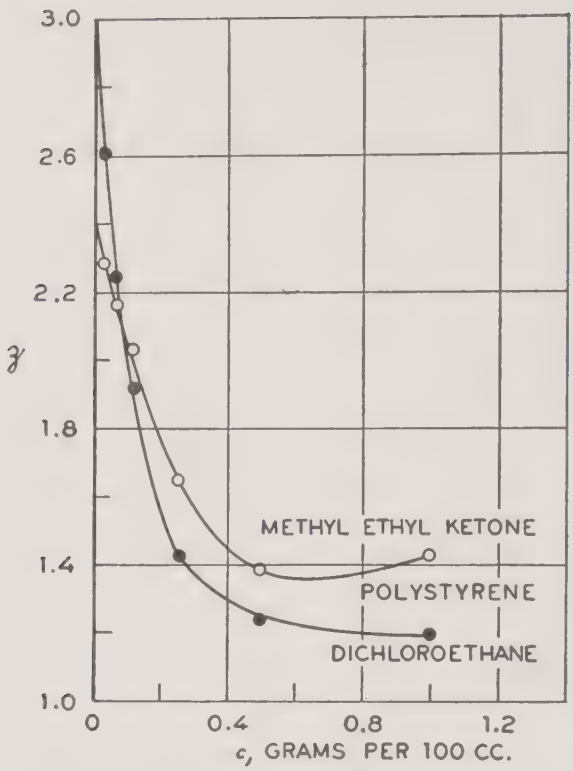

Fig. 8. The dissymmetry, z, as defined by the ratio of the intensity scattered under 50° and 130° *vs.* the concentration of the solute. The polymer is a polystyrene fraction; the solvents are methyl ethyl ketone and dichloroethane.

behavior is illustrated in Figure 8 which contains dissymmetry measurements with polystyrene fractions in various solvents (42). Because of the noticeable dependence of z upon concentration, Zimm has proposed carrying out a graphical extrapolation to infinite dilution and using for all further considerations the *intrinsic dissymmetry* $[z]$.

This intrinsic dissymmetry is now dependent only upon a parameter which refers to the ratio between a characteristic dimension of the polymer molecule and the wave length. Figure 9 represents three curves expressing this dependency for spheres (*1*), rigid rods (*2*), and random coils (*3*); the characteristic dimensions are the *diameter* of the sphere, the *length* of the rod, and the *root mean square extension* of the random coil, respectively, which, with the aid of these curves, can be read directly from a determination of $[z]$.

This discussion of dissymmetry shows that there are two ways of determining molecular weights of polymers in solution from turbidity measurements:

(*1*) From Figure 6 it can immediately be seen that, in the neighborhood of the primary beam, the phase differences between waves emerging from different parts of a polymer molecule are small, even if the molecules approach the wave length of the scattered light; this *small-angle scattering* can, therefore, be used to determine intensities, which are unaffected by destructive interference and which lead to the turbidity, τ, as used in equation (21) to compute the molecular weight of the dissolved polymer. Measurements under small angles are, however, not too easy to carry out and it seems preferable, therefore, to use the other prodecure.

(2) One measures first at a given concentration the intensity scattered under 90° and, at the same concentration, the intensities scattered in the forward and backward direction symmetrically about 90°, *e.g.*, under 50° and 130°, respectively. If the dissolved macromolecules are small enough, the scattering (after correcting for polarization) under all three angles will be the same and equation (21) can be used directly. In the case of larger molecules the values will increase from $I(130°)$ over $I(90°)$ to $I(50°)$ according to the curves in Figure 6. It is therefore apparent that the value measured under 90° is noticeably affected by destructive interference and is smaller than it would be if the theory outlined in the second paragraph (page 123) were correct. If the 90° intensity as measured is introduced into equation (21), a molecular weight is obtained which is too small and, therefore, must be multiplied by a *correction factor*, f, to account for the destructive interference in the 90° direction.

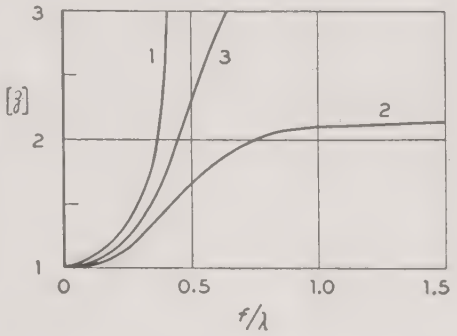

Fig. 9. Intrinsic dissymmetry, $[z]$, *vs.* f/λ, where f is a characteristic dimension of the scattering particle according to equations (24) and (26).

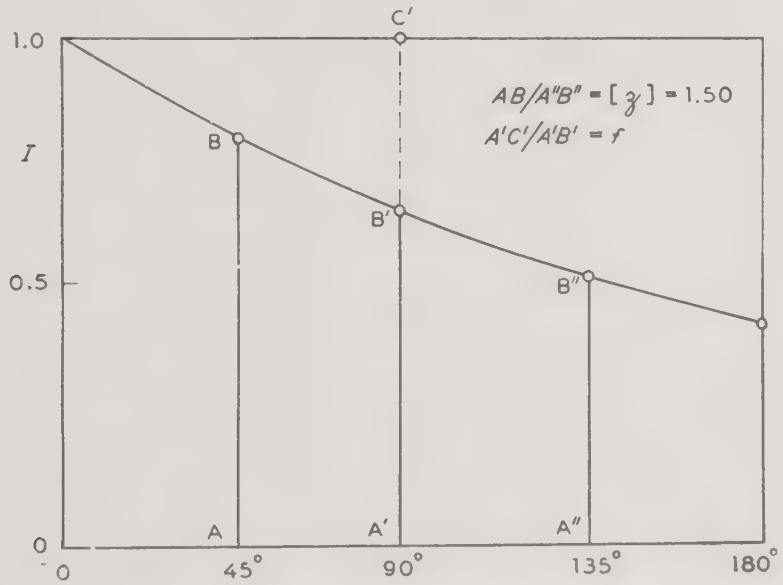

Fig. 10. I *vs.* θ for dissymmetric scattering from a particle having the shape of a random coil.

This correction factor can be obtained from z in the following way. It must first be decided which of the three models—sphere, rod, or random coil—should be applied; in general, the rod model will be used for free-draining chains and the coil model for matted particles. Let us assume that for a given polymer we have decided to use the model of a random coil. In this case we use curve *3* in Figure 9 and arrive, from the measured value, at the corresponding D/λ-value of the dissolved molecules. This value is then introduced into equation (25) which is now only a function of θ and the graph showing I *vs.* θ is drawn. Let us assume that it has the shape shown in Figure 10, where $I(50)/I(130)$ has an assumed value of 1.50. Then it is evident that the destructive interference under 90° has diminished the scattered intensity from its proper value, $A'C'$, to the actually measured value, $A'B'$. In order to obtain the correct value, we must therefore, multiply the observed value, $A'B'$, by the *correction factor*, $f = A'C'/A'B'$, which we can take directly from the graph of Figure 10. The value of f apparently depends upon the shape of the I *vs.* θ curve which in turn depends upon D/λ. Stein and Doty (41) have, for the special case of cellulose acetate in acetone, worked out the relation between f and z, which is represented in Figure 11, where the correction factor can directly be taken from the measurement of the dissymmetry coefficient, *viz.*, of the intrinsic dissymmetry. Such graphs are very useful and become necessary for the application of equation (21) as soon as a given system displays any appreciable angular dissymmetry of the scattered radiation.

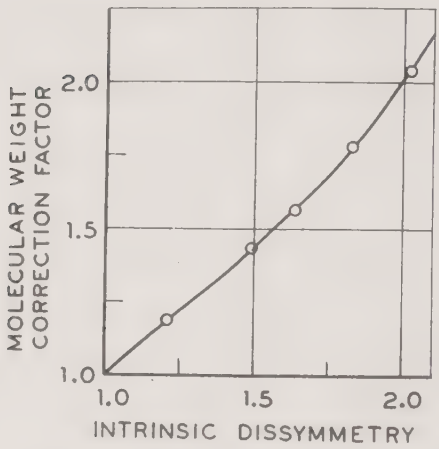

Fig. 11. Correction factor, f, for the intensity scattered under 90° *vs.* the intrinsic dissymmetry.

Tables presenting similar data are contained in an unpublished report by P. Debye and J. A. McCartney to the Office of Rubber Reserve, Reconstruction Finance Corporation.

From this brief discussion it becomes apparent that it is always highly recommendable to measure the scattered intensity in at least three directions. If there is no dissymmetry, one can be sure that the dimensions of the dissolved macromolecules are small as compared with the wave length of the light in all directions, whereas if a scattering dissymmetry is en-

countered, it must be taken into account to arrive at the correct values of the molecular weight and can also be used to obtain some information about the largest dimensions in the polymer molecules. In both procedures it is necessary to decide upon which model—sphere, rod, or random coil—the calculations should be based. This introduces a certain ambiguity and may produce misleading results, if the wrong model is picked. However, Doty and Zimm have pointed out that in most cases which have been treated hitherto, such as cellulose acetate, polystyrene, polyvinyl chloride, etc., the dissymmetries are usually not larger than 1.6 or 1.7. Figure 9 shows that the three dissymmetry curves for sphere, coil, and rod, respectively, do not diverge very much from each other in this range. If the rod curve is used at $z = 1.7$, an L/λ-value of 0.50 is obtained, whereas the corresponding D/λ-value on the coil curve is about 0.35; this is not too bad a deviation, if one keeps in mind the fact that even the order of magnitude of the dimensions of macromolecules in solution is sometimes of considerable interest.

In order to eliminate this uncertainty, the scattering measurements would have to be carried out under different angles with different wave lengths to find out whether, at values of L/λ larger than 0.75, the curve flattens out as indicated in Figure 9 for rods or whether it continues to rise, which is characteristic for coils.

Equations (23) and (25) contain the wave length, λ, implicitly in *two* places: first, in I^0, where it appears in the factor $(1/\lambda)^4$, and second, in x and v, where L and D are measured in terms of λ. Hence, if I is determined at a given angle θ for different wave lengths, deviations from the simple $(1/\lambda)^4$ dependency should be expected. Heller (24) has pointed out that these deviations can be also used to discover the presence of particles which are not small (as compared with λ) in every direction. In fact, every scattering phenomenon always permits the observation of a certain effect, either by measuring the angular-intensity distribution at constant wave length or the wave-length dependency at constant angle.

VI. Depolarization of Scattered Light

Equations (7), (23), and (25) which express the angular distribution of the intensity scattered by small and large molecules predict that the light scattered under 90° should be completely polarized; its electric vector should oscillate in a plane perpendicular to the plane which is defined by the incident beam and the direction of observation. This is a simple consequence of the transversal nature of the vibrations of the light. Experi-

ments with gases, liquids, and solutions have now shown that, in most cases, the light scattered under 90° has a small horizontal component. The ratio of this horizontal component to the vertical component represents the *depolarization* of the scattered radiation. In the theory outlined previously this effect has been neglected; it is, in general, rather small in gases, liquids, and normal solutions and has been treated in a number of articles by Mie (30), Gans (21), and particularly Krishman (26); compare also (4,6). The depolarization of solutions containing polymer molecules has recently been studied by Doty and Kaufman (16) for cellulose acetate in acetone, polyvinyl chloride in methyl ethyl ketone, and polystyrene in toluene and methyl ethyl ketone.

If depolarization exists, two general conclusions can be drawn:

(*1*) The intensity measured under 90° is now somewhat larger than it should be according to the simple theory embodied in equations (13) or (21) because of the existence of the horizontal component. The turbidity of a solution exhibiting depolarization will, therefore, be larger than it should be according to equation (13) and the molecular weights determined from relation (21) will be too large. In order to arrive at their true values, it will be necessary to multiply them by a correction factor, f, the computation of which we shall discuss briefly later.

(*2*) The scattering particles do not behave like isotropic elements but exhibit a certain degree of intrinsic anisotropy which can be measured and which may allow interesting conclusions about the structure of the dissolved macromolecules.

In the elementary theory, as briefly outlined in the previous paragraphs, it was assumed that the electrons in the scattering particles oscillate exactly parallel to the vector of the incident light, which implies that the polarizability, α, is independent of direction and can be considered to be a *scalar* quantity. In the general case, however, α depends upon the direction and the scattering particles must be characterized by an *ellipsoid of polarization*. Each single particle carries with it such an ellipsoid of polarization with three principle axes of polarizability. In the course of the random movements of the individual molecules in the gas, the liquid, or the solution, these ellipsoids will become randomly oriented in all directions. Their orientation, however, will exhibit fluctuations and these additional *fluctuations of orientation* are responsible for the fact that anisotropic molecules scatter *more* light in a given direction than isotropic ones.

By introducing these orientation fluctuations to the theory it is found that α^2 in equation (7) must be replaced by:

$$\alpha^2 f = \alpha^2 \cdot \frac{6 + 6\rho}{6 - 7\rho} \qquad (27)$$

The depolarization, ρ, is, in general, of the order of magnitude of 10^{-2} and the value of f is, therefore, usually between 1.02 and 1.10; its application reduces the molecular weight as found without considering polarization by 2 to 10%. In investigating cellulose acetate fractions in acetone Doty and Kaufman (16) have found depolarization values from 0.017 to 0.045 and have computed that the molecular weights of four fractions had to be decreased from 116,000, 91,700, 60,200 and 47,200 to 114,000, 87,700, 55,600 and 43,000, respectively (*cf.* 39). This is not a very large correction in the case of the fractions of high molecular weight, in which the particles have essentially the character of kinked coils, but amounts to almost 10% in the case of the lowest fraction, in which the molecules apparently almost approach the shape of rods and have little tendency to curl back on themselves. This is also borne out by the fact that the depolarization, ρ, is essentially independent of concentration but noticeably dependent upon molecular weight. It indicates the presence of comparatively unflexible, anisotropic chain molecules with only little mutual interaction. In the case of polyvinyl chloride in methyl ethyl ketone, it was found by a similar investigation that the molecules are coiled up in solution to a considerable degree; in the case of polystyrene it turned out that polymers prepared at different temperatures (1) exhibit different tendencies to coil up in solution even though the molecular weights are essentially the same; it appears that polystyrene molecules prepared at 100°C. are smaller but more isotropic than molecules prepared at 70°C.

Thus it appears that depolarization measurements not only provide for a necessary correction in the computation of the molecular weight but also contribute interesting information on the question of the average shape of macromolecules in solution.

Before closing the theoretical section of this review and going on to the description of the experimental procedure, it should be indicated that the *fluctuation theory* of light scattering operates with assumptions which, to a certain extent, represent a considerable simplification of the problem.*

One of these is the assumption that the fluctuations in density, concentration, etc. in a given volume element are completely independent of those in the surrounding volumes. Ornstein and Zernicke (32) and Zimm (43) have discussed this problem and have shown that this is only justified

*Some of the questions raised here are taken up in a forthcoming article by P. Debye, *J. Phys. Chem.*, in press.

if the range of intermolecular forces is small as compared with the wave length of light. This will in general be true, but in polymer solutions, in which the molecules themselves are comparable or even larger than the wave length of light, it is doubtful whether the concentration fluctuations in adjacent volume elements can be considered to be independent of each other.

Another assumption is that each volume element of the scattering medium vibrates essentially under the influence of the primary wave *alone*, whereas in a condensed system the surrounding volume will appreciably contribute to the polarization of a given volume element. It is therefore necessary to consider the forced vibrations of a given molecule to be produced by an *effective field* which is not identical with, but proportional to, the external field. The computation of the proportionality coefficient is a problem which has not yet been solved satisfactorily. According to Lorentz (29), the effective field can be approximately calculated by considering the medium to be a continuous uniform fluid enclosing a cavity in which the volume element under consideration is placed. It is then found that the factor characterizing the effective field depends strongly on the shape of the cavity, ranging in value from n^2 for a needle-shaped cavity parallel to the field to unity for a cubic or disclike cavity cutting across the field; for a sphere, the value is $(n^2 + 2)/3$. In all articles reported here, the effective field has been assumed to be equal to the external field, but it would be highly desirable to have this point cleared up by more experimental work with solutions of substances with low molecular weights.

Finally, it may be that the part of the effective field which comes from the influence of the surrounding volumes fluctuates as the polarization of these volume elements changes, and that these fluctuations are related to the fluctuations in concentration. This would introduce an additional correction factor, the magnitude of which is difficult to predict without a rather complete analysis. Such a treatment of our problem is still lacking (41).

VII. Experimental Methods for Measuring Turbidity and Dissymmetry

In order to apply the formulas derived in the previous paragraphs, it is necessary to measure *two* quantities: the *turbidity*, τ, and the *refractive index*, μ, of a transparent solution. The *turbidity* can be measured in two principally different ways:

(*a*) *Transmission Method* (12,24). In this method the quantity I in

equation (1) is determined. As I_0 and l are known, the turbidity, τ, can be computed. This method is reliable and accurate if the product τl has a value not too small as compared with unity and if no true absorption of the light occurs in the medium. For absorption tubes of reasonable lengths this is the case only if visibly turbid emulsions or suspensions are investigated; for such systems the transmission method has been used with good success. For dilute (less than 0.5%) polymer solutions, however, τ is of the order of magnitude of 10^{-3} to 10^{-4} and it would, therefore, be necessary to operate with tubes several meters in length, to reduce the primary intensity to a noticeable degree. In such cases the second method is preferred.

(*b*) *Direct Measurement of Laterally Scattered Light.* In this method a comparatively small intensity must be measured with an accuracy of about 2–5% of its value. If the solution is clean and colorless this is a relatively easy task which can be carried out either by *visual* observation or by *photoelectric* registration (11,12,17,39).

A turbidimeter for visual observation,* which has been used fairly successfully for a large number of measurements, is shown in Figure 12 (14,15,17,39). A vertically mounted mercury arc (AH-4, 100-watt, General Electric bulb) furnishes the light which is rendered monochromatic by the filters (*B*) and parallel by the lens (*C*) and square diaphragm (*D*). A glass plate (*E*) mounted at 45° reflects a small fraction of the incident light on an opalescent glass plate (*F*).

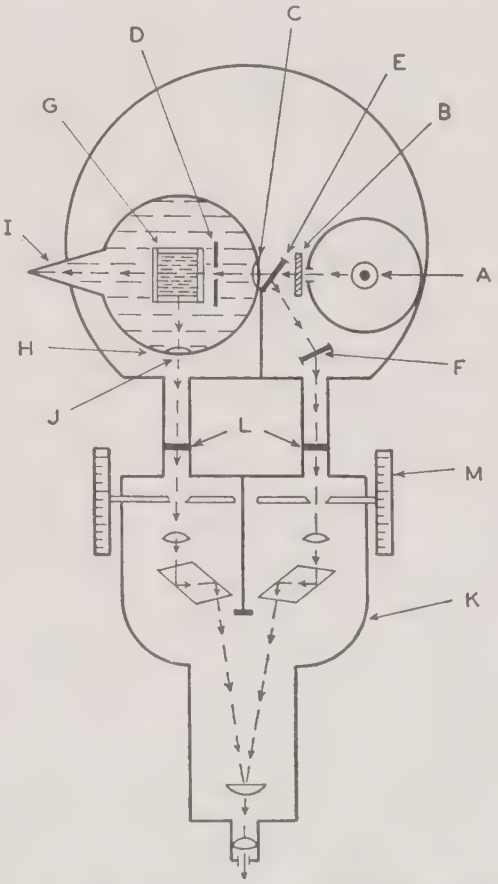

Fig. 12. Instrument for the visual measurement of the intensity scattered under 90°, according to P. M. Doty (turbidimeter).

*Instruments of this type are manufactured by General Gauge and Tool Company, 30 Irving Place, New York.

The square cell (G) containing the polymer solution is immersed in a water-filled chamber (H). A false bottom in this chamber permits temperature control by circulating water from a thermostat. The water in the cell also serves to minimize reflections at interfaces. After passing through the solution, the incident beam is absorbed, through multiple reflection, by the cone (I) at the far end of the chamber. The lens (J) transmits some of the light scattered at 90° into one side of a Zeiss Pulfrich photometer (K) which is used to compare visually the intensity of this light with that coming from the opalescent plate (F), the reference standard. Provision is made for inserting neutral filters (L) into the connecting tube of the photometer in order to limit the intensity during the calibration. The two beams pass through precision diaphragms of adjustable area and, by means of a prism and lens system, illuminate the two halves of a divided field. The slit areas are adjusted until the two half-fields appear to be equally bright. The relative intensities are then inversely proportional to the respective slit areas, which are indicated on graduated scales on the adjusting dials (M) of the slit area.

The calibration of the instrument just described, as well as all others based on a similar principle, requires only a means of diverting a very *small* but *accurately known* fraction of the incident light beam into the transverse direction. If the intensity of this small fraction of the incident beam is i_0 at a distance r from the beam then the turbidity is given by:

$$\tau = \frac{16\pi}{3} \cdot \frac{i_0 r^2}{I} \tag{28}$$

where I is the intensity of the incident beam. The fraction i_0/I must be of the order of 10^{-6}. Two methods have been used to obtain this ratio. One has been based on a reflection either from magnesium carbonate (with subsequent reduction with filters) (41) or from multiple reflections on glass plates (12). The other method involves the use of a solution. The *only* requirements for the solution are (*a*) that it scatters light symmetrically about the transverse direction (Rayleigh scattering) and (*b*) that it scatters sufficiently to permit an accurate determination of its turbidity by transmission measurement. These conditions are best satisfied by a pure protein solution or polymer of low molecular weight. Such a solution which satisfies these two requirements can be used for direct calibration. The response which the instrument gives to the solution corresponds to the turbidity determined by the transmission measurement.

For the measurement of the *dissymmetry* another visual instrument

was designed, which is shown in Figure 13. Inasmuch as the theory indicates that the angular distribution is characterized by only one parameter for particles of homogeneous size in the range we are investigating, and since the influence of very small amounts of colloidal impurities on the dissymmetry is often great enough to limit considerably the accuracy attainable, it was felt that a simple apparatus capable of measuring only a

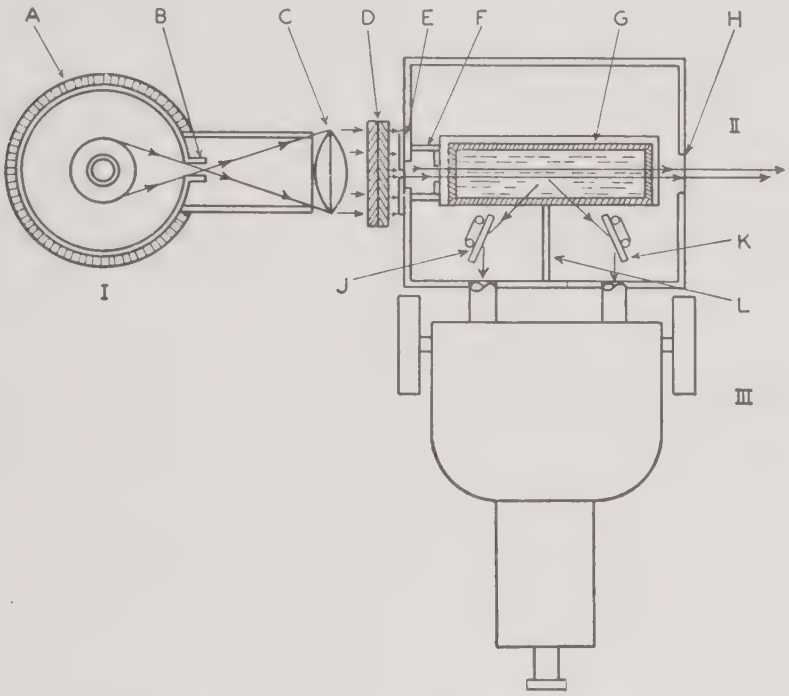

Fig. 13. Instrument for the measurement of the dissymmetry of the scattered light, according to P. M. Doty (Rayleighometer).

few points on the intensity-angle curve would be adequate for the problem at hand.

A cylindrical, water-cooled vertical lamp housing (*A*) contains a vertically mounted AH-4 mercury arc. A narrow slit (*B*) in the front of the housing serves as a secondary source. The convex lens (*C*) renders the light parallel, while a set of Corning color filters (*D*) isolates the desired mercury line. Two 1/8-in. vertical slits (*E*) and (*F*) collimate the beam into a narrow rectangular pencil.

The principal component of the instrument is a metal box, 7 in. long, 6 in. wide, and 3 in. high, which contains the solution and the mirrors. A rectangular glass cell (*G*), 100 mm. long, 20 mm. wide, and 50 mm. high,

is located in the center of this box by metal guides. The cell is open at the top and is partially filled with a solution of the high polymer. The light beam, upon leaving the collimating slits, passes through the center of this cell and out through the exit hole (*H*). Light is scattered in all directions from the solution, and two surface mirrors (*J*) and (*K*) are so mounted as to reflect two symmetrically scattered rays of light out of the box perpendicularly through two circular holes in the front wall. The mirrors are mounted on bases having dowel pins which fit into holes drilled through the bottom of the box. Several sets of these holes are provided so as to permit variation of the mirror angles symmetrically about the 90° axis. A central barrier (*L*) serves to help prevent stray light from striking the mirrors. The interior of the box is coated with an optically black lacquer.

A Zeiss Pulfrich photometer, similar to that used with the turbidimeter, is placed so as to receive the light passing out through the holes in front of the box. Its function is to measure the comparative intensity of these two light rays. At balanced fields, the ratio of the intensities of these two rays should be inversely proportional to the respective dial readings of the photometer.

The instrument may be tested for symmetry of construction by measuring the dissymmetry of the fluorescent light radiating from a solution of fluorescein placed in the cell. Such a solution should radiate light equally in all directions, and the indicated dissymmetry coefficient should be zero. The effect of stray light may be determined by measuring the dissymmetry of the radiation from successive dilutions of the fluorescein. If stray light enters the photometer unsymmetrically (as it would probably do if it is present), the observed dissymmetry should become more apparent at lower concentrations. The instrument was tested in this manner and was found to give fairly satisfactory measurements in the intensity range over which the scattering measurements were to be made.

A simple *photoelectric turbidimeter* was constructed (17) to measure the temperature dependence of the light scattered from a polymer solution under 90°; it is shown in Figure 14. The source of illumination is a 100-watt AH-4 lamp (*A*) which is mounted in a metal housing (*B*). The light from this lamp is rendered parallel by a lens (*C*) mounted in the housing, and it then passes through a glass filter (*D*) which transmits the green mercury line (5461 Å). This nearly parallel monochromatic light is then partially reflected by means of two pieces of plate glass (*E*) mounted at 45° to the incident beam to a Weston photronic cell (*F*). The photronic cell is mounted about six inches away from the main part of the apparatus to minimize temperature changes due to the thermostat, since the photronic

cell output is somewhat sensitive to temperature. The cell is used to measure the intensity of the beam produced by the mercury lamp, since it receives a small constant fraction of this light from the two glass plates. It has a sensitivity of about 4.4 microamp. per foot-candle to white light

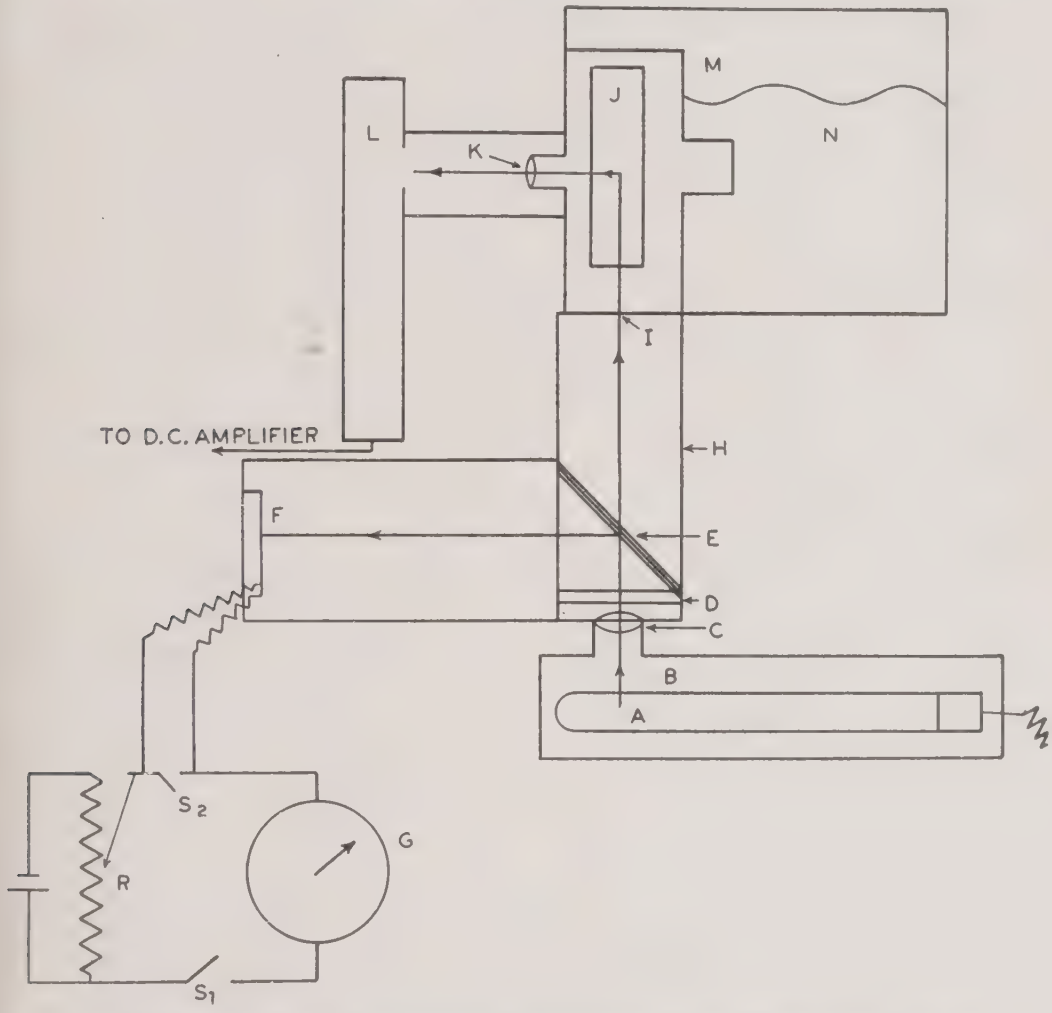

Fig. 14. Photoelectric turbidimeter, according to Doty, Singer, and Wagner.

and its response is very nearly linear, especially when there is close to zero potential difference across it. This may be accomplished by using the circuit shown in the lower left of Figure 14. To take a reading switch S_1 is closed and the ammeter, G, is read. With S_1 still closed, S_2 is also closed and the ammeter is read again. If the two ammeter readings do not agree, the potential across the photronic cell is not zero and so the rheostat is

adjusted until it is. This arrangement helps to increase the sensitivity, reduce the effect of temperature variations, and improve the linearity of response.

In order to determine whether the response was linear, the transmission of a piece of optically flat glass, essentially a neutral filter, was measured in a photoelectric colorimeter and in the turbidimeter described above. The agreement was within experimental error for this one measurement, as well as for successive measurements made with several pieces stacked together. In the latter case, the value of the known transmission (%) of the graph was taken as the transmission for a single piece of the nth power, where n is the number of pieces.

The major fraction of the light beam continues upward, enclosed by a wooden box (H) which is painted a dull flat black on the inside to reduce the stray light caused by internal reflections. It then passes through an aperture (I) so that a beam about one-half inch in cross section enters the solution to be examined, which is contained in a glass cell (J). The position of the beam must be adjusted so that it passes through the center of the solution and does not hit the side of the cell.

At right angles to the cell and mounted on the outside of the thermostat is a lens (K) which serves to collect the scattered light from the sample and focus it onto the light-sensitive portion of the phototube (L). The output of the phototube is electronically amplified and the current produced when light impinges on the tube is determined with a sensitive galvanometer.* The instrument, most sensitive to wave lengths at the lower end of the spectrum, has a sensitivity of about 2×10^{-6} foot-candles per scale division in the blue region; this may be increased tenfold by switching out the shunt across the galvanometer. Since the galvanometer has 100 divisions and can be read to about one scale division, the precision depends to a large extent on the portion of the scale used. The response of the instrument is linear; the data were obtained in the same fashion as for the photronic cell.

The relative positions of the lens, glass cell, and phototube are so arranged that light from only the center of the solution reaches the photocell. This eliminates reflected light from the sides or corners of the glass cell. For the same reason enough liquid must be put into the glass cell to avoid reflections from the meniscus. The cell containing the liquid is mounted in a metal housing (M) which fits into a glass aquarium converted

*This entire photometer unit was purchased from Photovolt Corporation, 95 Madison Ave., New York.

into a thermostated water bath (N). The temperature may be raised to about 80°C.

Operation and Calibration. The instrument was calibrated indirectly. A gel of 1% polystyrene in acetyltributyl citrate was measured in a visual turbidimeter which had been calibrated absolutely by using solutions and pure liquids of known turbidity. The turbidity of the gel was found to be 2.68×10^{-3} cm.$^{-1}$, and the new instrument was checked before every series of readings with this secondary standard. Since the absolute value of the scattering of this gel was obtained, the proportionality factor between absolute scattering and instrument reading was obtained and used for all the solutions measured on that day. This procedure corrects for small day to day variations, such as dust on the lens or the glass plates.

To measure the turbidity of a solution, a glass cell is filled with at least 35 ml. of solution and set in place in the thermostat. Sufficient time is allowed for the solution to come to the appropriate temperature. A stop is placed in the path of the light beam and the galvanometer is adjusted to read zero; the stop is then removed and the galvanometer is read again. A third reading is now taken with the stop in place again. The two dark readings are taken to be sure the amplifier has not drifted appreciably while the reading was taken. These two dark readings, which should be near zero, are averaged and the result is subtracted from the reading obtained with the solution. Usually three such readings are taken, there being nine observations in all. The photronic cell ammeter is also read, as described above.

Calculation of Absolute Turbidity.

Let

P_s be the galvanometer reading for the unknown solution.
c_s be the photronic cell reading when P_s was measured.
P_0 be the galvanometer reading for the standard gel.
c_0 be the photronic cell reading when P_0 was measured.
K be the actual turbidity of the standard gel, 2.68×10^{-3} cm.$^{-1}$.

Then:
$$\tau_0 = \frac{KP_s c_0}{c_s P_0} \tag{29}$$

since the response of the phototube is linear. The scattering of the solvent must be subtracted from τ_0, the scattering of the solution, to obtain the turbidity, τ, due to concentration fluctuations, from which the molecular weight may be obtained. This is done by measuring τ for various concen-

trations, plotting Hc/τ as a function of concentration, and setting the intercept equal to $1/M_2$.

It was found necessary to filter carefully all the solutions used, since the presence of any foreign particles would obviously give erroneous results. The most prevalent and frequent contaminant was dust. All vessels were carefully rinsed and then dried by evaporation of solvents to avoid lint from the towels. The solutions were then put through sintered glass filters, first through one of coarse or medium pore size, and then through one of fine pore size. The solutions were usually filtered directly into the glass cell in which they were to be measured, thus eliminating an intermediate step which might have caused contamination. The solution was considered dust free when no particles could be seen at right angles to an incident mercury lamp beam.

A very elaborate *photoelectric* instrument for turbidity determinations by *transmission* and *scattering* was constructed by P. P. Debye; it also permits measuring the scattered intensity at angles between 0° and 125°. The following description is taken from Debye's paper (12).

The light-scattering unit, a photograph of which is given by Debye (12), contains four separate phototubes (RCA 929 type) which can be connected interchangeably to a special d.c. amplifier.* The light intensities are read on a built-in taut-suspension galvanometer, which is shunted in order to have a variable sensitivity range of 1 : 2 : 5 : 10 : 20 : 50. Before and after each series of measurements the primary light beam intensity is obtained by reflection on a magnesium carbonate block under 45° with respect to the primary light beam and with an additional dark glass filter interposed. In this way long-term fluctuations of the light source as well as of the amplifier can be eliminated.

The light-scattering unit has three separate and easily interchangeable lamp houses: one contains a high-intensity tungsten-filament bulb, the other a water-cooled high-pressure mercury arc (H-6), and the third a medium pressure-forced air-cooled mercury arc of the AH-4 type. It has been found that a simple electrical stabilizing circuit makes the light output of the AH-4 bulb quite satisfactorily constant.

The arrangement of the optical parts is shown schematically in Figure 15. The light of the mercury arc illuminates an opal glass (O) situated in front of a slide (A), having various interchangeable apertures of different sizes; then it passes a monochromatic-glass color filter (F) and a stationary lens (L_2) with iris diaphragm (D). The parallel beam of light which leaves

*Photovolt Corporation, 95 Madison Ave., New York.

the lens can then be intercepted by a Polaroid (P) and/or an extra plain glass slide (G). The latter is used to calibrate the electrical parts by decreasing the primary light intensity by small but known amounts. This is useful in the case of transmission measurements where the zero of the galvanometer is suppressed by electrical means. Between the aperture slide and the color filter there is a removable additional lens (L_1) which, because of its higher numerical aperture, gives greater light intensities. It focuses the first aperture in the center of the solution cell (S).

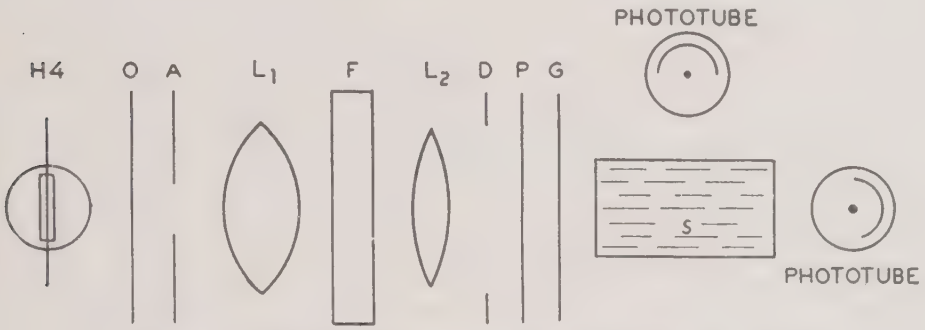

Fig. 15. Optical design of the photoelectric turbidimeter, according to P. P. Debye.

As shown in Figure 15, one phototube is situated close to the solution cell for measuring turbidity by 90° scattering. The other phototube is used for transmission measurements but it can also be applied to measuring angular distribution; the latter is done by moving the tube in a semicircle around the solution cell. The perpendicular axis of this motion extends through the bottom of the unit and is connected to an indicator arm on the outside of the case where a pointer shows the position of the tube (in degrees) with respect to the primary beam. The motion covers an angle interval from 0 to 125°.

The measurement of μ can be carried out in a *Pulfrich refractometer* or, better, in a special differential refractometer, which determines directly $(\mu_s - \mu)$ as used in equation (13). It was constructed and described by P. P. Debye (12). The differential refractometer (Fig. 16) allows the measurement of μ with great convenience and an accuracy of about 3×10^{-6}. An adjustable precision slit (S) is illuminated by monochromatic light from a mercury arc (AH-4) and an image (I) of this slit is formed at a distance of about 190 cm. in the field of a filar micrometer. A rectangular glass cell (C) containing the solvent is placed between the two lenses (L_1 and

L_2) in the parallel light beam. Suspended in the solvent cell (C) is a hollow prismatic glass cell (P) containing the solution. The refraction angle of the prism is approximately 125°. If there is any difference in refractive index of solvent and solution, the image of the slit which can be observed in the eyepiece of the filar micrometer will undergo a deflection. If the difference in refractive index ($\mu_s - \mu$) is not too large, the image deflection will be proportional to the refractive index difference. For this instrument the full-scale deflection is still in the linear range.

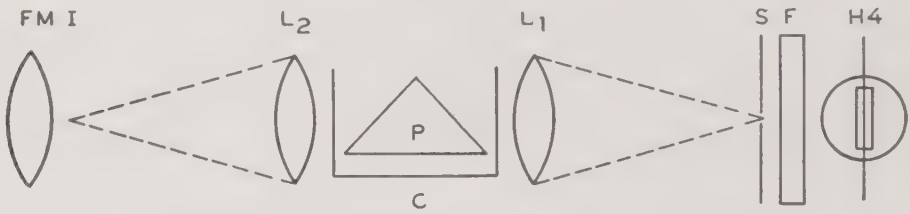

Fig. 16. Optical design of the differential refractometer, according to P. P. Debye.

The image deflection can be calculated by the following equations. If the top angle of the prism is A, the angular deflection α, and prism and cell have the refractive indices μ_s and μ, respectively, then:

$$\alpha = 2(\mu_s - \mu) \tan A/2 \tag{30}$$

With a lens of focal length f, this gives an image deflection X:

$$X = \alpha f = 2f \tan A/2 \cdot (\mu_s - \mu) \tag{31}$$

The relation shows that the image deflection, X, depends linearly on the refraction difference ($\mu_s - \mu$) only in first approximation (for small deflections).

The equation for the image deflection (X) also shows that X is independent of the refractive index of the solvent (μ). The instrument can therefore be calibrated with, for instance, an aqueous sucrose solution and then be used for any other solvent–solute system.

The differential method employed in this instrument has the great advantage of being fairly insensitive to small temperature changes. On this account a good enclosed-type mercury regulator will work well for the temperature control of the water which is pumped through the jacket surrounding the cells. In practice the temperature equilibrium of prism and cell is attained in 5–7 minutes.

Before continuing to the discussion of the results obtained with the light-scattering method up to date, it may be in place to add a few remarks about the preparation and purification of solvents and solutions before they can be considered to be ready for measurements. The polymer specimens usually are the products of repeated fractionation of commercial materials or of samples polymerized under certain controlled conditions. Two types of impurities, which can never be completely eliminated, require special attention and care:

(*a*) *Low Molecular Weight Impurities of Solvent and Polymer.* All solvents should be carefully distilled until their properties, such as density, boiling point and refractive index, do not undergo any changes upon further purification. Some solvents, *e.g.*, dioxane, formic acid, etc., retain water very tenaciously and have to be kept carefully dry, because even small amounts of water affect the refractive index noticeably. The polymers should be dissolved and reprecipitated before they can be brought into the solution which is finally used for the measurements. It seems advisable to prepare a 2–3% solution of the original polymer in the same solvent in which the final measurements are contemplated, and to precipitate it with a volatile precipitant. The precipitate is filtered off and thoroughly washed with the precipitant. It is then slowly dried at low temperatures in a vacuum; fast drying under more vigorous conditions, such as elevated temperature, leads in certain cases to hornification of the samples, which makes subsequent dissolving difficult and eventually even leads to solutions containing minute gel particles, which may cause excessive scattering. This process of purification through precipitation should be repeated one or more times; some polymers, *e.g.*, polystyrene, are relatively easily separated from traces of monomer, catalysts, or stabilizers; others, *e.g.*, nylon or rubbery copolymers, retain impurities rather tenaciously. It does not seem easy to give any strict prescription at present, and it will be necessary to collect further data until certain standard procedures can be recommended.

(*b*) *Coarse Impurities of Solvent and Polymer.* All solvents and solutions have to be filtered repeatedly until they appear optically clean and until further filtration does not decrease the turbidity any more. All solvents contain a certain amount of dust of mostly inorganic origin, which can be satisfactorily reduced to an insignificant amount by repeated filtration through glass fritters and bacterial filters. All polymers contain coarse impurities of various types. Dust of inorganic origin, having large particle sizes (several microns), is comparatively easily removed by precipitation,

washing, redissolution, and final filtration through glass fritters. Haze, of organic origin, is frequently due to chemical and structural heterogeneity of the polymer, such as too highly (or too little) acetylated fractions in cellulose acetate or branched (even cross-linked) constituents in vinyl polymers and copolymers. This type of haze, which is chemically closely related to the investigated material and differs from it only slightly in its solubility characteristics, sometimes offers very serious obstacles and eventually can prevent the application of the light-scattering method altogether. It seems that a comparatively successful way to reduce this haze is to precipitate the polymer three or four times, using another solvent each time and eventually also more than one precipitant. It can be directly observed in such cases that the turbidity of the solution decreases visibly after each precipitation, but even a solution which appears completely transparent to the eye may still contain enough haze to give wrong results. These very large complexes affect the light scattering in about the same way as they affect specific viscosity, because of the fact that they contribute to the total effect according to their weight. Their large size (1000 Å or more), on the other hand, makes it possible to obtain independent experimental evidence about their presence by measuring the dependence of the turbidity upon the angle between incident and scattered light in any apparatus described previously (page 153).

In choosing a solvent for this type of work, one must be mindful of the great importance of the difference in index of refraction between solvent and solute. This difference should be greater than 0.0005 refractive index units between a 1% solution and the solvent. In fact, it is just this difference which determines the lowest molecular weight which can be measured with a given accuracy, for, obviously, the greater the refractive index difference, the lower the molecular weight (of the solute) that will give the same scattering. The lowest molecular weights measured were close to 10,000, where $\partial n/\partial c = 0.07$ for the system investigated. To measure molecular weights lower than this $\partial n/\partial c$ would have to be increased by use of a different solvent or less accuracy would have to be expected. Thus at present the method is limited to molecular weights above 10,000. Colored solutions offer some difficulty; however, by using light with a wave length that is outside the absorption band of the solution, no trouble is encountered.

At the end of this section it may be reiterated that the few recommendations made are far from constituting a well worked-out technique. They only represent the limited experience collected during a short period and will have to be improved and expanded in the future.

VIII. Experimental Data and Discussion

1. Proteins

The turbidity of protein solutions was studied very carefully in 1935 by Putzeys and Brosteaux (34). They measured the light scattered under 90° from dilute aqueous solutions of ovalbumin, (MW = 34,500), amandin (MW = 208,000), excelsin (MW = 212,000) and hemocyanin (MW = 5,000,000). The weight-average molecular weights of these substances are known from previous observations in the Svedberg ultracentrifuge. Scattering measurements were made at different wave lengths, at different protein concentrations, and at different *p*H values. The degree of depolarization was determined and the correction factor, $(6 + 6\rho)/6 - 7\rho)$, was applied. The measurements were evaluated with the aid of a relation of the form $\tau = KM_2c_2$, which can be derived from Rayleigh's law of scattering in gases and which is essentially identical with equation (17). The constant K, however, was introduced as an *empirical quantity* and the purpose of the investigation was not so much to determine absolute molecular weights of proteins in solution, but rather to show that the intensity of the scattered light is proportional to the molecular weight of the protein. This was demonstrated to be true for materials with molecular weights ranging from about 30,000 to about 5,000,000. Later (35,36) Putzeys, Brosteaux, and Lontie contributed a number of interesting papers to the light scattering and especially the depolarization of the scattered light in protein solutions.

More recently Heller and Klevens (24) have investigated aqueous solutions of egg albumin with the use of an 18-cm. tube by the transmission method. The material was characterized by an osmotic molecular weight of 42,000–45,000, whereas measurements in the ultracentrifuge gave 40,000–44,000. Turbidity determinations gave a molecular weight of 47,000 immediately after the preparation of the sample at 4°C.; this value increased to 64,000 after 24 hours and to 81,000 after 72 hours. This is apparently due to aggregation (denaturation). The solutions did not show any noticeable dissymmetry.

2. Vinyl Polymers

Recent experiments (13) on some fractions of polystyrene confirm the assumptions just mentioned and in addition furnish useful information on the size of polystyrene molecules as a function of molecular weight and of the solvent ability of the liquid in which they are dissolved. Measurements

were made on three polystyrene fractions in methyl ethyl ketone (*JNZ*). The limiting dissymmetry coefficient, called the intrinsic dissymmetry coefficient, is actually most conveniently evaluated by plotting the reciprocal dissymmetry coefficient ($1/q$) *vs. c*. The first part of Table VI shows the dissymmetry coefficient, [q], for these three fractions as well as the value of R obtained from Figure 9. From the molecular weight, the value of M/R^2 can be calculated. The values are very nearly constant. A different fraction, *RT-H*, of molecular weight 4,000,000 was dissolved in four solvents of different solvent abilities and the turbidity, dissymmetry, and viscosity were measured. These results are shown in the lower part of Table VI.

TABLE VI

DISSYMMETRY COEFFICIENTS FOR VARIOUS POLYSTYRENE FRACTIONS

Fraction	Solvent	M	[q]	R	[η]	M/R^2
JNZ-7	Butanone	2,080,000	0.64	1350	1.82	1.14
JNZ-4	Butanone	4,800,000	1.41	2100	3.30	1.08
JNZ-1	Butanone	9,800,000	2.00	2770	4.10	1.27
RT-H	Toluene	4,000,000	1.59	2370	7.6	
RT-H	Ethylene dichloride	4,000,000	1.64	2390	5.3	
RT-H	Butanone	4,000,000	1.39	2100	2.3	0.91
RT-H	Butanone + 15% methanol	4,000,000	1.19	1900	1.6	

The behavior of q with concentration for different solvents is just that expected, for toluene and ethylene dichloride are good solvents, butanone is intermediate and with 15% methanol added is on the verge of being nonsolvent.

It is interesting to note that the actual value of R has decreased on going to a poorer solvent, but hardly enough to account for the fivefold change in intrinsic viscosity. This point is discussed in the original paper (13). The demands of consistency are great in the molecular weight measurements of the *RT-H* fraction in the four different solvents because of the widely different correction factors required for the measured turbidities. Nonetheless, satisfactory results were obtained. The molecular weight values obtained in the four liquids spread between 3,100,000 and 4,900,000. Even so, this should certainly not be considered the highest accuracy obtainable, for the whole work was done with only routine care.

Polystyrene fractions of various samples, prepared at different tem-

peratures, are now being reinvestigated by osmotic and light-scattering observations with increased accuracy and it is hoped that these results will throw light not only on the sharpness of the various fractions, but also on the question of what difference exists in the internal chain configuration of such polymers (1,25).

Interesting evidence on this question was contributed by Doty and Kaufman (16), who measured the depolarization of the light scattered from three polystyrene fractions in toluene and methyl ethyl ketone. One of them came from a sample prepared at 70°C., whereas the two others were cuts from a sample polymerized at room temperature. All fractions were obtained by only one single step of fractionation and, consequently, probably had a comparatively limited sharpness. The number-average molecular weights and the depolarization coefficients for unpolarized incident light of these fractions at 1% concentrations are given in Table VII.

TABLE VII

DEPOLARIZATION MEASUREMENTS OF THREE POLYSTYRENE FRACTIONS

Fraction	Molecular weight	Depolarization	
		In toluene	In methyl ethyl ketone
F (70°)	500,000[a]	0.075	0.012
F_1(25°)	400,000	0.095	0.015
F_2(25°)	3,000,000	0.065	0.011

[a]The viscosity-average molecular weight of this sample was found to be 800,000, which leads to a number average of about 500,000.

First it can be seen that in both solvents, ρ decreases with increasing degree of polymerization, indicating that the longer chains are capable of coiling up into more isotropic configurations. Furthermore, in all cases, toluene solutions exhibit much stronger anisotropy. This is in line with the corresponding behavior of the μ_{12}-values taken from osmotic measurements, with the intrinsic viscosities, and with the dissymmetries (compare Table VI on page 164) and reaffirm the conclusion that toluene is a thermodynamically good solvent in which each polymer chain is closely surrounded by solvent molecules and therefore prevented from coiling back on itself too closely. Methyl ethyl ketone, on the other hand, has less tendency to stick to the chains and permits the establishment of comparatively frequent spots of polymer–polymer contact. This results in more or less randomly

coiled particles, whose statistical character does not lead to any outspoken anisotropy. Hence the small values of ρ in the fourth column of Table VII. By comparing $F(70°)$ and $F_1(25°)$, which have approximately the same molecular weight and hence should have about the same anisotropy in both solvents, Doty and Kaufman conclude from measurements of the anisotropy of polarized light at various concentrations that the scattering particles of these two fractions are virtually identical in size and anisotropy in toluene, whereas in methyl ethyl ketone $F_1(25°)$ behaves as if the dissolved macromolecules were smaller in size and more isotropic than those of $F(70°)$. From this one may conclude that a solvent with strong solvent–solute interaction, such as toluene is for polystyrene, solvates both types of molecules to approximately the same extent and produces solute particles of about the same shape and anisotropy. In methyl ethyl ketone, on the other hand, the intrinsic architecture of the dissolved macromolecules is not so much affected by solvation and manifests itself to a higher degree. The data of Doty and Kaufman thus indicate that the molecules prepared at room temperature have a higher capacity to assume the shape of a random coil than those polymerized at 70°C. Whether this is due to a bottle-brush or feather-type branching of the latter polymer (1) or to a different distribution of the phenyl groups along the chain, as proposed by Huggins (25) can hardly be decided with the experimental data available at present. More work to elucidate this question is under way in the Polymer Research Institute at the Polytechnic Institute of Brooklyn, and will be presented in forthcoming theses and publications (*cf.* 13,15).

Polyvinyl chloride (Geon 101) and *polyvinyl chloride-acetate* (Vinylite) have been studied in methyl ethyl ketone and dioxane. These polymers exhibit considerable tendency toward aggregation and association as discovered and studied by Doty, Wagner, and Singer (17). Osmotic and light-scattering measurements have therefore been carried out at various temperatures with the aid of the instruments described on pp. 151 *et seq.* and shown in Figures 12 and 13; they disclose a noticeable temperature dependence of the *particle weight* and indicated the existence of a reversible association equilibrium in these systems. Table VIII shows this effect for two polyvinyl chloride fractions in dioxane, in which the apparent molecular weight decreased from about 12,000,000 and 17,000,000 at 28°C. to about 2,000,000 at 63°C. These solutions exhibit a considerable degree of dissymmetry and the molecular weights have therefore been corrected for nonsymmetrical scattering as described on pages 145 and 146. Osmotic measurements were carried out with the same samples, which revealed

TABLE VIII

DEPENDENCE OF APPARENT WEIGHT-AVERAGE MOLECULAR WEIGHT OF TWO POLYVINYL CHLORIDE FRACTIONS (IN DIOXANE) UPON TEMPERATURE

Fraction	Temperature	Weight-average molecular weight
7	28.5	16,700,000
7	48	4,500,000
7	63	2,040,000
12	28.5	12,500,000
12	51	2,400,000
12	62.5	1,800,000

that the number-average molecular weights of these polymers were much smaller than the weight averages determined from turbidity. Table IX

TABLE IX

DEPENDENCE OF APPARENT NUMBER-AVERAGE MOLECULAR WEIGHT OF FRACTION 7 (IN DIOXANE) UPON TEMPERATURE

Temperature, °C.	Number-average molecular weight
14	210,000
38	210,000
47	141,000
68	112,000
77	90,000

contains the results obtained with fraction 7 by Doty and his co-workers. It can be seen that the temperature dependence corresponds to that of Table VIII; the number-average molecular weight decreases from 210,000 at 14°C. to 90,000 at 77°C. The absolute values, however, are less than 1/20 of those obtained by light scattering. A study of these same fractions in other solvents and with the aid of the ultracentrifuge (17) revealed that this discrepancy is due to the existence of a rather broad molecular-weight distribution in these samples, which is probably characterized by two maxima, one of which is (at room temperature) in the neighborhood of 15,000,000, whereas the other lies at about 200,000. It seems that the species of high molecular weight consists of clusters, formed by aggregation

of the true chemical molecules (about 90,000) and that these association complexes break up in a reversible manner during heating.

This explanation was further corroborated by depolarization measurements (15,17) which disclosed an increasing anisotropy at higher temperatures. The random clusters of the individual polymer units are distinctly less anisotropic than these (smaller) chain molecules themselves, which, according to dissymmetry and viscosity measurements, have the character of moderately undulated free draining chains.

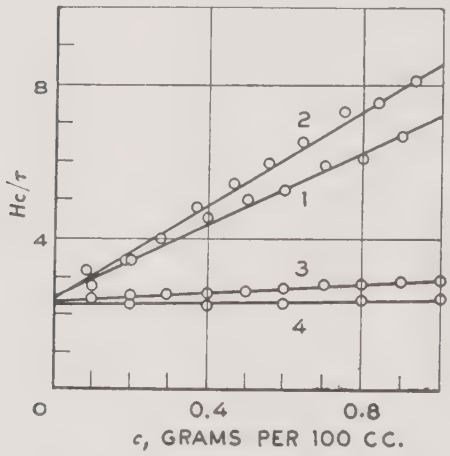

Fig. 17. Hc/τ values of four polyvinyl *n*-butyl ether samples *vs.* solute concentration, according to P. P. Debye.

P. P. Debye (12) has investigated several *polystyrenes* in toluene and a number of polyvinyl *n*-butyl ether samples in benzene. The Hc/τ *vs.* c plots of the polystyrenes gave fairly parallel straight lines, corresponding to weight-average molecular weights of 560,000, 410,000, and 140,000, respectively. A very interesting effect was observed with unmilled and milled samples of polyvinyl *n*-butyl ether. Figure 17 shows the Hc/τ *vs.* c plots of four samples of this polymer in benzene. Curve *1* is the original material, which has a molecular weight of about 220,000; curve *2* represents the material after aging in solution for 48 hours at 65°C.; the molecular weight is virtually unchanged (221,000) whereas the slope of the line is noticeably increased. Curves 3 and 4 represent two samples, which were milled for 10 and 45 minutes, respectively; the molecular weights are essentially the same as that of the initial polymer. The slopes of the lines, however, are sharply decreased; this might indicate that milling is accompanied by a slight oxidation of certain groups in the chain, whereby a somewhat less soluble material is produced.

3. Cellulose Derivatives

Cellulose acetate in acetone was subjected to a very careful study by the light-scattering method by Stein and Doty (41). Four fractions were used which had been fairly well characterized by previous osmotic viscosity and ultracentrifuge measurements. Turbidity (90°), dissymmetry (51° and 129°), and depolarization measurements (15) were carried out and the

results present a comparatively thorough characterization of these solutions. Table X contains (second column) the *osmotic* molecular weights of

TABLE X

SUMMARY OF DATA ON FOUR CELLULOSE ACETATE FRACTIONS

Fraction	Molecular weight			
	Osmotic	Uncorrected	Corrected for ρ	Corrected for z
8B	163,000	118,000	114,000	173,000
23B	133,000	92,000	88,700	135,000
18B	75,000	60,000	55,600	77,000
32B	65,000	47,000	43,000	60,000

these four fractions, which were the result of fairly careful fractionation of a commercial cellulose acetate (2) and probably represent as narrow molecular-weight distributions as have yet been obtained by fractional precipitation. In the third column are listed the *turbidity* molecular weights as computed directly from the 90° scattering, whereas the fourth column contains the data corrected for *depolarization*. The figures in this column are somewhat smaller than those in the third column, because they have been obtained by multiplication by a factor $(6 - 7\rho)/(6 + 6\rho)$. The last column shows the values corrected for *dissymmetry*; they are noticeably larger than those in the fourth column because the dissymmetry of these solutions was quite appreciable (see Table XI). It can be seen that the ultimate light-scattering molecular weights of the four fractions agree remarkably well with the osmotic figures.

These fractions were some of those which were prepared by W. J. Badgley during his thesis work in 1944 and 1945. Osmotic and viscosity measurements were made for all fractions by Dr. Badgley and a fairly thorough analysis in the ultracentrifuge was carried out by Stern, Singer, and Davis (39).

As pointed out previously (compare page 145) it is possible to compute the maximum effective dimensions of dissolved macromolecules from the dissymmetry coefficients if a certain characteristic average shape—sphere, rod, or coil—is assumed for the particles. Stein and Doty assumed the shape of a random coil to be most suitable for their case and arrived at the results indicated in Table XI. The second column of this table contains the corrected molecular weights, the third, the actually measured dissymmetry coefficient $(z - 1)$, and the fourth, the root mean square separation

TABLE XI

DIMENSIONS OF CELLULOSE ACETATE MOLECULES IN ACETONE SOLUTION

Fraction	Molecular weight	$(z-1)$	Average distance between ends for a coil, Å	Length of completely stretched chain, Å
8B	163,000	0.60	1340	3100
23B	135,000	0.60	1340	2400
18B	75,000	0.43	1120	1440
32B	65,000	0.43	1120	1250

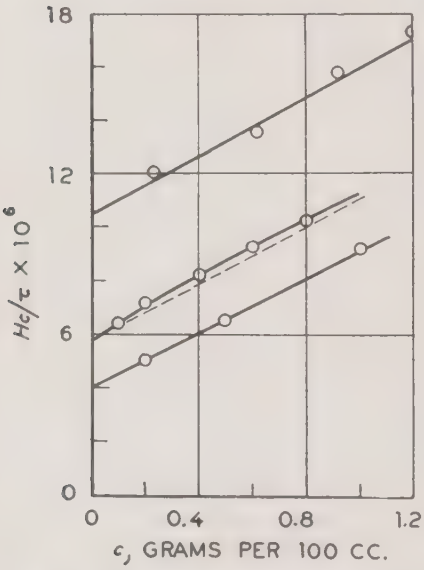

Fig. 18. The two straight lines intercepting at 4.0 and 10.6 were obtained by Zimm and Doty from two polystyrene fractions. The line intercepting at 5.9 is a 1 : 1 mixture of the two fractions; the points are no longer on a straight, but on a slightly curved line.

between the ends of a random coil as computed from z. In the last column the lengths of the molecules are presented on the basis of their being completely straight chains. The figures show that in the two larger fractions the chains are coiled up to about 40 and 60% of their maximum lengths, whereas the molecules of the two lower fractions are almost straight chains. This is in agreement with axial ratio calculations by Nichols and Kraemer* from sedimentation and viscosity measurements and with the observations of depolarization by Doty and Kaufman (16).

Before closing this brief paragraph on the present experimental data on light scattering from polymer solutions, it may be appropriate to mention the possibility of determining the *molecular weight distribution function* of a dissolved polymer by turbidity measurements. Zimm and Doty (44) and Debye (10) pointed out that the Hc/τ *vs.* c plot is only a straight line as long as the investigated samples are fairly homogeneous, but that a curved line is to be expected if the sample is a mixture of several molecular

*Compare the article on ultracentrifuge analysis of high polymers by E. O. Kraemer in the first volume of this series and the chapter of J. B. Nichols and E. O. Kraemer in The Svedberg and R. O. Pedersen, *The Ultracentrifuge* (Oxford Univ. Press, London, 1940, p. 430).

species. Zimm and Doty have investigated very carefully a mixture of equal amounts of two fractions of polystyrene with molecular weights of 95,000 and 250,000, respectively, and have found that the intercept of the graph gave a weight average of 172,000, whereas 172,500 should be expected. The Hc/τ *vs.* c plots of the two components were well-defined straight lines, whereas the plot of the mixture was noticeably curved. Their results are presented in Figure 18 which shows the plots for the two components and for the mixture. A similar phenomenon was observed by P. P. Debye (12) in his study of polyvinyl *n*-butyl ether in benzene, who found that the Hc/τ *vs.* c plots of polymers in the molecular-weight range from 120,000 to 680,000 show a noticeable downward curvature indicating the presence of a number of molecular species having different molecular weights. Whether the heavier species are actually chemical molecules of very high polymerization degree or whether they are agglomerates of the lighter species cannot be decided unless the temperature dependence of this effect is studied (compare page 167).

Note Added in Proof

A few important publications have appeared since this article was written that should at least be mentioned here briefly. R. H. Ewart, C. P. Roe, P. Debye, and J. R. McCartney, *J. Chem. Phys.*, **14**, 687 (1946), have extended the theory of light scattering in an inhomogeneous dielectric medium and applied it to the study of polystyrene methacrylate solutions in solvent–precipitant mixtures. They have shown that, in such systems, correct values of the molecular weight by the usual interpretation of the turbidity are obtained only if the solvent and precipitant have the same refractive index. On the other hand, if different refractive indices of solvent and precipitant are chosen, light-scattering measurements can give information about the extent of selective absorption of the solvent by the polymer molecules.

G. Oster, P. M. Doty, and B. H. Zimm, *J. Am. Chem. Soc.*, **69**, 1193 (1947), have studied the light scattering of tobacco mosaic virus suspensions. The length of the rod-like particles determined from the dissymmetry of the scattering was found to be 2700 Å; the corrected weight-average molecular weight is 40,000,000. These data are in remarkable agreement with the results obtained by the electron microscope (particle length around 270 mμ) and by viscosity studies of Lauffer, who applied the theory of Simha on the intrinsic viscosity of tobacco mosaic virus solutions and arrived at a particle length of 260 mμ.

References

1. T. Alfrey, A. Bartovics, and H. Mark, *J. Am. Chem. Soc.*, **65**, 2319 (1943).
2. W. J. Badgley, *Polymer Bull.*, **1**, 17 (1945).
3. W. J. Badgley and H. Mark, in *High Molecular Weight Organic Compounds* (Frontiers in Chemistry, Vol. VI). Interscience, New York, 1948.

4. S. Bhagavantam, *The Scattering of Light and the Raman Effect.* Chemical Pub. Co., Brooklyn, 1942.
5. H. Blumer, *Z. Physik*, **32,** 119 (1925); **38,** 304, 920 (1925); **39,** 195 (1925).
6. M. Born, *Optik.* Springer, Berlin, 1933.
7. J. Cabannes, *Diffusion moléculaire de la lumière.* Presses Universitaires de France, Paris, 1939.
8. P. Debye, *J. Applied Phys.*, **15,** 338 (1944); *J. Phys. Colloid Chem.*, **51,** 18 (1947).
9. P. Debye, Lecture given at the High Polymer Group of the American Physical Society, Rochester, June 23–24, 1944, and at Gibson Island, July, 1944.
10. P. Debye, Lecture given at the High Polymer Group of the American Physical Society, Evanston, November 12–13, 1943, and lecture given at the High Polymer Seminar at the Polytechnic Institute of Brooklyn, November 25, 1944.
11. P. P. Debye, *Doctoral thesis*, Cornell University, 1944.
12. P. P. Debye, *J. Applied Phys.*, **17,** 392 (1946).
13. P. M. Doty, W. A. Affens, and B. H. Zimm, *Trans. Faraday Soc., in press.*
14. P. M. Doty and W. J. Badgley, *J. Polymer Sci., in press.*
15. P. M. Doty and E. Edelson, *in press.*
16. P. M. Doty and H. Kaufman, *J. Phys. Chem.*, **49,** 583 (1945).
17. P. M. Doty, H. Wagner, and S. Singer, *J. Phys. Colloid Chem.*, **51,** 32 (1947).
18. P. M. Doty, B. H. Zimm, and H. Mark, *J. Chem. Phys.*, **12,** 144 (1944).
19. P. M. Doty, B. H. Zimm, and H. Mark, *ibid.*, **13,** 159 (1945).
20. A. Einstein, *Ann. Physik*, **33,** 1275 (1910).
21. R. Gans, *ibid.*, **37,** 881 (1912); **47,** 270 (1915); **62,** 330 (1920); **65,** 97 (1921).
22. S. D. Gehman and J. S. Field, *Ind. Eng. Chem.*, **29,** 793 (1937).
23. E. Guth and H. Mark, *Monatsh.*, **65,** 93 (1934).
24. W. Heller and H. B. Klevens, *Phys. Rev.*, **67,** 61 (1945). W. Heller, *ibid.*, **68,** 5 (1945).
25. M. L. Huggins, *J. Am. Chem. Soc.*, **66,** 1991 (1944).
26. R. Krishnan, *Proc. Indian Acad. Sci.*, **A7,** 21, 91, 98 (1938).
27. W. Kuhn, *Kolloid-Z.*, **68,** 2 (1934).
28. V. K. LaMer, *J. Colloid. Sci.*, **1,** 71, 79 (1946).
29. H. A. Lorentz, *Ann. Physik*, **9,** 641 (1880).
30. G. Mie, *ibid.*, **25,** 377 (1908).
31. T. Neugebauer, *ibid.*, **42,** 509 (1943).
32. L. S. Ornstein and F. Zernicke, *Physik. Z.*, **27,** 261 (1926).
33. F. Perrin, *J. Chem. Phys.*, **10,** 415 (1942).
34. P. Putzeys and J. Brosteaux, *Trans. Faraday Soc.*, **31,** 1314 (1935).
35. P. Putzeys and E. Dory, *Ann. soc. sci. Bruxelles*, **60,** 37 (1940).
36. P. Putzeys and J. Brosteaux, *Mededeel Konink. Vlaam. Acad. Wetenschap.*, **3,** 1 (1941). Compare also R. Lontie, *ibid.*, **6,** 5 (1944); and P. Putzeys and M. L. Beckmans, *Bull. soc. chim. biol.*, **28,** 503 (1946).
37. C. V. Raman and K. R. Ramanathan, *Phil. Mag.*, **45,** 213 (1923). C. V. Raman, *Ind. J. Phys.*, **2,** 1 (1927).

38. R. J. Rayleigh, *Phil. Mag.*, **41,** 107, 274, 477 (1871).
39. K. G. Stern, S. Singer, and S. Davis, *Polymer Bull.*, **1,** 31 (1945).
40. M. von Smoluchowsky, *Ann. Physik*, **25,** 205 (1908).
40*a*. H. Staudinger and I. Henel-Immendörfer, *J. makromol. Chem.*, **1,** 185 (1944).
41. R. S. Stein and P. M. Doty, *J. Am. Chem. Soc.*, **68,** 159 (1946).
42. B. H. Zimm, *unpublished observations*, which will be incorporated in a number of Doctoral theses at the Polytechnic Institute of Brooklyn in 1947.
43. B. H. Zimm, *J. Chem. Phys.*, **14,** 164 (1946).
44. B. H. Zimm and P. M. Doty, *ibid.*, **12,** 203 (1944).
45. B. H. Zimm, R. S. Stein, and P. M. Doty, *Polymer Bull.*, **1,** 90 (1945).

VI. *The Nature of Inorganic Gels*

MIROSLAV W. TAMELE

Shell Development Company, Emeryville, California

I. Introduction

THE LARGE INCREASE in the number of industrial catalytic processes in the chemical industry and, on a particularly large scale, in the petroleum industry, has created a renewed interest in the nature of inorganic gels. Catalysts and catalyst carriers are frequently prepared as porous, dry gels by desiccation of precipitated, hydrous gels. This procedure offers the advantage of obtaining materials of a relatively large surface. In addition to the extent of the surface, the architecture of the surface, its accessibility to the reacting molecules, its chemical nature and purity, and the preservation of the desirable characteristics of the surface while the reaction proceeds—often at elevated temperatures—are some of the most obvious considerations in catalyst preparation.

Unfortunately, it is a rather common experience that two catalysts prepared from two gels, which in turn have been prepared by what appear to be two identical procedures, differ substantially in their catalytic properties. It seems unavoidable to conclude that either the hydrous gels or the desiccated products differ in some physical or chemical properties, even though such differences may not be apparent and may escape detection by any known method of measurement. It is apparent then that the knowledge of the nature of inorganic gels is, at present, rather inadequate and incomplete, in spite of a large amount of observational material which has

been accumulated by the early workers in the field. Some of the older data found in the literature may be laboriously reinterpreted in the light of the general advances in the fields of physics and chemistry, and this has been attempted in some recent critical reviews. A few summaries of more recent work deal for the most part only with certain phases of this subject (1–6). Substantial progress can be expected only from new and original approaches with modern methods and techniques.

II. Definition of Gel

The term gel was used originally by Graham to describe any coagulated material; at present, this term is generally used in a more restricted sense, but no general agreement appears to exist regarding its exact use. If this term is restricted to semisolid systems comprising the entire liquid originally present, and retaining the form of the vessel, gelatinous precipitates are recognized formally as different from gels. Weiser (7), from a survey of the older literature as well as his own experimental work, concluded that only a gradual change in preparative conditions is responsible for the formation of a gel or a gelatinous precipitate of the same inorganic substance and, consequently, no sharp line can be drawn between the two. In his terminology, "gelatinous precipitates and jellies" are the two forms of solid or semisolid colloids included under the general term *gel*. Thomas (8), and many others, prefer to restrict the term jelly to those gels which are heat-reversible to sols, as, for example, aqueous gelatin, or agar-agar, or cellulose acetate–benzyl alcohol systems.

Freundlich (9) defined gels as collodially dispersed systems consisting of a solid and a liquid which, in spite of having a high liquid content, exhibit some properties of solids, namely, definite form, rigidity, and elasticity. Kraemer (10) observed, in 1931, an almost universal acceptance of the view that gels possess a ramifying, more or less coherent solid framework, but pointed out the considerable uncertainty regarding the condition of the liquid component.

This uncertainty still exists at present. Some progress has been made in the theoretical analysis of the forces holding together the framework, which can often be so extensively attenuated as to make material contact between the particles most unlikely. The role of the liquid component, at least in partly dried gels, is now better accessible to study because of general progress in understanding the adsorption and desorption of vapors on porous bodies (11). Information on the size of the primary aggregates in the framework of the gels, and the identification of the solid phases, is

becoming available through systematic application of x-ray and electron diffraction techniques to the numerous inorganic gel systems (2).

In view of the uncertainty regarding the structure of gels, many previous attempts to classify gels into several general types have not been altogether satisfactory and have been largely abandoned; certain arbitrary classifications based on external behavior and bulk properties of gels are, however, useful. The separation into swelling and nonswelling gels draws a rough line between organic and inorganic gels. It is based on the behavior of dried gels toward water or organic liquids. Swelling gels absorb water (or a properly selected solvent) and continuously increase in volume, sometimes until the original volume before desiccation has been reached. Nonswelling gels (mostly dried inorganic gels) absorb water and organic liquids without an appreciable volume change.

The term xerogel, originated by Freundlich, is often used with advantage to denote a gel dried enough to present the external appearance of a dry solid, but without regard to the actual water content which may be as high as 50%.

III. Formation of Inorganic Gels

The most general methods of gel formation are based on reactions leading to precipitation of insoluble solids, although many instances are known of gels formed by chemical attack on solids (*e.g.*, attack of acids on certain insoluble silicates, and of high pressure steam on quartz).

Precipitation from solution may be accomplished by hydrolysis of salts or by metathesis of two soluble electrolytes. Formation of a new solid phase does not, however, always lead to a gel. The solid phase may appear as a distinctly granular, coagulated precipitate, or else it may remain suspended in the liquid phase as a colloidal dispersion of very small particles (a lyophobic sol). The sol, by proper treatment, may be converted again either to a precipitate, or to a gel.

A great number of observations regarding the appearance of solid phase from a solution led to the conclusion that a certain amount of resistance has to be overcome to make possible the separation of the solid phase. It has been established experimentally that some degree of supersaturation often precedes the separation of a solid phase, and that the separation begins on nuclei, about the nature and origin of which little is known. Further growth proceeds preferably on existing fragments. Von Weimarn (12) attempted to formulate these ideas on a quantitative basis. The velocity of growth on the nuclei was considered as determined by a balance

between precipitation pressure (proportional to supersaturation) and precipitation resistance (proportional to the solubility of coarse crystals), and a development of an orderly, organized crystal structure was assumed to require time. Von Weimarn was able to present a useful semiquantitative picture of various situations which agrees roughly with experience. Thus, in very dilute solutions, the velocity of nuclei formation is small, and the velocity of growth is small: the precipitated substances, therefore, have a tendency to assume a highly organized, crystalline form. On the other hand, reactions in concentrated solutions can reasonably be expected to lead to higher supersaturation, higher velocity of nuclei formation, and a very rapid separation of solid phase with less orderly growth of particles.

Von Weimarn assembled an enormous amount of experimental material to support his theories. He succeeded in preparing, in the form of gels or gelatinous precipitates, a number of inorganic substances, such as barium sulfate and sodium chloride, which were at the time considered to be typically crystalline materials. He thus contributed substantially to the conclusion that the fine structure of the freshly separated solid phase depends not only on the material itself but also on the external conditions and the environment in which it is formed.

Von Weimarn's ideas represent, at best, a great oversimplification, and neglect many factors, such as the effect of adsorption, complex formation, variation in solubility with the size of primary particles, agitation, and above all, the influence of structural factors—differences in the way molecules, or ions, or any intermediate complex ions in solution may be put together to form a solid phase, as well as the changes which ions, or complex ions, or molecules undergo when leaving the liquid phase to become the building blocks of a solid phase. Unfortunately, very little progress has been made so far along these lines. Many inextricably interdependent variables, and an unknown number of as yet unappreciated variables, combine to determine the structure and chemical properties of gels, for example, intermediate formation of basic salts which may be only slowly transformed by the excess of reagent (thus introducing time as a variable), concurrent variations in hydrogen ion concentration, and the adsorption of by-products of reaction and their influence on the rate of growth of particles. It would be premature at this stage of the art to attempt any generalization, except to state that each system must be carefully analyzed in all its steps.

It appears that so far only the reactions leading to the formation of silica gel by acidification of alkali silicates have received any appreciable consideration (1,5,6). In certain ranges of acidity and concentration, inter-

mediate formation of orthosilicic acid, followed by condensation of the terminal Si—OH groups appears probable. Presence of primary valence chains connected by Si—O—Si bonds has been demonstrated beyond doubt in many crystalline silicates, but their presence in amorphous silica gel is still a matter of contention supported only by indirect experimental evidence. Commercial sodium silicate presumably contains chains of the pyroxene type; the viscosity (among other properties) of solutions of water glass indicates the presence of relatively long chains. The striking elastic properties of concentrated solutions of water glass are in agreement with this interpretation (13). Gelation would appear then to be an incident in the life of the primary particles occurring when a certain critical number of Si—O—Si bonds have been formed by the condensation reaction, in general agreement with Flory's statistical picture of the gelation of space polymers (14).

It would be dangerous to generalize from these observations to other systems, particularly to those in which the nature of the intermediate reaction products which are in "equilibrium" with the newly formed solid phase is not known. Thus, for example, it is very improbable that alumina, which forms definite hydrates (mono- and trihydrates, but no dihydrates), follows the same pattern of simple condensation as does silica, which is known to form no definite hydrates. The study of the changes which occur in the aluminum salt solutions upon the addition of hydroxyl ions and the study of the decomposition of aluminate solutions by acids have scarcely been begun.

Treadwell (15), from a potentiometric study of a solution of 1 mole of aluminum in 1 mole of hydrochloric acid, concludes that AlO^+ or $Al(OH)_2^+$ cations are present, which, on addition of sodium hydroxide, polymerize with $Al(OH)_3$ to 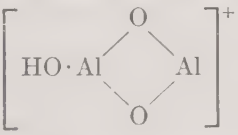 cations. Presumably no such intermediates are formed by rapid addition of sodium hydroxide to aluminum chloride. Various interpretations of the formation of alumina, chromia, and other hydrous oxides via complex formation in solution have been advanced by Bjerrum, Willstätter, Thomas, and others (15). Jander and Winkel (16) studied the size of cations in Al salts by measuring their diffusion rates in presence of an excess of indifferent salts. The measurements showed that with addition of alkali the mean size of the cation increased, tending toward an equilibrium value at the precipitation of the solid phase. Similar experiments were performed with Cr and Fe salts.

A study of the mechanism of precipitation of alumina from sodium aluminate solutions has appeared recently (17).

IV. Inorganic Sols

Whatever the mechanism of the formation of the primary gel particles, it is generally true that primary particles are small enough (of the order of 10–1000 Å) to be influenced by the bombardment of molecules of the liquid phase in which they originated and are therefore subject to Brownian movement. The surface of such small particles may be relatively large per unit of mass of the solid phase and thus any phenomena normally occurring at the liquid–solid interface will assume a significance not apparent for the corresponding bulk phase. Because of the heteropolar nature of inorganic oxides, hydroxides, and salts, adsorption of ions from solution will be marked. The presence of electrical charges (ions of its own species, or adsorbed foreign ions) may be sufficient—together with thermal agitation—to keep sol particles in more or less stable suspension.

Sols show macroscopically all the properties of the liquid phase: the presence of the dispersed solid phase, however, can be readily demonstrated. If allowed to age, some sols separate a solid phase spontaneously under the influence of gravity, or may be induced to do so by centrifuging. Very stable sols may be precipitated by dialysis, using properly selected membranes permeable only to particles of molecular dimensions. The presence of particles of the solid phase may be established—without disturbing the dispersion—by optical methods, such as Tyndall scattering or ultramicroscopy.

The solid phase can be very rapidly and completely separated by the addition of a suitable electrolyte, although silica sols are remarkably insensitive to electrolytes. On the other hand, it is generally agreed that traces of electrolyte are essential for stability, and cannot be removed without destroying the dispersity and causing the separation of the solid phase (*e.g.*, by persistent purification by dialysis). The stability of sols appears to be related to the presence of traces of electrolytes closely associated with the dispersed particles.

The shape of the sol particles is often characteristic of the material of which they are composed; it may, however, also be influenced by the method used in the preparation. Particles in which all three dimensions are of the same order of magnitude are generally described as corpuscular, and may actually be nearly spherical or, more likely, polyhedral; those with one axis much shorter are laminar, or disc- or plate-shaped; and those with

but one long axis, are fibrillar, or rod-shaped particles. Red gold sols, silver, platinum, and arsenic trisulfide sols are approximately spherical. Iron oxide, blue gold sol, and bentonite clays contain discs or platelets. Tungstic oxide and vanadium pentoxide contain rod-shaped particles. Information on particle shape has been obtained from optical effects observed under the ultramicroscope. Spherical particles large enough to be observed under the ultramicroscope and agitated by Brownian movement exhibit continuous radiation. Small elongated particles become luminous only when they assume a certain correct position, that is, when light strikes the particle approximately in the direction perpendicular to its long axis (and the particle is not perpendicular to the plane of observation), and "scintillation" is produced.

The shape of the particles can often be deduced from the intensity of light reflected in certain directions after giving a mass of nonspherical particles a common orientation, *e.g.*, by linear flow, or by an electrical or magnetic field. Optically isotropic elongated particles when oriented by flow may cause a very weak rodlike double refraction. This effect is pronounced when rod-shaped particles are themselves doubly refracting (vanadium pentoxide). The general conclusions from these studies have been confirmed recently by electron microscopy. Polyhedral particles were observed in solutions of colloidal gold (18), rod-shaped particles in vanadium pentoxide (19), and platelets in samples of montmorillonite (20).

Application of x-ray diffraction methods to the study of sol particles disclosed that particles of colloidal dimensions are essentially fragments of the solid phase with properties such as we know from the studies of bulk materials, often crystalline, less often amorphous or pseudoamorphous, and having a structure subject to the same limitations of crystallographic rules deduced from x-ray and electron diffraction studies of matter. This was demonstrated very early by Scherrer in co-operation with Zsigmondy. The study of various crystalline forms produced in the early stages of precipitation, and their changes with aging, is one of the most active phases of the study of sol and gel formation at present (2).

From all properties of sols it has been concluded that the degree of stability and dispersion depend on the method of preparation and the particular set of conditions at the time of preparation, and the series of subsequent changes which proceed more or less rapidly, all tending to decrease the relatively large surface of the sol particles. This process is known as coarsening of sol particles and is dependent chiefly on the solubility of the dispersed phase and on other variables determining solubility, *e.g.*, temperature and the presence of salts which increase the solubility. Thus,

the rate of coarsening of silver iodide sols increases enormously if potassium iodide is added to the sol (21).

Although sols are not stable with respect to the slow process of coarsening, as long as coarsening has not progressed too far, some sols have a definite stability to coagulation, that is to aggregation of the particles into clusters in which the individuality of the particles is more or less preserved. Coagulation of sols is a relatively rapid process and is accessible to study only in systems which do not coarsen too fast.

The relative stability of inorganic sols is due primarily, but not wholly, to the repulsion of charges of like sign on the particles. The dispersing action of thermal movement also contributes to stability by opposing spontaneous aggregation. Very little is known of the possible protective influence of adsorbed layers of solvent (lyospheres), particularly polar solvents like water, which are thought to exist on sol particles. Unfortunately, no direct evidence of such lyospheres has as yet been obtained, although their existence is suggested by the studies of sedimentation volumes of suspensions, and related phenomena (22).

Unfortunately, the electrical forces connected with the charges of particles are also inaccessible to direct measurement. Nevertheless, the presence of the charges is readily demonstrated by the movement of sol particles in an electrical field (electrophoresis), and the velocity of particles evaluated from such experiments. The conductivity is invariably considerably low, indicating a relatively small number of charges per unit of mass. The velocity of migration is smaller than that of electrolytic ions, but is comparable.

From electrophoretic measurements it is possible to calculate the value of the electrical potential associated with the particles without detailed assumptions regarding the nature and distribution of the charges. A physical theory satisfactory for this purpose was advanced many years ago by Helmholtz (23) who assumed the presence of two rigid layers of charges of opposite sign, one located on the surface, the other very near the surface, in the liquid phase.

If the distance between the layers is d, the surface charge density e, and ϵ is the dielectric constant of the medium, the system constitutes an electrical double layer which can be considered, as a first approximation, to be a parallel plate condenser whose potential:

$$\zeta = 4\pi ed/\epsilon \tag{1}$$

When a particle moves through the liquid medium under the influence of an electrical potential E, at a uniform rate u, then the electrical force

Ee driving the particle, is equal to the frictional force, $\eta u/d$, where η is the coefficient of viscosity of the liquid and u/d is the velocity gradient in the double layer (assuming the liquid to be at complete rest at the surface of the particle), or:

$$Ee = \eta u/d \tag{2}$$

By combination of (1) and (2), the potential ζ can be calculated in terms of the migration velocity, u:

$$\zeta = 4\pi\eta u/\epsilon E \tag{3}$$

Equation (3) is, with minor refinements, still suitable for calculation of ζ potentials, in spite of certain modifications of the Helmholtz original concept of a rigid layer.

Subsequent investigations resulted mainly in a better understanding of the fine structure of the double layer. The origin of charges is considered to be the result of nonuniform distribution of ions at the interface, the charges on the particles being either adsorbed ions or ions originating from the dissociation of the surface itself.

The layer of ions of the opposite charge to the surface is not considered rigid, but, following Gouy (24) and Chapman (25), it is assumed to extend some distance into the solution, with composition progressively approaching the uniform random distribution of ions in the solution.* The most complete theory of the double layer was proposed by Stern (27); in this theory consideration is given to chemical adsorption potentials of adsorbed ions, as well as to the diffuseness of the mobile portion.

The ζ potential may be compared to the electrostatic potential of a charged body; it is all located in one phase only and is measured between two points, one about one atomic diameter from the surface, and the other in the interior of the liquid phase at a distance where uniform random ionic composition prevails (28). It is not to be confused with the more complex potential known as the electrochemical potential which is related to the potential difference between an ion in the interior of the solid phase and the same ion placed in the liquid phase. Following the development of the Debye-Hückel theory of interionic attraction, numerous attempts have been made to apply it to the calculation of the potentials and forces in the neighborhood of sol particles. Most recent work of Verwey and Overbeek, however, casts some doubt on the general applicability of the theory

*The thickness of the double layer in a 0.001 N solution has been estimated to be about 10 mμ. In very pure water, it may be about 100 mμ (26).

in its present form to colloidal particles which carry considerably larger charges than electrolytic ions (45).

V. Sol–Gel Transformation

By a relatively small change in conditions, such as temperature change or addition of an electrolyte, sols may be induced to separate a solid phase in the form of macroscopic particles or flocks, either dense or voluminous, distinctly crystalline or gelatinous, which settle to the bottom of the container. Under less drastic circumstances, the whole mass of sol may congeal, retaining essentially the volume and the form occupied by the sol, thus including practically all the liquid phase originally present. The mobility, characteristic of a liquid, disappears and the mass now displays certain characteristics of a solid.

If the mass is sheared to some extent, a more or less permanent force tends to restore it to its former state. This force is transmitted through gel structure; the gel is elastic. A greater force readily destroys the structure. On the other hand, many of the properties of the liquid sol, such as its optical properties, electrical conductivity, and rate of diffusion of electrolytes, are not measurably affected by gelation.

On closer inspection, it is found that thermal agitation of sol particles has partially or completely ceased. In many instances gels can be redispersed by gentle shaking to sols of substantially identical particle size and electrical properties; freedom from disturbance causes the sol to set again to a gel (reversible gelation, thixotropic gels). This operation may be repeated several times with certain alumina sols, ferric oxide sols, bentonite clays, and many others. With sols readily susceptible to particle growth and coagulation, this property may be lost after a few trials.

It is apparent that, on gelation, the disgregating forces of electrical repulsion and thermal agitation are balanced by some attractive forces between the particles. It is generally agreed that some solid, skeletonlike framework, has been formed within the mass which can be easily destroyed even by mild interference. Very little is known, however, about the fine structure of this framework or about the condition of the liquid component held firmly within the structure. Separation of water on standing from some gels (under isothermal conditions, known as syneresis) suggests that the building of the gel structure continues in such cases for some time following gelation.

Various mechanisms have been advanced to account for gel structure. It is conceivable that systems comprising a liquid, and small anisodimen-

sional particles of a solid, are capable of building a framework by mechanical entangling or enmeshing of particles, thereby filling up relatively large spaces with but little solid substance. Such systems are known to exist, but when formed in the absence of any permanent directing and restoring forces between the particles, merely by piling up of particles, they are easily and permanently destroyed by mild mechanical interference, and the liquid and solid phase are readily separated. To this class belong certain gel-like materials formed by precipitation of masses of needlelike crystals, such as a gel-like mixture obtained by shaking calcium hemihydrate with a solution of ammonium sulfate. Weiser and Moreland demonstrated that the material consists of an entangled mass of relatively long needlelike crystals, and no true gel is formed (29).

In systems with nearly spherical or polyhedral particles, mechanical entanglement is not to be expected, but bridging (formation of chains) by adhesion of particles is conceivable. The void spaces between very small particles in dilute suspensions are much smaller than one would be tempted to estimate. Kraemer (30) calculated that in a 6.5% (by volume) suspension of uniform spheres in cubic arrangement, the thickness of the films between adjacent spheres is equal to their diameter. If the particles are 10–100 $m\mu$ in diameter, corresponding to common lyophobic sols, it is evident that the capillary spaces in a 6.5% dispersion are exceedingly fine. Relatively few particles need to adhere to each other in order to immobilize the entire dispersion, and the rigidity of the structure will usually suffice to prevent closer packing. Such structure may possibly be formed when finally divided carbon is dispersed in organic solvents. McDowell and Usher observed that 1% suspensions of lamp black in organic solvents acquired perceptible electrical conductivity when allowed to stand undisturbed whereas tapping and violent shaking always reduced the conductivity greatly (31).

The formation of a network without material contact between particles is also conceivable, provided that the particles are, at least partly, immobilized by a balance of attractive and repulsive forces emanating from the particles. The behavior of certain thixotropic sols and gels strongly suggests arrangement of particles without material contact, immobilized in positions of minimum potential energy.

Some thixotropic sols set in exceedingly short periods of time, and the process of redispersion to the sol and subsequent setting can be repeated several times, indicating some restoring force between the particles, rather than mechanical entanglement. The period required for setting of slow setting sols is usually quite definite and reproducible, and is characteristic

for a given sol. It can, furthermore, be altered by the addition of electrolytes in the direction expected from the known influence of electrolytes on the electrical forces between particles.

In extremely dilute sols, such as 0.1% chromic oxide gels of Weiser (32), or 0.05% suspensions of bentonite studied by Hauser, which on setting acquire a measurable yield value, a balance of forces would have to be operative over a calculated distance of some 1000 Å. The possibility that the effective diameter of the particles is many times larger than the observed diameter because of several layers of water adsorbed has been suggested. From recent studies of Hauser and LeBeau it appears unlikely, however, that the water hulls, or lyospheres, are thick enough to account for immobilization of all water and establishment of material contact between particles (33).

The role and the exact nature of attractive and repulsive forces which are presumably operative in gelation (as well as in coagulation) is, as yet, far from clear. Hardy (34) believed that a complete loss of electrical charge was necessary for coagulation, but Powis later demonstrated (34) that only a lowering of the electric potential ζ below a certain critical value was required. Since reduction in ζ potential may occur by the reduction in the thickness of the double layer by the added electrolyte, a loss or decrease in charge need not occur at all.

Rapidly accumulating experimental evidence eventually demonstrated that the consideration of the ζ potential alone was unsatisfactory. The critical value of the ζ potential leading to coagulation was found to be, as a rule, considerably higher for the addition of uni-univalent than for other electrolytes. Kruyt and Willigen (34) observed that the ζ potential actually increased to a certain critical value when arsenic trisulfide sol was coagulated with solutions of potassium chloride or potassium ferrocyanide.

In 1929–1930, von Buzágh (35) in a series of brilliant experiments demonstrated the existence of adhesion without direct contact between material particles. Relatively large quartz particles were found to adhere to the bottom of a quartz plate submerged in water. By selecting particles of proper size, he was able to determine the region in which adhesion just balanced the combined disgregating forces of gravity and thermal movement. Particles of this size, although not in material contact with the plate and still performing a lateral thermal motion, confined their movements to a small area in the neighborhood of a fixed point. Addition of electrolytes had a profound influence on the quantitative aspects of this phenomenon, strikingly analogous in detail to the influence exerted by electrolytes on the coagulation of sols.

In 1932 Kallmann and Willstätter (36) suggested that London-van

der Waals' forces of adhesion may operate over considerable, previously unsuspected distances between particles. These forces are known to decrease extremely rapidly with distance ($\backsim 1/r^6$), but are believed to be additive for aggregates of molecules or atoms. Following their method of calculation, an attraction between a quartz wall and a small quartz particle (2–3 μ diameter) would decrease with the negative second power of the distance ($\backsim 1/r^2$).

Freundlich and Rubin (37) demonstrated that the superposition of such attractive forces on electrical forces of repulsion ($\backsim e^{-\kappa r}$, where κ = Debye's constant dependent on valence and concentration of the electrolyte), leads to shallow potential energy minima at a certain critical distance between colloidal particles; the calculated values were of a reasonable order of magnitude, and were taken as characteristic of thixotropic systems. Coagulation was considered to result upon closer approach of the particles, caused either by overcoming the potential barrier (thermal agitation) or by alteration of the electrical forces (*e.g.*, by further addition of electrolyte).

Hamaker (38) developed similar views in considerably greater detail, and following J. H. de Boer, expanded the methods of calculating van der Waals' interactions. Later workers attempted to calculate the electrical forces with greater precision [Eversole (39), Derjaguin (40), Verwey (41), Corkill and Rosenhead (42), Levine (43), Langmuir (44)].

The present state of the theory is not a happy one. Levine, starting largely from the Debye-Hückel theory of interionic attraction, calculated that electrical forces between two colloidal particles with ionic atmosphere are repulsive at small distances and become attractive at larger distances. Langmuir considers the assumption of long-range van der Waals' forces acting in a sol medium to be very improbable, and calculates, with the aid of Debye-Hückel theory, that the interaction of all charged particles and counter ions in a sol leads always to an excess of attraction which must be balanced by some forces of repulsion in excess of thermal agitation.

Most recently, Verwey (45) rejected the Debye-Hückel theory in its present form as inapplicable to colloidal particles and, starting from the Gouy-Chapman theory of the double layer, concluded that double layer interaction always leads to repulsion. This conclusion appears justified by the consideration that energy (including chemical energy) is gained in the double layer formation which must again be supplied to force this layer away, as in the case of interaction. These theories do not lend themselves readily to experimental verification; so far, only Verwey's newest theory has the distinction of leading to theoretical derivation of an experimentally well-established rule relating the valence of the coagulating ions to the critical concentration causing coagulation (Hardy-Schulze rule).

VI. Structural Changes on Drying of Gels

The dehydration of an inorganic hydrogel, depending upon the nature of the substance, may be a rather complex process. Besides removal of free or unbound water, there may likewise be removed water held by adsorption and by capillarity, the vapor pressure of which may be substantially lower than that of free water. The volume changes which accompany the removal of water have a profound influence on the structure of the resultant gel framework. At elevated temperatures, the removal of water of constitution may result in phase changes (*e.g.*, hydroxide to oxide) which cause additional changes in the structure.

The dehydration of silica gel at room temperature has been well described in the monumental work of van Bemmelen (46), and is illustrative of the phenomena occurring with many inorganic gels.

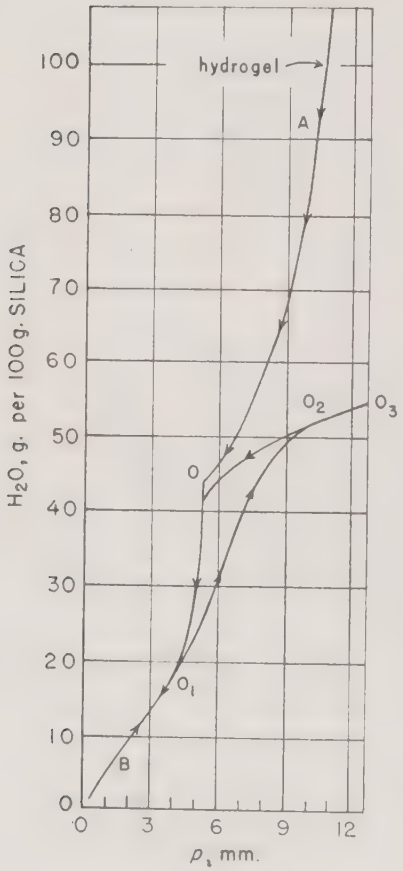

Fig. 1. Dehydration and rehydration of silica gel (46). (Saturation vapor pressure of water at 15 °C. = 12.67 mm.).

A freshly set silica gel was found to contain 180 grams of water per 100 grams of silica (SiO_2). At this stage the gel has the vapor pressure of water. Water can also be squeezed out, and it is quite evident that a considerable amount of free water is present. The structure of the network is not yet rigid, and as more water is removed, the network shrinks. When still more water is removed, the vapor pressure becomes gradually lower, the volume decreases, shrinking of the framework continues, and the pore volume decreases. If it is assumed that the pores are small capillaries, their average diameter decreases during this phase. This intermediate stage of the dehydration of the gel is illustrated by point *A* of Figure 1.

At point *O* the network becomes sufficiently rigid so that further dehydration does not affect it, in other words, the capillary pore volume remains constant. At this point the material contained 31–47 g. of water per 100 g. of silica. The pores are

of submicroscopic size, and the gel presents a glassy, lustrous surface, but is opaque. On further dehydration to point O_1, the gel becomes clear again (water content 20 g. per 100 g. of silica). Substantially complete dehydration is achieved at point B (about 5 g. per 100 g. of silica).

The appearance of opaqueness led the early investigators to erroneous conceptions of the structure, namely large honeycomb-like cavities filled with water. It is now generally agreed that these inhomogeneities are traceable to the presence of fairly large areas comprising numbers of interconnected submicroscopic pores, filled alternately with gas and liquid, *i.e.*, bubbles trapped in the gel framework.

On rehydration, the first part of the curve to point O_1 can be retraced reversibly. From point O, however, a different path is followed. Likewise, the total capacity for water imbibition, measured by point O_3, is lower than for the original hydrogel. Obviously, an irreversible shrinkage of the gel has taken place. On second dehydration, the path $O_3O_2OO_1B$ is followed, demonstrating that the structure does not undergo further change and has assumed a definite final state.

Discovery by Kistler (47) of a process by which water can be removed from a hydrogel without the collapse of its structure, shed some light on the forces which contribute to the collapse of the structure. Kistler replaced the water by a succession of organic solvents, the last of which was then evaporated above its critical point. In this manner the strong contractive forces of the meniscus of the evaporating solvent were avoided and the collapse of the structure was prevented. It is very probable that such a method yields a gel in which the original framework existing in the hydrogel is largely preserved. Such gels Kistler called "aerogels."

From an examination of aerogels and from consideration of other evidence, Kistler visualized the probable structure of silica gel as a mat or felt of filaments forming a three-dimensional network, rather than a rigid solid body with a system of cylindrical capillaries. Heat conductivity measurements indicated that the average distance from one wall to another in aerogels was about 700 Å. It is very likely that the same filaments, only more closely packed, would be present in gels desiccated without Kistler's precautions, since xerogels of the same surface area, but of much smaller pore volume, can be prepared by ordinary drying procedure (specific surface, *ca.* 600–800 square meters per gram; average pore size, 20–60 Å).

VII. Solid Framework of Dried Gels

The solid framework of gels is the product of aggregation of small particles, the existence of which in the sols has been well established. The

nature of the forces which cause the aggregation into hydrogels has already been discussed; even less is known about the changes which occur on desiccation.

It is probable that the particles often preserve their individuality, and this would account for the great friability of certain gels. On the other hand, great mechanical strength and hardness of other gels suggests in those cases a very strong attachment of individual particles. It is to be expected that the final mode of attachment and the nature of the bonds responsible for the rigidity should vary with the nature of the substance and the characteristics of the surface of the aggregating particles. The solid framework of the gel may be crystalline or amorphous, just as the sol particles from which it originated. In the case of crystalline frameworks, x-ray diffraction before and after desiccation may supply some information on the possible growth of individual crystallites, although, in general, no unambiguous answer can be expected regarding the individuality of particles constituting the framework, particularly if crystallites are smaller than the original sol particles, or when points of contact of aggregating crystallites are relatively few.

VIII. Porosity of Gels

The structure of most gels is without doubt a three-dimensional network of solid permeated with free space more or less accessible to molecules of liquids or gases. Large segments or all of this space may be interconnected by passages of various sizes, called pores, whose shape and size is largely determined by the shape, size, and mode of aggregation of the original particles. The free space is called the "total internal volume" or the "pore volume" of the gel. The surface of the pores is the "internal surface" of the gel, which is often so large in comparison with the external surface as to be synonymous with "total surface."

The volume of the gel determined by displacement of a liquid which does not penetrate into the pores is the "apparent volume" and the ratio of internal volume to apparent volume is the "porosity":

$$V_i/V_a = N$$

At this point it may be useful to introduce a differentiation between micropores (very small pores) and macropores (large and very large pores), which is perhaps not fully justified in principle, but is very useful from the experimental point of view. We will arbitrarily assign the term "macro-

pores" to pores larger than about 1000 Å in diameter, and the term "micropores" to pores with diameters smaller than this value. This differentiation as to size is based on the ease of filling of pores by condensation of gases. With nitrogen gas at liquid nitrogen temperature (the experimental conditions widely used for this type of measurement) the dividing line corresponds to a partial pressure of gas approximately 0.98 of saturation pressure. Micropores according to the above description will be filled at or below this partial pressure, while macropores remain unfilled.

It is not possible at present to arrive at a complete picture of the pore structure. While certain characteristics of porous gels can be measured with good accuracy, for example, the surface area of the pores and the total volume of the pores, others, particularly the shape of the pores, are still not accessible to anything like quantitative evaluation.

The measurement of the total pore volume is often relatively simple and can be performed by measuring the displacement of helium gas by the framework of the gel. It can be reasonably assumed that helium gas is not adsorbed on most substances but does penetrate into all pores larger than the helium atom itself. By admitting a measured amount of helium gas into an evacuated bulb of known volume containing the sample of the gel, the data necessary to calculate the volume of the gel framework are obtained. Complications may arise from the slow diffusion of the helium gas into the very narrow channels of the gel.

The value of the pore volume can often be derived from measurement of the apparent volume of the gel, provided that the density of the framework material is known or can be assumed with reasonable accuracy. Apparent volume is obtained by measuring the displacement of a liquid which does not penetrate into the pores of the adsorbent. Mercury often satisfies this requirement.*

The most fruitful method of approach to the pore structure of gels is the investigation of the isothermal adsorption of gases below their critical temperatures with pressures increasing up to the saturation pressure of the gas being studied. Thus, beginning with the gel cleaned of adsorbed gases by heat and evacuation, adsorption is conducted in progressive steps through the stages of incomplete coverage of the surface, formation of the multilayers, filling of the pores by coalescence of multilayers growing on opposite walls of the pore, and filling of the pores by capillary condensation,

*The size of pores penetrated by mercury at different pressures can be calculated by the equation of Washburn. Recently these values were experimentally confirmed by Ritter and Drake (48).

followed by a reversal of these steps by progressive reduction in the gas pressure with attendant desorption of the gas.

The interpretation of the data obtained from such observations is, of course, dependent upon the correctness of the theories applied to them. The first major step in this direction was taken by Zsigmondy (49), who, from his extensive studies of the optical behavior of silica gels, and their appearance under the ultramicroscope, realized that the pores, instead of being the large honeycomb-like empty spaces ($\backsim 1\ \mu$) envisioned by Bütschli and van Bemmelen, must be very much finer, of the order of the size ($\backsim 0.005\ \mu$) where the Kelvin theory of capillary condensation (50) could be applied. The pores were conceived by Zsigmondy as fine capillaries in which gases could condense at a pressure lower than the saturation pressure in accordance with the equation derived from Kelvin's work:

$$p = p_0 e^{-2\sigma V/rRT}$$

where p is the pressure at which a gas having a saturation pressure p_0 ($p < p_0$), will condense in a capillary of radius r to produce a liquid of surface tension σ, and molal volume V.

Zsigmondy was aware that capillary condensation was preceded by reversible adsorption, but apparently considered this fact of secondary importance. He brilliantly hurdled the difficult problem of hysteresis by advancing a plausible explanation. According to Zsigmondy, the hysteresis was due to incomplete wetting of the clean gel surface and distortion of the advancing meniscus. The receding meniscus was presumably in equilibrium with the vapor, and the desorption rather than the adsorption branch of the isotherm was therefore better suited for the calculation of pore diameters.

Anderson (51), in Zsigmondy's laboratory, furnished the first experimental support for the theory of capillary condensation. With the simplifying assumption that the pores could be treated as small cylinders, Anderson obtained very good agreement of pore size values calculated from adsorption data for vapors of three very different liquids, namely water, alcohol, and benzene.

The theory was widely accepted as the result of Anderson's work. However, instances began to appear which disclosed the shortcomings of the capillary condensation theory as applied originally to adsorption isotherms. Complete disregard of adsorption is obviously erroneous; it is clearly evident that, if adsorption on the walls of the unfilled pores is taking place prior to or simultaneously with, capillary condensation, the effect must somehow be separated from capillary condensation in any pore

size computation. Particularly, the point at which capillary condensation sets in must be established. The difficulty is especially marked when the gel contains very small pores comparable to molecular dimensions. It is then obviously not justified to calculate the curvature of the "meniscus" and to substitute for surface tension and molal volume in Kelvin's equation values established for bulk liquids. If the calculation is nevertheless performed, pore diameters smaller than the diameter of the molecules of adsorbate and, hence, without physical meaning, may be obtained from adsorption measurements at low pressures (52,53). The pore sizes of a number of materials were investigated by Kubelka (54) who accepted the Kelvin equation but concluded that the surface tension and molal volume of free liquid when applied to very small capillaries led to erroneous results when used in the calculation. Schukowitzki (55) was the first to point out the specific effect upon the calculated pore size of neglecting adsorption, but his considerations were not followed actively, and it remained for Kistler (56) to make a definite correction for monomolecular adsorption in the low-pressure region of the adsorption isotherm. The value of such procedure is, however, doubtful in view of the remarkable success of the theory of multilayer adsorption in accounting for the general shape of all possible types of adsorption isotherms, at least in the low-pressure region (11).

The sorption is pictured by Emmett and Brunauer as taking place by true adsorption only for the first layer. Additional layers may be condensed on top of the first layer even when the coverage by monolayer is not completed. In the first stages only a relatively small fraction of the total surface is covered by more than a monomolecular layer. The theory provides a means of calculating the exact amount of gas necessary to cover the surface with a monolayer; it provides, furthermore, a new mechanism for filling the pores by multilayer adsorption and coalescence of the two layers growing on the opposing walls of the pores. The theory does not exclude the possibility of the occurrence of capillary condensation at pressures near saturation; however, efforts to include capillary condensation in the theory of multilayer adsorption have, as yet, not been completely successful, and lead to very complicated algebraic expressions for the adsorption isotherms (11,57).

A survey of the literature on physical adsorption revealed that five general types of adsorption isotherms may be encountered. The multilayer theory of adsorption offers a general equation which accounts satisfactorily for all five types over a significant portion of the pressure range. The equation is rather complex but certain simplifying assumptions can often be made to qualify the equations for practical use.

1. Pore Size Distribution

The pores in gels are not necessarily of uniform size, and it is to be expected that a distribution of sizes will invariably be encountered. It is, however, a matter of considerable interest that, in many cases investigated, the micropores have either a fairly narrow size distribution or that, at least, the sizes are uniformly distributed about a mean or average value. The curves indicating such distribution resemble the probability curves very closely.

Pore size distribution may be derived from the adsorption isotherms by the use, either of the capillary condensation theory, or the theory of multimolecular adsorption. The application of the capillary condensation theory rests essentially on the fact that (neglecting the adsorption layer) a certain pore size can be assigned to each value of the pressure at which condensation presumably takes place, according to the Kelvin equation. It is possible to substitute directly for the fractional pressures p/p_0 and calculate the radii values. The total volume of adsorbed gas at any point on the isotherm is the total volume of pores of radii equal to or smaller than the given radius. It is convenient to utilize such curves in their differentiated form and to plot only the increments of volume corresponding to small increments of radius, obtaining thereby the so-called "structure curves."

The application of the multilayer theory consists essentially in the evaluation of the constant n of equation 41, page 154 of Brunauer's book (11), for each volume increment. This is beyond doubt a complex algebraic operation and, to the author's knowledge, is not widely followed (58). Data recorded in the literature indicate that the two theories give fairly concordant results and it is likely that the values calculated from capillary condensation theory are at least of the correct order of magnitude. Exact evaluation of the errors involved is at present not possible.

Very little is known concerning the distribution of pore sizes in the region of macropores; a convenient method for the evaluation of sizes and the distribution of sizes of macropores has, however, been recently developed (48). The method consists essentially in forcing mercury under pressure into the pores and calculating the pore sizes from Washburn's equation for the penetration of liquids into capillaries. Since by going into high, but experimentally feasible, pressures with mercury, pore sizes well into the micropore size range can be determined, this method supplies an additional check against the pore size distribution obtained by the application of the Kelvin capillary condensation equation to low-temperature gaseous adsorption isotherms.

2. Shape of the Pores

So far, only the capillary condensation theory is in a position to give some indications of the geometry of the pores. It is recognized that the assumption of cylindrical pores is only a mathematical convenience; it is, indeed, difficult to reconcile the assumption of cylindrical pores with the possible structure of gels, such as a three-dimensional network of filaments or an aggregation of more or less spherical particles.

It has been suggested that the phenomenon of reversible hysteresis in adsorption and desorption of vapors is in some way related to the shape of the pores; Kraemer (59), and later McBain (60), suggested that the presence of capillary spaces with narrow communicating channels would account qualitatively for hysteresis. Such spaces would be completely filled by capillary condensation at a pressure corresponding to the curvature of the meniscus in the wide portion, but could empty only at a lower pressure determined by the radius of the narrow channels. Foster (61) suggested that hysteresis was due to a delay in the formation of the meniscus in open pores during adsorption. Later Cohan (62) and Coelingh (63) developed the theory of capillary condensation in open cylindrical pores. In such pores the filling is assumed to proceed by condensation on the cylindrical walls, the emptying, via a meniscus formed by the coalescence of the condensate. The radius of curvature of the spherical meniscus is twice as large as that of the cylindrical wall, and thus emptying of the pore (desorption) can take place only at a lower pressure. In a recent paper, Cohan (64) has developed further, and in greater detail, the relationship between hysteresis and a number of probable pore shapes, and suggested experimental techniques for exploration of the relative number of each species.

References

1. H. Freundlich, *J. Phys. Chem.*, **41,** 901 (1937).
2. H. B. Weiser and W. O. Milligan, "The Constitution of Colloidal Systems of the Hydrous Oxides," in E. O. Kraemer, *Advances in Colloid Science,* Vol. I. Interscience, New York, 1942.
3. C. F. Goodeve, *Trans. Faraday Soc.*, **35,** 342 (1939).
4. H. R. Kruyt, *Chimie & industrie,* **42,** 587 (1939).
5. P. C. Carman, *Trans. Faraday Soc.*, **36,** 964 (1940).
6. C. B. Hurd, *Chem. Revs.*, **22,** 403 (1938).
7. H. B. Weiser, *Colloid Chemistry.* Wiley, New York, 1939, p. 271.
8. A. W. Thomas, *Colloid Chemistry.* McGraw-Hill, New York, 1934, p. 471.
9. H. Freundlich, *Colloid and Capillary Chemistry.* Dutton, New York, 1922.

10. E. O. Kraemer, in H. S. Taylor, *A Treatise on Physical Chemistry*. Van Nostrand, New York, 1931, p. 1710.
11. S. Brunauer, *The Adsorption of Gases and Vapors*. Princeton Univ. Press, Princeton, 1943.
12. See, *e.g.*, H. B. Weiser, *Colloid Chemistry*, Wiley, New York, 1939, p. 117, for a brief summary and references to von Weimarn's work.
13. K. H. Meyer, *Natural and Synthetic High Polymers* (High Polymers, Vol. I). Interscience, New York, 1942, p. 66.
14. P. F. Flory, *J. Am. Chem. Soc.*, **63,** 3083, 3091, 3096 (1941).
15. W. D. Treadwell, *Helv. Chim. Acta*, **14,** 473 (1931). See A. W. Thomas, *Colloid Chemistry*, McGraw-Hill, New York, 1934, for a review of this subject.
16. G. Jander and A. Winkel, *Z. physik. Chem.*, **A149,** 97 (1930); *Z. anorg. allgem. Chem.*, **200,** 257 (1931).
17. K. L. Elmore, C. M. Mason, and J. D. Hatfield, *J. Am. Chem. Soc.*, **67,** 1449 (1945).
18. B. von Borries and G. A. Kausche, *Kolloid-Z.*, **90,** 132 (1940).
19. H. von Ardenne, *Elektronen Übermikroskopie*. Springer, Berlin, 1940.
20. B. T. Shaw, *J. Phys. Chem.*, **46,** 1032 (1942).
21. E. J. W. Verwey and H. R. Kruyt, *Z. physik. Chem.*, **A167,** 137 (1933).
22. See *e.g.*, A. von Buzágh, *Colloid Systems*. Technical Press, London, 1937, pp. 156, 163. Also E. A. Hauser, *Colloidal Phenomena*. McGraw-Hill, New York, 1939.
23. H. Helmholtz, *Ann. Physik Chem.* (*Wiedemann*), **7,** 337 (1879).
24. G. Gouy, *J. phys.*, **9,** 457 (1910); *Ann. phys.*, **7,** 129 (1917).
25. D. L. Chapman, *Phil. Mag.*, **25,** 475 (1913).
26. E. O. Kraemer, in H. S. Taylor, *A Treatise on Physical Chemistry*. Van Nostrand, New York, 1931, p. 1680.
27. O. Stern, *Z. Elektrochem.*, **30,** 507 (1924).
28. N. K. Adams, *Physics and Chemistry of Surfaces*. Oxford Univ. Press, London, 1941.
29. H. B. Weiser and F. B. Moreland, *J. Phys. Chem.*, **36,** 1 (1932).
30. E. O. Kraemer in H. S. Taylor, *A Treatise on Physical Chemistry*, p. 1709.
31. C. M. McDowell and F. L. Usher, *Proc. Roy. Soc. London*, **A131,** 564 (1931).
32. H. B. Weiser, *Colloid Symposium Monograph*, **1,** 38 (1923).
33. E. A. Hauser and D. S. LeBeau, *J. Phys. Chem.*, **45,** 54 (1941).
34. W. B. Hardy, *Proc. Roy. Soc. London*, **66,** 110 (1900). F. Powis, *Z. physik. Chem.*, **89,** 186 (1915). H. R. Kruyt and P. C. van der Willigen, *ibid.*, **130,** 170 (1927).
35. A. von Buzágh, *Kolloid-Z.*, **47,** 370 (1929); **51,** 105, 230 (1930); **52,** 46 (1930); *Naturwissenschaften*, **18,** 444 (1930).
36. H. Kallmann and M. Willstätter, *Naturwissenschaften*, **20,** 952 (1932).
37. H. Freundlich and J. Rubin (J. R. Vinograd), in H. Freundlich, *Thixotropy*. Hermann, Paris, 1935.

38. H. C. Hamaker, *Rec. trav. chim.*, **55,** 1015 (1936); **56,** 3, 727 (1937). Compare also *Hydrophobic Colloids* (Symposium of the Nederlandsche Chemische Vereeniging at Utrecht), Nordemann, Amsterdam, 1937.
39. W. G. Eversole and P. H. Lahr, *J. Chem. Phys.*, **9,** 530 (1941). W. G. Eversole and A. J. Hanson, *ibid.*, **10,** 460 (1942).
40. B. Derjaguin, *Trans. Faraday Soc.*, **36,** 203 (1940).
41. E. J. W. Verwey, *ibid.*, **36,** 192 (1940); *Chem. Weekblad*, **39,** 563 (1942).
42. A. J. Corkill and L. Rosenhead, *Proc. Roy. Soc. London*, **A172**, 410 (1939).
43. S. Levine, *ibid.*, **A170,** 145, 165 (1939). S. Levine and G. P. Dube, *Trans. Faraday Soc.*, **35,** 1125 (1939); **36,** 215 (1940).
44. I. Langmuir, *J. Chem. Phys.*, **6,** 873 (1938).
45. E. J. W. Verwey, *Philips Research Repts.*, **1,** 33 (1945).
46. J. M. van Bemmelen, *Z. anorg. Chem.*, **13,** 233 (1897).
47. S. S. Kistler, *Nature*, **127,** 741 (1931).
48. H. L. Ritter and L. C. Drake, *Ind. Eng. Chem., Anal. Ed.*, **17,** 782 (1945).
49. R. Zsigmondy, *Z. anorg. Chem.*, **71,** 356 (1911).
50. W. Thomson (Lord Kelvin), *Proc. Roy. Soc. Edinburgh*, **7,** 63 (1869–70).
51. J. S. Anderson, *Z. physik. Chem.*, **88,** 191 (1914).
52. S. Brunauer, *The Adsorption of Gases and Vapors*, p. 134.
53. A. S. Coolidge, *J. Am. Chem. Soc.*, **46,** 596 (1924).
54. P. Kubelka, *Kolloid-Z.*, **55,** 129 (1931); **58,** 189 (1932).
55. A. A. Schukowitzki, *ibid.*, **66,** 139 (1934).
56. S. S. Kistler, E. A. Fischer, and I. R. Freeman, *J. Am. Chem. Soc.*, **65,** 1909 (1943).
57. S. Brunauer, L. S. Deming, W. E. Deming, and E. Teller, *ibid.*, **62,** 1723 (1940).
58. V. Dietz and L. F. Gleysteen, *Bur. Standards Bull.*, R. P. 1496 (1942).
59. E. O. Kraemer, in H. S. Taylor, *A Treatise on Physical Chemistry*, p. 1661.
60. J. W. McBain, *J. Am. Chem. Soc.*, **57,** 699 (1935).
61. A. G. Foster, *Trans. Faraday Soc.*, **28,** 645 (1932).
62. L. H. Cohan, *J. Am. Chem. Soc.*, **60,** 433 (1938).
63. M. B. Coelingh, *Kolloid-Z.*, **87,** 251 (1939).
64. L. H. Cohan, *J. Amer. Chem. Soc.*, **66,** 98 (1944).

SUBJECT INDEX

A

Activated state, 4
Activation energy, concept, 3
Active centers and poisoning of catalysts, 16
Adhesion, analogue of coagulation, 186
Adsorption, interpretation, 193
Aerogels, structure, 189
Aldehydes, dipole moment, 40
Aliphatic resonance, 36
Alkenes, catalytic reactions, 19
Alumina, theory of gel formation, 179
Ammonia, chemisorption of hydrogen on, 14
Aromatic resonance, 31
Atomic number, effective, and electronic orbitals, 62
Atomic orbitals and bond configurations, 79
Atomic radii and isomorphism, 2
Avogadro's number from light scattering, 127

B

Benzene, structure, 26
Beryllium acetylacetonate, physical properties, 58
Binding energy, 4
  three-atom system, 5
Binuclear complex, resolution, 94
Biological specificity and structural similarity, 17
Bond configurations and atomic orbitals, 79
Bond distribution, elements, 83

C

Capillary condensation, gels, 192
Carbon black, graphitization, 112
  random-layer structure, 108
  structure, 110
  x-ray pattern, 109
Carbonyl compounds, reduction by hydrogen and deuterium, 14
Catalyst(s), gel structure, 175
  lattice spacings and surface reactions, 12
  poisoning, 15
Cellulose acetate, light scattering, 169
Cellulose derivatives, light scattering, 168
Chemisorption of hydrogen, 11
Chromium complex compounds, 73
Cis-bridging, coordination compounds, 71
Cis-trans isomerism, coordination compounds, 67
Coagulation, theory, 182
Cobalt complex compounds, 72
Complex compound(s). See also *Coordination compound(s)*.
  classification, 57
  definition, 54
Complex ions, instability constant, 55
  ionic potential, 59
Complex salts, definition, 55
Complex silicate structures, 106
Complex structure determination, 106
Compound of higher order, 54
Compressibilities of liquids from light scattering, 130
Coordinate covalence, 60
Coordination complex, 56
Coordination compound(s), classification, 57
  deduction of structure, 65
  definition, 54
  dipole moments, 77
  electron diffraction, 76
  isomerism, 66
  magnetochemistry, 80
  optical properties, 82
  radioactive isotopes, 81
  structure, 53–100
  substitution reactions, 71
  x-ray studies, 74
Coordination isomerism, 67
Coordination linkages, nature, 59
Coordination number, definition, 56
  in crystallography, 76
Coordination number two, 83
  three, 84
  four, 84
  five, 90
  six, 90
  seven, 95
  eight, 96
Coordination ratios of radii, 64
Coordination sphere, 55
Covalence, definition, 60
  Sidgwick's rule, 60
Crystalline structures, 103
Crystallochemical rules, 2
Crystal structure, x-ray diffraction patterns, 102

D

Debye equation, 24

Dehydration, hydrogel, 188
Dehydrogenation of six-membered rings, 9
Depolarization, scattered light, 147
Deuterium exchange, olefins, 15
Dichloroethylene, structure, 26
Dielectric constant and phase transition, 30
Differential refractometer, 159
Dipole(s), molecule as, 23
  movable, 28
Dipole moment(s), coordination compounds, 77
  experimental determination, 24
  and resonance, 31
  solvent effect, 25
Dissymmetry coefficients of several polymers, 164
Dissymmetry measurements, visual observation, 153
Dissymmetry of light scattering, experimental method, 150
Double bonds, hydrogenation, 15
Double layer, electrophoretic theory, 182
Double salts, definition, 55
Drying of gels, structural changes, 188

E

Effective atomic number and electronic orbitals, computation, 63
Electrical potential of particles in sol, 182
Electron-density methods, crystal structures, 107
Electron diffraction, coordination compounds, 76
Electronic configurations, 62
Electronic orbitals, and effective atomic number, 62
  theory, 78
Electrovalence, definition, 60
Elements, bond distribution, 83
Ethylene, hydrogenation, 12
Ethylene dihalides, restricted rotation, 28
Exchange energies, 4

F

Fluctuation of optical density, 132
Forced configuration, coordination compounds, 86
Four-atom system, molecular geometry, 6
Free-draining chains, 141–143

G

Gas on surface, molecular energy, 10
Gel(s), classification, 177
  definition, 176
  inorganic, formation, 177
    nature, 175–197
Gel(s) *continued*
  pore size distribution, 194
  pore structure, 191
  porosity, 190
  shape of pores, 195
  solid framework, 189
  structural changes in drying, 188
Gelation, 184
  electropotentials, 186
Gel formation, theory, 178
Geometrical structure, dipole moment for determination, 26
Geometry, heterogeneous reactions, 8
  homogeneous liquid systems, 19
  homogeneous reactions, 5
  and reaction mechanism, 1–22
Giant molecules, complex structure, 76
Goldschmidt's crystallochemical rules, 2
Graphite, structure, 108
Graphitization, carbon black, 112

H

Heat of reaction, 4
Heitler-London forces, 4
Heterogeneous reactions, geometry, 8
Hindrance of rotation, 30
Homogeneous liquid systems, molecular geometry, 19
Homogeneous reactions, geometry, 5
Hydrocarbons, resonance, 36
Hydrogel, dehydration, 188
Hydrogen, chemisorption on synthetic ammonia, 14
  three-atom complex, 5
Hydrogenation, double bonds, 15
Hydrogen molecule, adsorption and geometry, 11
Hydrous oxides, theory of gel formation, 179
Hysteresis, necessity of gels and pores, 195

I

Ideal gas, light scattering, 125
Impurities, low molecular weight, 161
Inner sphere, molecule, 55
Inorganic gels, formation, 177
  nature, 175–197
Inorganic sols, particle shape, 180
Instability constant, complex ions, 54
Intermediate complex, molecular geometry, 5
Intrinsic dissymmetry, light scattering, 144
Ion-dipole bond, nature, 59
Ionic bonds, dipole moments, 31
Ionic potential, complex ions, 59
Ionization isomerism, 67
Ionization sphere, 56

Ions, identification in complex compounds, 66
in crystals, shapes, 75
Isomerism, *cis-trans*, coordination compounds, 67
coordination compounds, 66
Isomorphism and chemical constitution, 1

L

Lattice spacing, influence on surface reactions, 12
Light scattering, direct measurements of, 151
experimental results, 163
in homogeneous dielectric medium, 172
ideal gas, 125
intrinsic dissymmetry, 144
isolated small molecule, 123
large molecule solutions, 139
molecular weight distribution function, 170
order of magnitude, 137
physical fundamentals, 123
in polymer solutions, 121–173
proteins, 163
pure liquid, 127
rigid-rod model, 142
solution of small molecules, 131
transmission method, 150
vinyl polymers, 163
Linkage isomerism, coordination compounds, 66
Liquid(s), compressibilities, 130
pure, light scattering, 127
London equation, 5
Long-range order in alloys, 113
Luminescent processes, kinetic characteristics, 18

M

Magnetic susceptibilities, Sidgwick-Bose rule, 80
Magnetochemistry, complex compounds, 80
Melting and molecular rotation, 30
Molecular geometry, historical survey, 1
and reaction mechanism, 1–22
Molecular rotation, complex compounds, 94
and solid–solid transitions, 30
Molecular structure, resonance, dipole moment, 23–51
Molecular weight distribution function, 170
Molecular weights, turbidity, 135
Movable dipoles, 28
Multiple adsorption theory—Burk, 8
Multiplet hypothesis—Balandin, 8

N

Nitriles, dipole moment, 44
Nitrobenzenes, resonance, 33
Nitroso and nitro complexes, 67

O

Octahedral configurations, coordination compounds, 91
Olefinic molecules, interaction, 15
Olefins, deuterium exchange, 15
Optical density, fluctuation, 132
Optical isomerism, coordination compounds, 70
Order-disorder in alloy, Cu_3Au, 113
Order-disorder randomness, 113
Osmotic molecular weight, 134
Outer sphere, molecule, 56
Oxalate compounds, magnetic susceptibilities, 80

P

Phase transition, determination through dipoles, 30
Photoelectric turbidimeter, 154, 158
Planar configuration, coordination compounds, 87
Platinum complex compounds, dipole moments, 77
Platinum metal complexes, effective atomic number, 64
Poisoning of metal catalysts, 15
Polyatomic systems, molecular geometry, 7
Polymerization isomerism, coordination compounds, 68
Polymer molecules, randomly kinked coils, 142
Polymer solutions, absolute method for weight-average molecular weight, 122
light scattering, 121–173
turbidity, 137
Polystyrene, depolarization measurements, 165
dissymmetry coefficients, 164
weight-average molecular weight, 168
Polystyrene solutions, turbidity, 135
Polyvinyl chloride, apparent weight-average molecular weight, 167
Pore shape, gels, 195
Pore size distribution, gels, 194
Pore volume, measurement, 191
Porosity, gels, 190
ζ-Potential, 183
Potential barrier, 4
rotation and dipoles, 29
Potential energy, rotation, 29
Proteins, turbidity of solutions, 163
Purity of solutions for turbidimetry, 161

Q

Quantum mechanical valence theory, 4

R

Radioactive isotopes, coordination compounds, 82
Radius ratio rules, 63
Random-layer structure of carbon black, 108
Randomly kinked polymer coils, 142
Randomness, discussion, 119
in structures, 108
x-ray studies, 101
Reaction mechanism and molecular geometry, 1–22
Refractometer, differential, 159
Rehydration, silica gel, 189
Resonance and dipole moment, 31
Rigid-rod model, polymer molecule, 141
Rotation, repulsive potential energy, 29
restricted and dipoles, 28

S

Scattered light, depolarization, 147
Short-range order in alloys, 115
Sidgwick-Bose rule, magnetic susceptibilities, 80
Sidgwick's rules of maximum covalence, 61
Silica gel, dehydration, 188
theory of formation, 178
Sol(s), electrophoretic analysis, 182
inorganic, particle shape, 180
optical analysis, 181
stability, 182
Sol–gel transformation, 184
Solid–solid transition and molecular rotation, 30
Solvent effect, dipole moment, 25
Sorption theory, 193
Specificity in surface catalysis, 17
Stability, sols, 182
Stereochemistry, 2
Stereoisomerism, coordination compounds, 67
Structure, deduction of coordination compounds, 65
definition, 53
Substitution reactions, for determining structure of coordination compounds, 71
Surface catalysis, specificity, 17

T

Tetrahedral configuration, coordination compounds, 85
Thermal density fluctuations in liquids, 128
Thixotropic sols, transformation, 185
Three-atom system, binding energy, 5
Tobacco mosaic virus suspensions, light scattering, 173
Transition elements, tending to form complex compounds, 62
Transmission method, light scattering, 150
Turbidimeter, photoelectric, 154, 158
visual observation, 151
Turbidimetry impurities of solution, 161
Turbidity, experimental method, 150
molecular weights, 135
of solution, 131

V

Valence, classification, 60
Valence forces, 4
Vinyl polymers, dissymmetry coefficients, 164
turbidity, 163

W

Water molecule, structure, 26
Weight-average molecular weight, absolute method, 122
apparent, of polyvinyl chloride, 167
of polystyrene, 168

X

Xerogel, definition, 177
X-ray diffraction patterns, crystal structure determinations, 102
X-ray studies, coordination compounds, 74
of randomness, 101

Checked
12/6/52

3/8/89 15.4.97

CHECKED 2008

C. F. T. R. I. LIBRARY, MYSORE.

Acc. No. 1810

Call No. E"x,1,N47 N48

VERIFIED 2013

Please return this publication on or before the last DUE DATE stamped below to avoid incurring overdue charges. 14/5/90

P. No.	Due Date	Return date

CFTRI-MYSORE
1810
Chemical archite

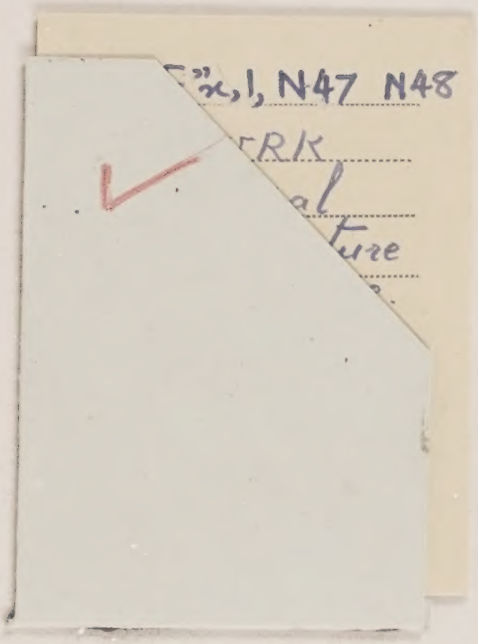
N47 N48
RK
al
ure